Leo Gilbride

From: Leo Gilbride
Sent: Wednesday, August 09, 2006 12:42 PM
To: Laine Adair
Cc: AAI Archive
Subject: (226-30) GENWAL Main West Retreat Analysis--Preliminary Results
Attachments: Figures 4-30.pdf; Figure 1.pdf; Figure 2.pdf; Figure 3.pdf

Laine,

I have prepared this email to summarize our preliminary analytical results for the proposed retreat mining sequence in the Main West barriers at GENWAL. We analyzed ground conditions using (1) the NIOSH ARMPS empirical design method and (2) the same LAMODEL stress and convergence model used in our Jul-20, 2006 analysis. Figure 1 shows the modeled areas.

ARMPS Modeling

The ARMPS method is an empirical design method developed by NIOSH based on 250 pillar retreat case histories. The database contains numerous cases representing ground conditions in the western U.S. and mining depths up to 2,000 ft, which makes the method relevant for conditions at GENWAL. The method computes a Stability Factor (SF) based on the ratio of pillar strength to pillar load averaged over the pillars within the active mining zone (near the edge of the gob). Lower SFs are supposed to indicate lower safety margins. Figure 2 plots the SFs as a function of mining depth for all the ARMPS case histories. The plot distinguishes between "satisfactory" and "unsatisfactory" case histories, where "unsatisfactory" case histories involved the following types of ground failures: excessive squeezing, bumps, and/or roof failure. The historical retreat panels in the 1st North Left block at GENWAL are computed to have a SF of 0.37 at a depth of 1,750 ft. Figure 3a shows the ARMPS model geometry used to compute the SF. The ARMPS database shows that industry experience is mixed for mines reporting similar SFs (0.16 to 1.05) at comparable depths (1,500 to 2,000 ft). Of these cases, slightly more than half were successful, while the remainder encountered ground control problems.

A SF of 0.53 is computed for the proposed retreat sequence in the Main West barriers under the deepest cover (Figure 3b). The ARMPS method recommends basing the depth of cover on sustained cover, and not on peak cover if the peak cover occurs over a limited area. Over Main West, 2,000 ft is the maximum sustained cover that is appropriate for the ARMPS calculation. Although a narrow ridge increases cover to 2,200 ft, this is too limited an area to significantly affect abutment loads in the ARMPS calculation. Elsewhere in the barriers and mains, a higher SF is computed. A SF of 0.67 is computed for pillaring east of the existing Main West seals (XC 118-119).

The ARMPS method recommends designing pillars for a 0.90 SF (for intermediate-strength roof) if site-specific data are not otherwise available. The authors of ARMPS suggest that the method is increasingly conservative at depth and that site-specific experience should be used to establish design SFs whenever possible. At GENWAL good success has been achieved at SFs below 0.90. Retreat conditions in the 1st North Left block were generally successful with a SF of 0.37, suggesting that a SF of about 0.40 is a reasonable lower limit for retreat mining at GENWAL. This is considered a lower limit because occasional problems with peeling top coal were encountered in the 1st North Left block. This required skipping pillars on retreat in some locations. Top coal is currently mined to minimize this risk and is not expected to be a problem in Main West.

The lowest SF for the proposed retreat sequence in Main West barriers is 0.53 under the deepest cover, which is approximately 43% higher than the "satisfactory" SF of 0.37 for the 1st North Left block. Implications are that the proposed retreat sequence in Main West will be successful in terms of ground control, even under the deepest cover (2,200 ft).

LAMODEL Modeling

The Main West retreat sequence was modeled in 9 steps, as shown in Figures 4 through 30. The model includes the actual variable depth of cover ranging from 1,200 to 2,200 ft, as shown on the map in Figure 1. The figures present modeled (1) vertical stress, (2) coal yielding, and (3) roof-to-floor convergence. Results show that convergence will be less than 2.0 inches in and around the active pillaring sections in the barriers. Results of the 1st North Left back-analysis model, discussed in the Jul-20, 2006 letter, concluded that convergence less than 2.0 inches is indicative of stable roof and pillar conditions in the model. Conclusions from LAMODEL corroborate the ARMPS results, principally that convergence can be adequately controlled with the proposed mine plan and that ground conditions should be generally good on retreat in the barriers, even under the deepest cover (2,200 ft).

The model predicts relatively high convergence during pillaring east of the existing Main West seals (XC 118-119) due to relatively large abutment loads around the wide gob area. This retreat block is approximately 1,400 to 1,600 ft deep. Model results show convergence in excess of 2.0 inches in and around the active pillaring areas, suggesting some risk for accelerated ground deterioration and increased reliance on ground support (i.e., bolts and mesh, and mobile roof support). The amount of convergence and ground squeezing is sensitive to the extraction sequence and the rate of extraction. A constant and relatively rapid rate of pillaring is beneficial for controlling the risk of excessive squeezing and bumping. The overall level of geotechnical risk is not considered excessive given GENWAL's history and favorable ground conditions. The mining plan and pillar layout as proposed are considered viable. The plan affords the contingency to leave occasional pillars for protection during retreat if conditions warrant, thus providing additional control of the geotechnical risk.

We can prepare a letter report to present these results at your discretion. In the meantime, please contact me at any point if you wish to discuss these results and recommendations.

Sincerely,

Leo Gilbride, PE
Principal

AGAPITO ASSOCIATES, INC.
715 Horizon Drive, Suite 340
Grand Junction, CO 81506
Telephone: (970) 242-4220
Fax: (970) 245-9234
www.agapito.com

Figure 1.pdf klg 9-21-07

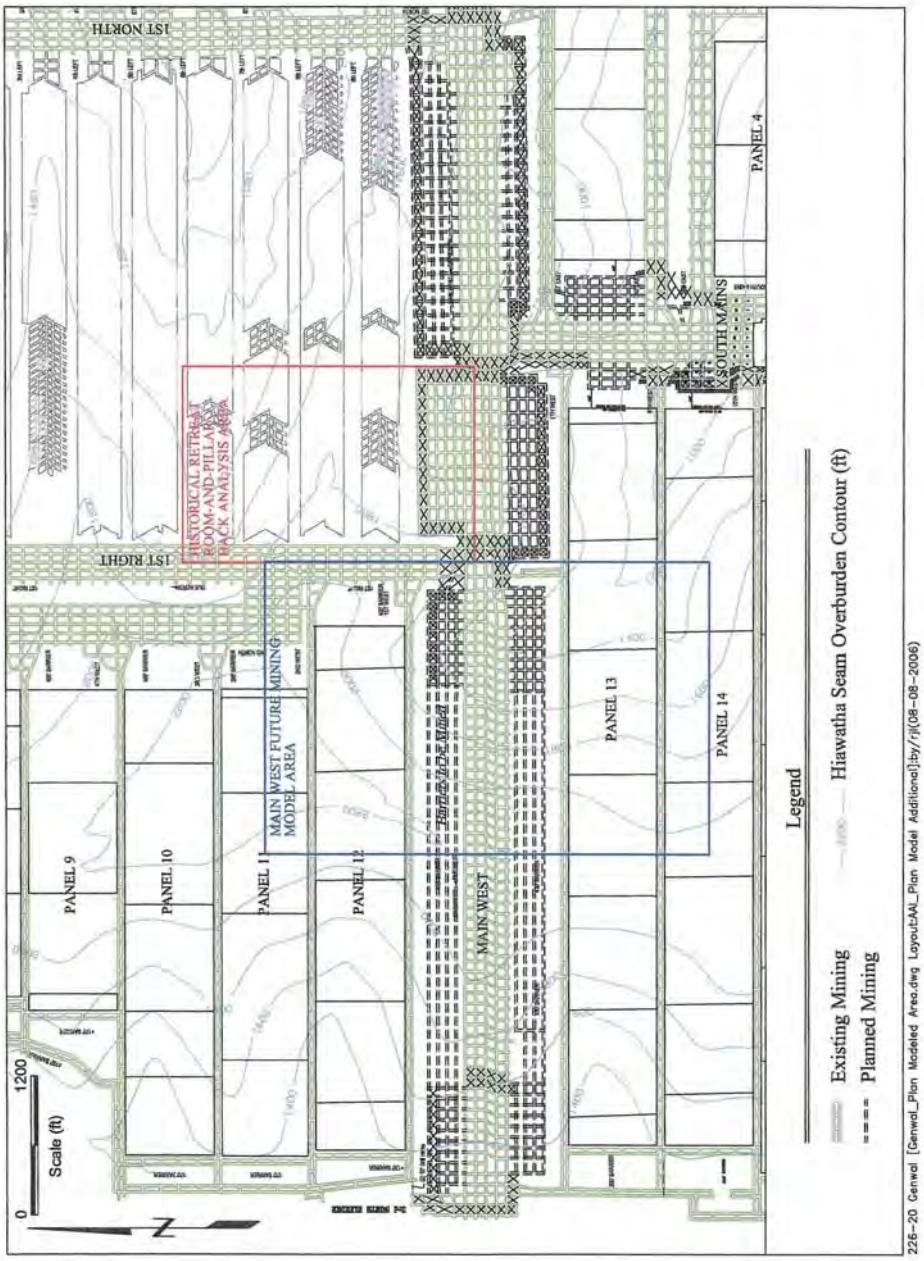

Figure 1. Main West Location Map Showing Exisitng and Future Mining and Modeled Areas

AAI000137

Figure 2.pdf klg 9-21-07

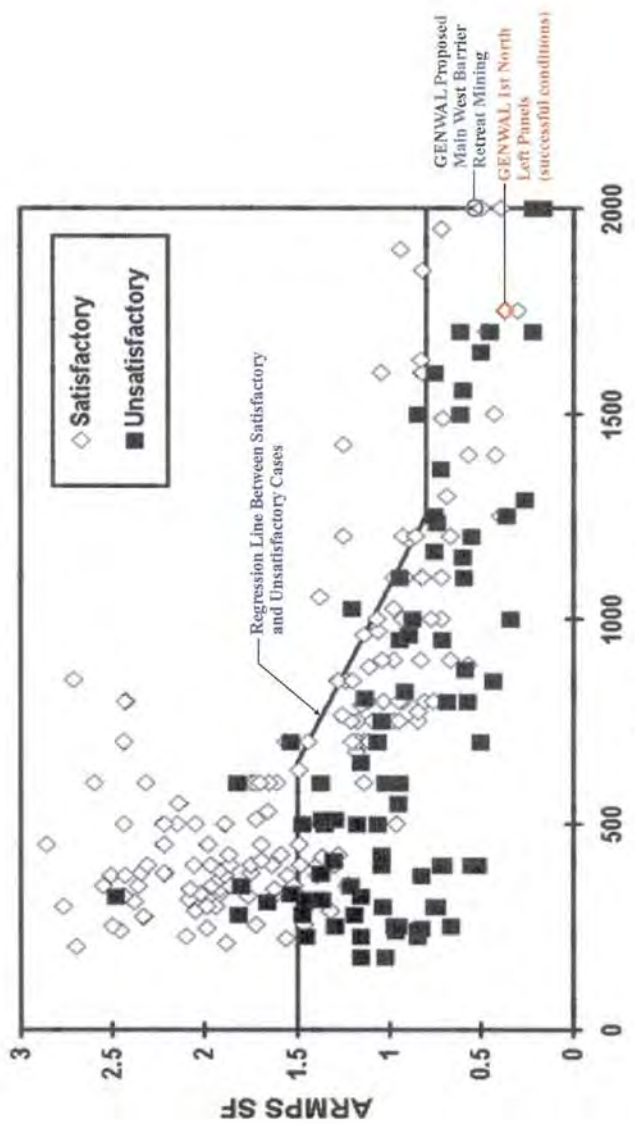

Figure 2. Comparison of GENWAL Past and Proposed Retreat Mining Stability Factors with ARMPS Case Histories

AAI000138

Figure 3.pdf klg 9-21-07

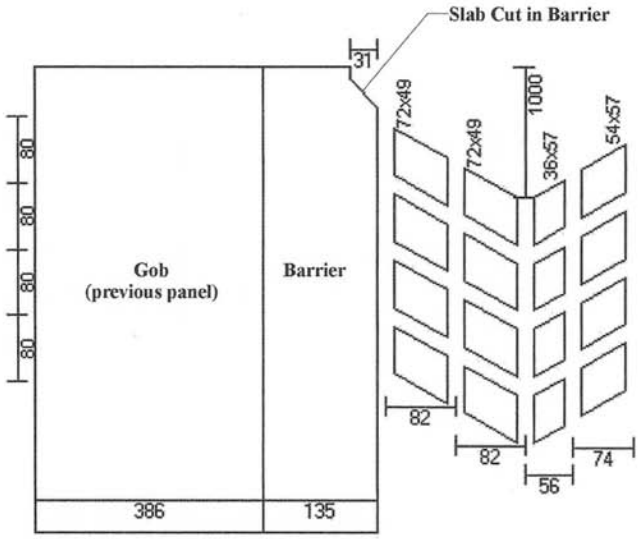

a) 1st North Left Typical Panel Retreat Geometry

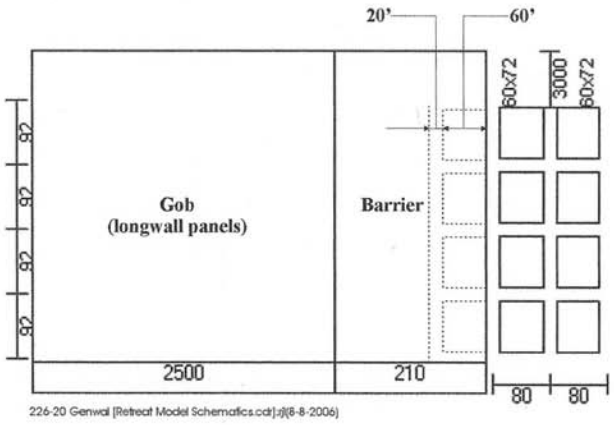

b) Main West Proposed Retreat Geometry

Figure 3. ARMPS Retreat Model Schematics

AAI000139

Figures 4-30.pdf klg 9-21-07

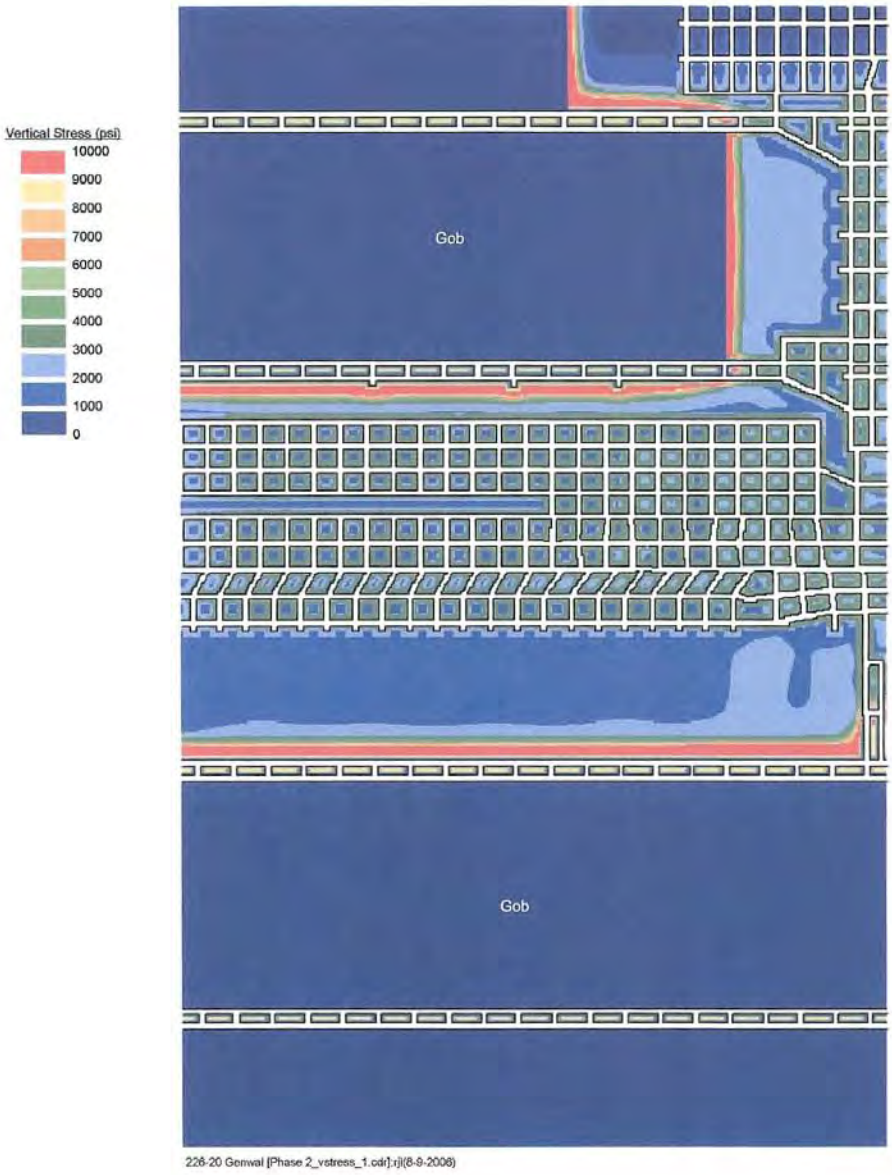

226-20 Genwal [Phase 2_vstress_1.cdr].rjl(8-9-2006)

AAI000140

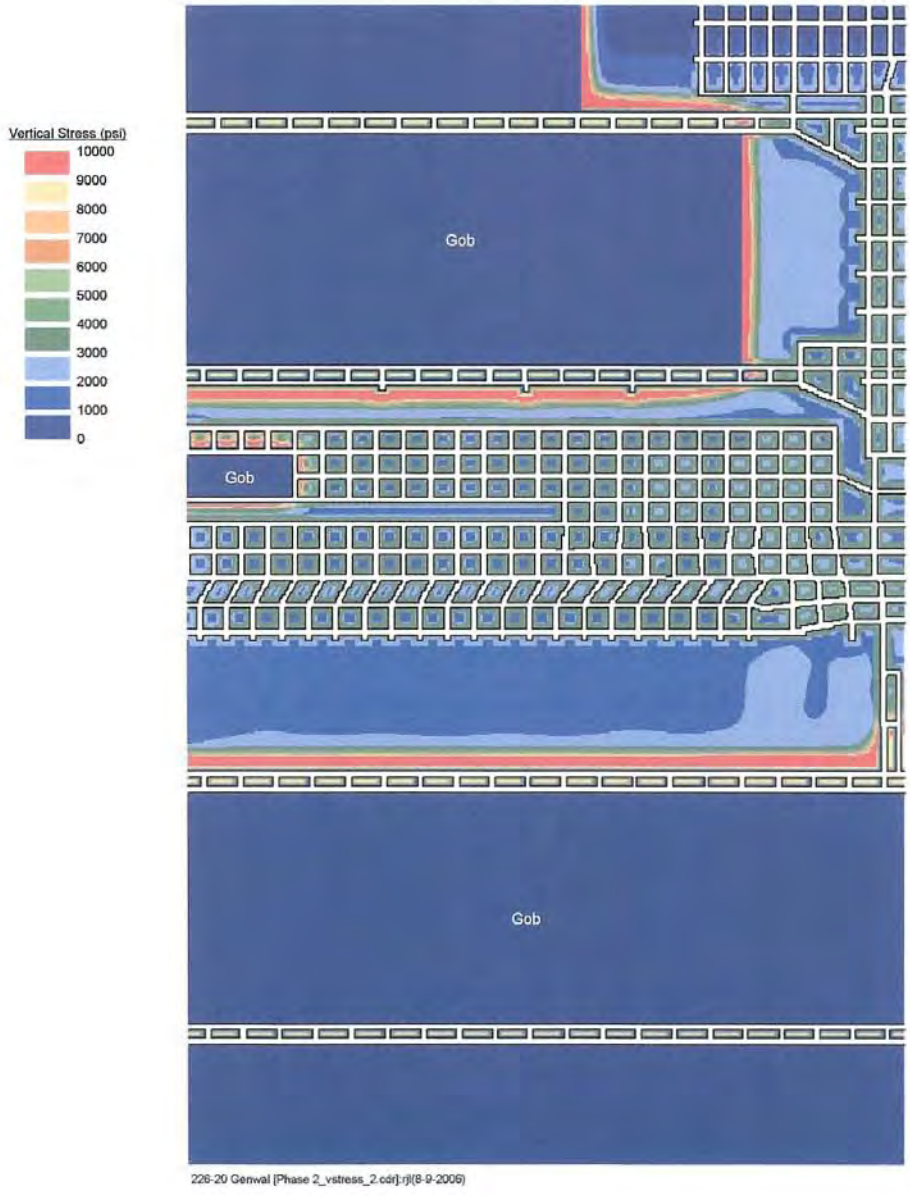
Vertical Stress (psi)
10000
9000
8000
7000
6000
5000
4000
3000
2000
1000
0
Gob
Gob
Gob
226-20 Genwal [Phase 2_vstress_2.cdr]:rj(8-9-2006)

AAI000141

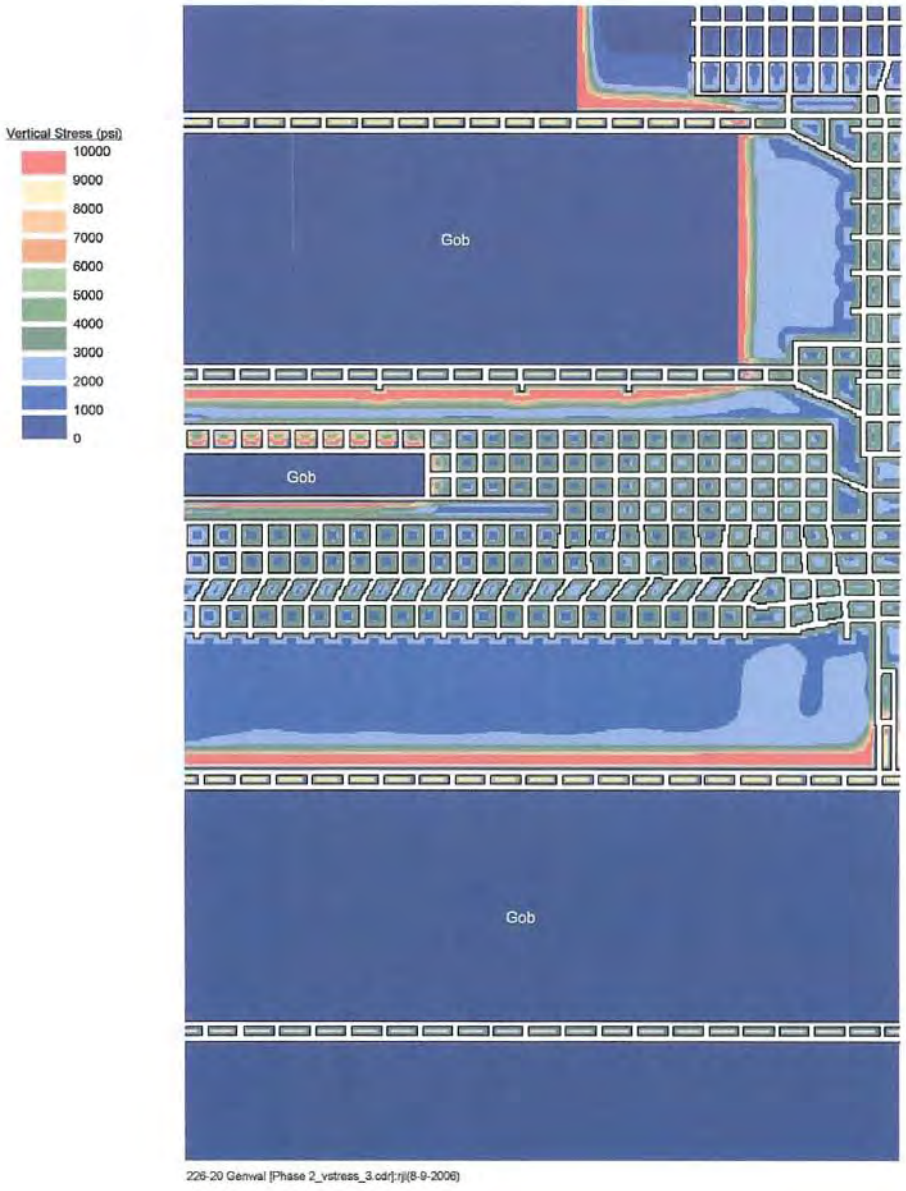
Vertical Stress (psi)
10000
9000
8000
7000
6000
5000
4000
3000
2000
1000
0
Gob
Gob
Gob
226-20 Genwal [Phase 2_vstress_3.cdr]:rji(8-9-2006)

AAI000142

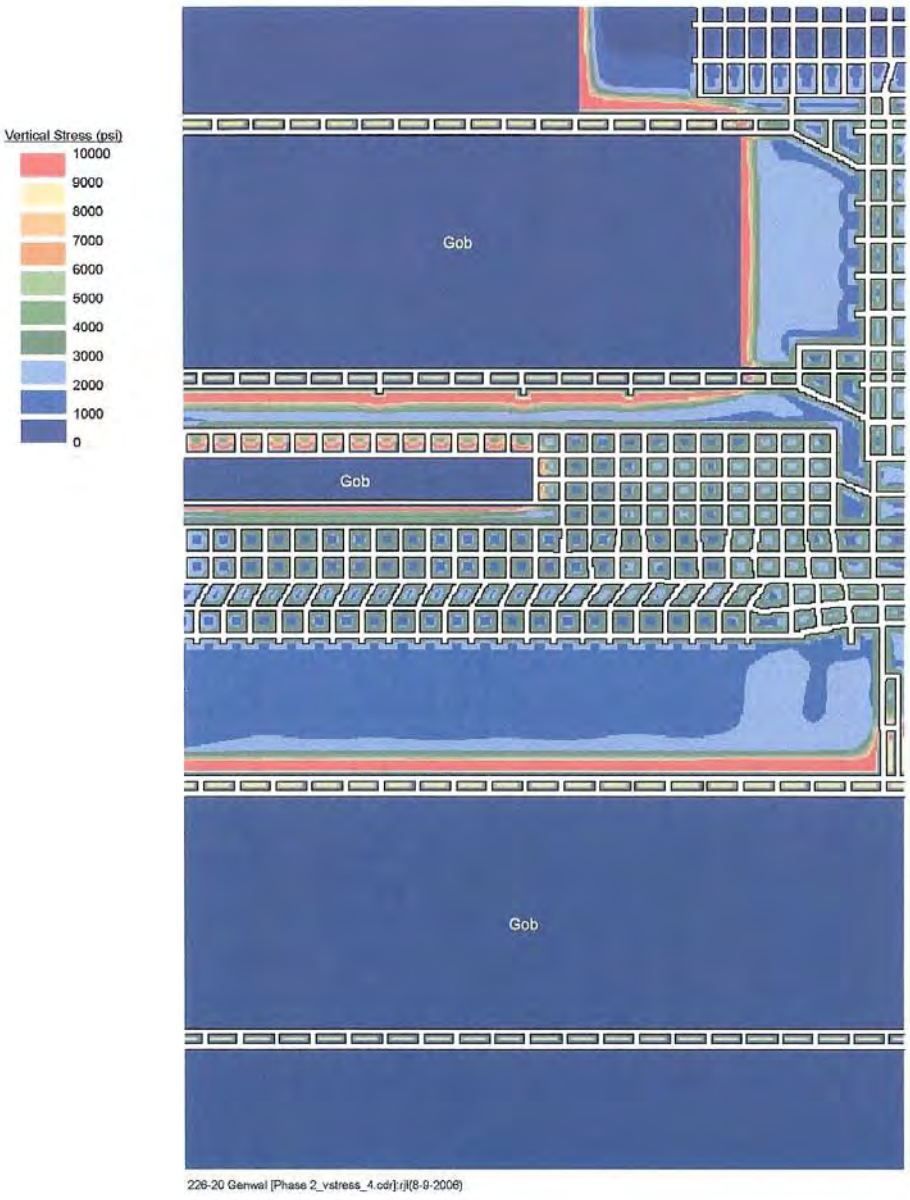
Vertical Stress (psi)
10000
9000
8000
7000
6000
5000
4000
3000
2000
1000
0
Gob
Gob
Gob
226-20 Genwal [Phase 2_vstress_4.cdr]:rjl(8-9-2006)

AAI000143

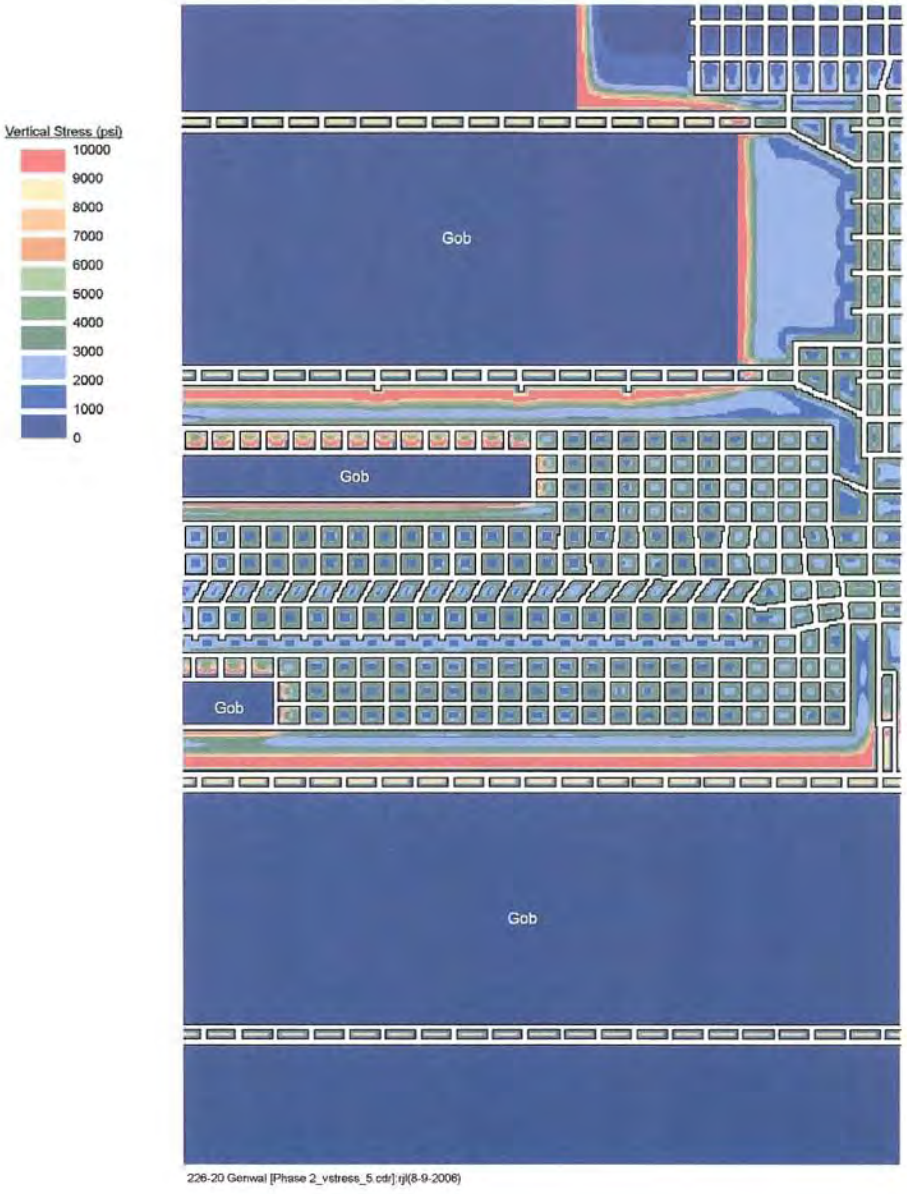
Vertical Stress (psi)
10000
9000
8000
7000
6000
5000
4000
3000
2000
1000
0
Gob
Gob
Gob
Gob
226-20 Genwal [Phase 2_vstress_5.cdr] rjl(8-9-2008)

AAI000144

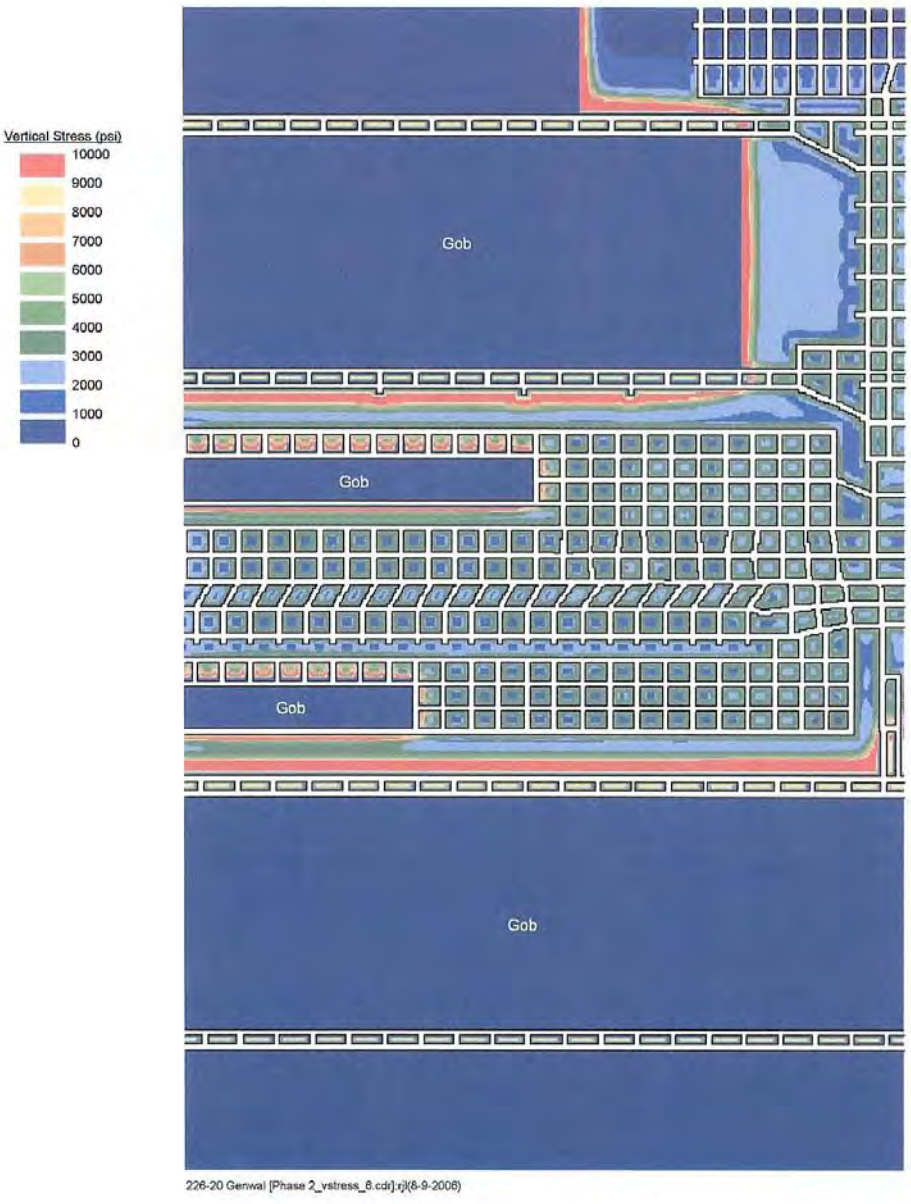
Vertical Stress (psi)
10000
9000
8000
7000
6000
5000
4000
3000
2000
1000
0
Gob
Gob
Gob
Gob
226-20 Genwal [Phase 2_vstress_6.cdr].rj(8-9-2006)

AAI000145

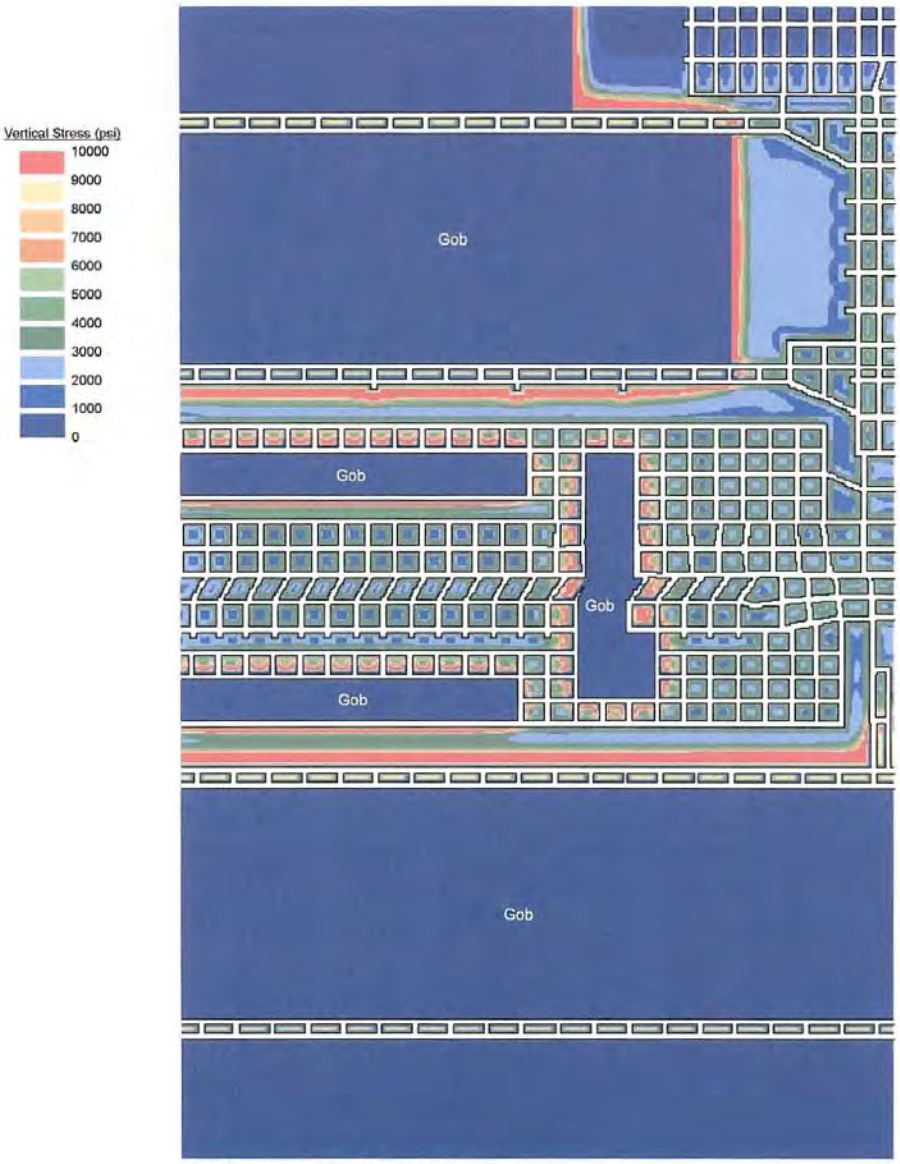
Vertical Stress (psi)
10000
9000
8000
7000
6000
5000
4000
3000
2000
1000
0
Gob
Gob
Gob
Gob
Gob
226-20 Genwal [Phase 2_vstress_7.cdr]:rji(8-9-2006)

AAI000146

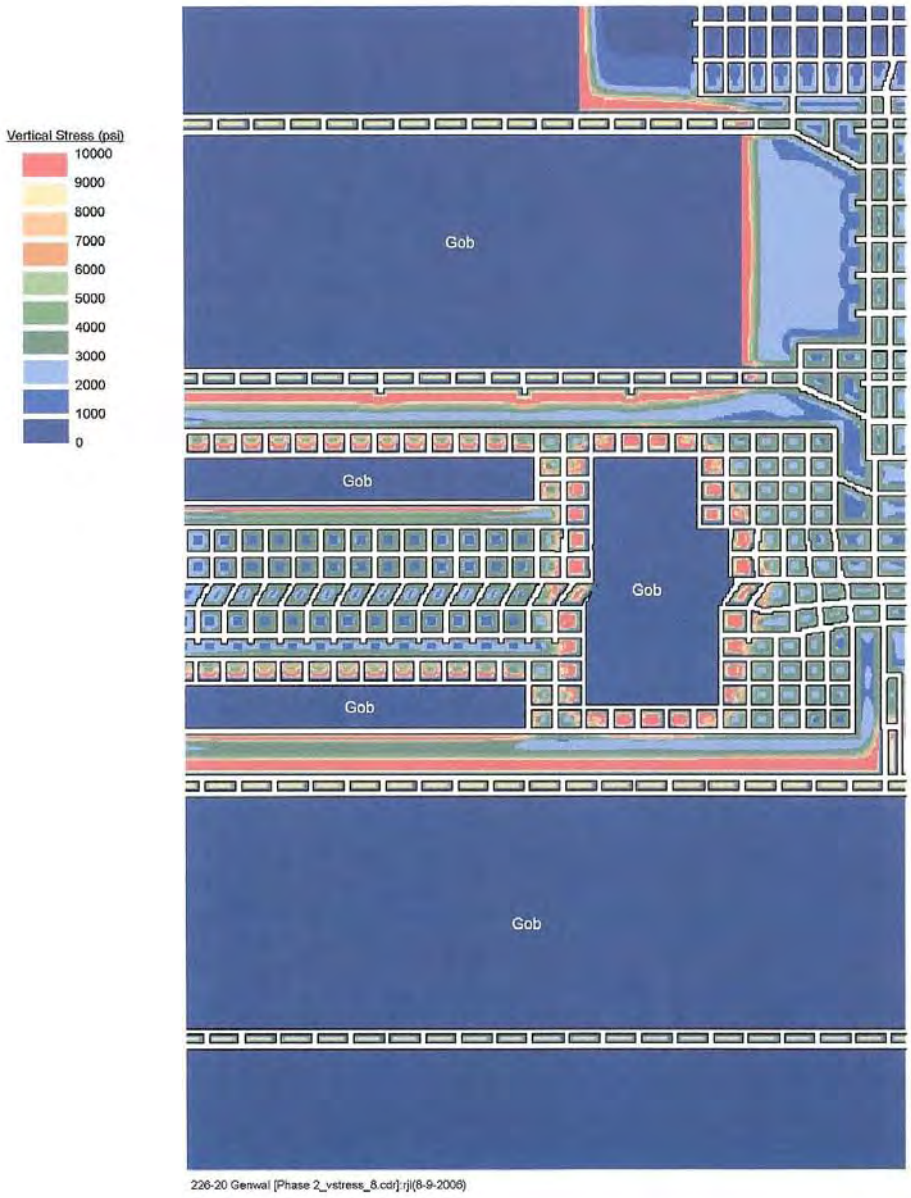
Vertical Stress (psi)
10000
9000
8000
7000
6000
5000
4000
3000
2000
1000
0
Gob
Gob
Gob
Gob
Gob
226-20 Genwal [Phase 2_vstress_8.cdr]:rjl(8-9-2006)

AAI000147

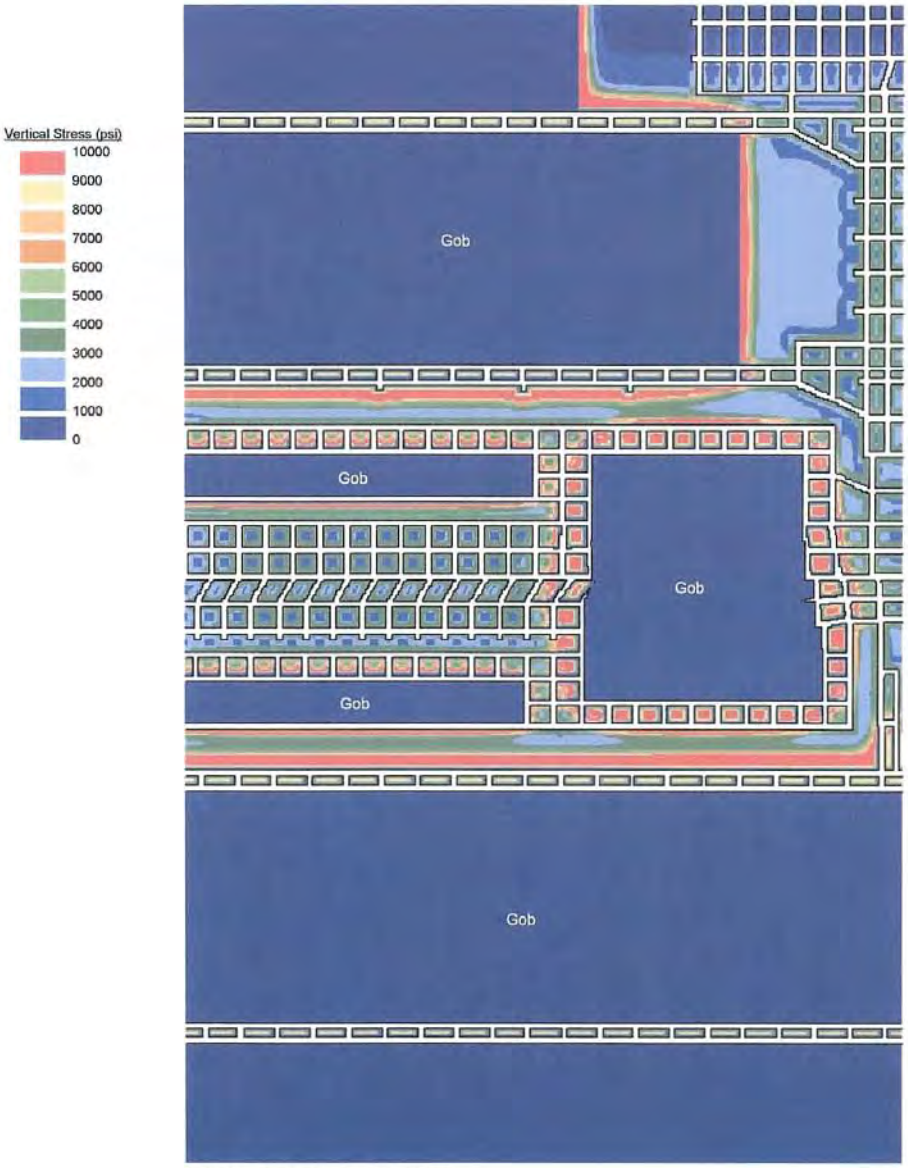
Vertical Stress (psi)
10000
9000
8000
7000
6000
5000
4000
3000
2000
1000
0
Gob
Gob
Gob
Gob
Gob
226-20 Genwal [Phase 2_vstress_9.cdr]:rjl(8-9-2006)

AAI000148

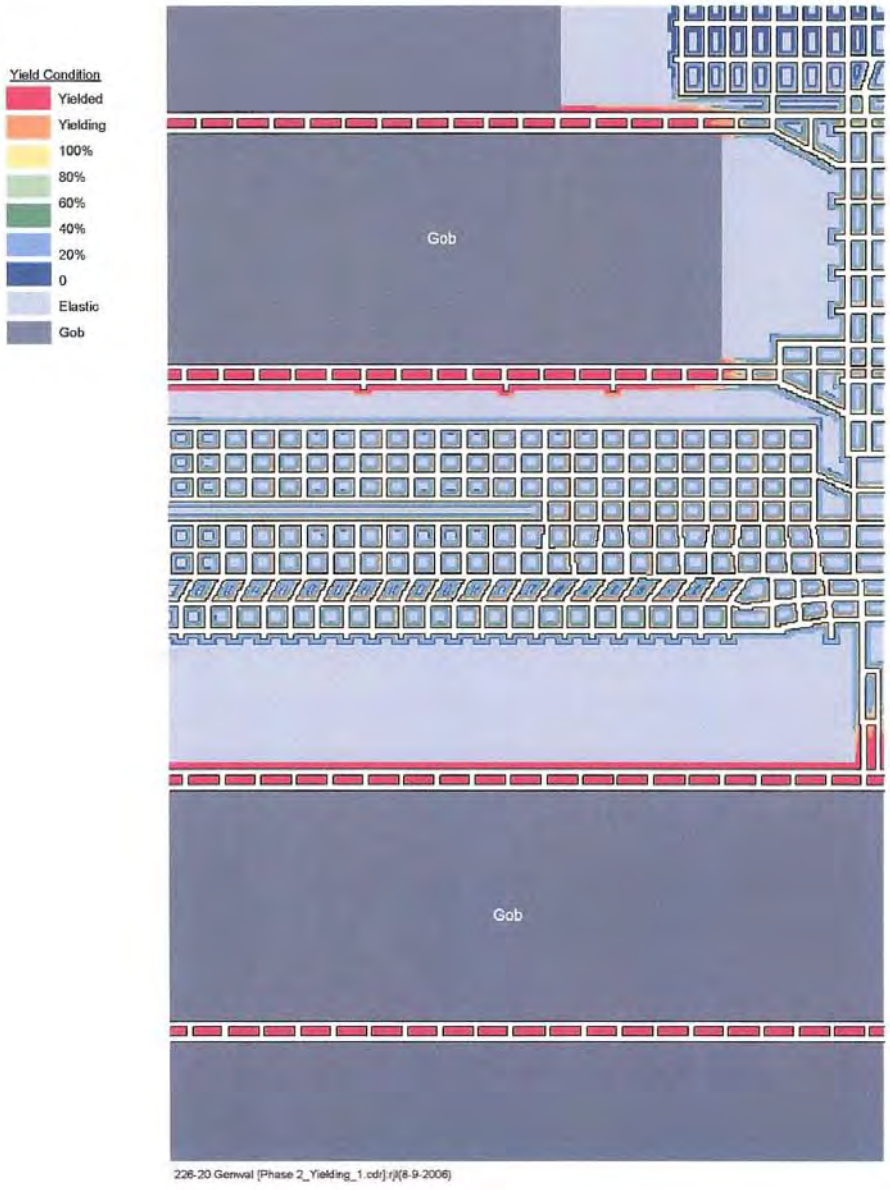
Yield Condition
Yielded
Yielding
100%
80%
60%
40%
20%
0
Elastic
Gob
Gob
Gob
226-20 Genwal [Phase 2_Yielding_1.cdr].rjl(8-9-2006)

AAI000149

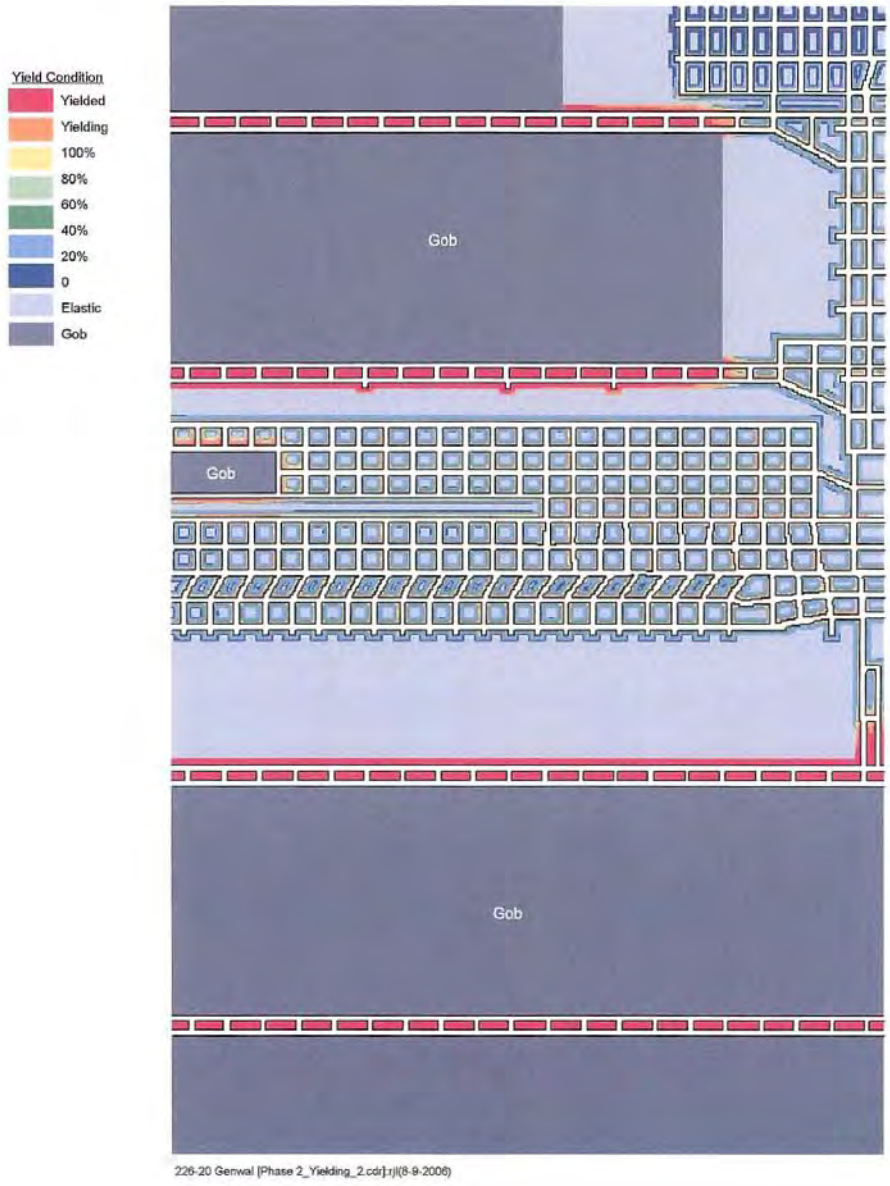
Yield Condition
Yielded
Yielding
100%
80%
60%
40%
20%
0
Elastic
Gob
Gob
Gob
Gob
226-20 Genwal [Phase 2_Yielding_2.cdr]:rjl(8-9-2006)

AAI000150

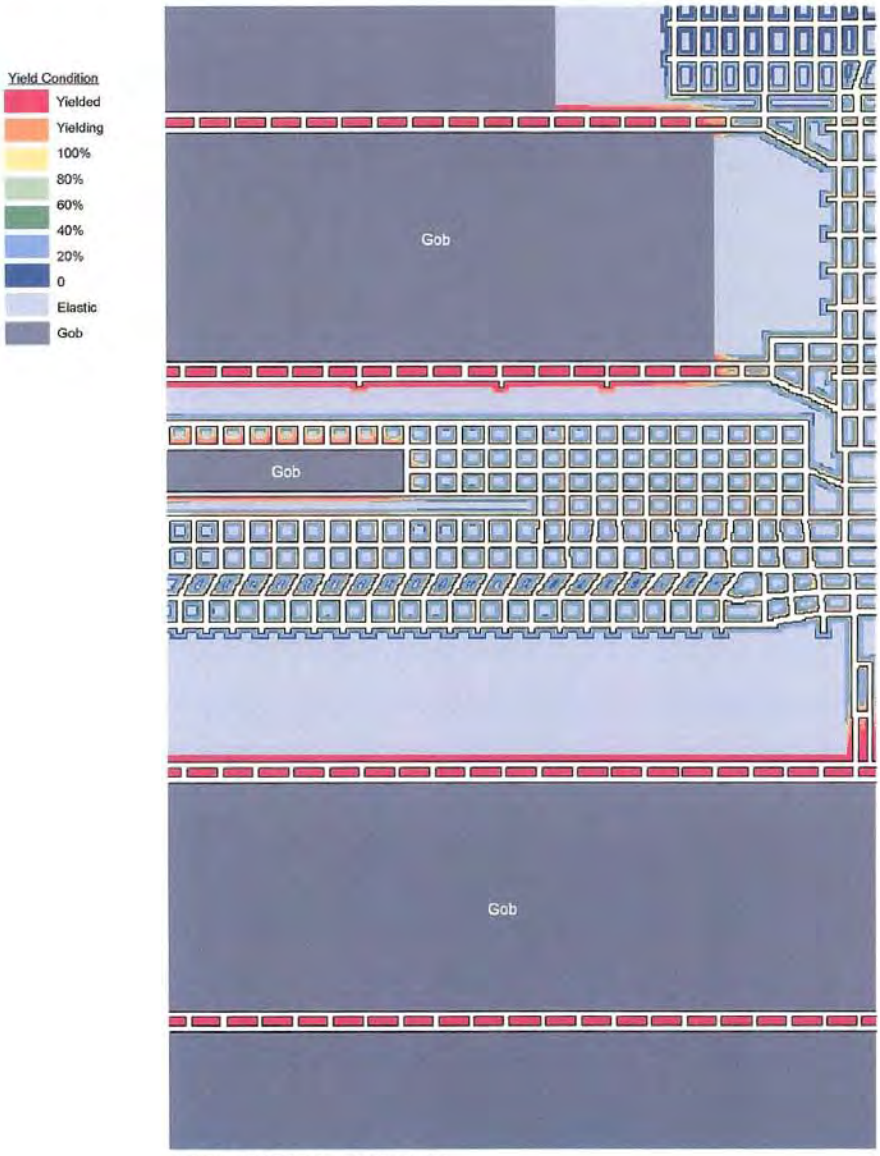
Yield Condition
Yielded
Yielding
100%
80%
60%
40%
20%
0
Elastic
Gob
Gob
Gob
Gob
228-20 Genwal [Phase 2_Yielding_3.cdr]:rjl(8-9-2006)

AAI000151

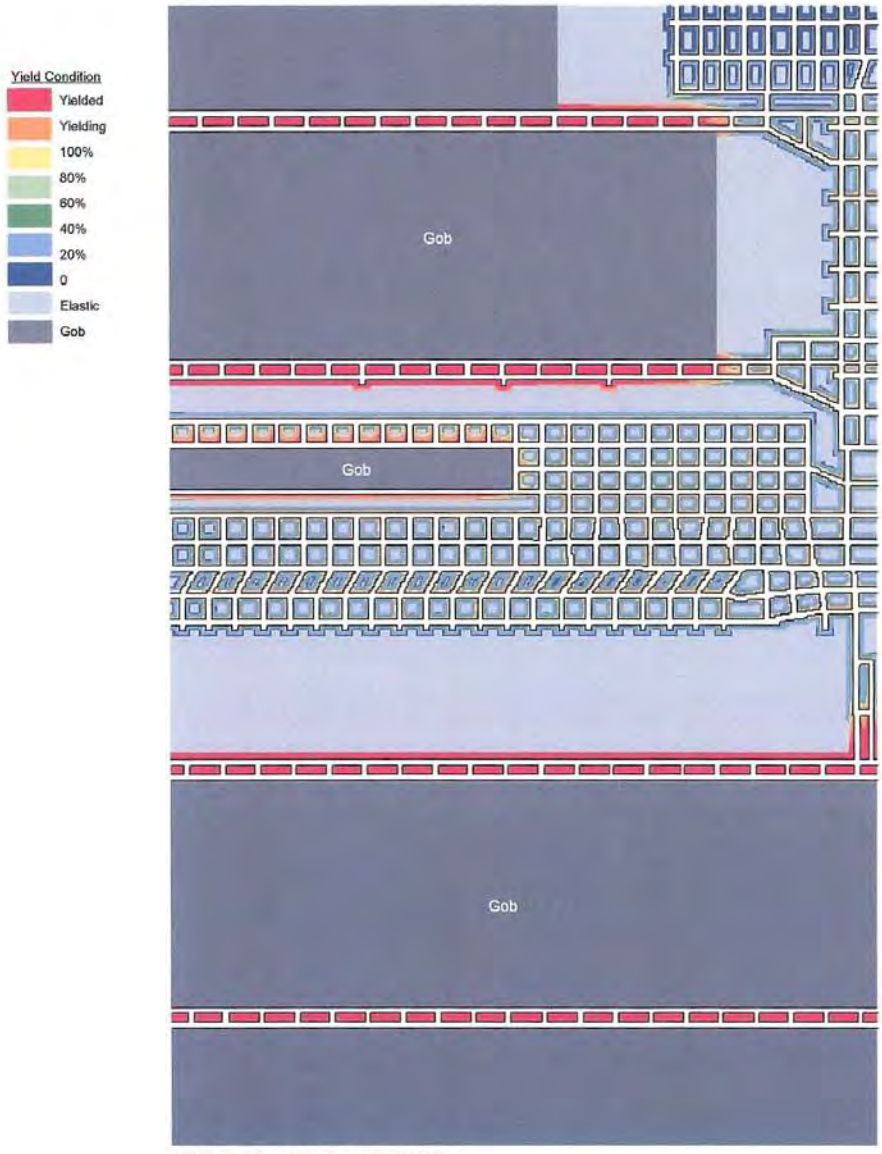

226-20 Genwal [Phase 2_Yielding_4.cdr].rjl(8-9-2006)

AAI000152

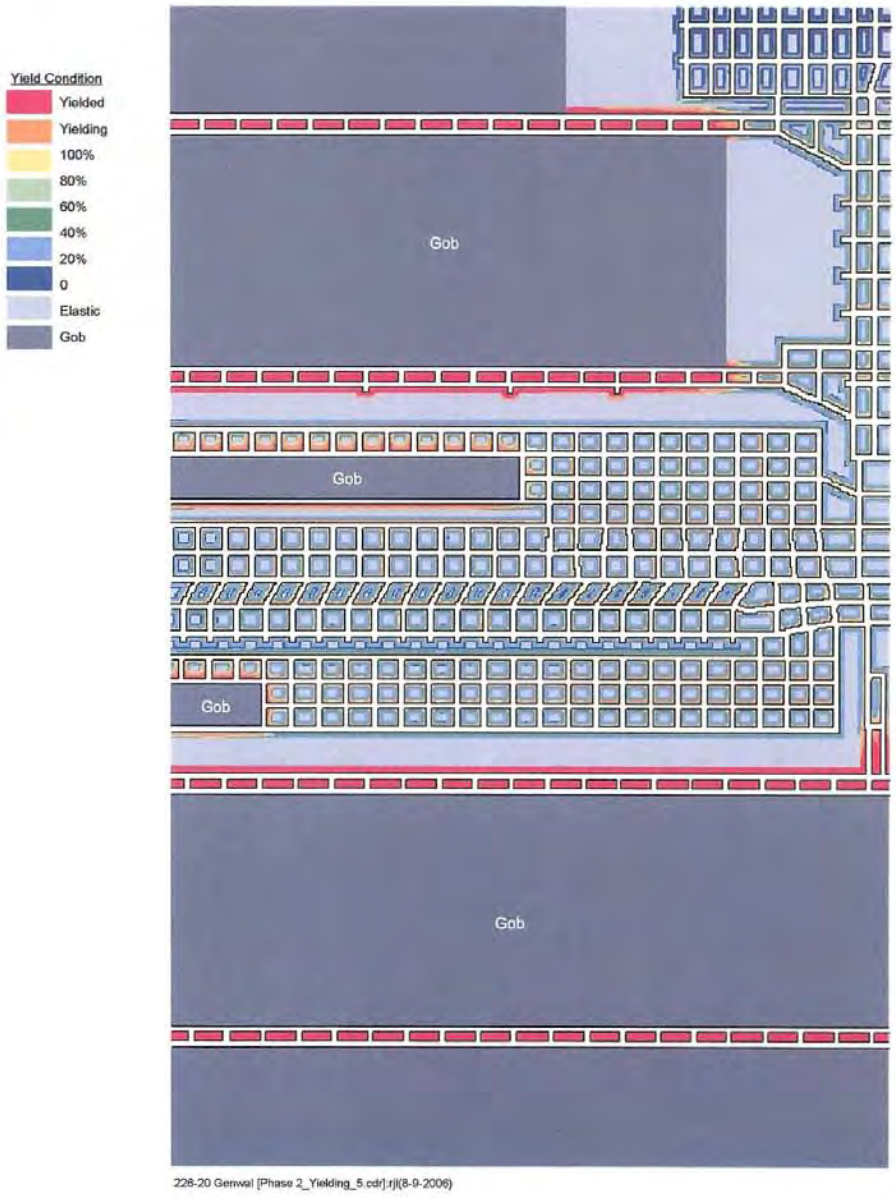
Yield Condition
Yielded
Yielding
100%
80%
60%
40%
20%
0
Elastic
Gob
Gob
Gob
Gob
228-20 Genwal [Phase 2_Yielding_5.cdr].rjl(8-9-2006)

AAI000153

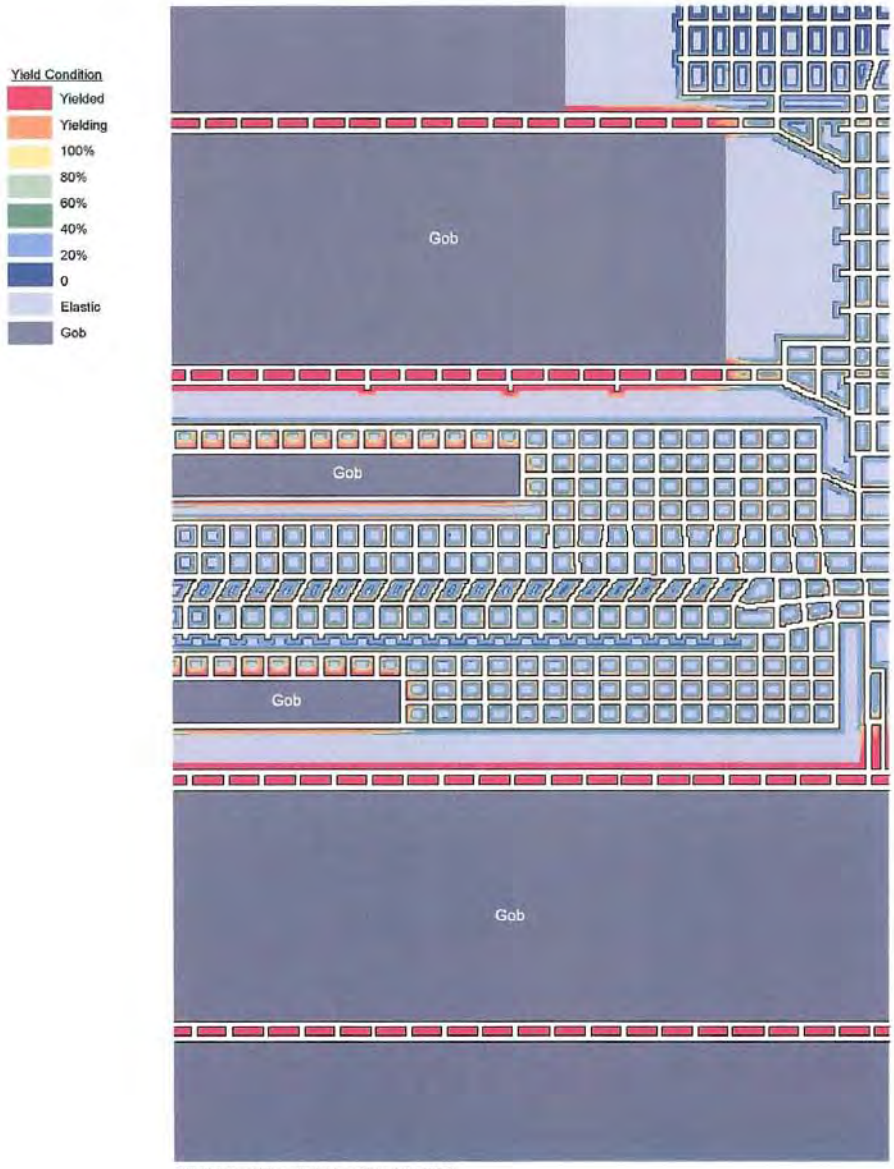
Yield Condition
Yielded
Yielding
100%
80%
60%
40%
20%
0
Elastic
Gob
Gob
Gob
Gob
226-20 Genwal [Phase 2_Yielding_8.cdr].rjl(8-9-2006)

AAI000154

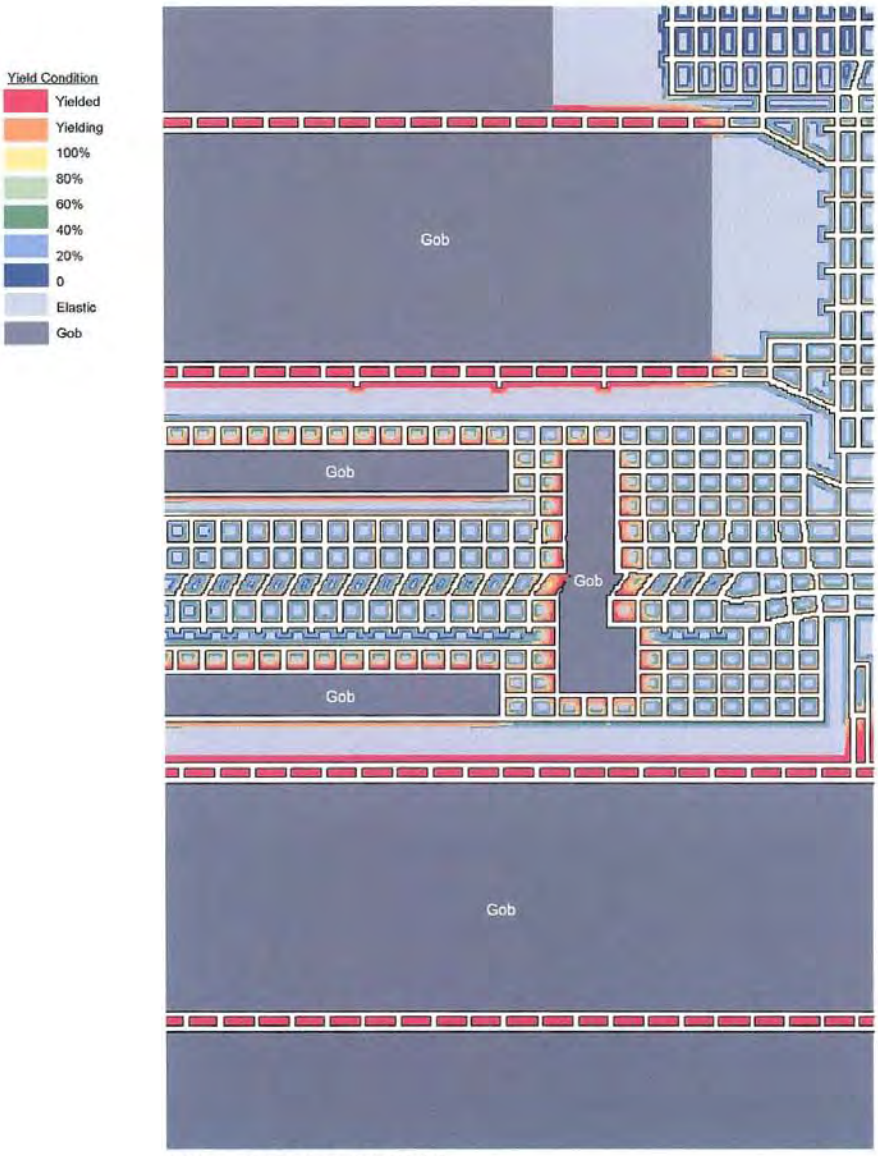
Yield Condition
Yielded
Yielding
100%
80%
60%
40%
20%
0
Elastic
Gob
Gob
Gob
Gob
Gob
226-20 Genwal [Phase 2_Yielding_7.cdr]:rjl(8-9-2006)

AAI000155

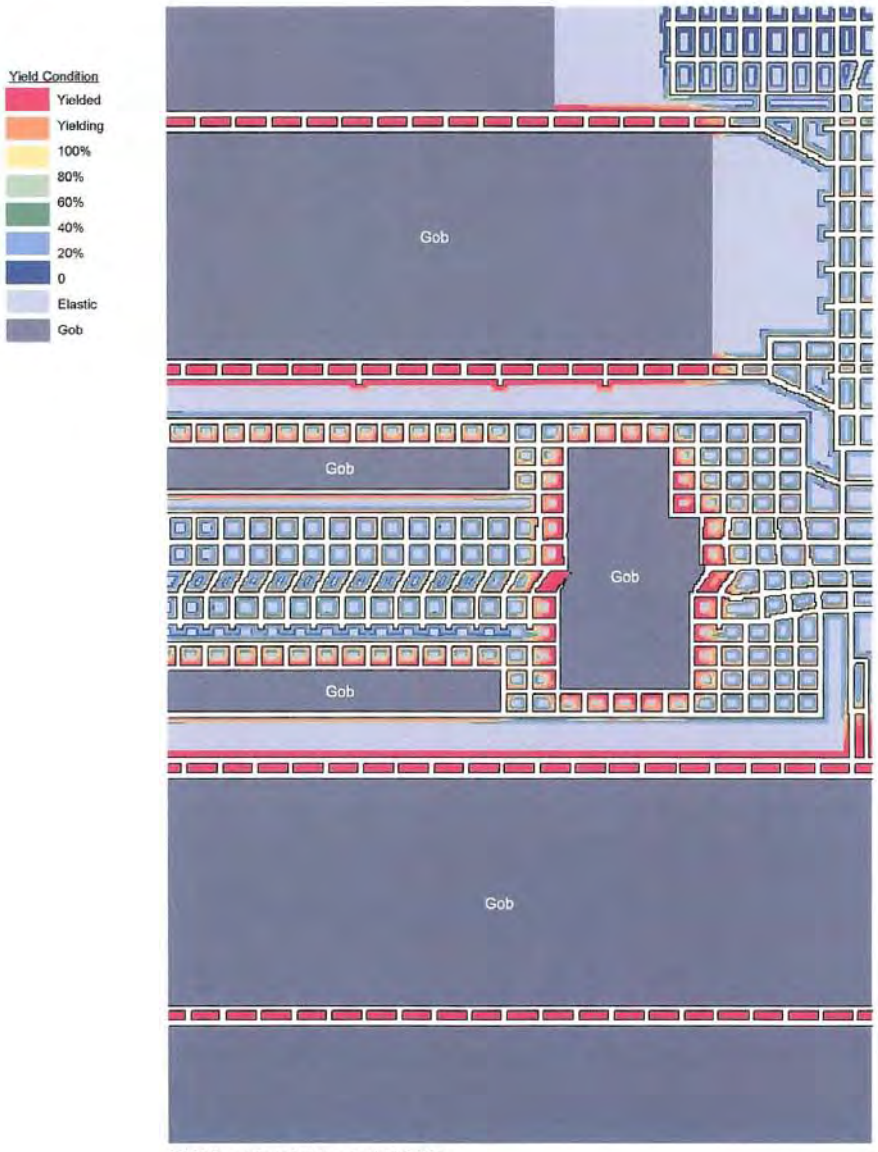
Yield Condition
Yielded
Yielding
100%
80%
60%
40%
20%
0
Elastic
Gob
Gob
Gob
Gob
Gob
226-20 Genwal [Phase 2_Yielding_6.cdr]:rji(8-9-2006)

AAI000156

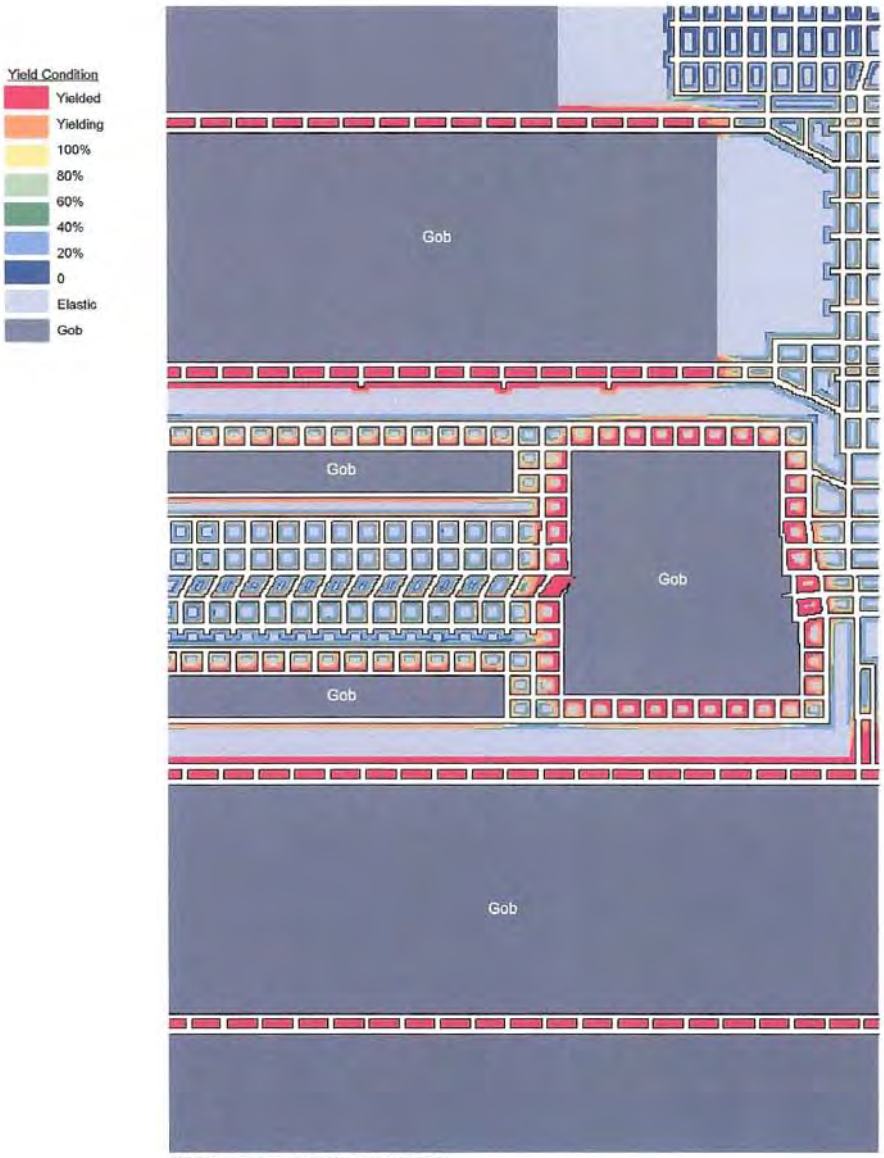
Yield Condition
Yielded
Yielding
100%
80%
60%
40%
20%
0
Elastic
Gob
Gob
Gob
Gob
Gob
226-20 Genwal [Phase 2_Yielding_9.cdr]:rjl(8-9-2006)

AAI000157

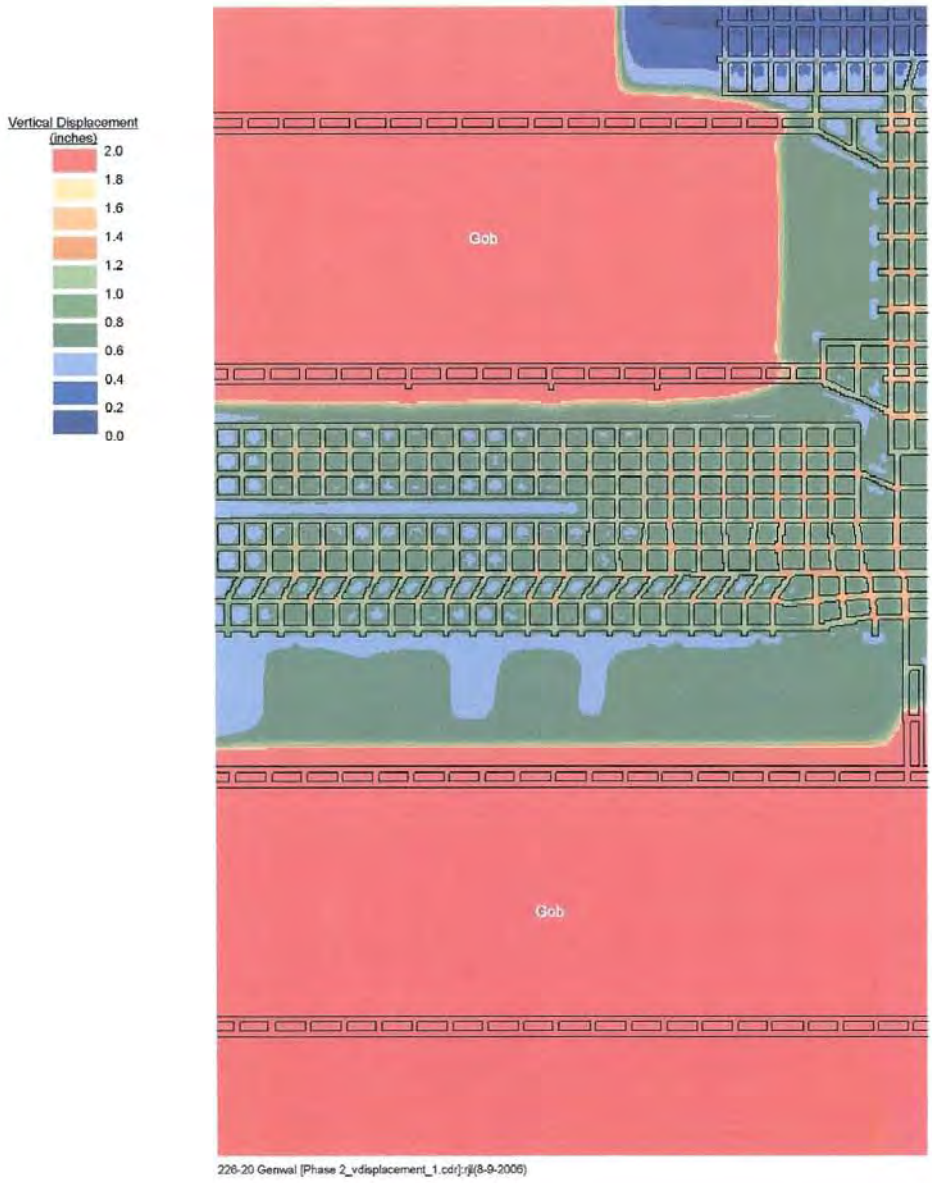
Vertical Displacement (inches)
2.0
1.8
1.6
1.4
1.2
1.0
0.8
0.6
0.4
0.2
0.0
Gob
Gob
226-20 Genwal [Phase 2_vdisplacement_1.cdr]:rjl(8-9-2006)

AAI000158

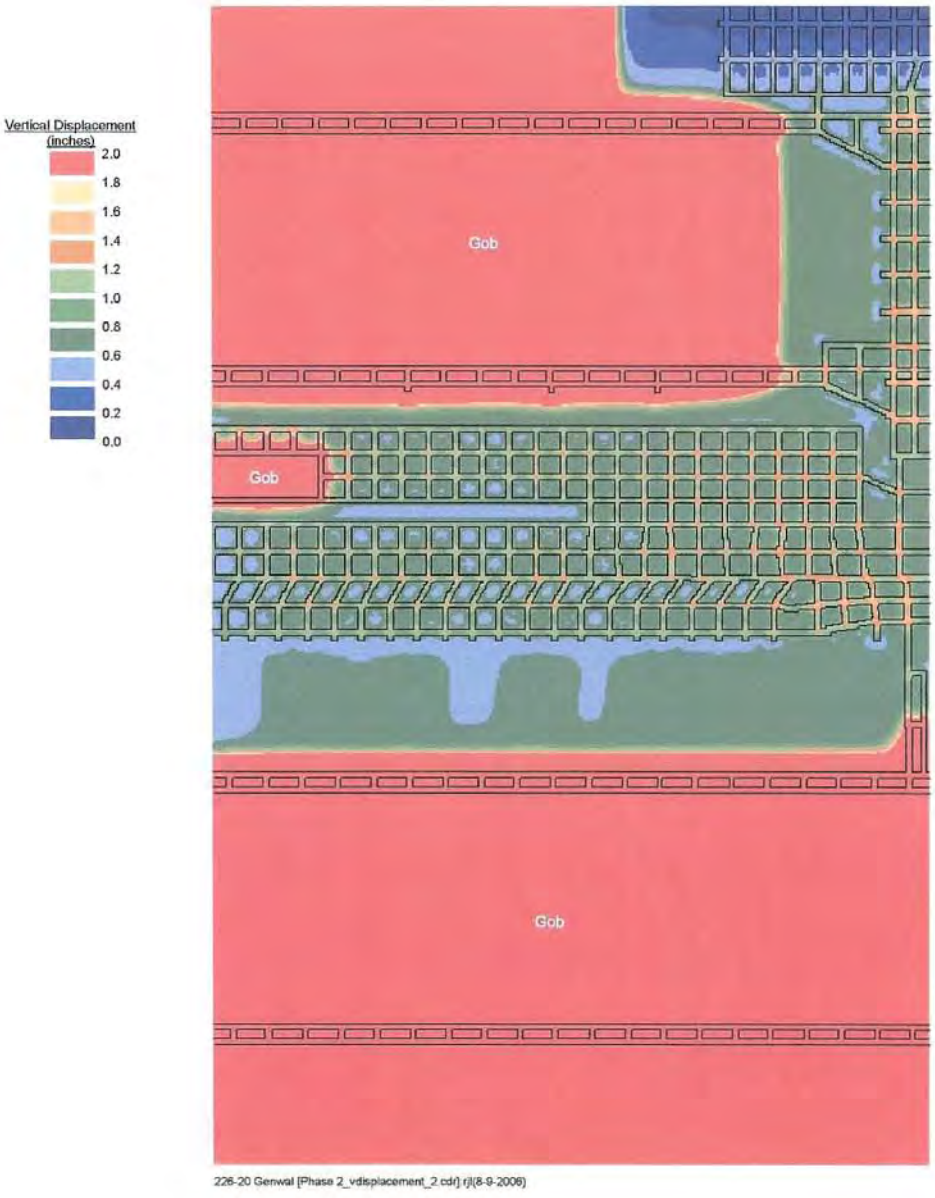
Vertical Displacement (inches)
2.0
1.8
1.6
1.4
1.2
1.0
0.8
0.6
0.4
0.2
0.0
Gob
Gob
Gob
226-20 Genwal [Phase 2_vdisplacement_2.cdr] rjl(8-9-2006)

AAI000159

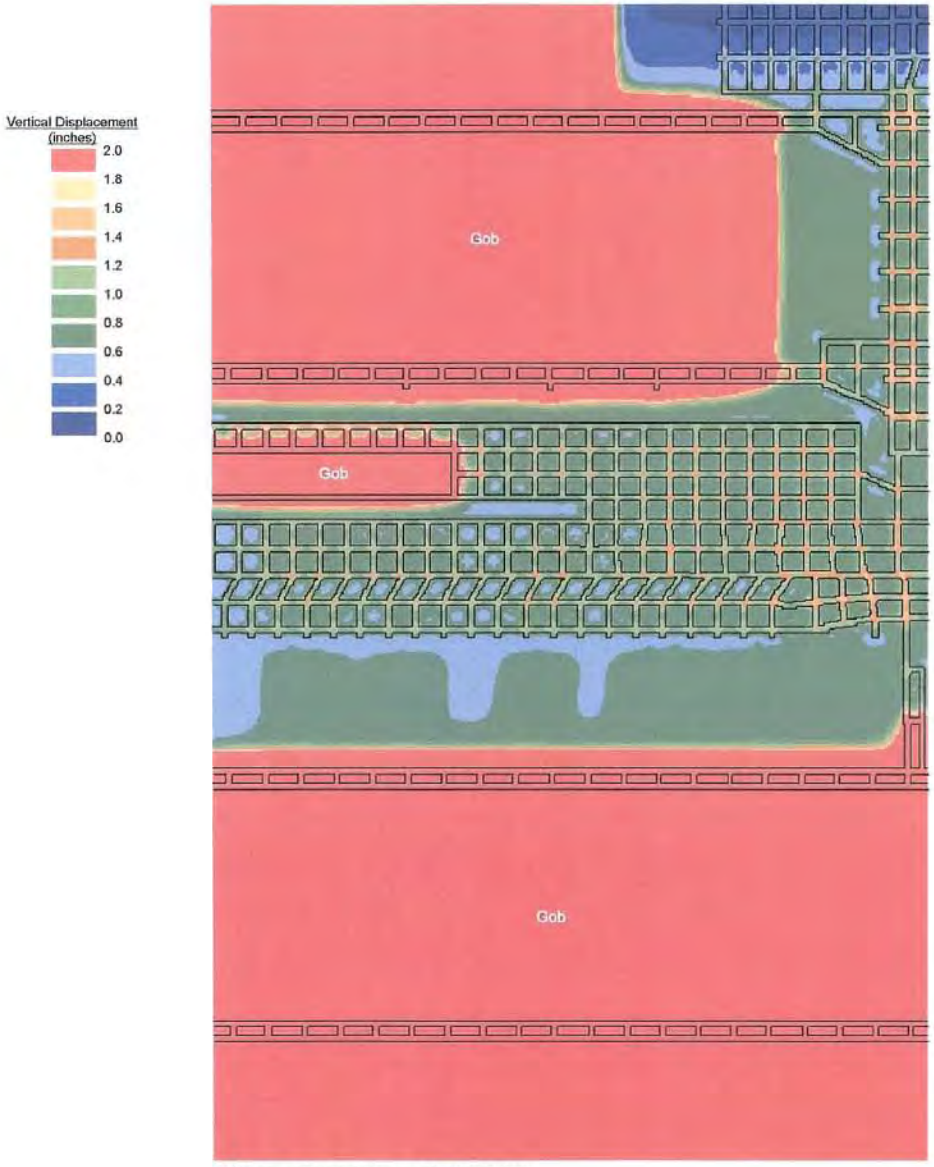
Vertical Displacement
(inches)
2.0
1.8
1.6
1.4
1.2
1.0
0.8
0.6
0.4
0.2
0.0
Gob
Gob
Gob
226-20 Genwal [Phase 2_vdisplacement_3.cdr].rjl(8-9-2006)

AAI000160

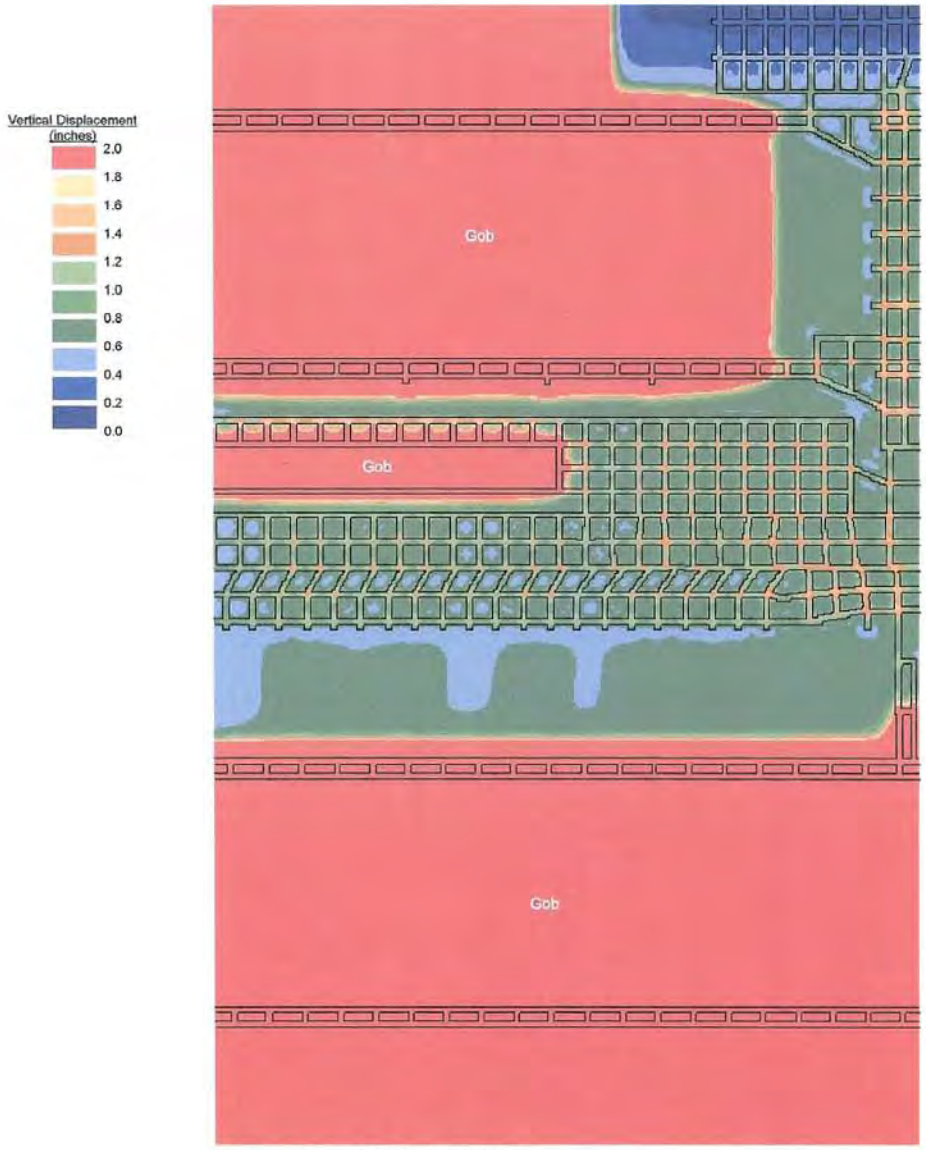

226-20 Genwal [Phase 2_vdisplacement_4.cdr]:rjl(8-9-2006)

AAI000161

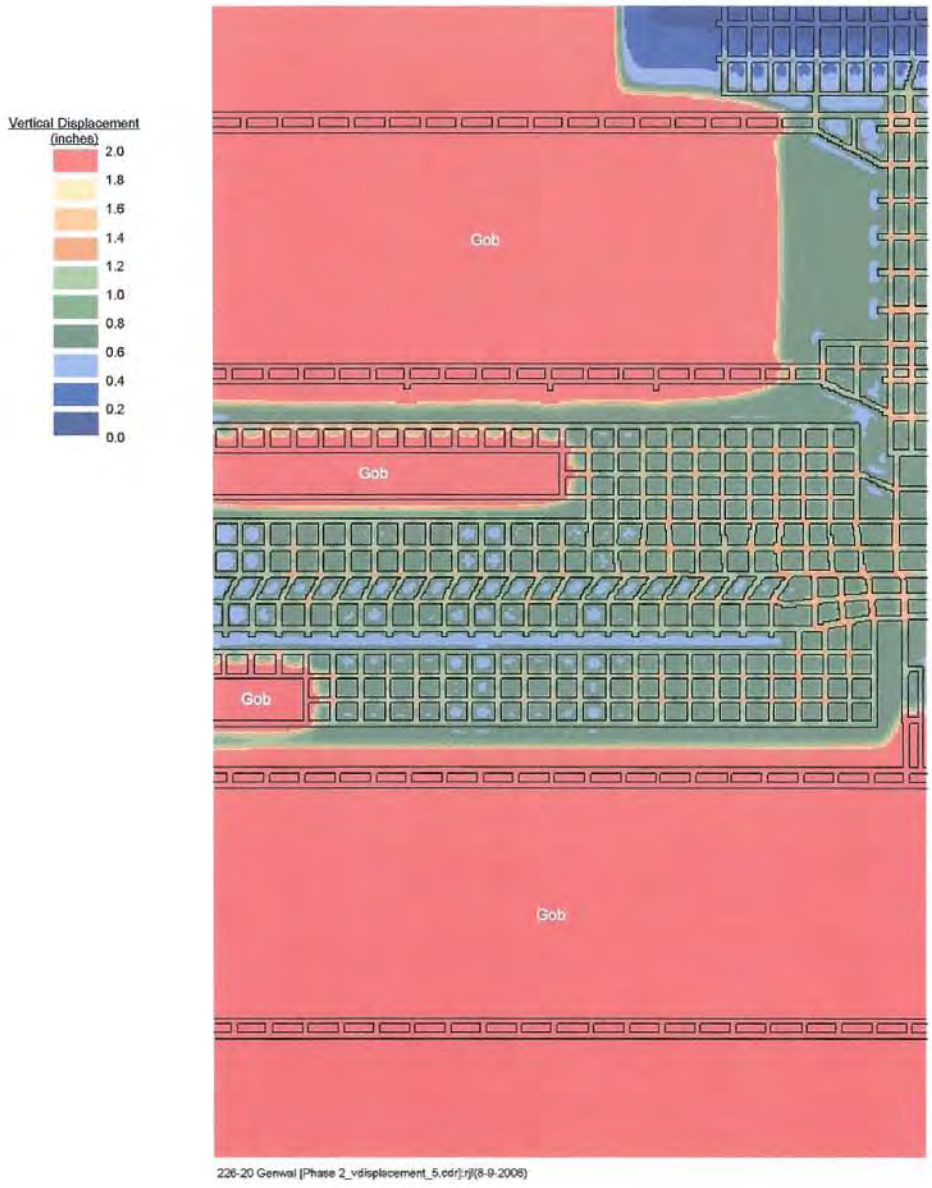
Vertical Displacement (inches)
2.0
1.8
1.6
1.4
1.2
1.0
0.8
0.6
0.4
0.2
0.0
Gob
Gob
Gob
Gob
226-20 Genwal [Phase 2_vdisplacement_5.cdr]:rjl(8-9-2006)

AAI000162

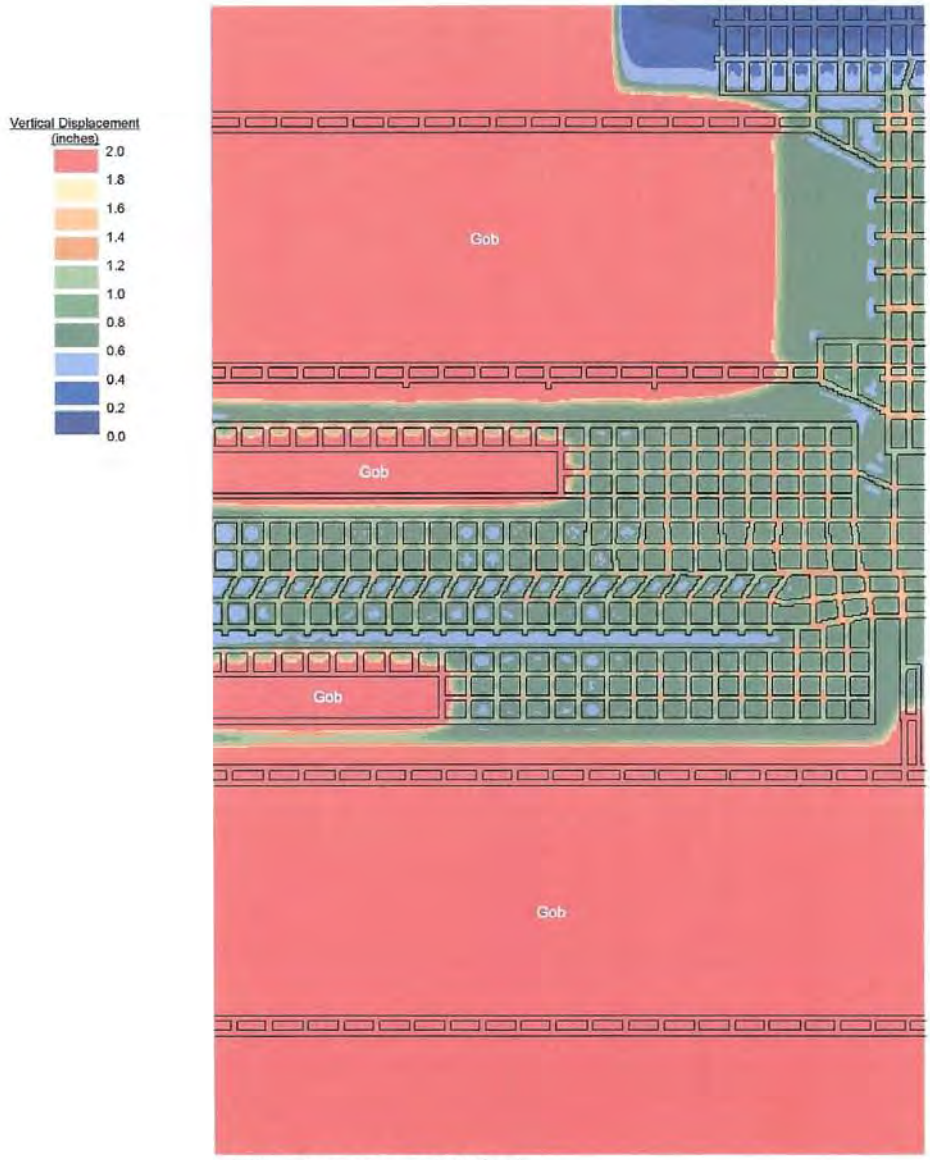
Vertical Displacement (inches)
2.0
1.8
1.6
1.4
1.2
1.0
0.8
0.6
0.4
0.2
0.0
Gob
Gob
Gob
Gob
228-20 Genwal [Phase 2_vdisplacement_6.cdr] rjl(8-9-2006)

AAI000163

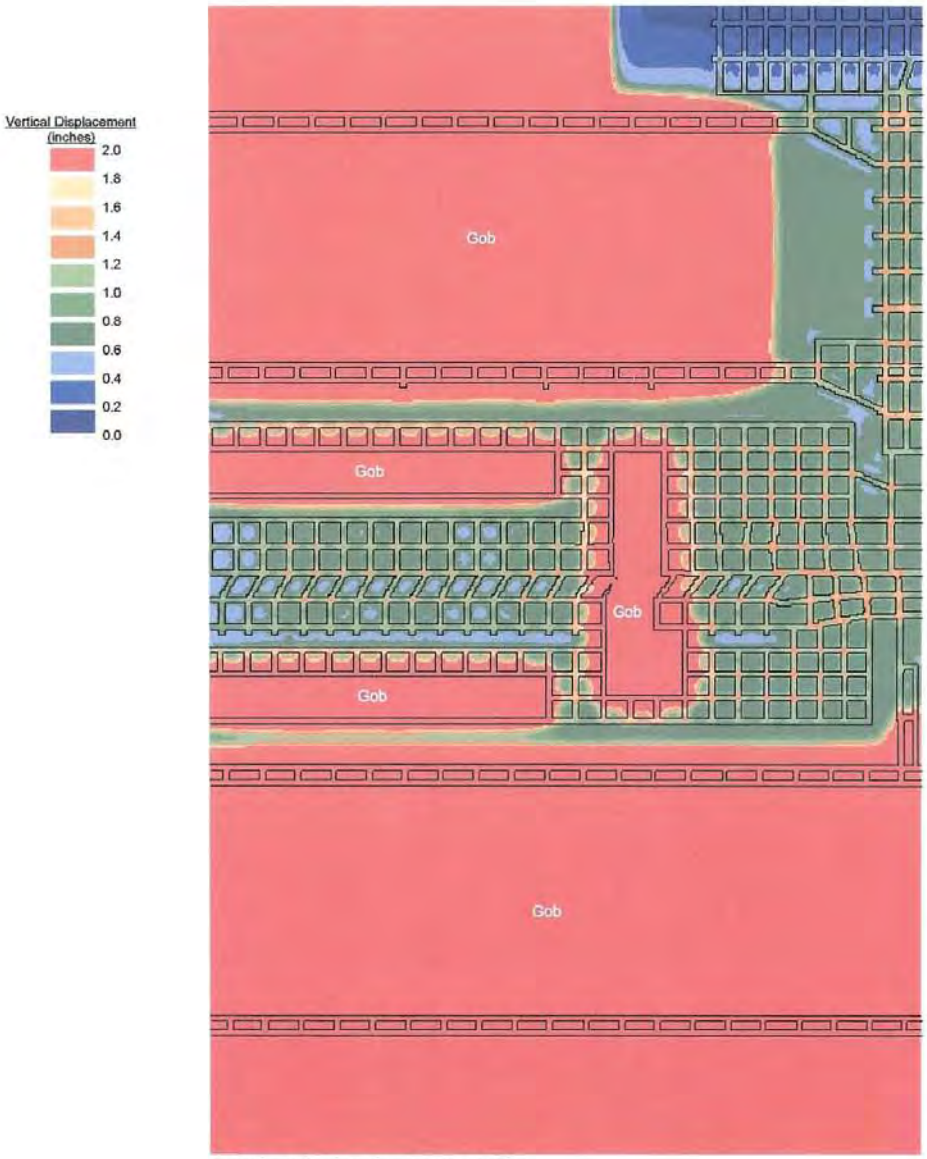
Vertical Displacement (inches)
2.0
1.8
1.6
1.4
1.2
1.0
0.8
0.6
0.4
0.2
0.0
Gob
Gob
Gob
Gob
Gob
226-20 Genwal [Phase 2_vdisplacement_7.cdr].rjl(8-9-2006)

AAI000164

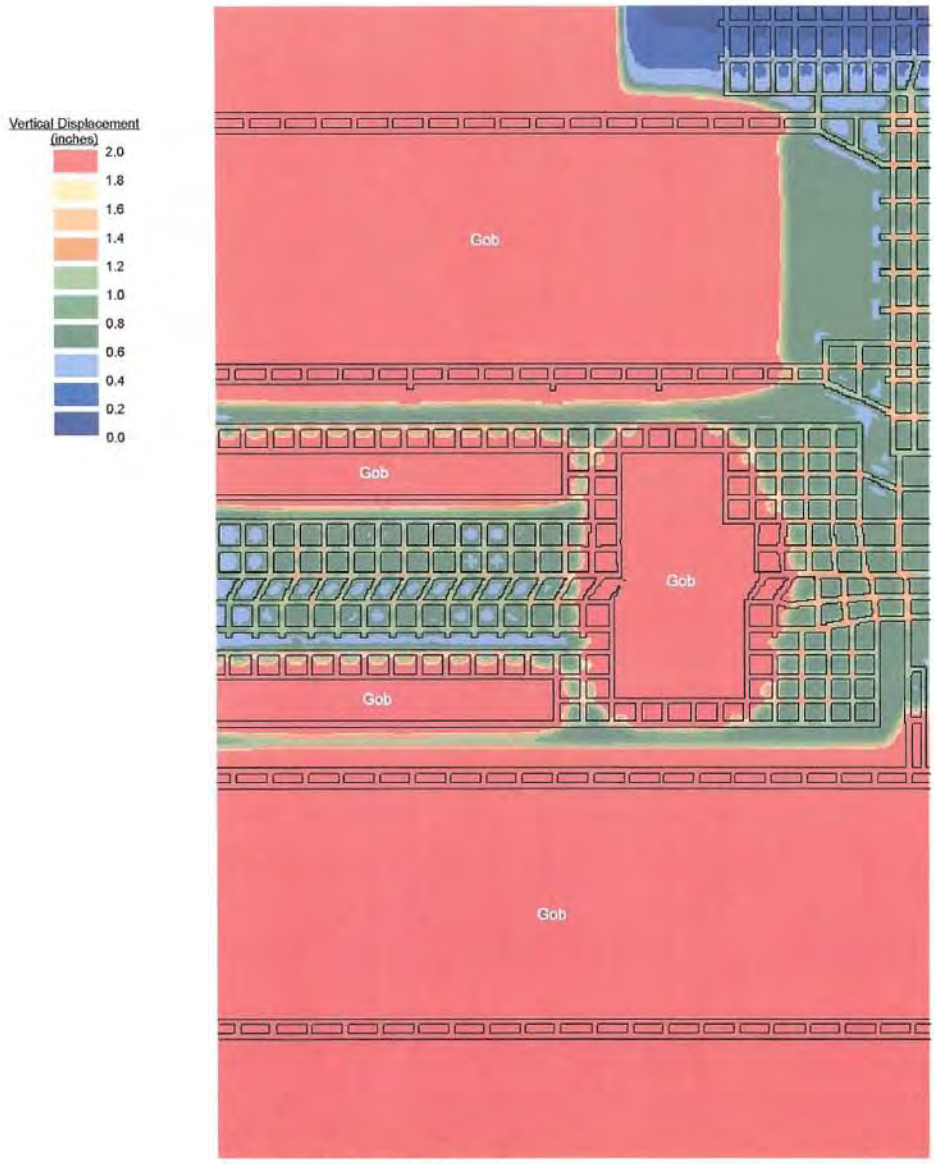
Vertical Displacement
(inches)
2.0
1.8
1.6
1.4
1.2
1.0
0.8
0.6
0.4
0.2
0.0
Gob
Gob
Gob
Gob
Gob
226-20 Genwal [Phase 2_vdisplacement_8.cdr]:rj(8-9-2006)

AAI000165

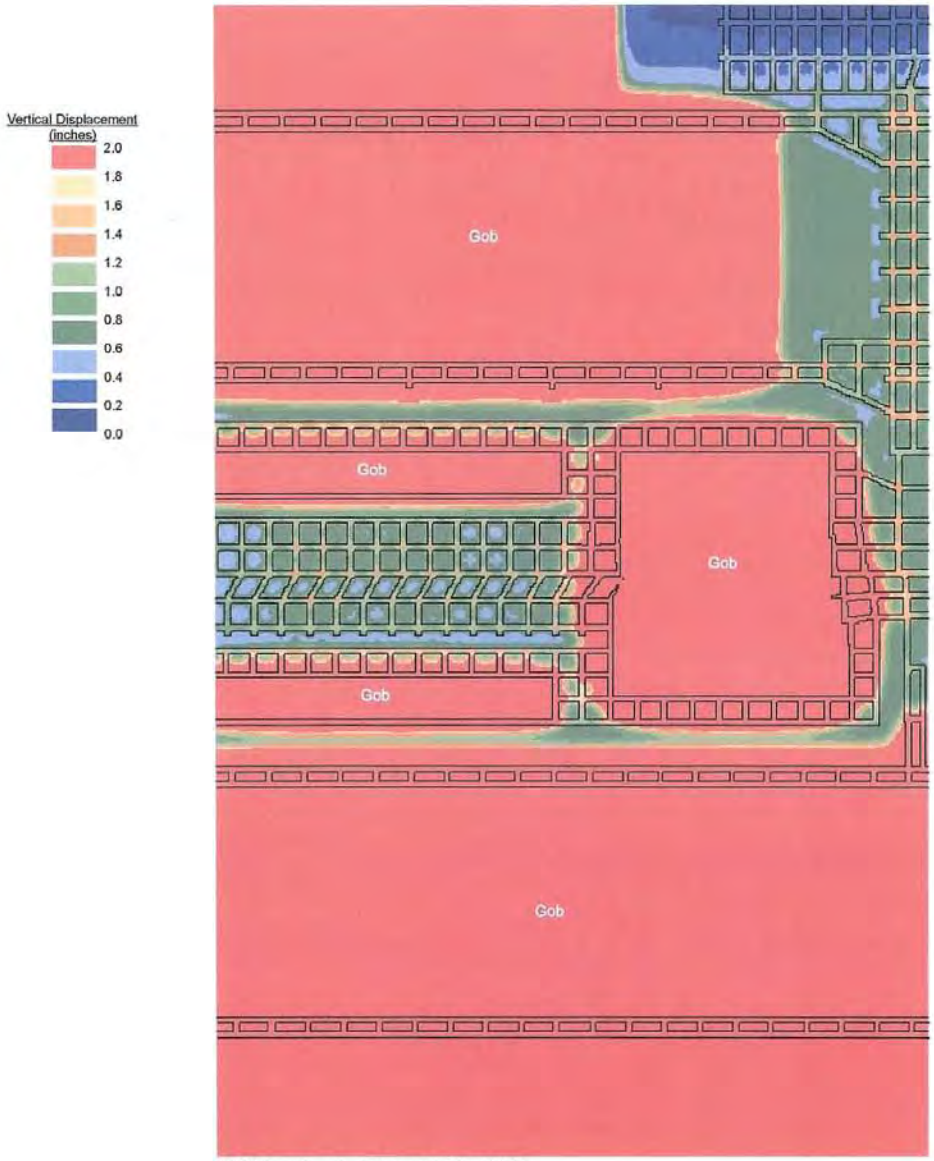

226-20 Genwal [Phase 2_vdisplacement_9.cdr] rjl(8-9-2006)

AAI000166

226-20 GENWAL Crandall Canyon Mine Trip Report 12-1-2006.pdf klg 9-22-07

AGAPITO ASSOCIATES, INC.
Mining & Civil Engineers & Geologists

715 HORIZON DRIVE
SUITE 340
GRAND JUNCTION, CO 81506
USA
VOICE 970.242.4220
www.agapito.com

GOLDEN OFFICE
303.271.3750

CHICAGO OFFICE
630.792.1520

December 8, 2006 226-20

Mr. Laine Adair
GENWAL Resources, Inc.
195 North 100 West
P. O. Box 1420
Huntington, UT 84528

Re: **Crandall Canyon Mine Ground Condition Review for Mining in the Main West North Barrier**

Dear Laine,

On December 1, 2006, Agapito Associates, Inc. (AAI), personnel, Michael Hardy, Gary Skaggs, and Bo Yu visited Crandall Canyon Mine to review the ground conditions of the room-and-pillar mining in the north barrier pillar along Main West. AAI personnel were escorted by Laine Adair.

Current plans in Main West include developing four entries in the north barrier west of the 1st Right Submains under cover ranging from approximately 1,300 ft to 2,200 ft. The mine plans were previously evaluated by AAI,[1,2] and the proposed mine plan with 60-ft by 72-ft (rib-to-rib) pillars was judged to be adequate for short-term recovery mining in the barriers.

At the time of our visit, four entries with 60-ft by 72-ft (rib-to-rib) pillars were developed in the Main West north barrier to Crosscut 123, where the depth of cover was almost 2,000 ft (See Figure 1). Entry widths were cut at 17 ft and were about 20 ft wide at pillar mid-height. Roof support included systematic bolting and rib-to-rib meshing. To the north and south of the mining area, 130-ft and 60-ft barriers were left, respectively, for the purpose of protection.

Good to excellent ground conditions were observed at all locations visited. Stable roof, floor, and ribs with only minor rib sloughage were observed in the recently mined areas in the

[1] Agapito Associates, Inc. (2006), "DRAFT—GEWNALL Crandall Canyon Mine Main West Barrier Mining Evaluation," prepared for Andalex Resources, Inc., July 20.
[2] Agapito Associates, Inc. (2006), "(226-30) GENWAL Main West Retreat Analysis—Preliminary Results," E-mail from Leo Gilbride to Laine Adair, August 9.

West Main barrier. Photo 1 shows only minor rib sloughing at Crosscut 123 in the entry immediately north of the West Mains. Photo 2 shows the second entry below longwall Panel 12 with minor sloughing at the rib between Crosscut 122 and Crosscut 121. The conditions of ribs along the north remnant barriers were good and consistent as shown in Photo 3. The rib was mildly yielded, but showed no evidence of blowouts, indicating that the 130-ft-wide remnant barrier pillar is wide enough to accommodate the load transfer from Panel 12 for short-term mining. The abutment load is expected to have alleviated since the time that Panel 12 was retreated in 1999 due to ground settlement and subsidence.

In summary, current ground conditions in Main West agree with our previous analysis. Roof, floor, and rib conditions were consistent with analytical predictions. There was no indication of problematic pillar yielding or roof problems that might indicate higher-than-predicted abutment loads. Conditions should continue to be carefully observed as mining progresses to the west under deeper cover.

We appreciate the opportunity to visit this area and directly observe ground conditions in the West Mains barrier. Please contact us if you have any questions.

Sincerely,

Michael Hardy
Principal
mhardy@agapito.com

BY:MPH/smvf

Attachments(4): Figure 1
Photos 1–3

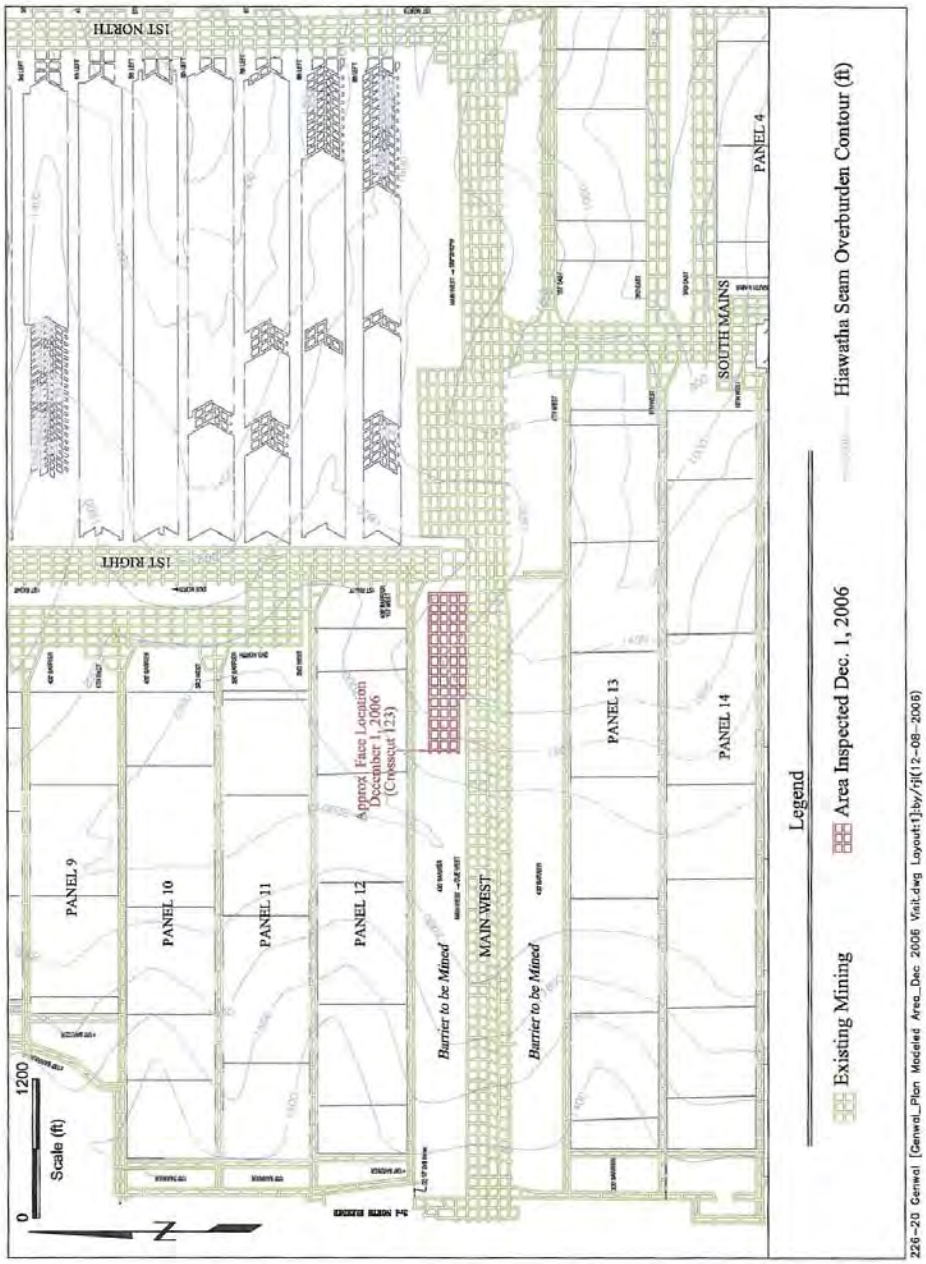

Figure 1. Main West Location Map Showing Extent of Main West North Barrier Mining at Time of Dec 1, 2006 Visit

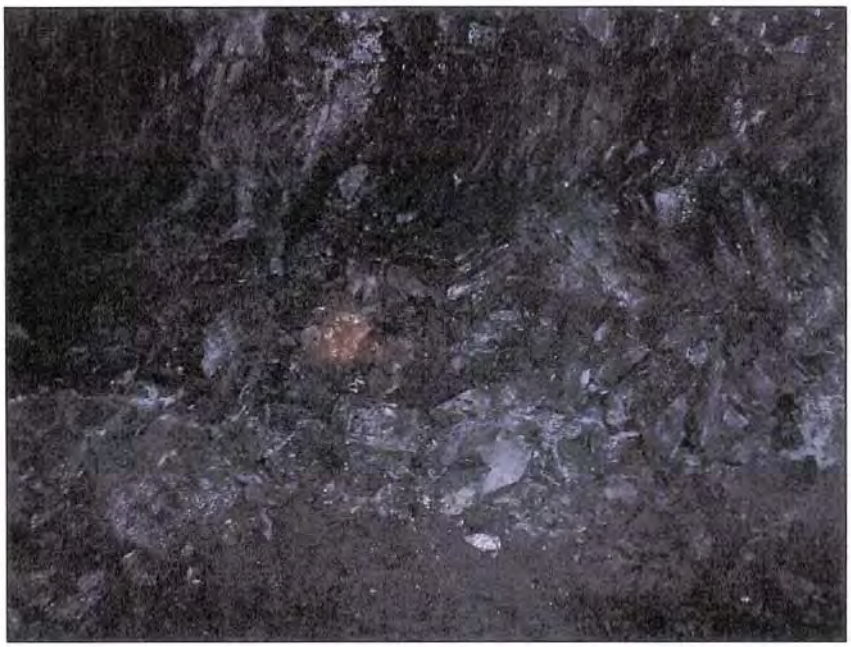

Photo 1. Rib Sloughing Near Crosscut 123 in the Entry North to the South Remnant Barrier Pillar

Photo 2. Minor Rib Sloughing at Crosscut 122 in the Second Entry from North Remnant Pillar

Photo 3. North Remnant Barrier Pillar Rib Condition Between Crosscuts 120 and 119

AGAPITO ASSOCIATES, INC.
Mining & Civil Engineers & Geologists

715 HORIZON DRIVE
SUITE 340
GRAND JUNCTION, CO 81506
USA
VOICE 970.242.4220
www.agapito.com

CHICAGO OFFICE
630.792.1520

GOLDEN OFFICE
303.271.3750

April 18, 2007 226-20

Mr. Laine Adair
General Manager
UtahAmerican Energy, Inc.
794 North C Canyon Road
Price, UT 84501

Re: **GENWAL Crandall Canyon Mine Main West South Barrier Mining Evaluation**

Dear Laine,

Agapito Associates, Inc. (AAI) has completed the geotechnical analysis of GENWAL Resources, Inc.'s (GENWAL) plan for room-and-pillar mining in the Crandall Canyon Mine Main West south barrier. AAI recommended the use of pillars on 80-ft by 92-ft[1] centers for retreat mining in both the north and south Main West barriers based on an earlier analysis documented in our July 20, 2007, report.[2] The design proved successful on development in the north barrier panel under maximum cover reaching 2,200 ft deep.

The panel was successfully retreated to crosscut (XC) 138 under approximately 2,100 ft of cover when poor roof conditions motivated moving the face outby and skipping pulling pillars between XCs 135 and 138. The retreat was re-initiated by pulling the two pillars between XCs 134 and 135 in early March 2007. A large bump occurred at this point resulting in heavy damage to the entries located between XCs 133 and 139. The remaining north panel was abandoned in favor of mining the south barrier.

AAI engineers Michael Hardy and Leo Gilbride visited the bump location on March 16, 2007, under the escort of Mr. Gary Peacock, GENWAL Mine Manager and Mr. Laine Adair, General Manager, UtahAmerican Energy, Inc. GENWAL commissioned AAI to refine the pillar design for the south barrier based on the response of the north panel pillars. AAI was able to analyze the stress and convergence conditions at the time of the bump and modify the pillar design accordingly to control the potential for similar events in the south barrier. The results of the analysis and recommendations for south barrier mining are summarized in the following letter.

[1] Pillar geometry stated in terms of center dimensions; entries typically mined 17 ft wide.
[2] Agapito Associates, Inc. (2006), "DRAFT—GENWAL Crandall Canyon Mine Main West Barrier Pillar Mining Evaluation," prepared for Andalex Resources, Inc.

ANALYSIS

Ground conditions were simulated using the calibrated NIOSH LAMODEL[3] displacement discontinuity model used in the preceding study.[2] The complete model area is illustrated in Figure 1. Simulated conditions at the time of the bump are shown in Figures 2, 3, and 4. Figure 2 describes the vertical stress distribution in the pillars leading up to the bump. Figures 3 and 4 show the corresponding degrees of coal yielding and roof-to-floor convergence. The figures incidentally show retreat mining in the south barrier, although this did not exist at the time of the bump. The two retreats were simulated in the same model for convenience, which is possible because the two areas are geomechnically isolated from one another in the model.

At the time of the bump, the cave was reported to be lagging inby XC 138. Also, the new start-up cave was minimally developed above the two pillars pulled between XCs 134 and 135. These lagging caves were simulated in the model by limiting load transfer through the gob, which causes higher abutment loads to be transmitted to surrounding pillars. The lagging caves can be recognized in Figure 1 by the white colored gob areas.

Model results show that high stresses were placed on the pillars from three contributing sources: (1) abutment loads from the main cave (inby XC 138), (2) abutment loads from the start-up cave (between XCs 134 and 135), and, to a lesser extent, (3) abutment loads from longwall Panel 12. Peak stresses were concentrated on the pillars located between the two caves (between XCs 135 and 138). Figure 3 shows significant yielding in these pillars indicative of overloading. Modeling suggests that the start-up cave contributed on the order of 5,000 psi additional stress to some parts of the surrounding pillars. This, coupled with the other abutment loads, is believed to have created a high stress region that allowed a localized bump in the pillars somewhere between XCs 134 and 135 to propagate to pillars over a much wider area.

Figures 2, 3, and 4 show stress, yielding, and convergence levels in the same sized pillars (80-ft by 92-ft[1]) in the south barrier for ordinary retreat conditions, where no pillars are skipped. The figures show that high-stress conditions attenuate quickly away from the face and that protected conditions exist as close as one crosscut outby the face.

Figures 5, 6, and 7 illustrate the benefit of increasing pillar size from 80-ft by 92-ft[1] to 80-ft by 129-ft[1]. The added 37 ft length, approximately equivalent to an extra full cut, increases the size and strength of the pillars' confined cores, which helps to isolate bumps to the face and reduce the risk of larger bumps overrunning crews in outby locations. For conservatism, a lagging cave was also assumed in the south panel. Plans are to slab the south barrier to a depth of about 40 ft. The wider span is expected to improve caving conditions compared to the north panel and reduced concentrated loads at the face.

The south barrier will be mined to about 97 ft wide (rib-to-rib) after slabbing. The slabbed barrier will be subject to side abutment loads from gob on both sides, resulting in elevated stress levels through the core. Model results indicate that the barrier will yield to a

[3] Heasley, K.A. (1998), *Numerical Modeling of Coal Mines with a Laminated Displacement-Discontinuity Code*, Ph.D. Thesis, Colorado School of Mines, 187 p.

depth of about 20 ft along the ribs, but that the core will remain competent. This is likely to result in some bumping in the gob, but is not considered to pose unusual risk to crews working at the face.

RECOMMENDATIONS

Based on the evidence from the Main West north barrier retreat and results of numerical modeling, we recommend mining with 80-ft by 129-ft[1] pillars, or similar, in the south barrier. This size of pillar is expected to provide a reliable level of protection against problematic bumping for retreat mining under cover reaching 2,200 ft. Pillars should be robbed as completely as is safe to promote good caving. Slabbing the south-side barrier is expected to benefit caving. Skipping pillars should be avoided in the south barrier, particularly under the deepest cover.

Please contact me to discuss these results, at your convenience, or if you have any questions.

Sincerely,

Leo Gilbride
Principal
gilbride@agapito.com

LG/smvf:klg
Attachments(7): Figures 1–7

Figure 1. Geometry of LAMODEL Model

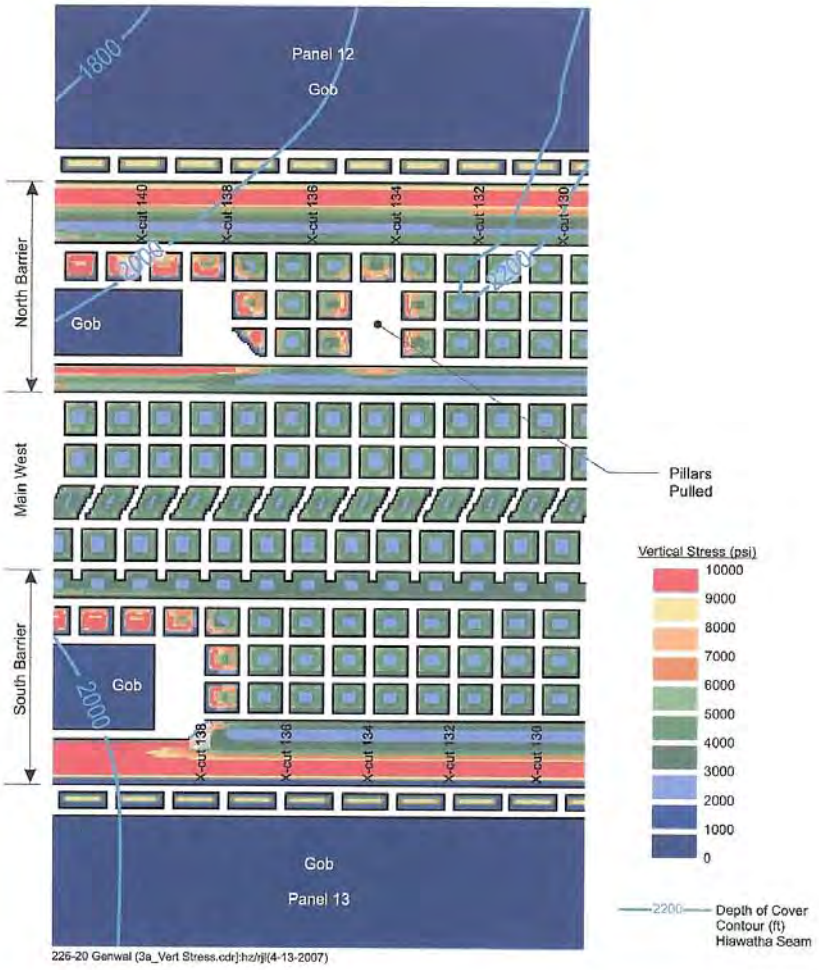

Figure 2. Modeled Vertical Stress—Existing Mining in the North Barrier and Optional Mining with 80-ft by 92-ft Pillars in the South Barrier

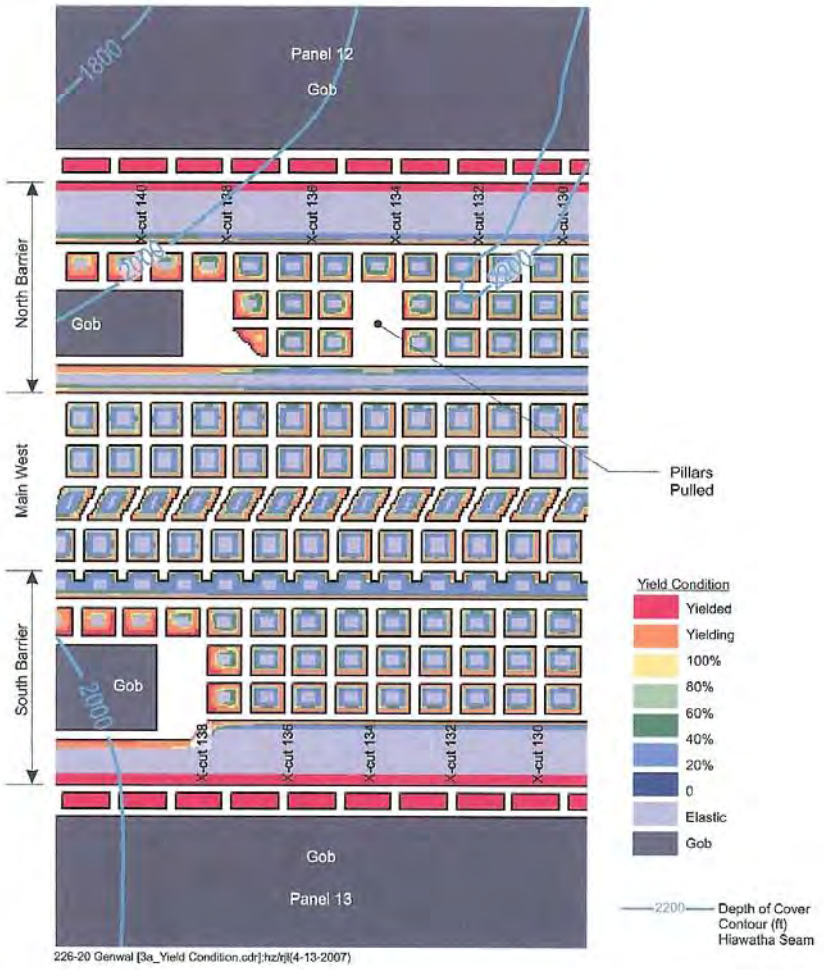

Figure 3. Modeled Coal Yielding—Existing Mining in the North Barrier and Optional Mining with 80-ft by 92-ft Pillars in the South Barrier

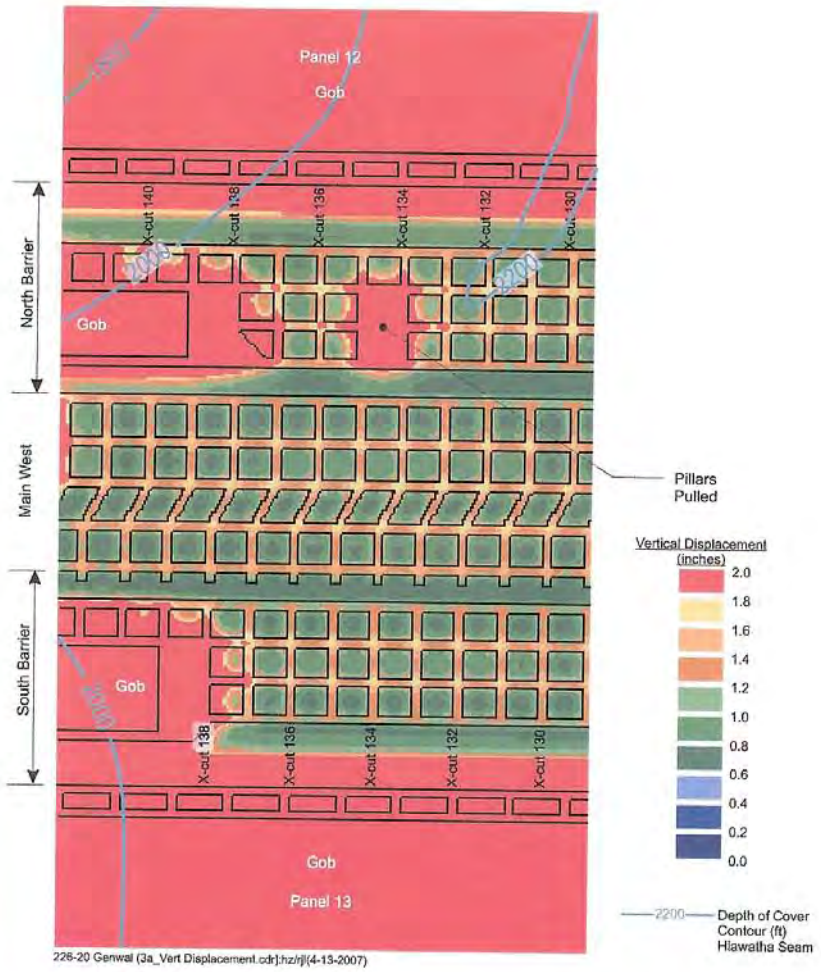

Figure 4. Modeled Roof-to-Floor Convergence—Existing Mining in the North Barrier and Optional Mining with 80-ft by 92-ft Pillars in the South Barrier

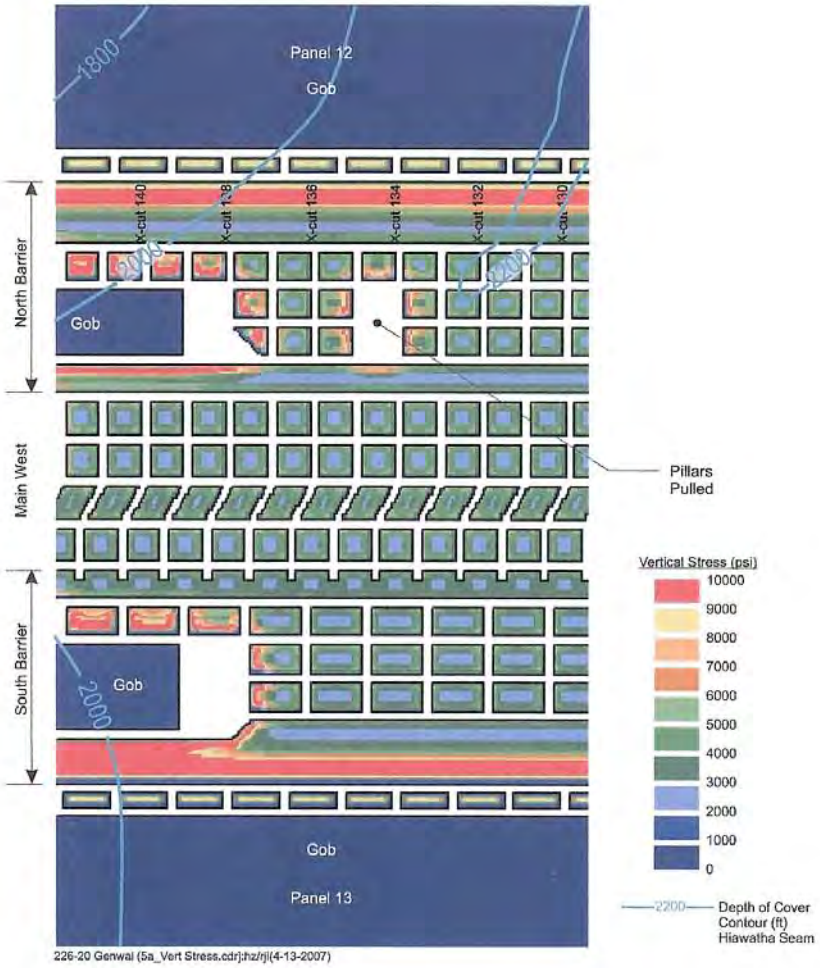

Figure 5. Modeled Vertical Stress—Existing Mining in the North Barrier and Optional Mining with 80-ft by 129-ft Pillars in the South Barrier

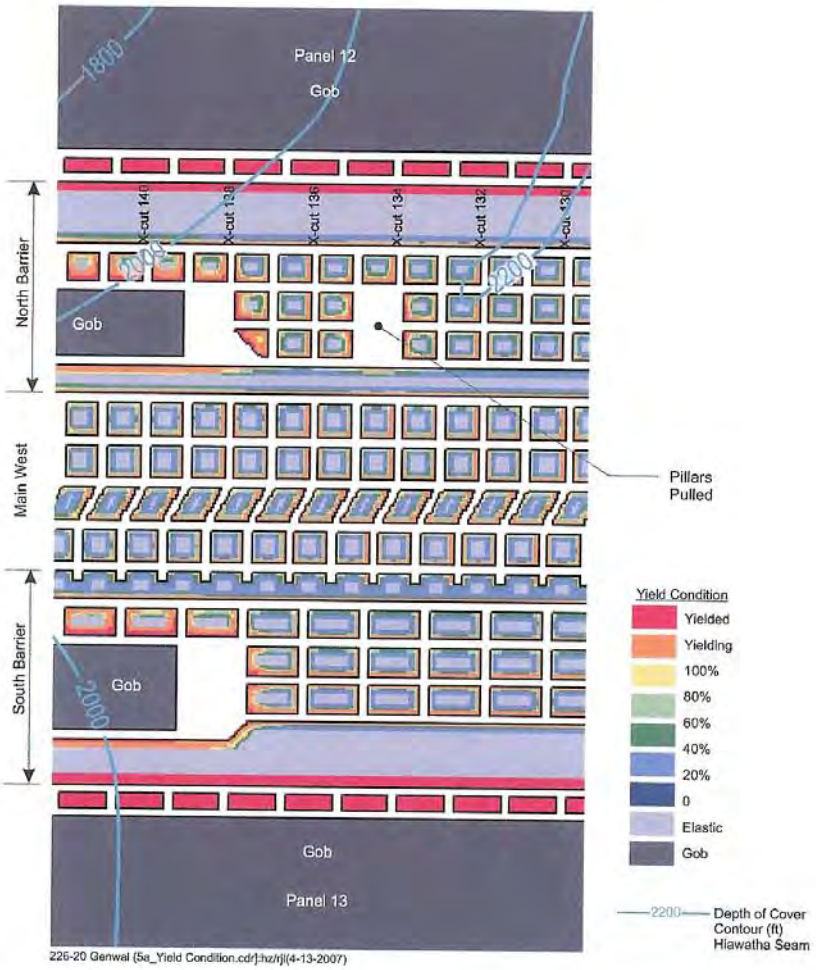

Figure 6. Modeled Coal Yielding—Existing Mining in the North Barrier and Optional Mining with 80-ft by 129-ft Pillars in the South Barrier

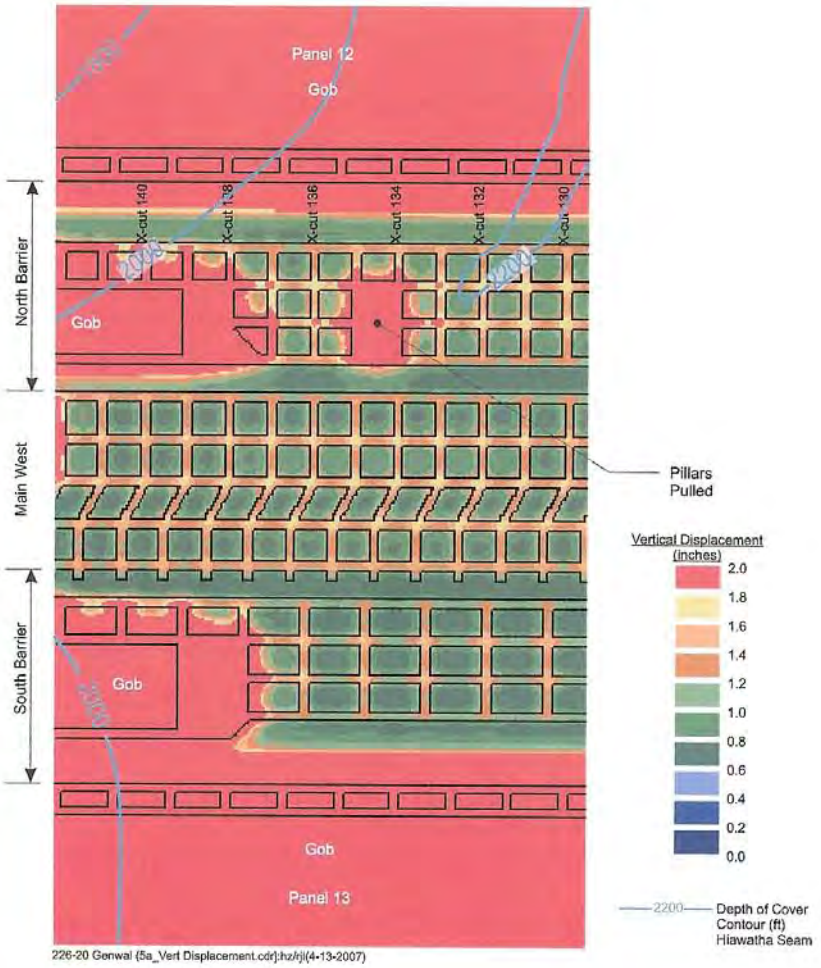

Figure 7. Modeled Roof-to-Floor Convergence—Existing Mining in the North Barrier and Optional Mining with 80-ft by 129-ft Pillars in the South Barrier

Appendix J - Roof Control Plan for Recovering South Barrier Section

RECEIVED MINE FILE
DATE FWD. 6-15-07
INITIALS MM

SURNAME	DATE
Owens	6/14/07
for KNEPP Owens	6/14/07

JUN 15 2007

Coal Mine Safety and Health
District 9

Gary Peacock
General Manager
Genwal Resources, Inc.
P.O. Box 1077
Price, UT 84501

RE: Crandall Canyon Mine
ID No. 42-01715
Roof Control Plan Amendment
Site-specific Pillaring Plan
Main West South Barrier

Dear Mr. Peacock:

The referenced roof control plan amendment is approved in accordance with 30 CFR 75.220(a)(1).

The submittal consisted of a cover letter, dated May 16, 2007, one page, and one drawing, addressing pillar mining of the Main West South Barrier. This amendment will be incorporated into the current plan originally approved on July 3, 2002.

This approval is site-specific for pillar mining the Main West South Barrier and will terminate upon completion of the project. Since this approval is site-specific, no pages in the roof control plan will be superseded. That is, this amendment will be added to the roof control plan as a separate attachment.

A copy of this approval must be made available to the miners and must be reviewed with all miners affected by this amendment.

If you have any questions regarding this approval, please contact Billy Owens at 303-231-5590 or 303-231-5458.

Sincerely,

William G. Denning

for Allyn C. Davis
District Manager

Enclosure

bcc: Price #2 FO (Copy surname letter & copy plan)
Price #2 FO UMF (Copy surname letter & copy plan)

Tom Hurst
Mining Engineer
Genwal Resources, Inc.
P.O. Box 1077
Price, UT 84501 (Copy letterhead letter and copy plan)

EC Plan File (Original surname letter & original plan)
RC MHF (Copy surname letter -Plus backup material)
RC Plan File (Copy surname letter & copy plan)
RC Reading 8646 B4-A19 (Copy surname letter)
A. Davis/D9 Chron 05/17/2007 (Copy surname letter)
WORD(T:\COAL\RC\bdo\mines\south Crandall\South Barrier Pillar B4-A19.doc)

BDO 5/17/07

Crandall Canyon Mine
a subsidiary

Hwy31 MP 33, Huntington, UT 84528
PO Box 1077, Price, UT 84501
Phone: (435) 888-4000
Fax: (435) 888-4002

UtahAmerican Energy, Inc.

8646 B4-A19

RECEIVED
MAY 17 2007
USDOL - MSHA
DISTRICT 4

May 16, 2007

Mr. Allyn C. Davis
District Manager
Coal Mine Safety and Health
P.O. Box 25367
Denver, Colorado 80225

Re: Crandall Canyon Mine ID# 42-01715 Roof Control Plan
Pillaring Main West South Barrier

Dear Mr. Davis:

Please find attached for your review and approval, a site specific roof control plan for pillaring the South Barrier of Main West at our Crandall Canyon Mine. The plan consists of one page of text and 1 Plate.

Please contact me with any questions at 435.888.4023.

Sincerely,

Tom Hurst

Tom Hurst
Mining Engineer
435.888.4023

Crandall Canyon Mine
MSHA ID # 42-01715
Main West Pillaring
South Barrier
Roof Control Plan

The mine is currently developing entries into the south barrier of the Main West area. This plan proposes to recover coal remaining in the pillars shown on attached Plate 1, Pillar Extraction.

Consultant reports indicate the development will avoid the majority of the side-abutment stress transferred from the adjacent longwall panels. These assessments have been validated by conditions experienced in the mine.

Plate 1, Pillar Extraction, shows the mining sequence and the blocks left in the mining process. This pillar recovery will be done in accordance with the approved Roof Control Plan.

Floor to roof support will be provided in the Bleeder entry. These timbers will be installed at the entrance to the crosscuts in number 4 entry. This support will consist of a double row of timbers (breaker row) installed on four (4) foot centers or closer if deemed necessary by the operator. There will be a minimum of four timbers in each row across the entry.

Also, should conditions warrant pillaring can begin at anytime in the panel. The pillar sequence and bleeder configuration will be same except that pillars will be left inby the beginning of the pillar line.

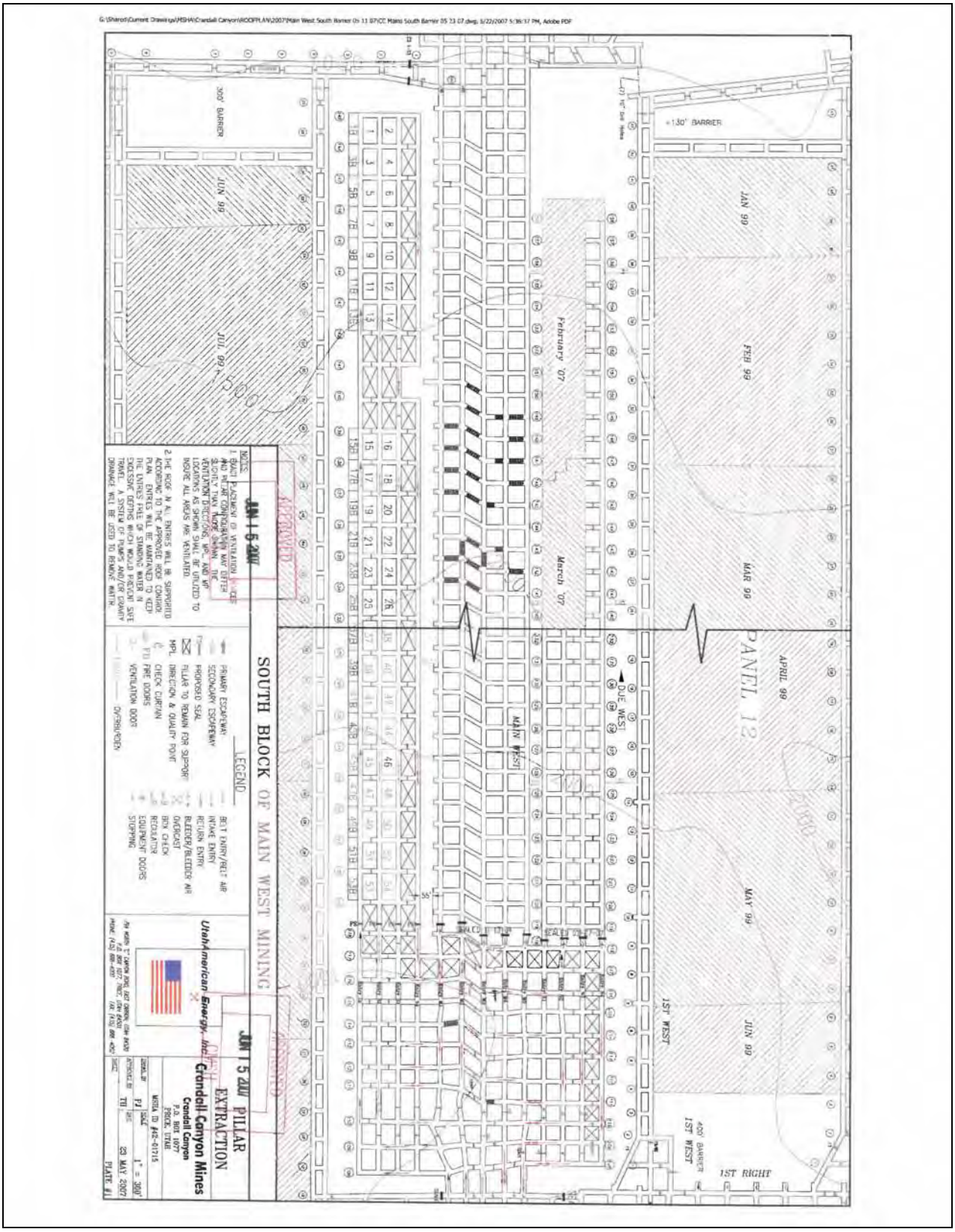
SOUTH BLOCK OF MAIN WEST MINING
PILLAR EXTRACTION
Crandall Canyon Mines
Crandall Canyon
P.O. BOX 1077
HUNTINGTON, UTAH
MSHA ID #42-01715
PANEL 12
MAIN WEST
1ST WEST
1ST RIGHT
300' BARRIER
130' BARRIER
JAN 99
FEB 99
MAR 99
APRIL 99
MAY 99
JUN 99
JUL 99
February '07
March '07
DUE WEST
LEGEND
PRIMARY ESCAPEWAY
SECONDARY ESCAPEWAY
PROPOSED SEAL
PILLAR TO REMAIN FOR SUPPORT
MPL
DIRECTION & QUALITY POINT
CHECK CURTAIN
FIRE DOORS
VENTILATION DOOR
OVERBOREN
BELT ENTRY/BELT AIR
INTAKE ENTRY
RETURN ENTRY
BLEEDER/BLEEDER AIR
OVERCAST
BOX CHECK
REGULATOR
EQUIPMENT DOORS
STOPPING
JAN 15 2007
APPROVED
23 MAY 2007
PLATE #1

Appendix K - Massive Pillar Collapse

The accident that occurred on August 6 at Crandall Canyon Mine was a rapid, catastrophic failure of coal pillars. In a very short time period, failure was manifested as pillar bursting that propagated over a broad area of the mine. Failure of coal pillars in "domino" fashion is referred to using a variety of terms such as massive pillar collapse, cascading pillar failure, or pillar run. At Crandall Canyon Mine the failure involved the violent expulsion of coal; however, other events characterized using the same terms (e.g., massive pillar collapse) may not.

Bureau of Mines investigations in the 1990's[19], documented more than a dozen massive pillar collapse events that occurred in U.S. coal mines. A detailed examination of these events revealed the following common characteristics:

- slender pillars (width-to-height ratio less than 3.0),
- low StF (less than 1.5),
- competent roof strata,
- collapsed area greater than 4 acres, and
- minimum dimension of the collapsed areas greater than 350 ft.

Based on these findings, Mark et al. recommended several strategies to reduce the likelihood of such catastrophic failures. However, the strategies pertain only to collapses involving small or slender pillars under relatively shallow overburden (i.e., the types of failure they had evaluated). Although these failures are sudden (often involving substantial air blasts), they are distinctly different from coal bursts. Mark et al. noted this distinction as follows:

> *Finally, it is important to note that the massive pillar collapses discussed in this paper are not to be confused with coal bumps or rock bursts. Although the outcomes may appear similar, the underlying mechanics are entirely different. Bumps* [bursts] *are sudden, violent failures that occur near coal mine entries and expel large amounts of coal and rock into the excavation (Maleki[20]). They occur at great depth, affect pillars (and longwall panels) with large w/h ratios, and are often associated with mining-induced seismicity. The design recommendations discussed here for massive pillar collapses do* ***not*** *apply to coal bump control.*

Pillars in the Main West and adjacent North and South Barrier sections were at low risk for the type of slender pillar collapse that Mark et al. studied. However, they were at significant risk for bursting.

The basic condition for a massive pillar collapse is a large area of pillars loaded almost to failure. Since all of the pillars are near failure, when one instability occurs, the transfer of load from that pillar to its neighbors causes them to fail and so on. In a large area of similarly sized pillars near failure, this process can continue unabated. Larger or more stable pillars (or barriers) that may stop the progression of failure are absent. Such was the case in the Main West area of Crandall Canyon Mine.

Furthermore, the pillars at Crandall Canyon Mine were not slender* and were capable of storing substantial amounts of energy that was released as a burst. Pillars with width-to-height (w/h) ratios between 5 and 10[21] are considered to be bump prone. Pillar w/h ratios at Crandall Canyon Mine ranged from 7 ½ to 8 ¾ in the collapse area.

* Slender pillars are those that are relatively narrow with respect to their height (e.g., width is less than 5 time the height).

Appendix L - Subsidence Data

Information was obtained from the U. S. Geological Survey (USGS) that defined the extent of surface deformation above the accident site. USGS scientists use radar satellite images (interferometric synthetic aperture radar or InSAR) to measure small movements on the earth's surface for their research on volcanoes, earthquakes, subsidence from groundwater pumping, and other ground disturbances from natural and man-made causes. The technique has been used in Europe to study mining subsidence since 1996, but its use has been limited in the U.S. coal mining industry. USGS applied this technology in the vicinity of the Crandall Canyon Mine and were able to identify an extensive subsidence region associated with the August 2007 accident. Neva Ridge Technologies (Neva Ridge) was contracted to verify the USGS study. The Neva Ridge report is provided in Appendix M in its entirety.

InSAR Surface Deformation

The InSAR deformation measurement technology relies on bouncing radar signals off the earth from satellites orbiting over the same area at different time periods. By studying the differences in the images, InSAR can detect small changes in the distance to the ground surface relative to the satellite. InSAR detects very small movements that can not be visually noticed. InSAR shows patterns of deformation as color bands with each band representing a few centimeters (cm) of movement. The following figures from the USGS publication *"Monitoring Ground Deformation from Space"* illustrate the use of the InSAR technology. Figure 96 depicts the orbiting satellites scanning the surface of the earth with transmitted radar waves bouncing back to the satellite.

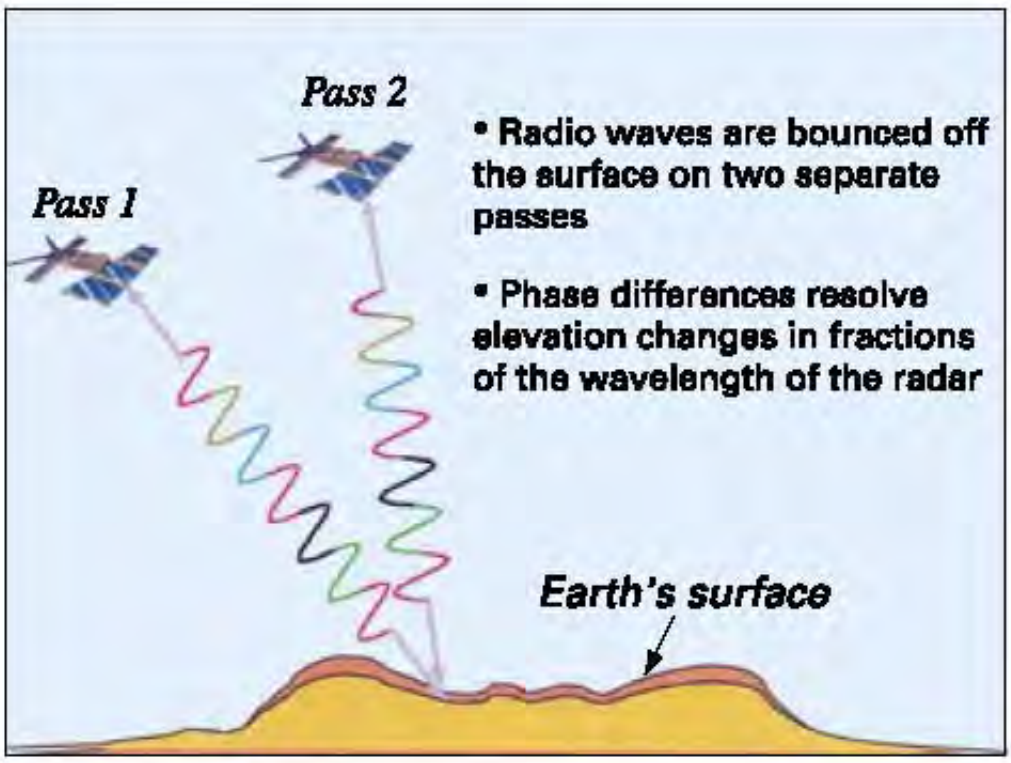

Figure 96 - How Satellites and Radar Interferometry Detect Surface Movement from USGS Fact Sheet 2005-3025

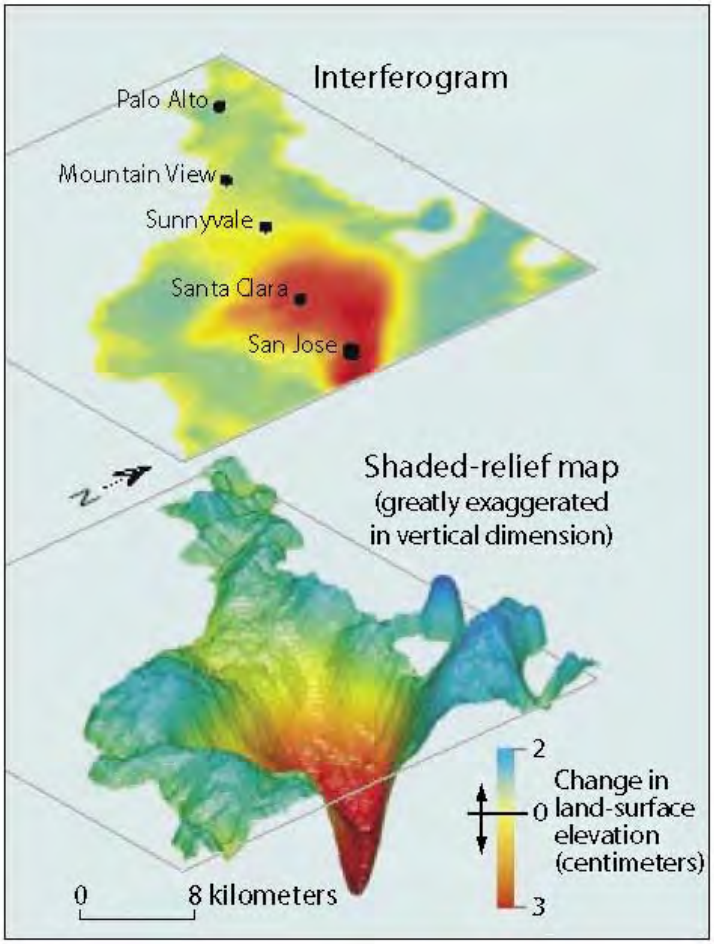

Figure 97 – Example of Interferogram Color Banding from USGS Fact Sheet 2005-3025

The radar images are processed to determine deformation. Figure 97 is an example from California showing the interferogram color banding generated from an InSAR analysis that depicts regional subsidence and localized uplift. Included in Figure 97 is the topographic detail of the subsidence and uplift for the study area with the vertical scale exaggerated.

Crandall Canyon Mine InSAR Surface Deformation.

There are only a limited number of InSAR images over the Crandall Canyon Mine area. The USGS identified a Japanese ALOS PALSAR satellite scan for June 8, 2007 (before the accident) that covered the Crandall Canyon Mine reserve area and another satellite scan on September 8, 2007 (after the accident). InSAR analysis of the radar imagery between the June and September time periods generated the InSAR deformation image shown in Figure 98. The image identifies a region of subsidence centered on the west flank of East Mountain in the vicinity of the Crandall Canyon August 2007 accident sites. Figure 98 shows the terrain surrounding the mine area, with nearby valleys identified for geographic reference. The Line-of-Sight (LOS) deformation in Figure 98 represents subsidence movement measured in a non vertical direction from the satellite. In the USGS analysis, the deformation is measured along a LOS of 39.7º from vertical. The InSAR images were processed and provided by a staff scientist of the Radar Project of Land Sciences at the USGS Earth Resources Observation and Science Center.

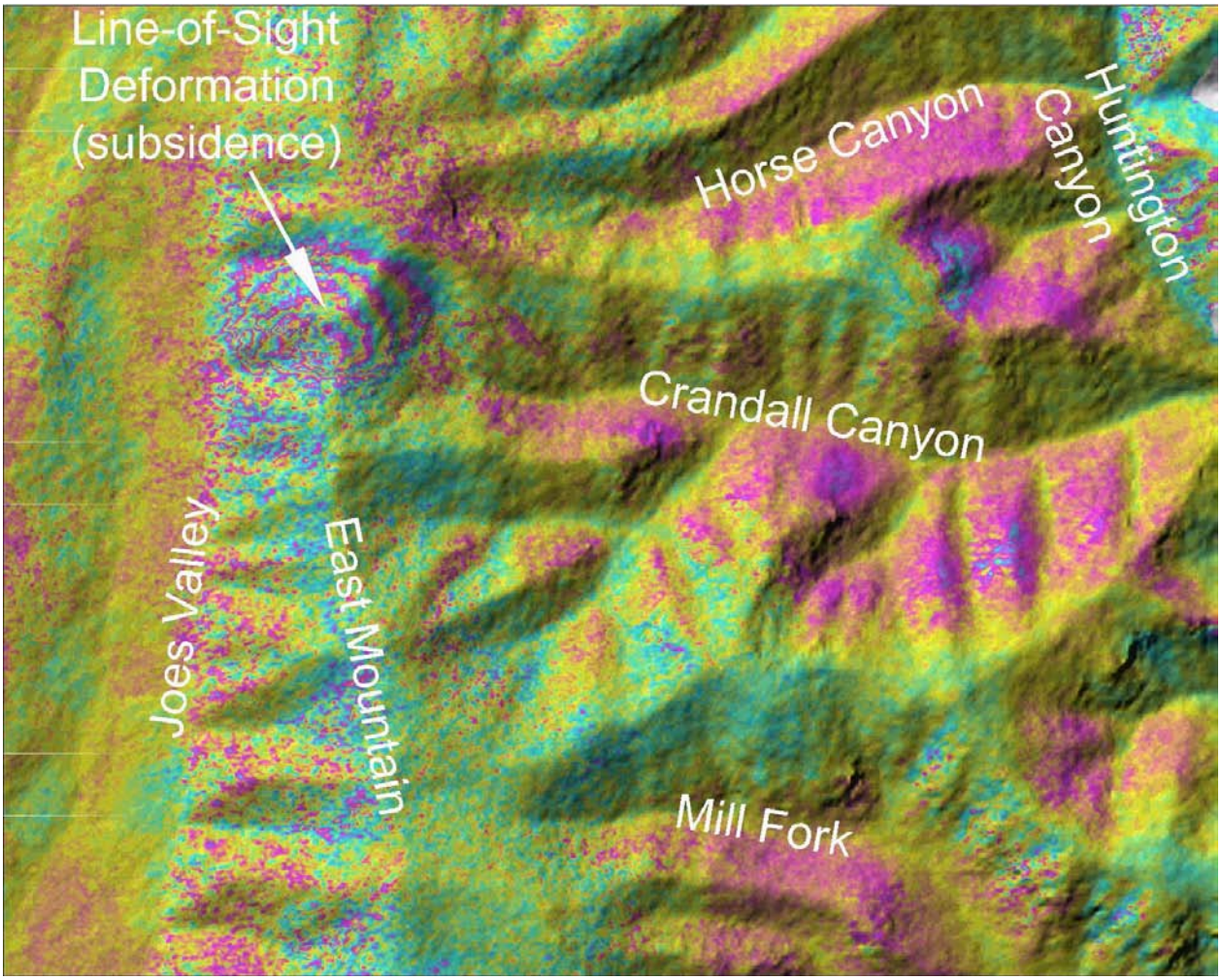

Figure 98 - USGS InSAR Image of Subsidence above the Accident Site.
The surface deformation depicted occurred between June 8, 2007, and September 8, 2007.

The InSAR image furnished by USGS was referenced by latitude and longitude, allowing conversion into state plane coordinates. The accident investigation team translated and rotated the InSAR image onto the Crandall Canyon Mine coordinate system using known state plane and corresponding mine local survey points. The InSAR deformation image with 5 cm color banding was contoured by the accident investigation team with some guidance from USGS to delineate the ground surface subsidence (see Figure 99).

The displacement contour values are Line-of-Sight (LOS) from the satellite. In Figure 99, maximum LOS subsidence contour is 20 cm (approximately 8 inches LOS). Each repetition of the color band (i.e., sequence of rainbow colors) represents 5 cm of LOS deformation with the repetitive color banding indicating successive 5 cm increments of movement. Mining subsidence is typically vertical; therefore, LOS subsidence values are multiplied by 1.29 (1/cos 39.7º) to determine vertical deformation. Consequently, the 20 cm LOS deformation contour converts to approximately 25 cm (approximately 10 inches) vertical surface subsidence. The movement is significant but, at a magnitude that cannot be detected visually on the mountainside.

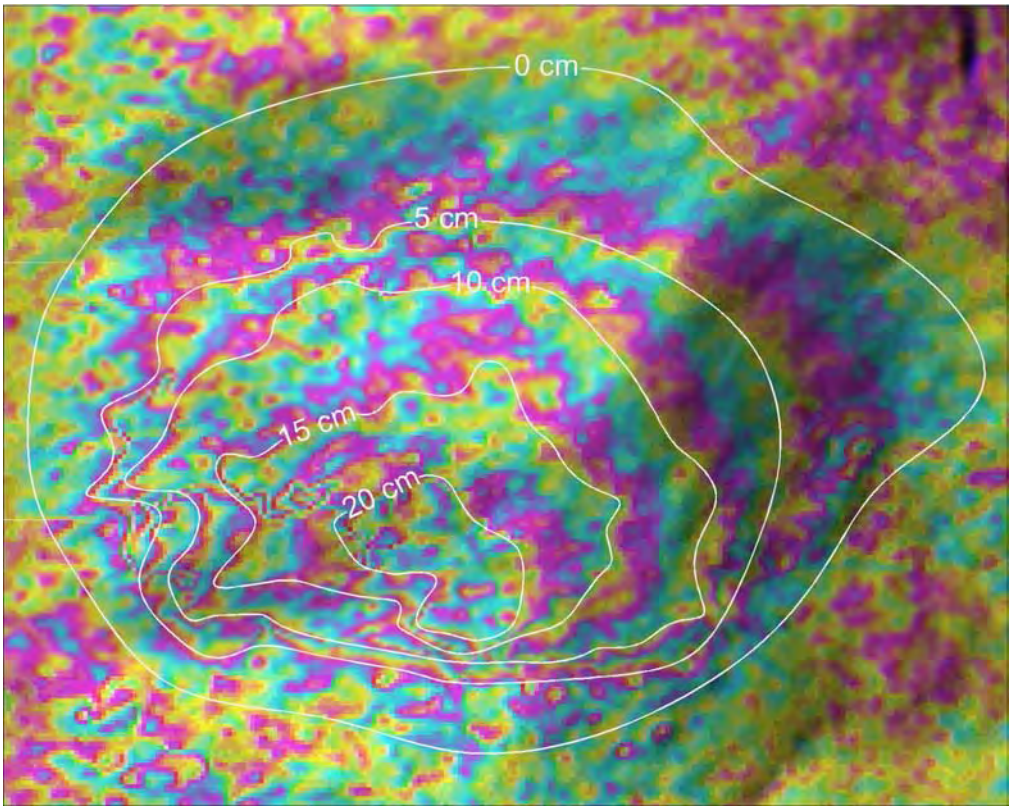

Figure 99 - Surface Deformation from USGS InSAR
Color banding contoured to delineate Line-of-Sight successive 5 cm subsidence movement. Maximum LOS movement of 20 cm (~8 inches) contoured.

The analysis performed by Neva Ridge included a contoured map of 5 cm vertical subsidence contours. The contoured map is included as Figure 100 below.

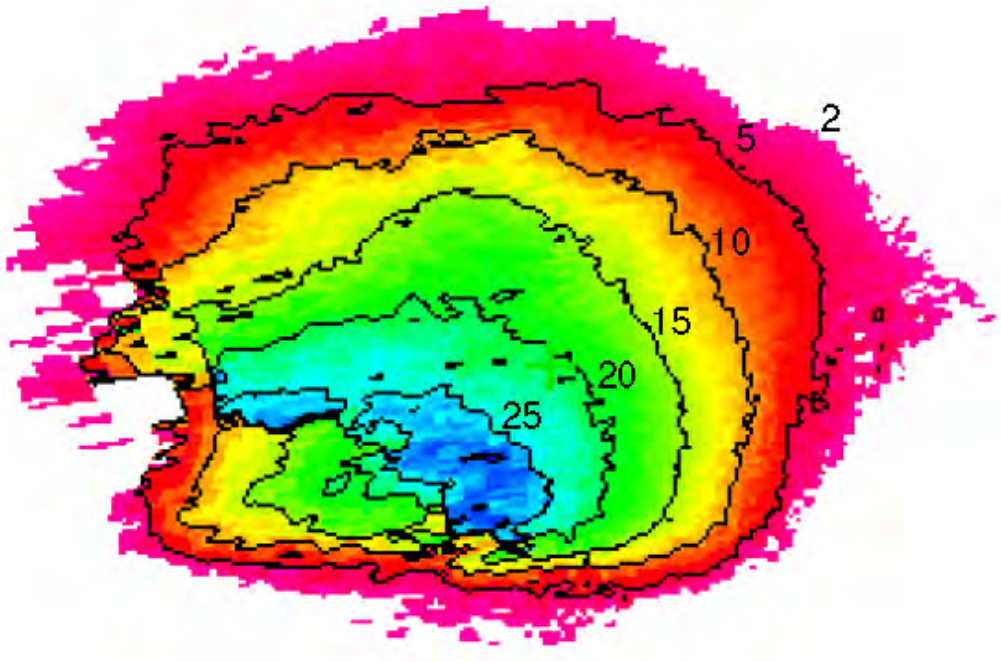

Figure 100 - InSAR Vertical Subsidence Contours (cm) from Neva Ridge

The contours on the USGS results were converted to vertical values and overlain on the Neva Ridge results for comparison. All measurements less than 2 cm were considered noise by Neva Ridge and removed from the map. The comparison of the two results is shown in Figure 101. The results are very similar except for the south-west portion of the depression. Tracing the contours of the USGS image was very difficult in this area due to the rapid rate of change, making it challenging to follow the color banding in Figure 99. The uncertainty in this area was a factor in retaining an independent analysis. The Neva Ridge contours developed by experts in InSAR analysis were therefore used throughout this report. The Neva Ridge InSAR surface subsidence contours were overlain onto the mine workings and identify a wide spread subsidence basin with the 25 cm (10-inch) vertical subsidence contour centered within the South Barrier section, roughly between crosscuts 133 and 139 (see Figure 31).

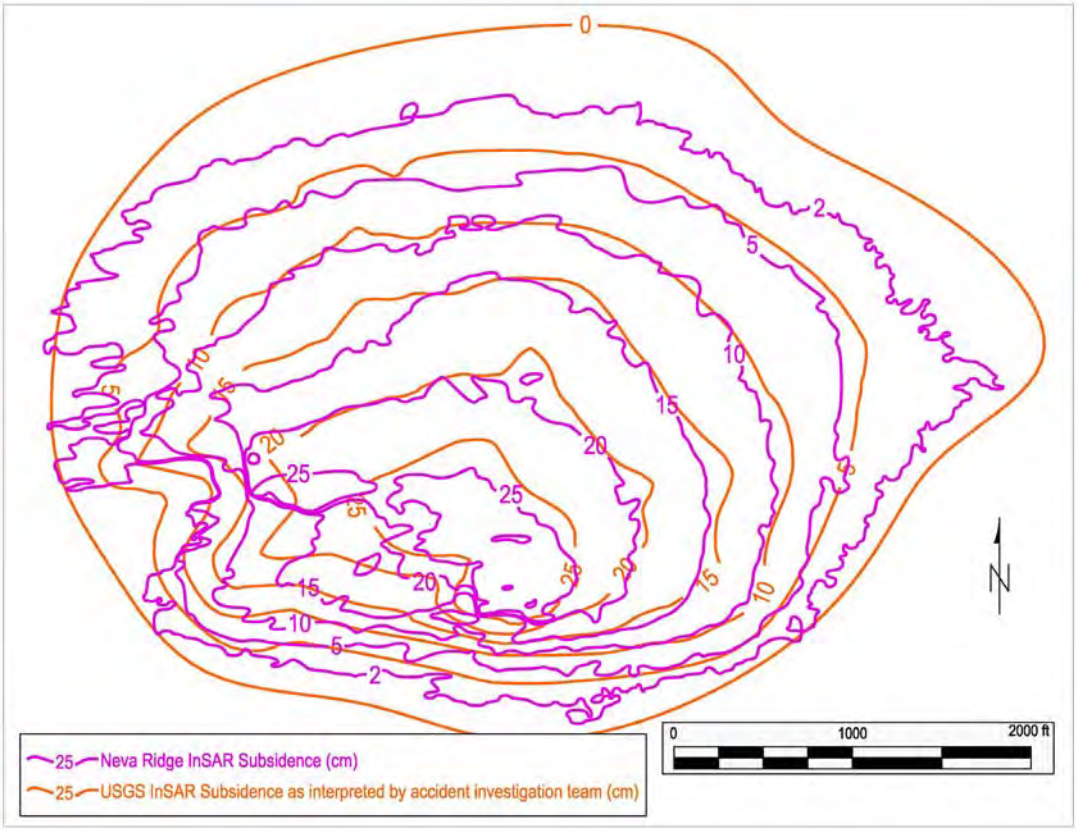

Figure 101 - Comparison of Vertical Subsidence from Interpreted USGS and Neva Ridge InSAR Results

The geometry of the InSAR surface subsidence depression indicates that the Main West and North and South Barrier sections have undergone extensive pillar failure. The knowledge that surface deformations radiate around collapse regions was used to extrapolate the extent of damage into adjoining regions that could not be traveled or investigated. Subsidence principles suggest that the extent of the collapse at seam level would be less laterally but greater vertically than the surface expression implies. The development of bed separations and other openings within the overburden can cause surface subsidence to be less than the full height of closure at mine level. Conversely, the collapse at mine level will draw the overburden downward with subsidence deformations radiating outward and laterally over an area greater that the collapsed area. Although subsidence research has primarily focused on full extraction mining, it is reasonable to expect that strata will respond similarly to a pillar collapse.

InSAR analyses were performed using satellite images from December 2006 and June 2007 specifically to determine if surface subsidence had been associated with pillar recovery in the

North Barrier section. No subsidence was detected. However, it is possible that subsidence occurred but the deformation was too small to measure or it was masked by ground surface conditions. December radar scans would be affected by snow cover and June's radar scans would not. Snow cover tends to generate data scatter (noise) that interferes with InSAR analyses.

InSAR Validation with Longwall Subsidence Monitoring Data

In 1999, a subsidence monitoring line was established on the north-to-south trending ridge of East Mountain. The survey line over a portion of Main West and Panels 13 to 17 was monitored from September 2000 to July 2004 by Ware Surveying, LLC (surveying contractor) using GPS survey technology. Surveys were performed using a Trimble GPS Total Station 4700 and Real Time Kinematics processing. The vertical accuracy of these surveys was reported to be ± 0.2-foot (roughly ± 6 cm). The survey monuments were 5/8-inch rebar driven into the ground.

Surface monuments were resurveyed on August 17, 2007, along the portion of the line from the center of Panel 14 to just north of Panel 13. These GPS subsidence measurements are the only reliable information available for comparison with the InSAR analyses. On August 17, six of 16 survey stations had been destroyed in the area of interest. However, some of the remaining monuments lie within the deformation crater identified using InSAR. The northern end of the survey line terminates along the 20 cm (8-inch vertical) deformation contour. The southern portion of the line lies outside of the 2 cm vertical subsidence contour (see Figure 102).

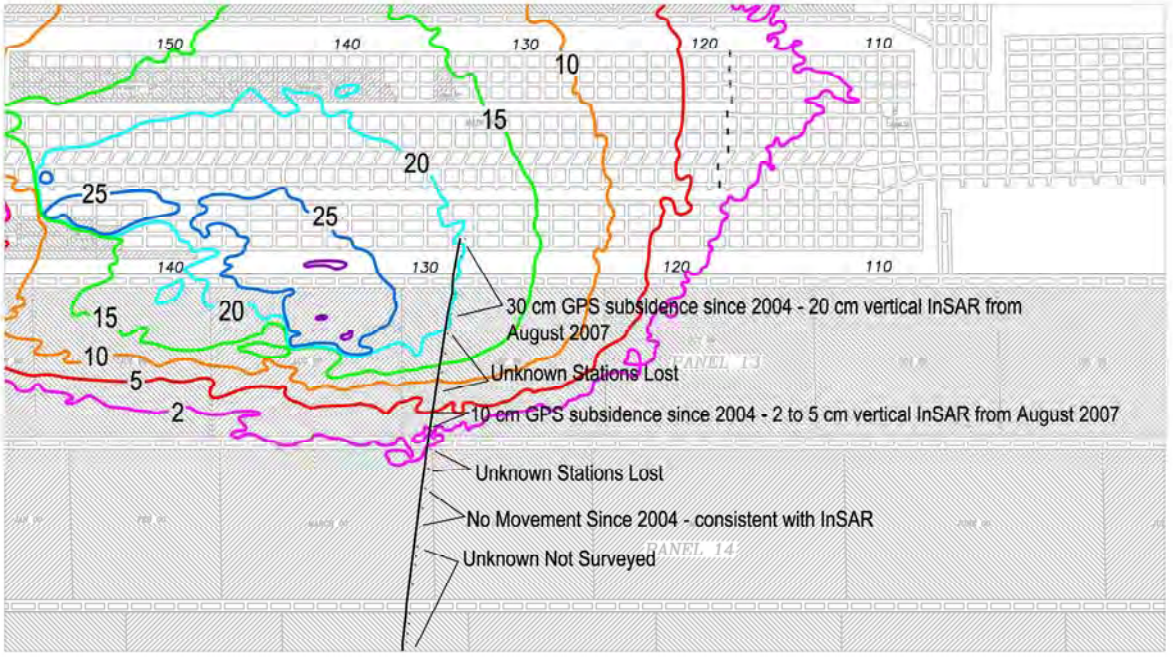

Figure 102 - InSAR Vertical Subsidence Contours & GPS Subsidence Line Data

Three stations near the southern end of the survey line showed no movement since 2004; this observation is consistent with the InSAR analysis in this area (see Figure 102). Two survey stations which showed approximately 10 cm of vertical movement (since 2004) were located within the 2 to 5 cm InSAR vertical deformation contours. Five stations at the northern end of the survey line showed 30 cm of vertical movement (since 2004) although they were located along the 20 cm InSAR vertical deformation contour.

InSAR provides a more reliable characterization of surface subsidence associated with pillar recovery in the South Barrier section since it only captures movement that occurred between June and September 2007. GPS survey data incorporates deformations that occurred over a longer time period between 2004 and August 17, 2007. For example, the five northern stations of the survey line showed remarkably similar displacements between 2004 and 2007 (i.e., 29 to 33 cm). These stations are situated near the edge of Panel 13 and the original unmined South Barrier. The data suggest that this area subsided gradually over the years between 2000 and 2004. It is possible that some amount of residual longwall subsidence and variations due to surveying precision ($\pm$ 6 cm) account for the 10 cm difference between the InSAR and GPS survey data.

Longwall Mining Subsidence History

Main West and adjoining barrier pillars near the accident area are bounded to the north and also to the south by six extracted longwall panels. To establish if unanticipated or unusual subsidence from the longwall extraction affected the region, the Panels 13 to 17 subsidence information was compared to information from handbooks and references. The data suggests that the Crandall Canyon Mine subsidence is similar to that published for deep longwall districts.

Data from the subsidence surveys show the development of the subsidence trough with the extraction of successive longwall panels. As illustrated in Figure 103 surface profiles do not begin to show the formation of a critical subsidence basin[22] (i.e., when subsidence reaches the maximum possible value) until 2001 when the third successive panel (Panel 15) was extracted. This delayed subsidence behavior is typical of the Wasatch Plateau where strong, thick strata in the overburden control caving characteristics. Similarly, these strong units can resist caving and form cantilevers at panel boundaries (as indicated by the absence of subsidence over more than half the width of Panel 13). Subsidence data collected elsewhere in the region indicates that the amount or extent of cantilevered strata at panel boundaries varies. These strata can be responsible for high abutment stresses and long abutment stress transfer distances.

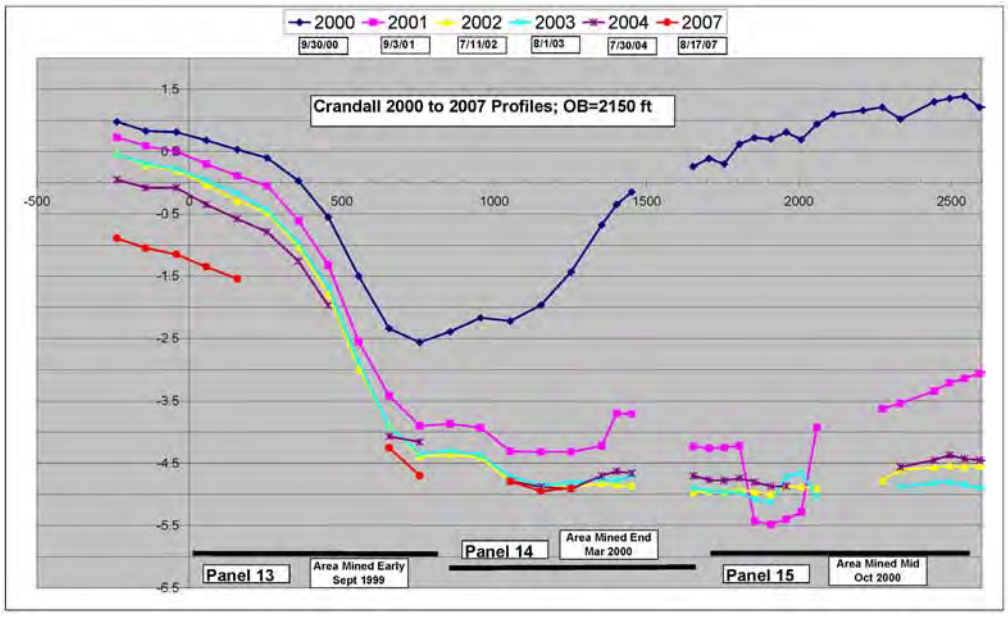

Figure 103 - Longwall Panels 13 to 15 GPS Surveyed Subsidence Profiles

Early measurements (2000 to 2002) show a surface elevation increase above the baseline from about the middle of Panel 13 to the barrier south of Main West. Cantilevered strata may be responsible for this movement. The data also suggest that the strata gradually subsided in this area over time.

Subsidence values derived from the surveyed profiles over Panels 13 to 17 are summarized in Table 14. The Panel 13 to 17 profile is supercritical in character where maximum subsidence (Smax) is achieved. Also, listed in Table 14 is the horizontal distance (d) from the excavation edge to the inflection point (point dividing the concave and convex portions of the subsidence profile). The supercritical width (W) for these Crandall Canyon Mine longwall panels is comparable to other Wasatch Plateau longwall panels. Also, the subsidence factor (Smax/m) shown in the table is typical for longwall mining.

The distance to the inflection point (d) was calculated from subsidence references using Panel 13 to 17 factors as shown in the lower portion of Table 14. This distance for the Panel 13 to 17 profile survey is roughly 500 feet. This value is similar to the values calculated from references. This information suggests that the Crandall Canyon subsidence and associated overburden bridging over extracted panels is comparable to other deep full extraction mining.

Table 14 - Crandall Canyon Longwall Subsidence Parameters, Values, and Comparisons

Parameter				**Values**		
Longwall Subsidence Data Source	**Approx. Depth (h), ft.**	**Mined Height (m), ft.**	**Approx. Maximum Subsidence (Smax), ft.**	**Approx. Supercritical Width (W), ft.**	**Smax/m**	**Approx. Distance to Inflection Point (d), ft.**
Crandall Canyon Mine Panels 13-17	2,150	7.9	5.0	2,300	0.63	500
Surface Subsidence Engineering Handbook[22]	2,150 used in Fig 2.4			2,300 used in chart Fig 2.4	0.63 used in Fig 2.4	495
Average Estimate from SDPS Chart[23]	2,150 used in Fig 3.2.1			2,300 used in Fig 3.2.1		505

Appendix M - Neva Ridge Technologies Report

Final Report

MSHA Contract DOLB08MR20605

April 18, 2008

Prepared by Neva Ridge Technologies

Contact: David Cohen, Ph.D.
Neva Ridge Technologies
4750 Walnut Street
Suite 205
Boulder, Colorado 80301
(303) 443-9966
cohen@nevaridge.com

1 Introduction

1.1 Data Description

Data from the ALOS/PALSAR sensor were obtained from the AADN (Americas ALOS Data Node, http://www.asf.alaska.edu/alos), located at the Alaska Satellite Facility in Fairbanks, Alaska. The dates of the acquisitions and the unique data designation numbers are shown in the table below.

Date	Designation
June 8, 2007	HH-ALPSRP072960780
September 8, 2007	HH-ALPSRP086380780

The ALOS satellite maintains a sun-synchronous, near polar orbit; this is a retrograde orbit that precesses in a plane that is at an inclination of 98.16 degrees. For the geographic location of this data collection, the following figure shows the geometry. Note that for these particular data acquisitions, the satellite was in the ascending portion of its orbit; the satellite looks to the right (starboard) side during data collection. Locally, then, the line-of-site is 38.7 degrees from the local vertical and 10.0 degrees above the local East direction.

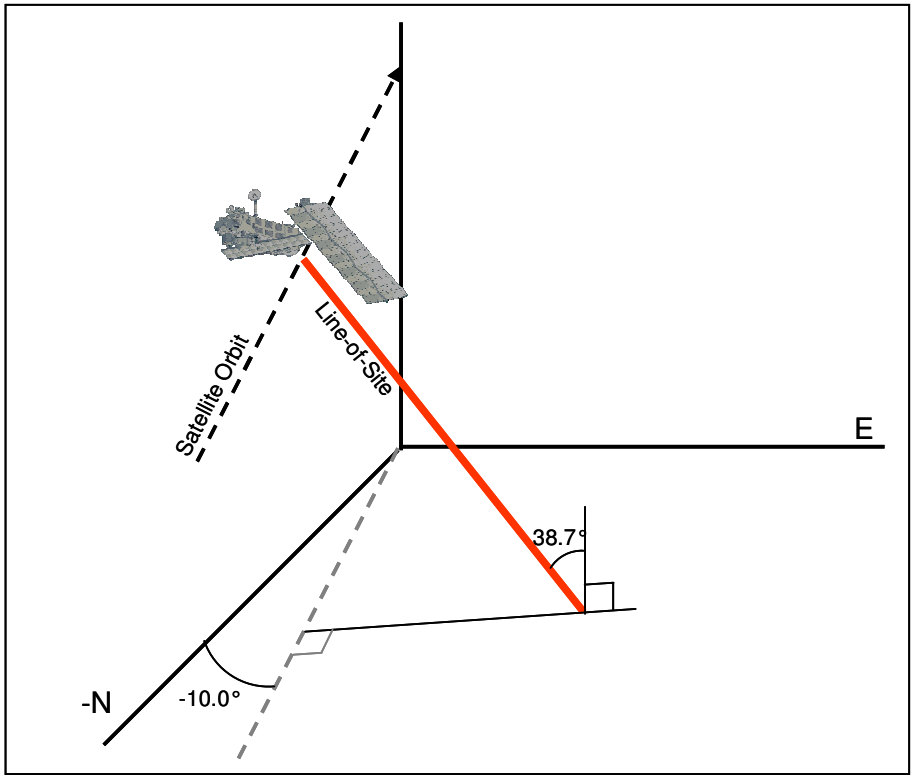

Figure 1. Diagram showing the geometry of the data acquisition at the site of interest.

1.2 Processing Description

Data were processed to complex SAR imagery using tools from Gamma Software. This is standardized processing software that ingests data from most civil SAR sensors. (Neva Ridge is a US distributor for this software.) The interferometry is performed with a combination of additional Gamma Software tools and internal Neva Ridge tools. Complex images are coregistered and the modeled phase due to topography is subtracted using the USGS 3 arcsecond elevation product. Following an iteration to remove errors in the estimated baseline, the *interferogram* is smoothed using a Goldstein filter[1] with a filter exponent of .6. The converted unwrapped results naturally represent the motion along the radar line-of-site (see previous figure) but can be converted to vertical motion with some assumptions. In particular, under the assumption that the ground motion is purely in the vertical direction, we can back-project the measured motion along the vertical direction. However, if we assume that the actual ground motion has a combination of horizontal and vertical components, there is no way to uniquely attach the measured line-of-site displacement to a unique set of horizontal and vertical displacements.

For display and some data manipulation, reprojection, and minor post-processing of the results, we use a combination of PCI Geomatics, Gamma display utilities, and internal tools.

2 Results

In the following sections, we include plan view diagrams (those specified in the SOW) representing the results of the interferometric processing. Each of the plan view figures below represent a region approximately centered on the coordinate NAD27 39°28'01.6"N, 111°13'16.2"W, with spatial extent of 3514 meters on a side.

In addition, in each of the plan view figures, reference points (shown as crosshairs) are included. The coordinates of these are:

Point	WGS 84
1.	111°14'04.9"W, 39°27'12.2"N
2.	111°13'13.3"W, 39°27'43.0"N
3.	111°13'09.1"W, 39°28'04.8"N

2.1 Line-of-Site InSAR Color Contours

In this representation, line-of-site displacements are presented as color-coded contours. In order to enhance the visual dynamic range of the image, the color scale *wraps* at a specified interval, which is shown on the adjacent color bar. For context, the color contours in Figure 2 are superimposed on the corresponding SAR image. As the interpretation of the SAR image is not necessarily intuitive, we have also annotated the physical regions represented by the SAR image shades/textures. The peak line-of-site subsidence measured in this data is 24 cm. Figure 3 shows the same information without the SAR image background layer.

[1] R.M. Goldstein, C.L. Werner, "Radar Interferogram Filtering for Geophysical Applications," *Geophys. Res. Letters, V25, No21, 1998*

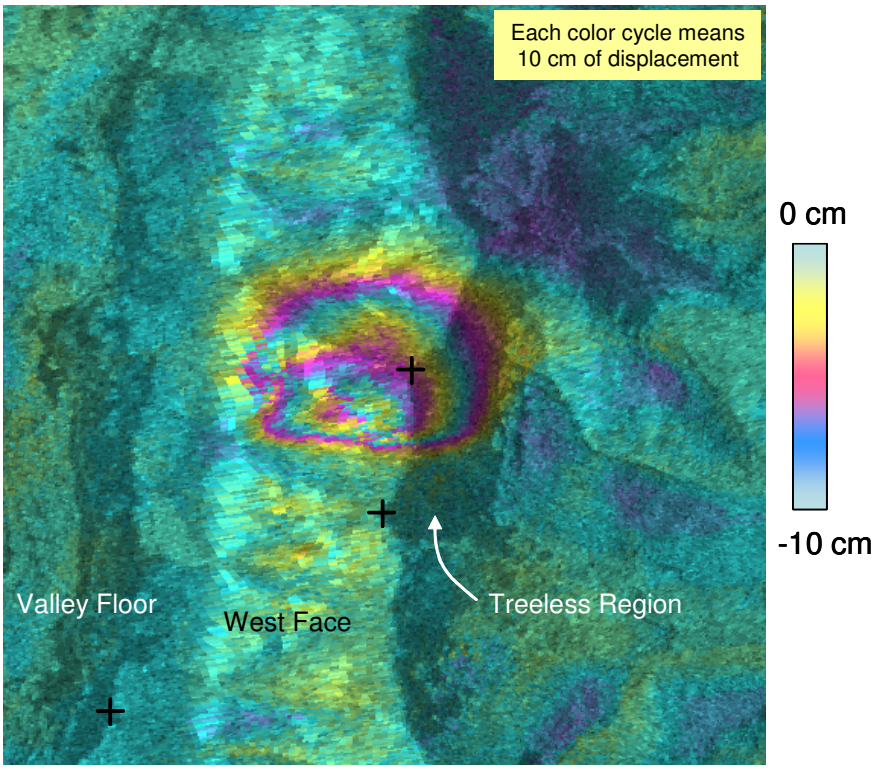

Figure 2. Color contours superimposed on the corresponding SAR image. A peak displacement of 24 cm (along the line-of-site, away from the radar) is measured.

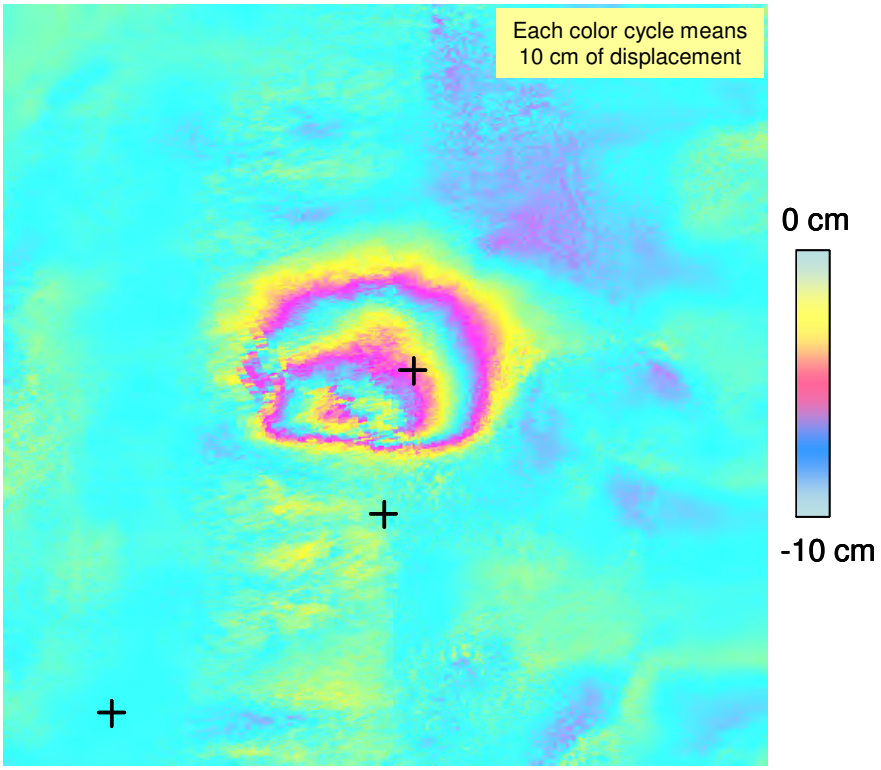

Figure 3. Color contour with no SAR image background layer. A peak displacement of 24 cm (along the line-of-site, away from the radar) is measured.

2.2 Line-of-Site Deformation Contours

The line-of-site deformation contours are produced at 5 cm intervals and are shown in Figure 4. It is not uncommon in InSAR measurements to contain atmospheric effects that are on the order of 1-2 cm. These are produced by moisture (dielectric) variations in the atmosphere that produce noise due to variable phase delays of the radar signal. Using an initial contour of 5 cm mitigates visual interference due to this low-level noise.

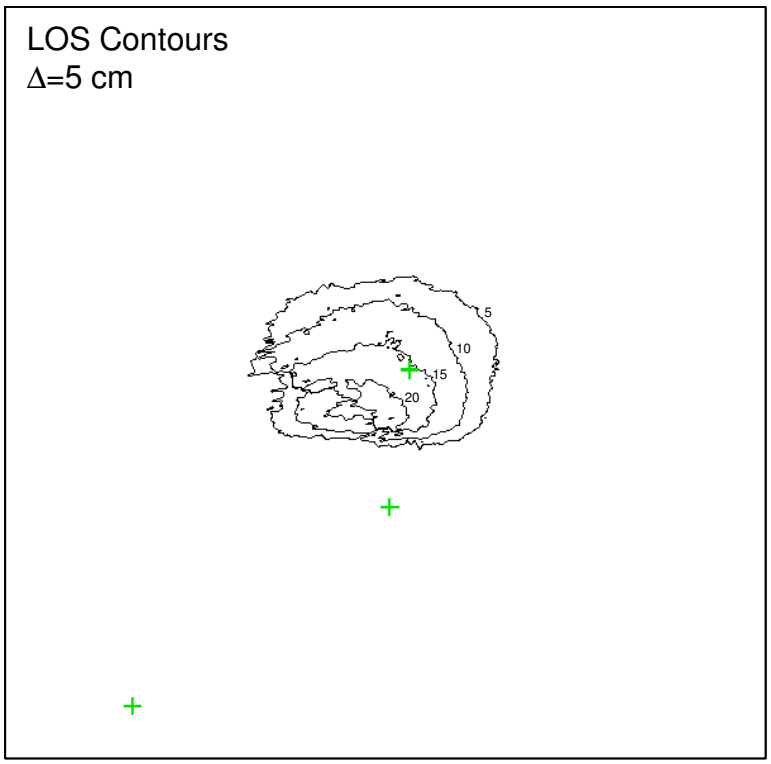

Figure 4. Line-of-site deformation contours with intervals of 5 cm. Motion is away from the radar.

2.3 Vertical Deformation Contours

Vertical deformation measurements may be derived from the line-of-site measurements under the assumption that motion is purely vertical. Based on the diagram in Figure 1, the relationship between the line-of-site measurement and vertical measurements is:

$$\delta_{vert} = \frac{\delta_{LOS}}{\cos(38.7)}$$

The result of this transformation is shown in Figure 5.

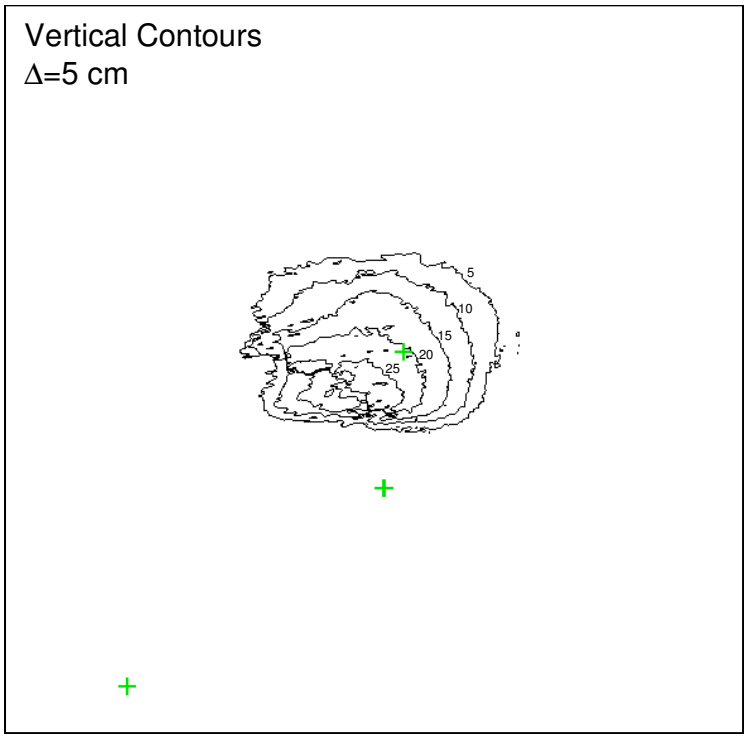

Figure 5. Vertical contours. A peak displacement of 30 cm (vertical, downward) is measured.

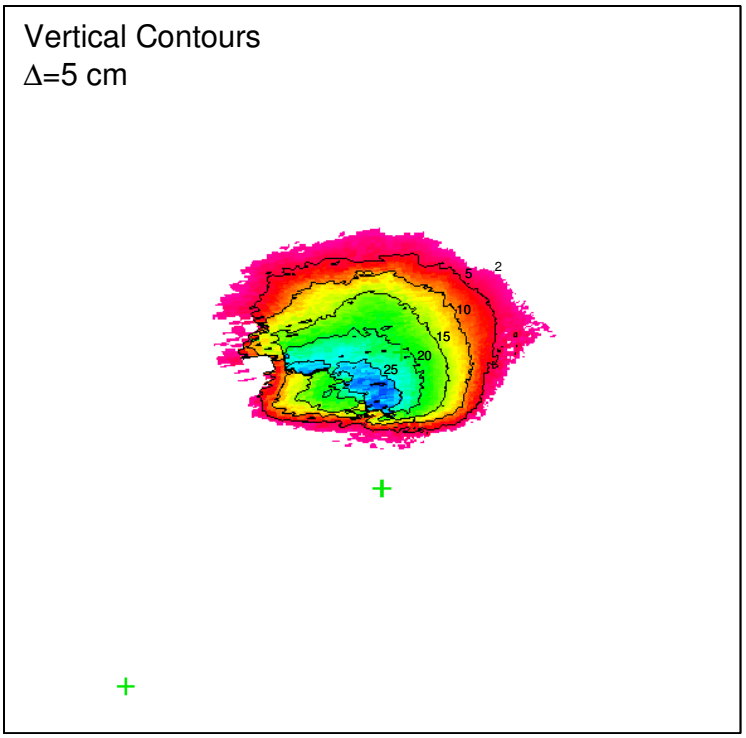

Figure 6. Vertical contours are combined with a color scale. For visual clarity, measurements outside the main feature, with values of 2 cm or less, have been removed.

2.4 Google Earth View

Figure 7 shows a Google Earth composite with the InSAR vertical displacements. The InSAR data have been filtered so as to remove measurements outside the main feature, with displacements of less than 2 cm. This results in a better visual representation of the data.

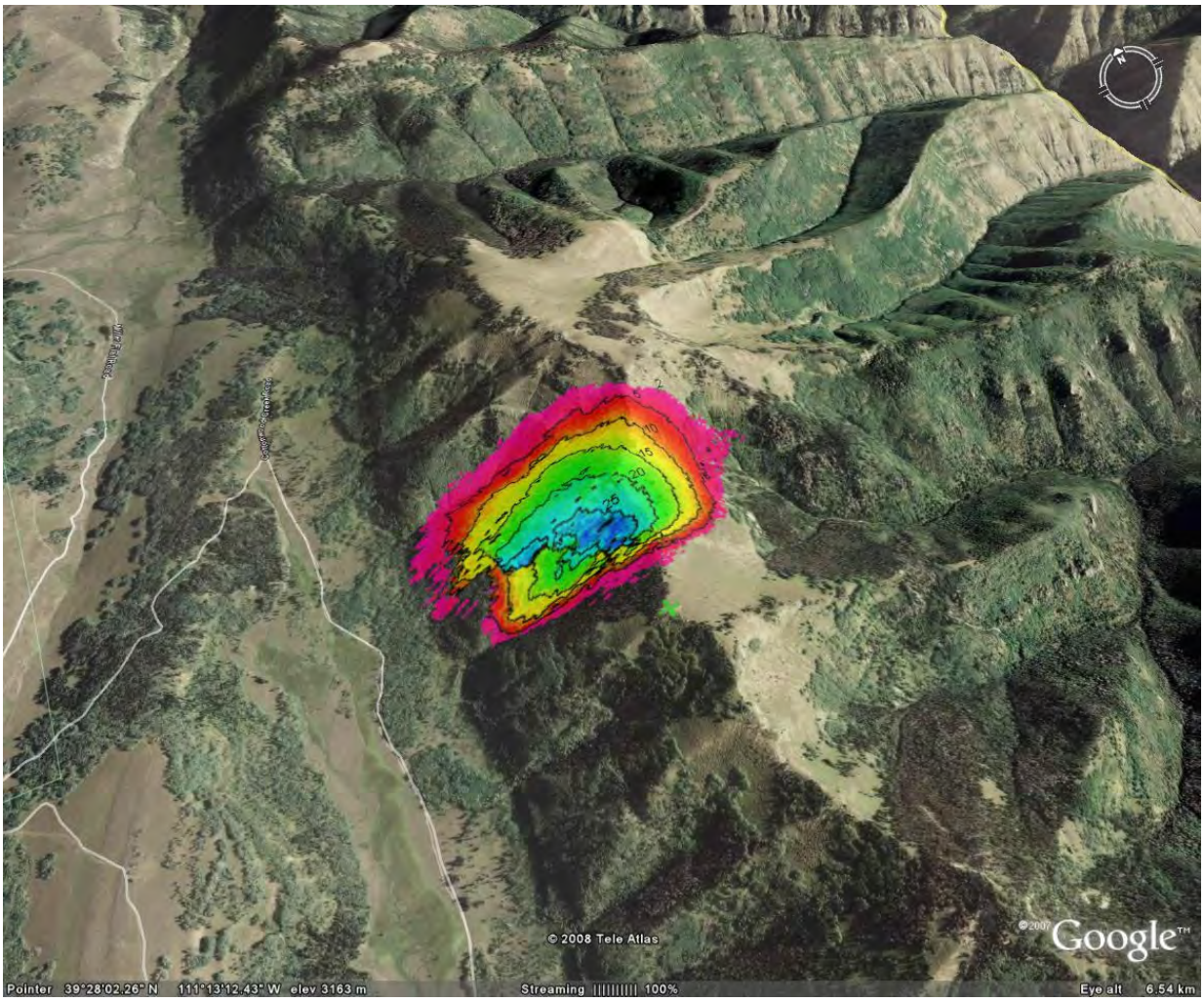

Figure 7. Google Earth composite image.

University of Utah Seismograph Stations

Continuous earthquake monitoring has been conducted at the University of Utah since 1907. The University of Utah Seismograph Stations (UUSS) is an entity within the Department of Geology and Geophysics. The mission of the UUSS is primarily academic research while also providing earthquake information to the general public and public officials. The UUSS is also a participant in the Advanced National Seismograph System (ANSS). The mission of the ANSS is to provide accurate and timely data for seismic events.

The UUSS maintains a regional/urban seismic network of over two hundred stations. An average of one thousand seismic events is detected in Utah each year. The number of events depends on the magnitude threshold of reporting. The number of recorded events includes those from natural sources (tectonic earthquakes) as well as those related to mining activity. In the Wasatch Plateau and Book Cliffs mining areas, at least 97% of the events have been identified as being related to mining activity. These events are termed mining-induced seismicity. Both tectonic and mining-induced seismic events can be referred to as earthquakes.

The majority of coal mining in Utah occurs in the Wasatch Plateau and Book Cliffs area. The coal fields form the shape of an inverted "U" in Carbon and Emery counties. In the coal mining region, nearly all the seismic events are mining-induced. Again, the number of events depends on the magnitude threshold. Special studies have recorded several thousand such events in a single year. Figure 104 is a plot of mining-induced seismicity from 1978 to 2007. Over 19,000 events are included. Mining-induced seismicity occurs regularly from normal mining activity in the Utah coal fields.

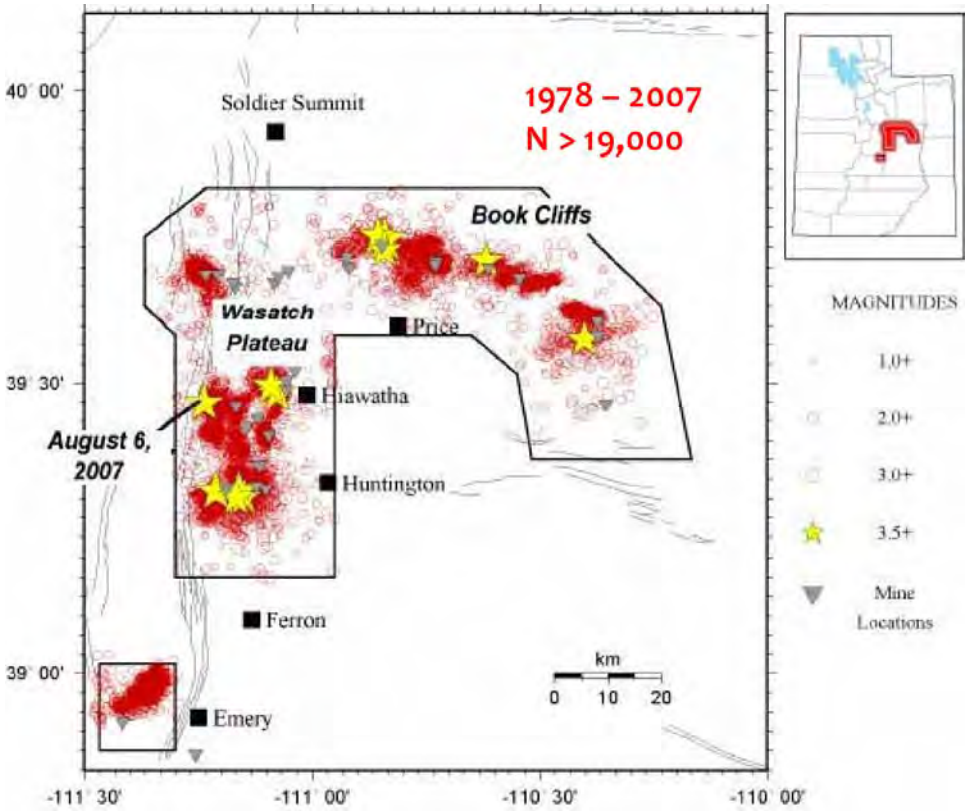

Figure 104 - Mining-Induced Seismicity in Utah
(from W. Arabasz presentation to Utah Mining Commission, November 2007)

The regional seismograph network includes several stations situated in the mining region. The location of these stations is shown in Figure 105. The stations are connected by telemetry to the UUSS central recording laboratory.

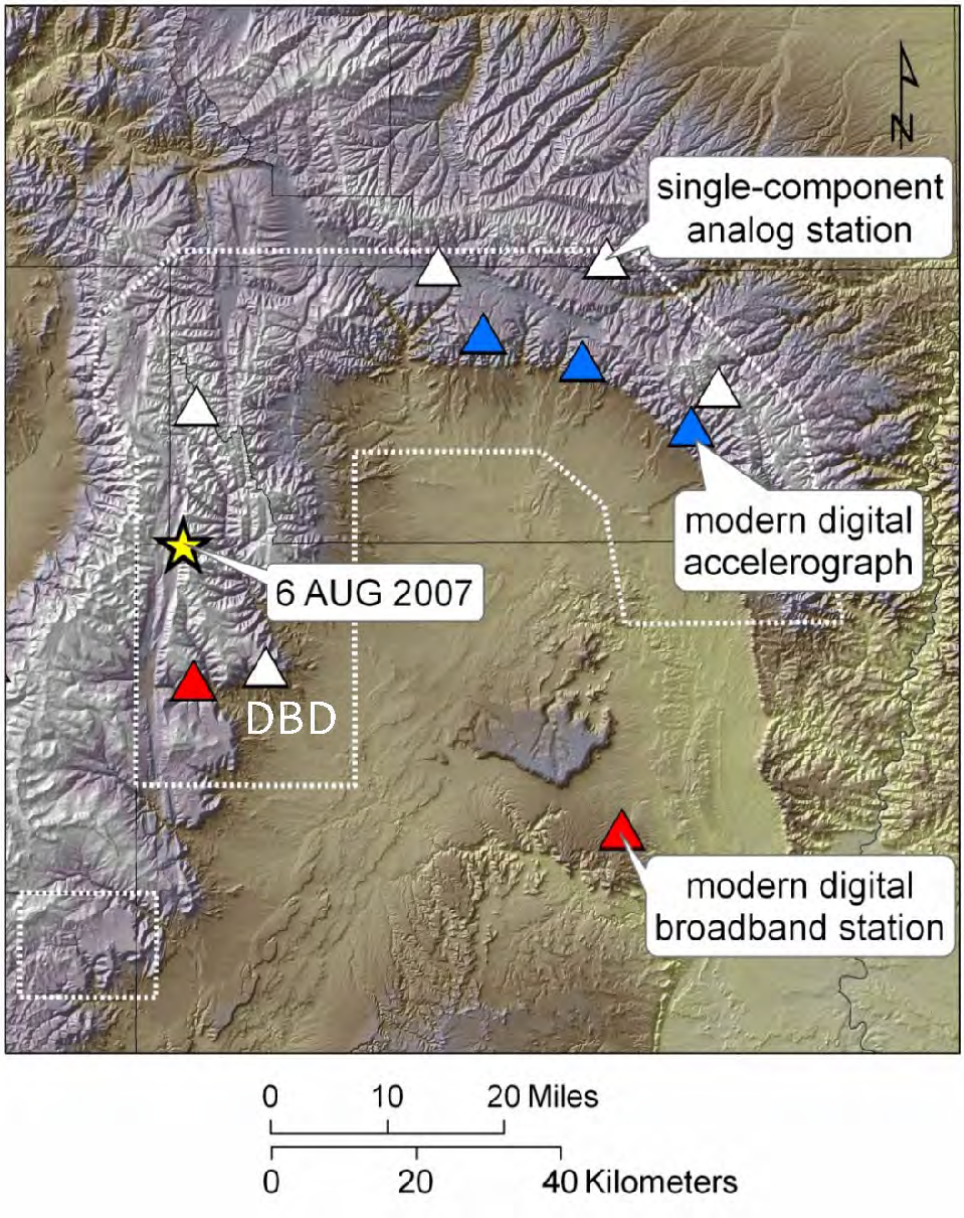

Figure 105 - Locations of UUSS Seismographs in the Wasatch Plateau In the Book Cliffs Mining Area[24]

Seismic Event Locations and Magnitudes

The magnitude of earthquakes is often reported in terms of the local magnitude (M_L). The local magnitude scale is a logarithmic scale developed by Charles Richter to measure the relative sizes of earthquakes in California. The scale was based on the amplitude recorded on a Wood-Anderson seismograph. The scale has been adapted for use around the world and is also known as the Richter scale.

Many additional scales have been used to measure earthquakes. Most scales are designed to report magnitudes similar to the local magnitude. The coda magnitude (M_C) is based on the length of the seismic signal. The coda magnitude scale used by the UUSS was calibrated to

provide similar results on average with the local magnitude scale for naturally occurring earthquakes. The UUSS has observed that mining related seismic events are shallow compared to most naturally occurring earthquakes and the duration or coda tends to be longer. This results in a slightly higher coda magnitude than local magnitude for mining-induced events.

It was not possible for the UUSS to calculate the local magnitude for all events. The coda magnitude was available for all reported events. While the local magnitude or M_L was the preferred scale, to maintain consistency, the coda magnitude or M_C was used in this report except where noted. The coda magnitude for the 3.9 M_L event on August 6, 2007, was 4.5.

Following the August 6, 2007, event, a location was automatically calculated and posted on the UUSS and USGS websites. The plotted location was not over the Crandall Canyon Mine and contributed to speculation that the event was not mining-related.

The location of a seismic event is determined by the travel times to each seismograph station and the velocity of the seismic wave through the earth. The velocity varies with depth. To calculate locations, a model of the velocity at different depths needs to be created. Any difference between the velocity model and actual velocities or lateral non-homogeneity in actual velocities can result in errors in the location.

Depths of the events were difficult to determine due to the distance to the nearest recording station and the shallow depths involved. According to UUSS seismologists, in order to accurately determine the depth of a seismic event, a seismograph station is generally needed at a distance less than or equal to the depth of the event. Because the depth of the August 6, 2007, accident was approximately 2000 feet, and the nearest station was approximately 11 miles away, the initial calculated depths were uncertain.

The UUSS deployed five additional portable units to the site to improve their ability to locate seismic events. Installation of the portable units began on August 7 and was completed on August 9, 2007.

A review of the seismic data revealed that several seismic events could be correlated to coal bursts that were observed underground. Known locations could be used to reduce the effect of errors in the velocity model, thus improving the accuracy for locating other events. Therefore, MSHA provided Dr. Pechmann of the UUSS with the known location of the August 16, 2007, accident to use as a fixed point to improve the locations for the other events. Two different methods were used by UUSS to improve the locations.

The first method was the calibrated master event method. In this method, corrections were made to the arrival times to fit the August 16 event to the known location. For each other event, the corrections were applied and new locations calculated. These corrections were applied to 189 recorded events going back approximately two years to August 2, 2005. This method relocated the August 6, 2007, event to the North barrier section at approximately crosscut 149.

The second method used by UUSS was the double difference method. This method determines the relative location between multiple events by minimizing differences between observed and theoretical travel times for pairs of events at each station.[25] Only 150 of the 189 events could be located using this method. Figure 106 shows the progressively refined locations for four selected events together with their known locations and the calculated locations for the August 6, 2007, accident. Shown on the figure are the initial standard locations, the locations as revised by the

master event method, and the locations as revised by the double difference method. As shown on the figure, the double difference locations match the known locations most closely. The location for the August 6 accident is given at the No. 3 entry of the South Barrier section between crosscuts 143 and 144. The August 6 accident was known to extend over a wide area. Because locations of seismic events are determined by the first arrival of the seismic waves, only the location of the initiation of the August 6 accident can be calculated. Therefore, the location shown indicates where the event began, not the center of the event.

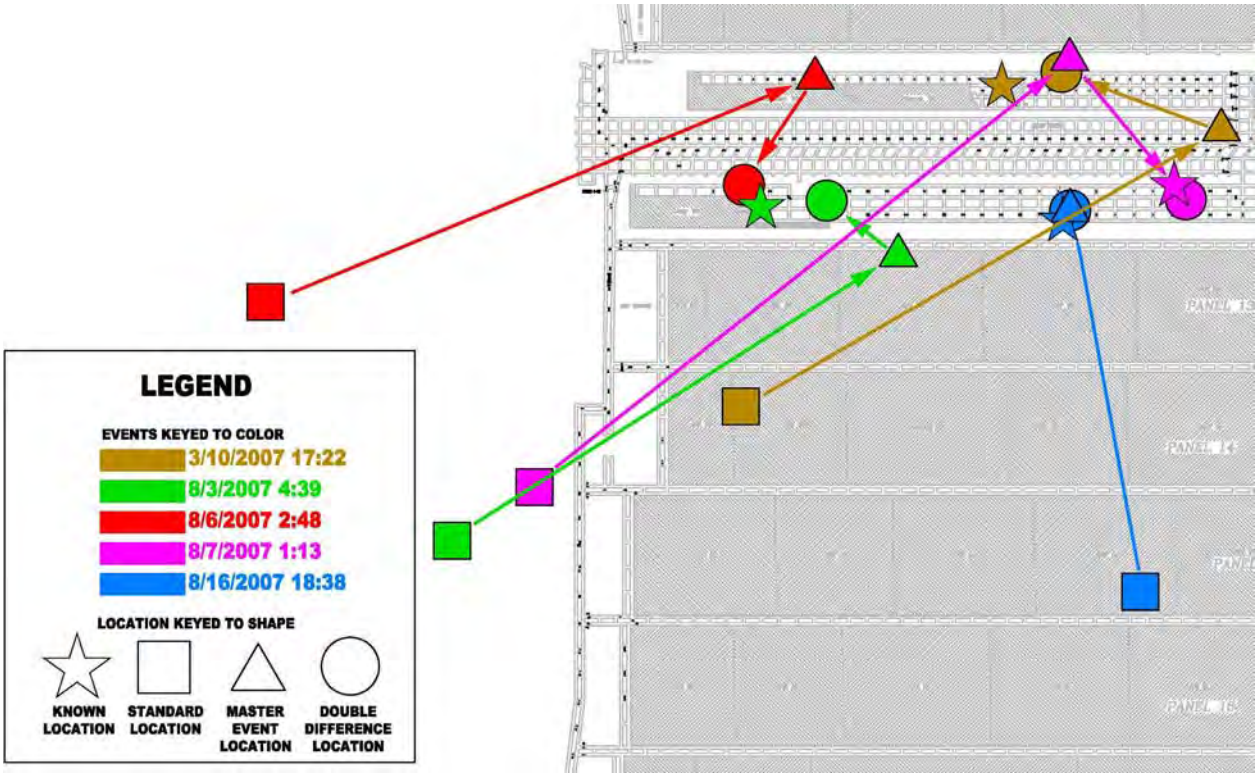

Figure 106 – Locations of Selected Events showing Progressive Refinements Using Three Methods

A review of mine records and records from the rescue and recovery operations revealed that ten events were both noted underground and recorded by the UUSS. Figure 107 shows the high degree of correlation with the underground locations and the double difference locations calculated by the UUSS. This provides some measure of the accuracy of the locations. Only the location of the August 16, 2007, accident had been provided to the UUSS. Excluding the August 16 accident event that was used for calibration, the mean distance between the reported locations and calculated locations was 450 feet. The median distance was 421 feet.

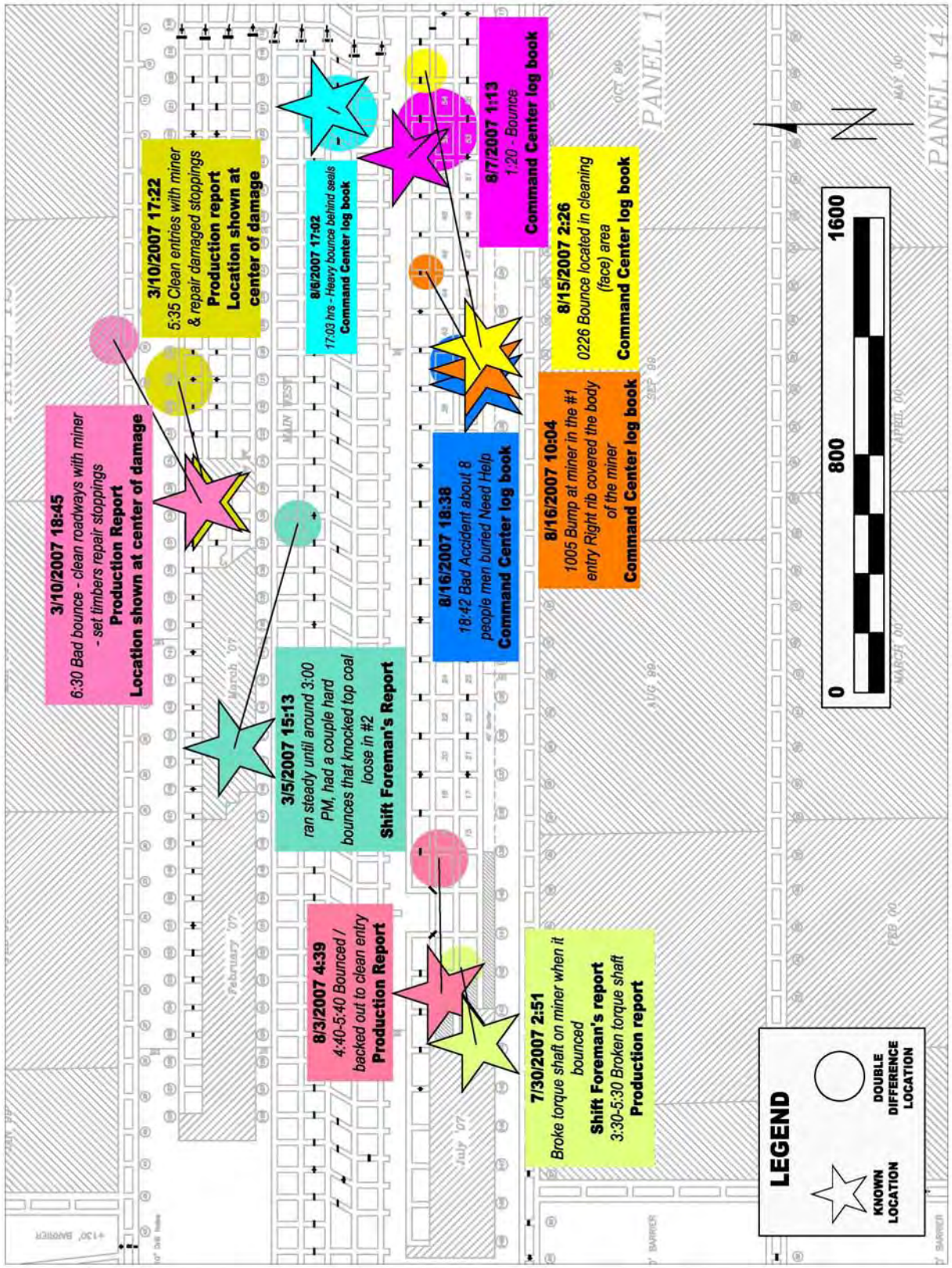

Figure 107 - Observed and Calculated Locations for Events

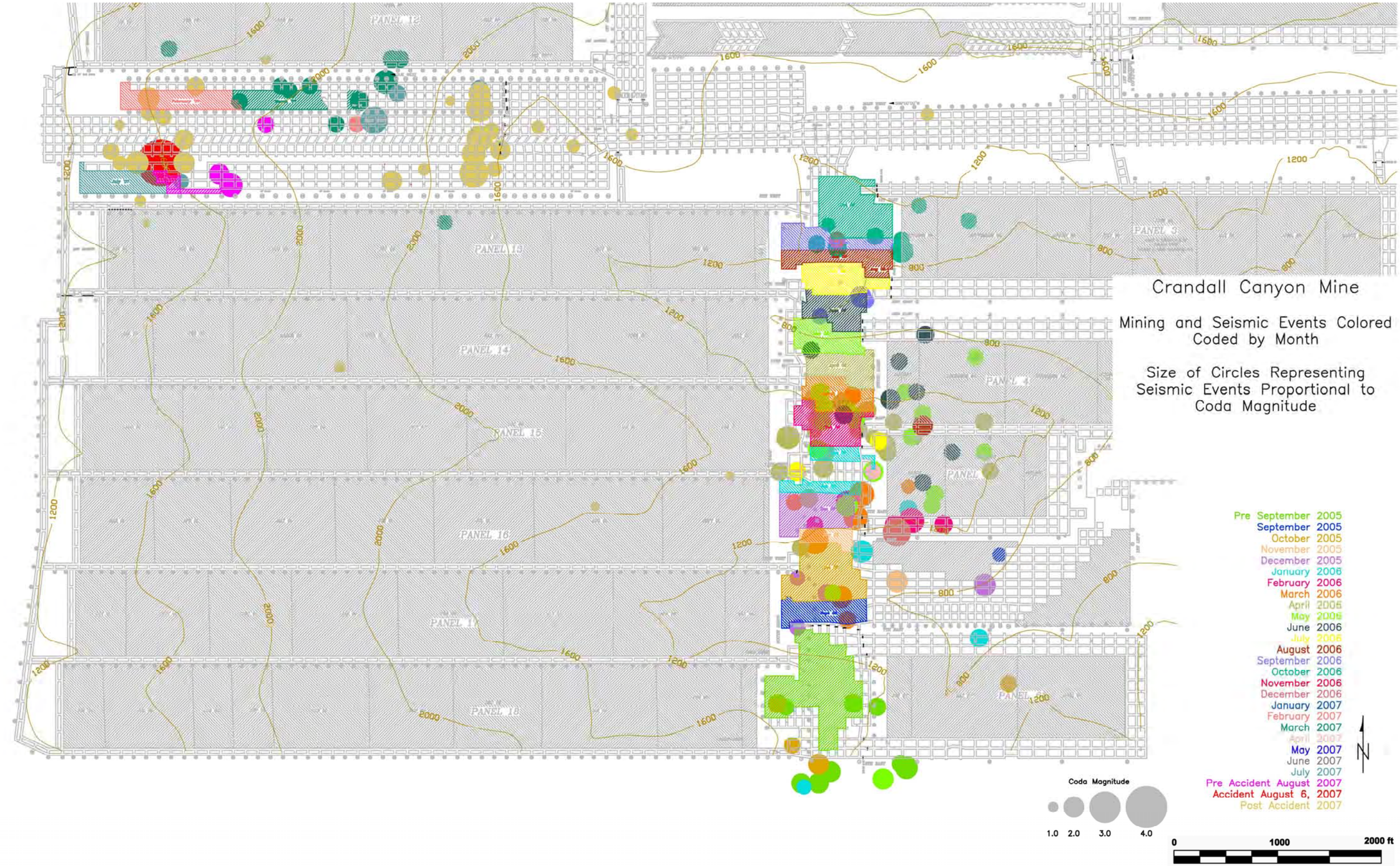

Figure 108 - Calculated Double Difference Locations and the Location of Mining Color Coded by Month

Figure 108 shows all of the calculated double difference locations and the location of mining activity color coded by month. The symbols are sized according to the coda magnitude of the events. The double difference locations show a high degree of correlation with pillar recovery mining in South Mains and the Main West barriers.

Figure 109 shows the seismic location of the August 6, 2007, accident in red. The events occurring after the accident on August 6 and 7 are shown in tan. Events occurring on August 8 to 27 inclusive are shown in blue. The locations of seismic events occurring on August 6 and 7 are notably clustered along a north to south line near crosscut 120 of the South Barrier section. The location corresponds with the outby extent of the collapse in the South Barrier section as determined by underground observation in the South Barrier section entries and Main West inby the breached seal. The seismic events extend from the South Barrier to the North Barrier. The initiation point for the collapse is located at the western boundary of the area. The collapse would have progressed to the east. The continuing events may have been the result of residual stress at the edge of the collapsed area. The events colored in blue occurred later and may represent settling at the west end of the collapse area.

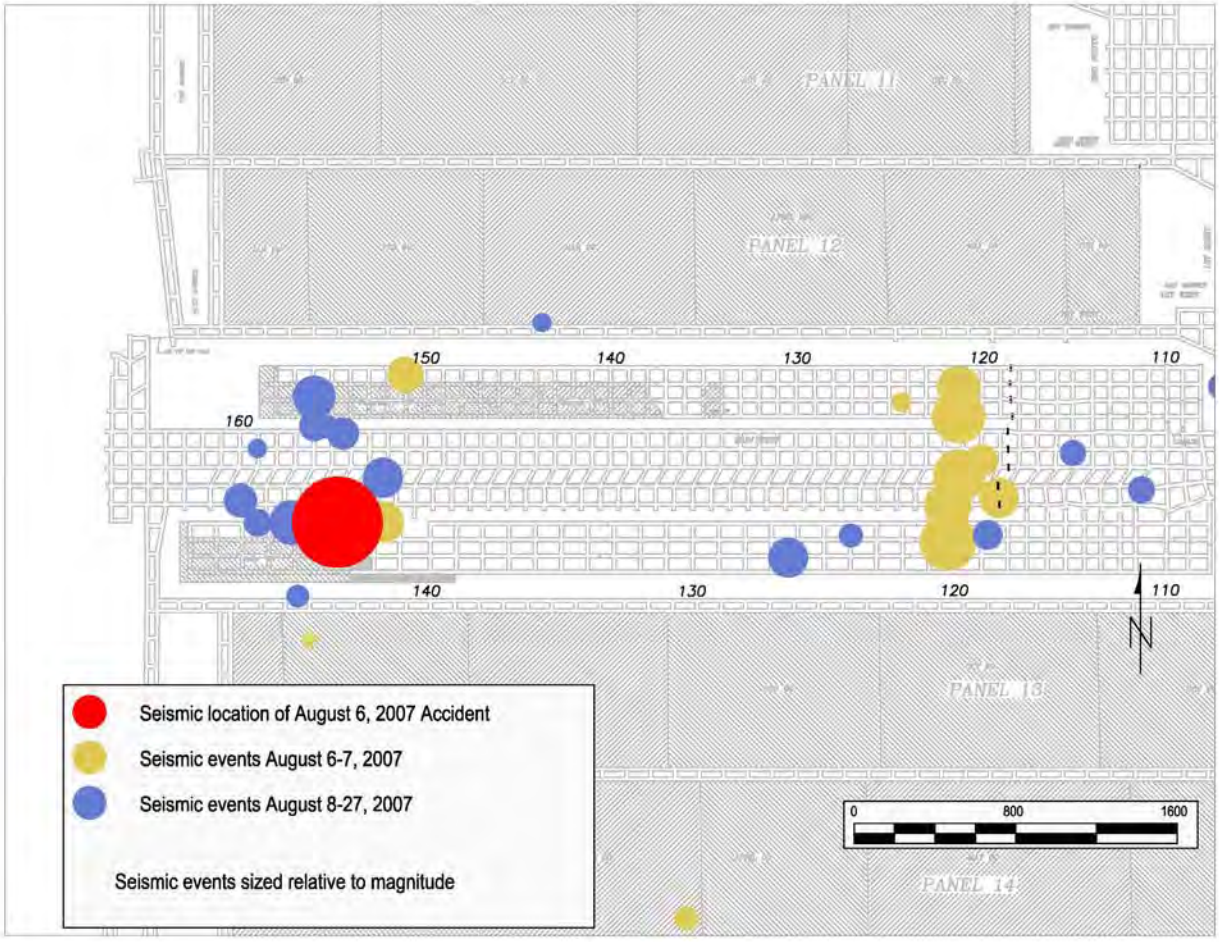

Figure 109 – Seismic Location of the August 6 Accident and Following Events

Analysis of the Seismic Event

The ground motions produced by the August 6, 2007, event were recorded on the UUSS seismographs. Earthquakes produce body and surface waves. Body waves travel through the interior of the earth. P-waves or primary waves and S-waves or secondary waves are types of body waves. P-waves are also known as compressional waves and consist of particle motion in

the direction of travel. P-waves travel faster than any other type of seismic wave and are the first to arrive at a seismograph station after an event.

A typical tectonic earthquake produced by a slip on a fault will result in part of the earth being placed in compression and part in dilation. This type of movement will typically generate P-waves with the initial or first motion on a vertical component seismograph in an upward direction or in compression at some locations and P-waves with a downward first motion or dilatation at other locations.

An analysis of the seismograph recordings from the August 6, 2007, event indicated that the initial or first motion recorded on a vertical component seismograph was downward in all cases (Pechmann 2008)[2]. This is characteristic of a collapse or implosion. Coal mining-related events are commonly collapse type events where caving or a coal burst has sudden roof-to-floor convergence. The lack of compressional or upward first motions is highly suggestive of a collapse but not conclusive. It may be possible that some upward first motions may have been missed. Figure 110 is a simplified diagram illustrating the types of motions expected for mine collapse and normal-faulting earthquakes.

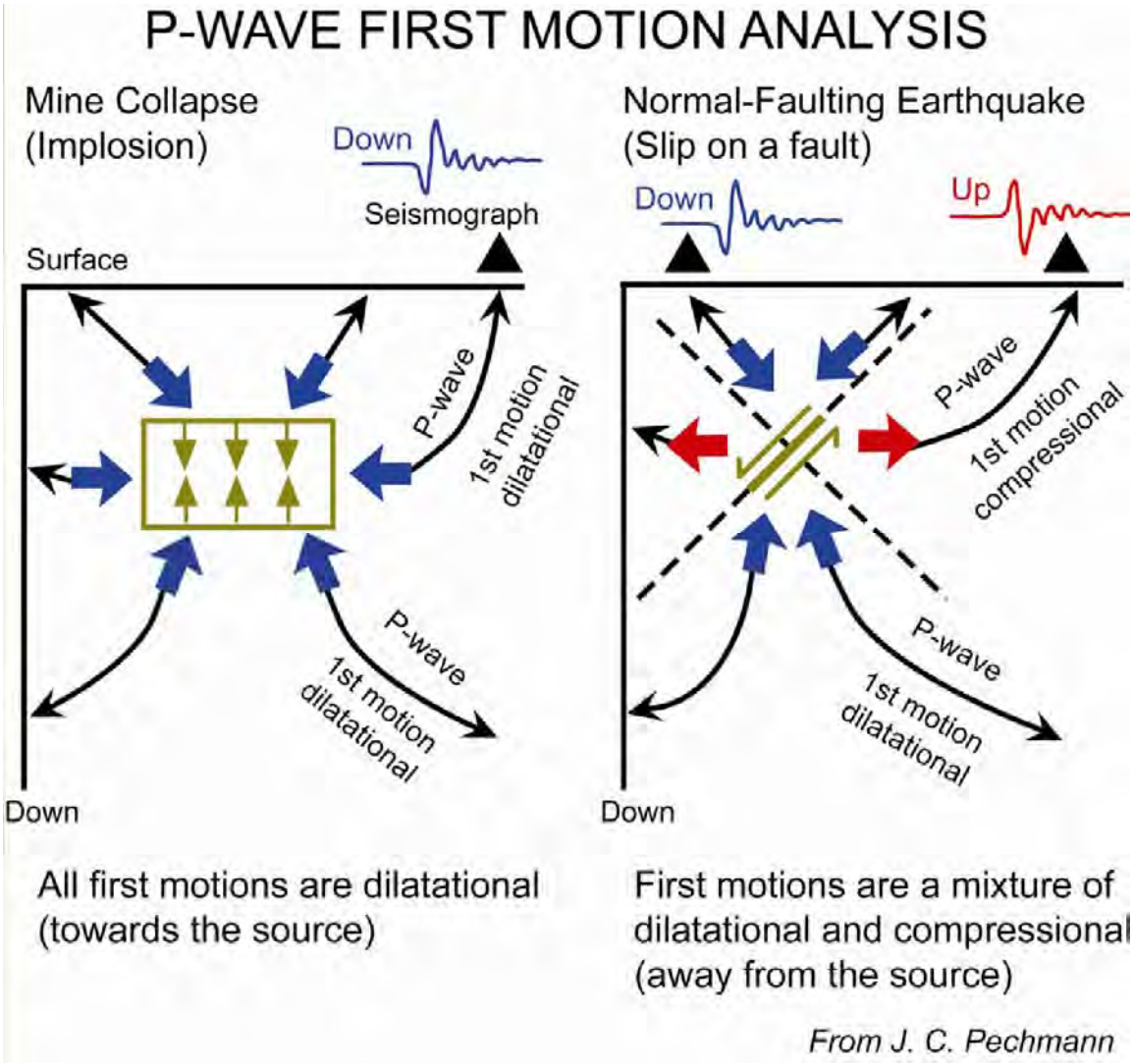

Figure 110 - P-Wave First Motion Analysis Examples
(from W. Arabasz presentation to Utah Mining Commission, November 2007)

Figure 111 shows the seismograph stations in place around the mining district as well as seismic waveforms of the vertical component from selected stations for the August 6, 2007, event. The waveforms are not shown to scale and are intended only to illustrate examples of first motions.

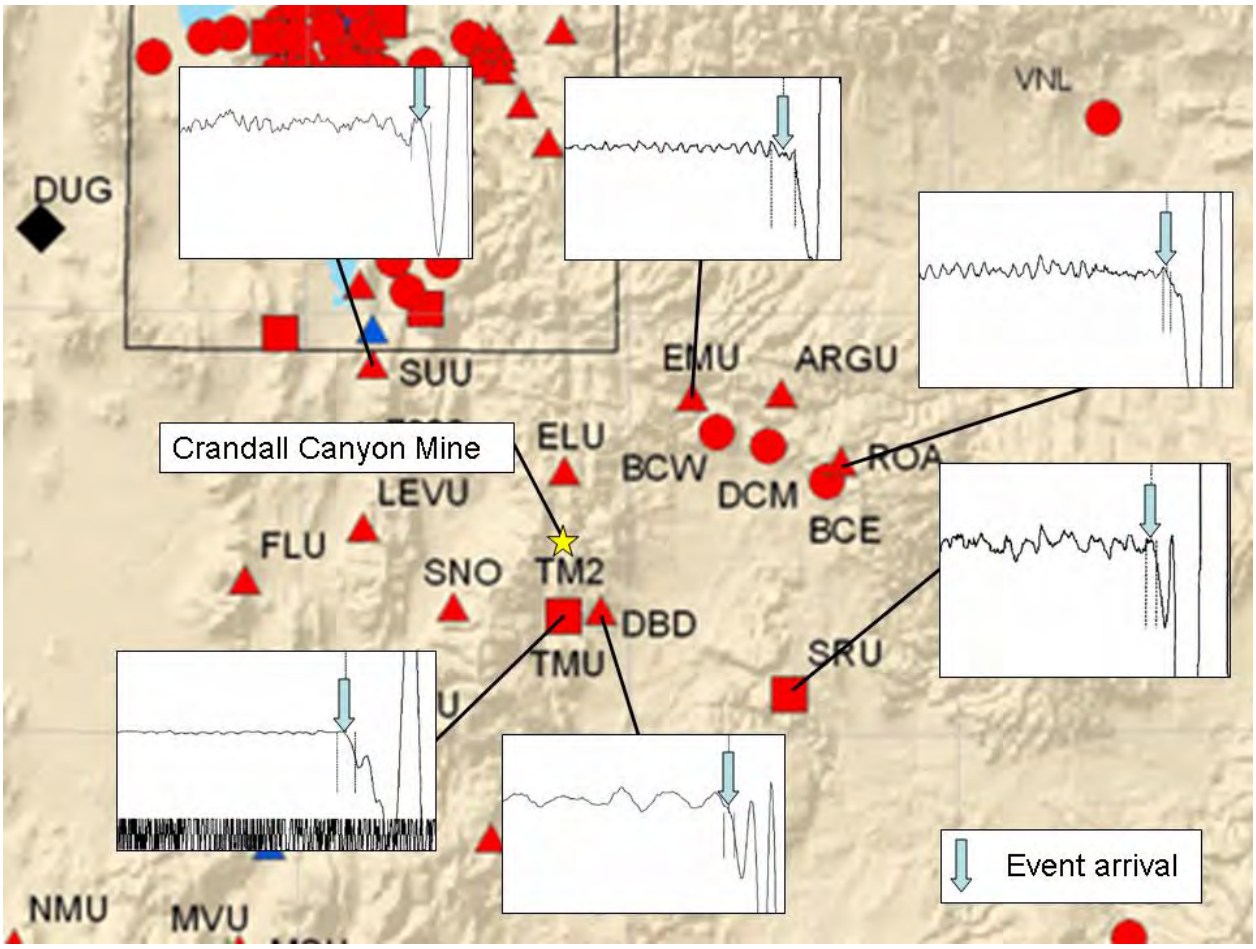

Figure 111 - Vertical Component Waveform Data for August 6, 2007 Event

The source mechanism of a mine collapse involves a change in volume at the source and is unusual compared to fault slip sources where the primary movement is slipping with no change in volume. These unusual mine collapse occurrences are of particular interest to persons engaged in monitoring to ensure compliance with the nuclear Comprehensive Test Ban Treaty. Considerable effort has been expended to distinguish man-made events from naturally occurring tectonic earthquakes.

As early as August 9, 2007, scientists at the University of California at Berkley Seismological Laboratory and the Lawrence Livermore National Laboratories studied the data and prepared a report titled *"Seismic Moment Tensor Report for the 06 Aug 2007, M3.9 Seismic event in central Utah"* that was made available on the UUSS website. A paper based on this analysis titled *"Source Characterization of the August 6, 2007 Crandall Canyon Mine Seismic Event in Central Utah"* also has been prepared[3]. The techniques employed in this analysis are beyond the scope of this report. However, the results can be summarized by Figure 112, reproduced from their paper, which shows seismic events plotted according to their source mechanism. The term DC refers to a double couple of forces or opposing forces which create shear or slip type movement resulting in natural earthquakes with no change in volume. The data for the August 6, 2007 event is shown as the red star. Its location characterizes it as an anti-crack or closing crack. This

would be consistent with an underground collapse. Natural or tectonic earthquakes plot near the center of this diagram. The orange star represents a natural tectonic earthquake of similar size that occurred on September 1, 2007 near Tremonton, Utah. The August 6 event is clearly outside this area. The explosion plotted in the figure was a nuclear test explosion. The three other collapses plotted were two trona mine collapses in Wyoming and a collapse of an explosion test cavity.

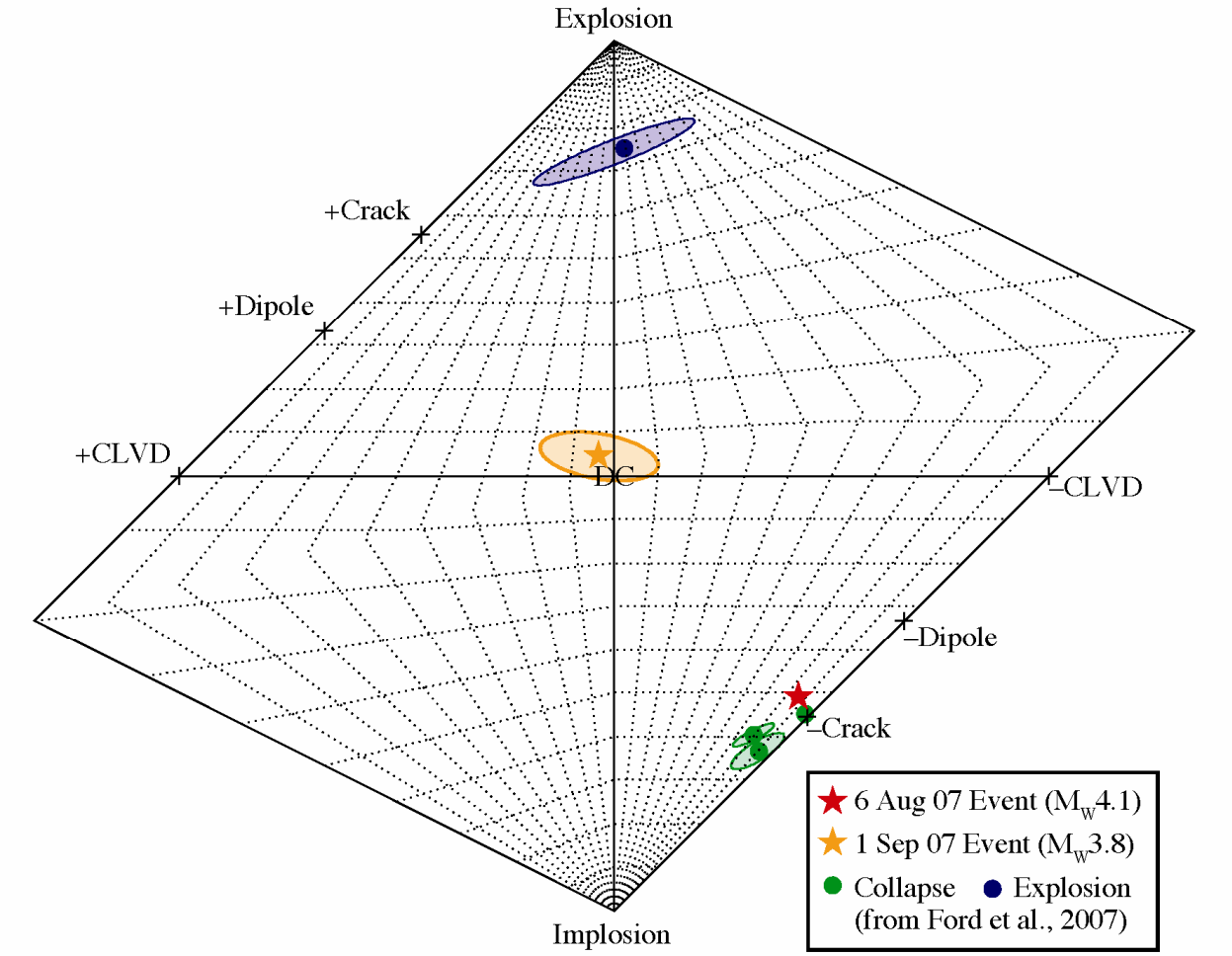

Figure 112 - Source Type Plot from Ford et al. (2008).

An analysis of the source depth for the August 6 event was conducted by Ford et al. (2008) Different depths for the event were assumed and the source type and variance reduction were calculated. Variance reduction is a measure of fit; the greater the reduction, the better the fit. Figure 113 shows the variance reduction results from the analyses in the inset box and the source type for the different assumed depths. As indicated, the shallowest depths (shown in red) result in the best fit. Even at depths up to 5 km, the source type remains as a closing crack and does not indicate the double-couple mechanism typical of natural tectonic earthquakes.

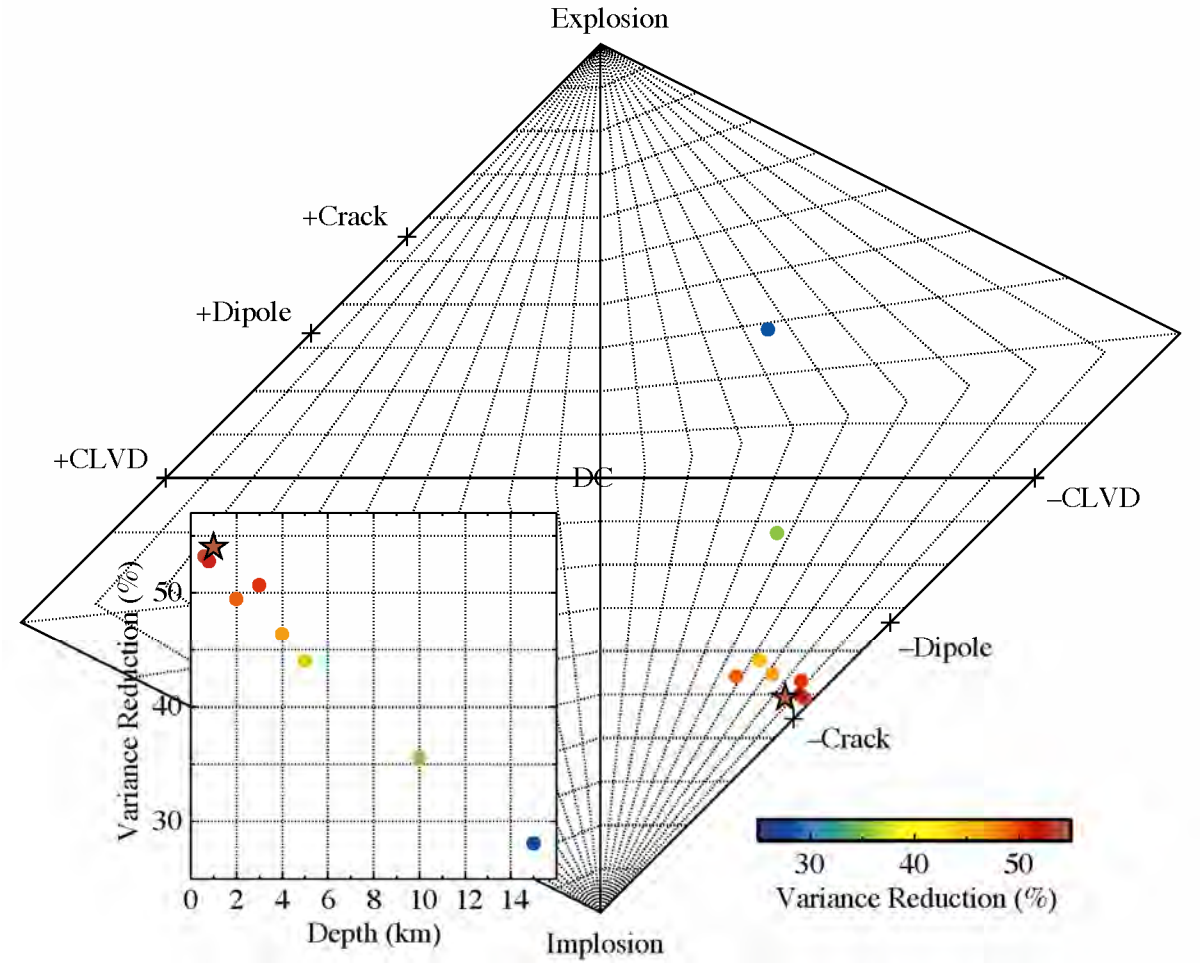

Figure 113 – Depth Analysis of August 6, 2007 event from Ford et al 2008.

Ford et al. (2008)[3] noted that while the primary and dominant source mechanism was a closing crack, the seismic record could not be explained by a pure vertical crack closure alone. Love waves that have motion horizontal to the direction of travel were present and can not be produced by the vertical closure. Possible explanations offered included that the collapse was uneven or that there was sympathetic shear on a roof fault adding a shear component to the collapse.

Pechmann et al. (2008)[2] similarly noted that while the event was dominantly implosional, there was a shear component. The most likely explanation offered was slip on a steeply dipping crack in the mine roof with a strike of approximately 150 degrees and motion downward on the east side.

Given that the event initiated at the west edge of the collapse area and seismic events occurred in the following 37 hours at the east edge of the collapse area (see Figure 109), the most likely explanation is that the event began at the western edge of the area and progressed eastward. The eastern edge, where the collapsed stopped, would have resulted in residual stress at the cantilevered edge and continued seismic activity.

Additionally, careful examination of the seismic waveforms by the UUSS did not reveal any indication of an event immediately preceding the main August 6, 2007 event. There was no evidence that the collapse was caused by an immediately preceding natural occurring event.

Duration of Seismic Events

It was initially reported in the media and by others that the August 6, 2007, event lasted four minutes. According to UUSS seismologists, the recorded length of vibratory motion of a seismograph will be orders of magnitude longer than the actual duration of the seismic source event. This is due to the arrival of seismic waves from many different and indirect paths. For example, the August 16 event generated one seismic record 63 seconds long[2] when the actual event was nearly instantaneous.

It is not straight forward to estimate the duration of a source event from the seismic record. The duration of the August 6 accident can be estimated by eye witness reports. One witness stated that the mine office building shook for several seconds and the shaking subsided quickly. None of the smaller events was reported to have any significant duration by underground witnesses. The building shaking may represent the collapse event and residual vibrations. The best estimate for the duration of the August 6, 2007, event is a few seconds.

Appendix O - Images of March 10, 2007, Coal Outburst Accident

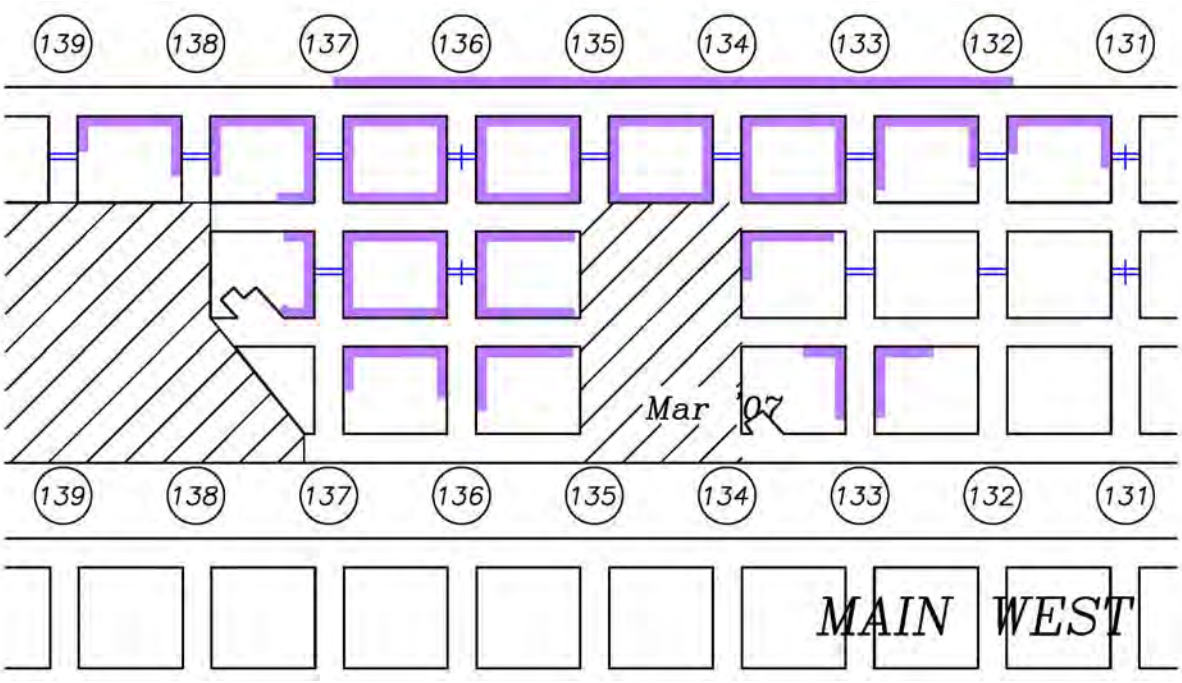

North Barrier Section after March 2007 Coal Outburst Accident

The following images were taken on March 16, 2007, during an investigation of the March 10, 2007, coal burst by Michael Hardy and Leo Gilbride of AAI and Laine Adair and Gary Peacock of GRI. A location diagram was inserted into each photo by the accident investigation team. The green arrow indicates the camera view point as determined from AAI's notes.


133
132
131
130

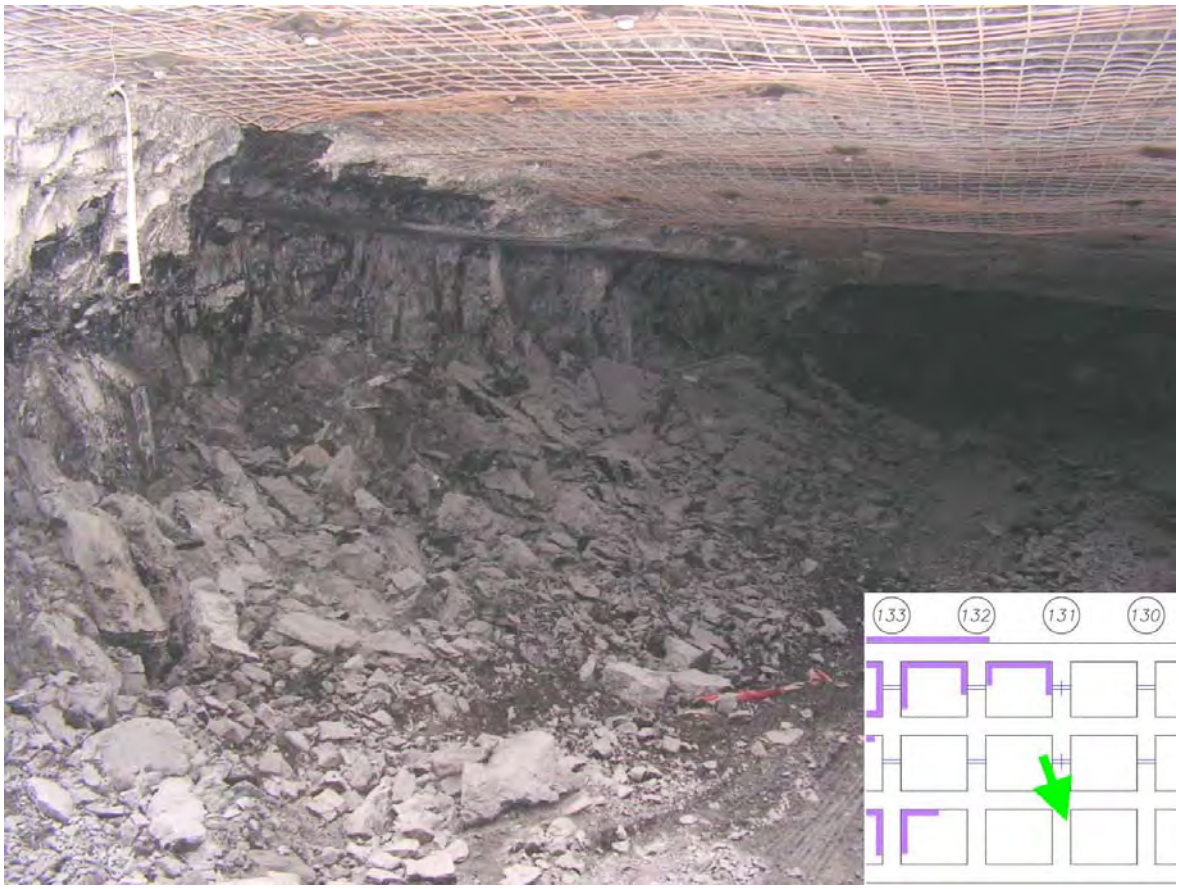
133
132
131
130

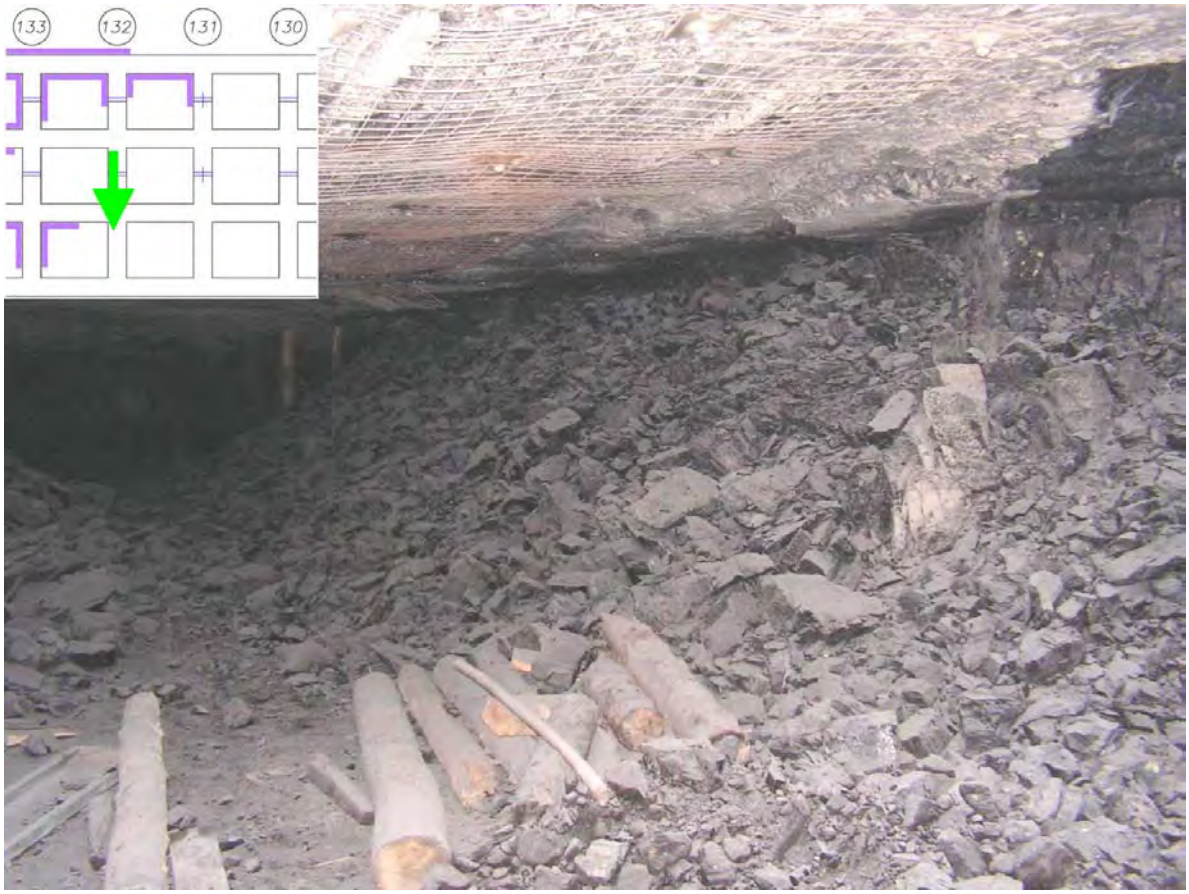
133
132
131
130


133
132
131
130


133
132
131
130

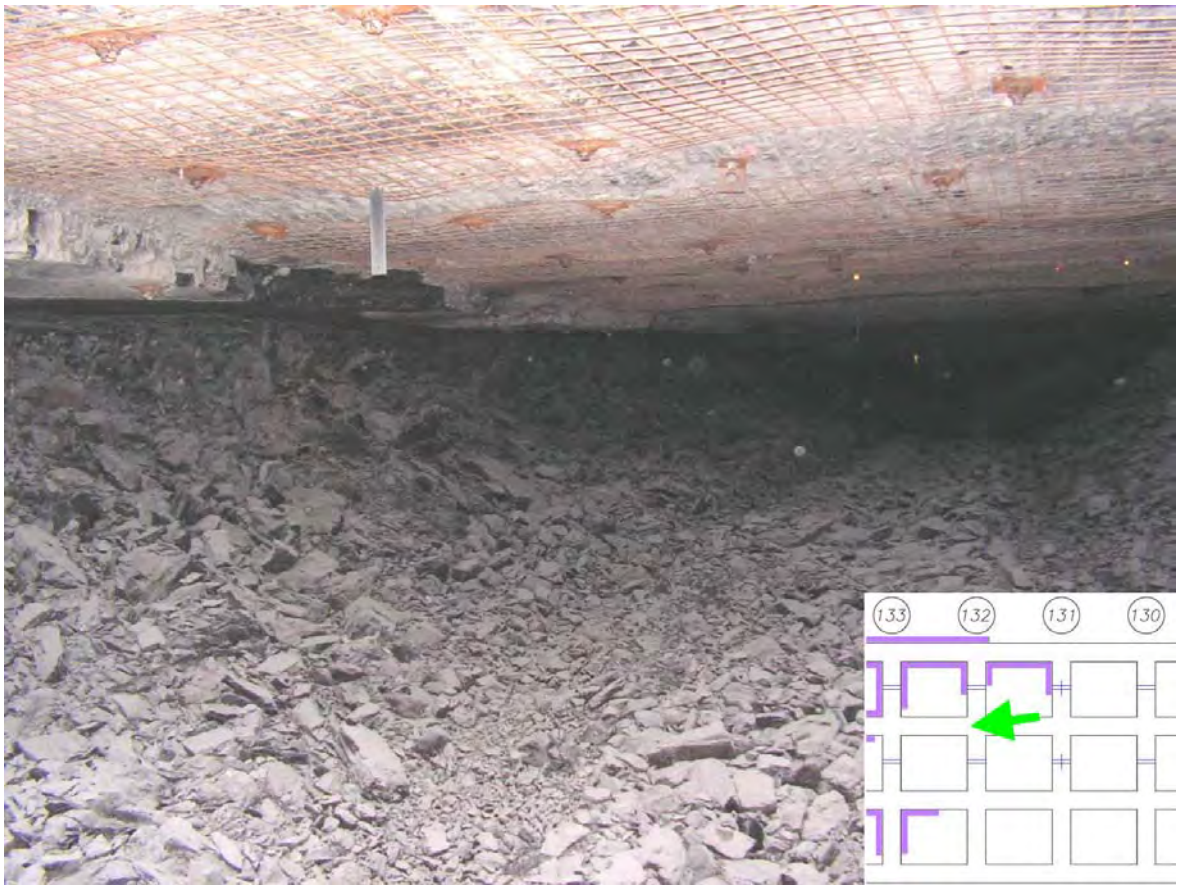
133
132
131
130


135
134
133
Mar
07

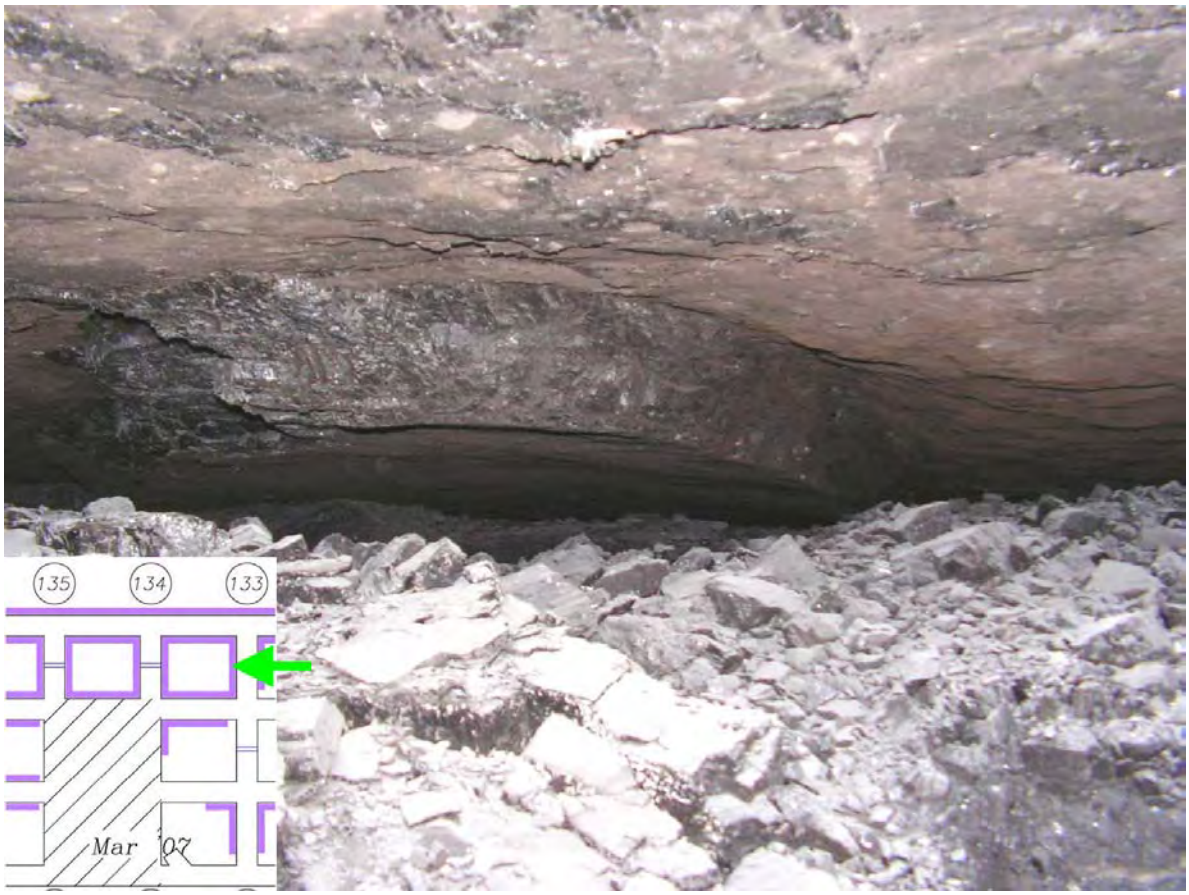
135
134
133
Mar
07

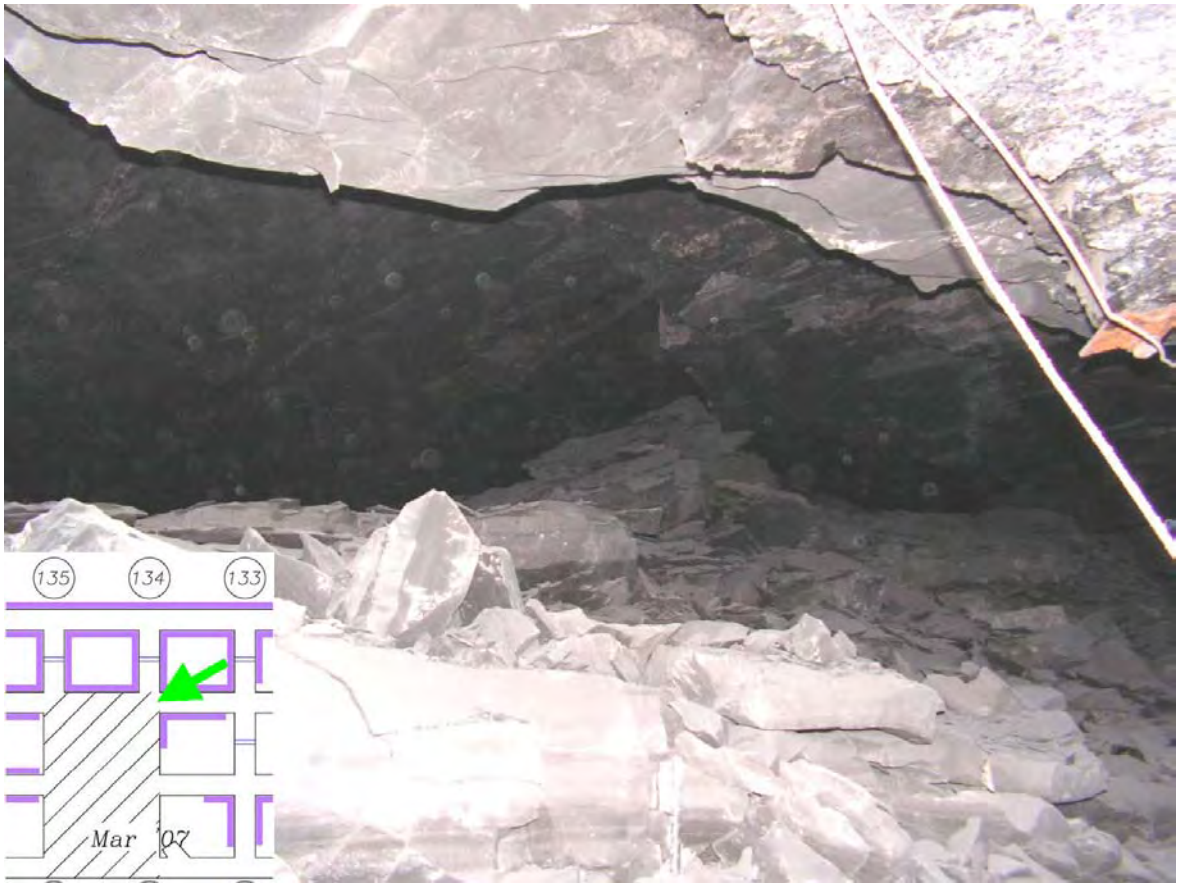
135
134
133
Mar 07

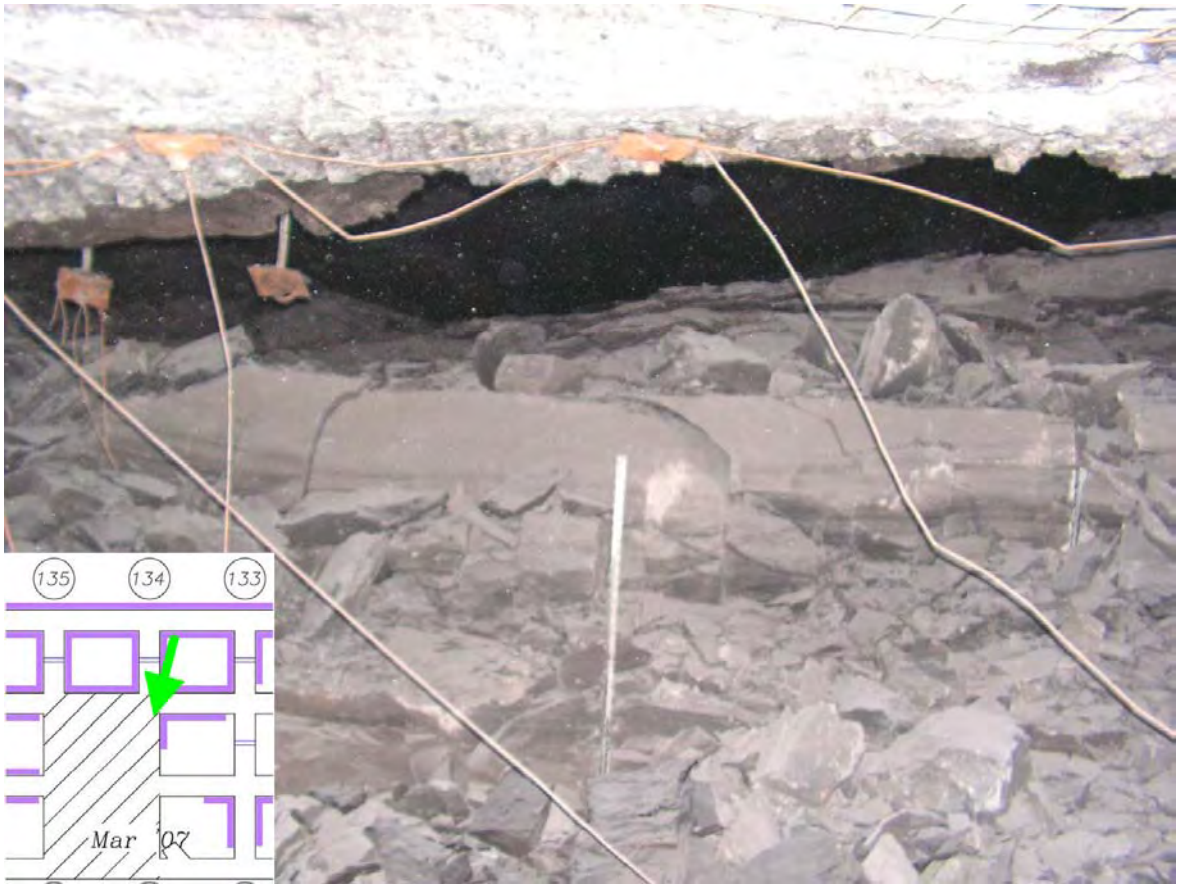
135
134
133
Mar 07


135
134
133
Mar

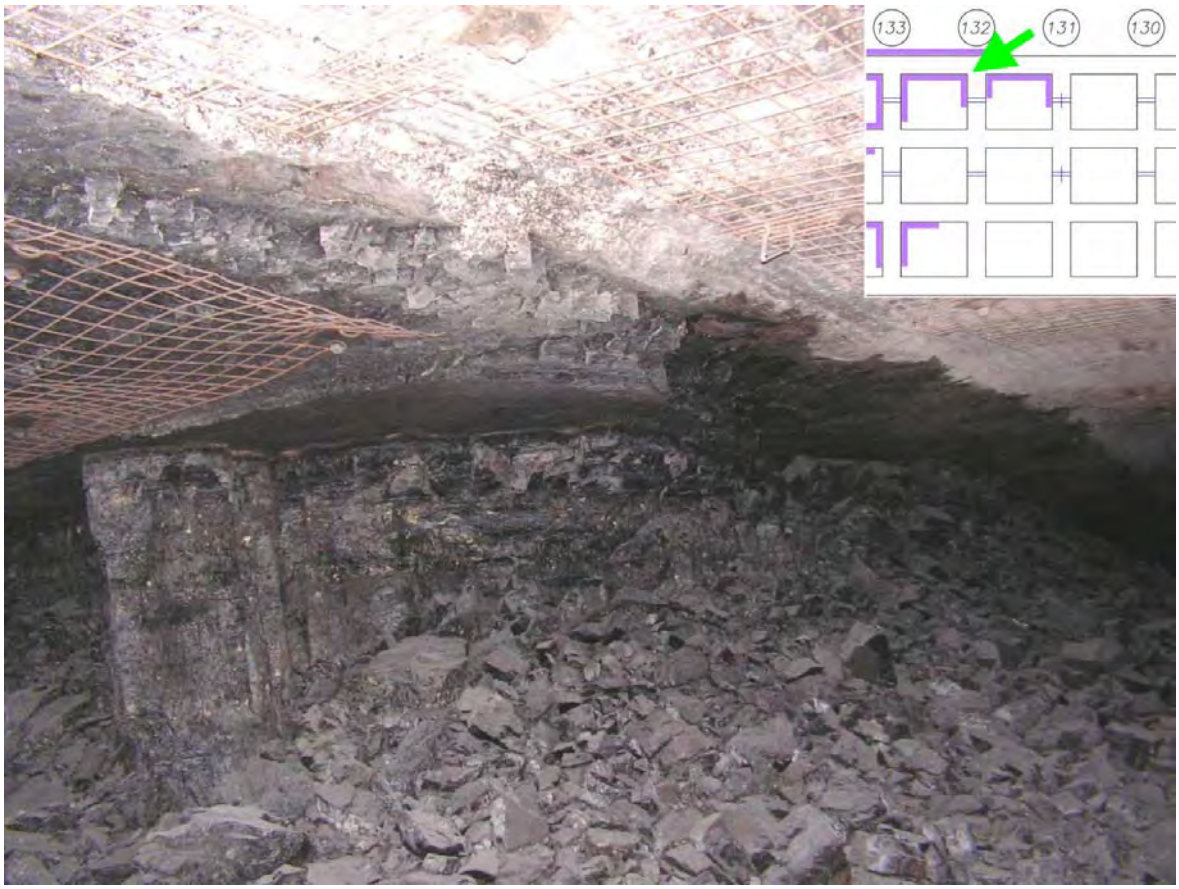
133
132
131
130


135
134
133
Mar '07


135
133
Mar '07


135
134
133
Mar '07


135
134
133
Mar '07


136
135
134
Mar


139
138
137
136

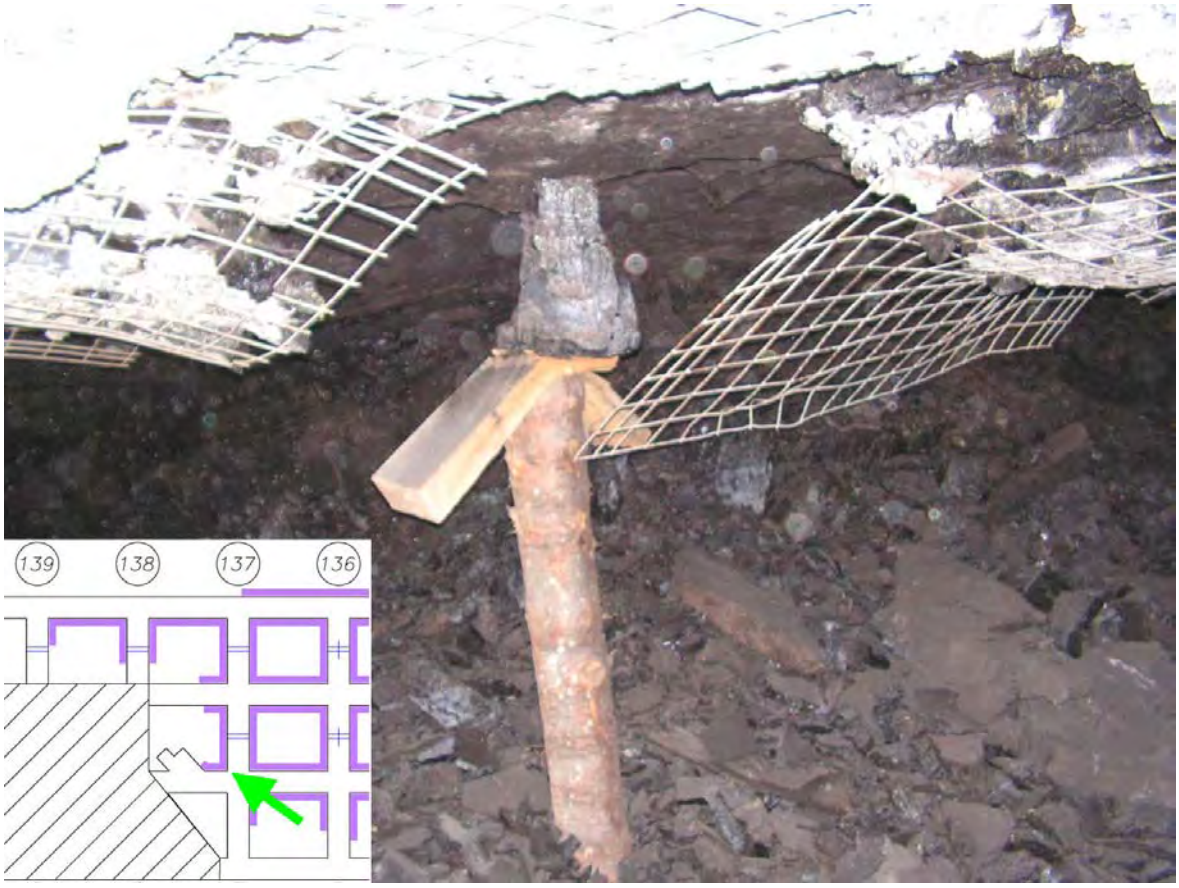
139
138
137
136

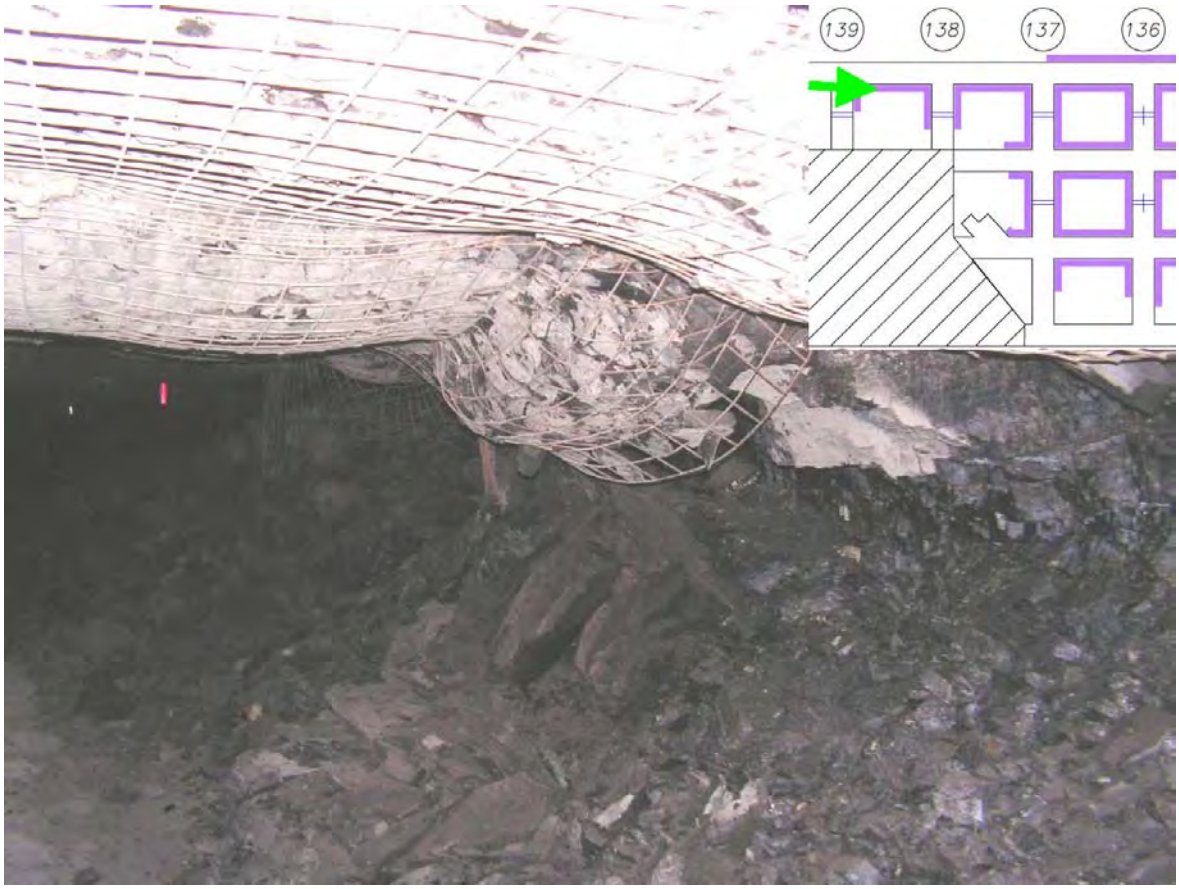
139
138
137
136

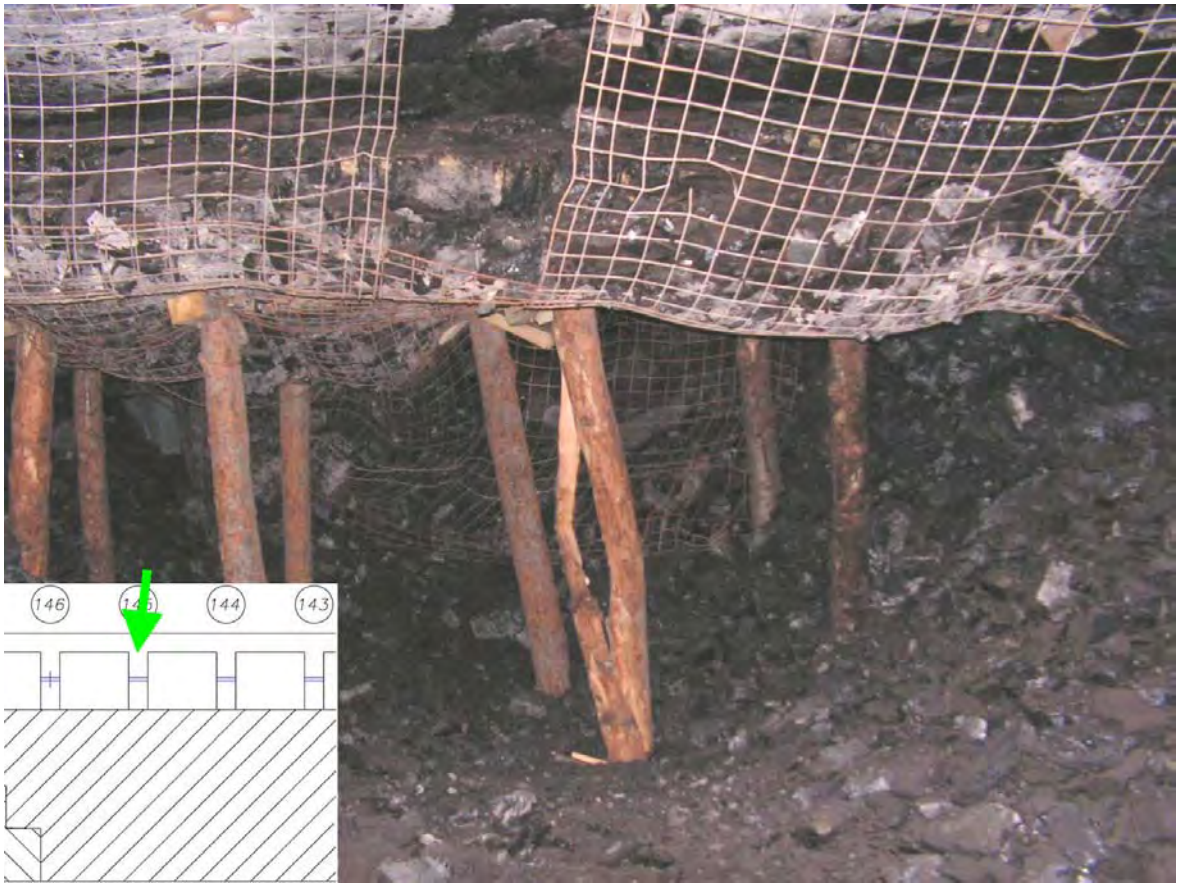
146
144
143

Appendix P- ARMPS Method Using Barrier Width Modified Based on Bearing Capacity

To account for the bleeder pillar being used as part of the barrier system, the bleeder pillar load bearing capacity is added to the load bearing capacity of the barrier to approximate the total load bearing capacity of the barrier system. This analysis method modifies the barrier width so that the load bearing capacity is adjusted to include a bleeder pillar. This process addresses those cases where the section pillar remains alongside the barrier pillar separating Active Gob and 1st Side Gob. The process involves mathematically modifying the barrier pillar system as outlined below:

1. Establish input parameters for mining geometry (i.e. overburden, pillar size, mining height, etc.).
2. Determine conventional stability factors by modeling the section as if all pillars are extracted. Note the PStF, BPStF, and remnant BPStF.
3. Note the load bearing capacity of the actual barrier width at the AMZ.
4. Note the load bearing capacity of the pillar that will be left alongside the barrier pillar.
5. Determine the equivalent load bearing capacity of a modified barrier system with the following:

$$\begin{matrix}\textit{Equivalent Barrier} \\ \textit{Capacity (tons)}\end{matrix} = \begin{matrix}\textit{Original Barrier} \\ \textit{Capacity (tons)}\end{matrix} + \frac{\textit{Pillar Capacity (tons) x AMZ Breath}}{\textit{Pillar Crosscut Center}}$$

6. Model the section with an Active Gob as retreating without the unmined section pillar (pillar line and section reduced by one pillar).
7. Modify the barrier width using the input screen, recalculate, and check the resultant barrier Capacity at the AMZ. Continue modifying the barrier width using this iterative process until the Equivalent Barrier Capacity is achieved.
8. Assign the resultant PStF for the AMZ, BPStF, and remnant BPStF as the values for the section pillars and the modified barrier pillar system stability values.

Appendix Q - Finite Element Analysis of Barrier Pillar Mining at Crandall Canyon Mine

by
William G. Pariseau
University of Utah

FINITE ELEMENT ANALYSIS OF BARRIER PILLAR MINING AT CRANDALL CANYON

Prepared for the Mine Safety and Health Administration
Arlington, Virginia

by

William G. Pariseau

University of Utah
Salt Lake City, Utah

May 26, 2008

CONTENTS

INTRODUCTION

This report discusses finite element analysis of mining in barrier pillars at the Crandall Canyon Mine in central Utah. Analyses are two-dimensional and represent vertical cross-sections from surface to about 1,000 ft (300m) below the mining horizon, the Hiawatha seam. The finite element program is UT2. This computer code has been in service for many years and well validated through numerous bench-mark comparisons with known problem solutions. UT2 has been used in many rock mechanics studies through the years, most recently in the study of inter-panel barrier pillars used in some Utah coal mines.

The study objective is to develop a better understanding of the strata mechanics associated with recent events (August, 2007) at the Crandall Canyon Mine. This mine is in the Wasatch coal field in central Utah, west of Price, Utah. There are three coal seams of interest in the stratigraphic column of the Wasatch Plateau, namely the Hiawatha seam and the overlying Cottonwood and Blind Canyon seams. Mining is not always feasible in every seam.

The Crandall Canyon property is developed from outcrop, as are almost all coal mines in Utah. Relief is high in the topography of the Wasatch Plateau region; depth of overburden increases rapidly with distance into a mine. Depth to the Hiawatha seam at Crandall Canyon varies with surface topography and ranges roughly between 1,500 and 2,000 ft (450 to 600 m). Thickness is also variable and of the order of 8 ft (2.4 m). Development consists of five nominally 20-ft (6-m) wide main entries separated by 70-ft (21-m) wide pillars driven in an east-west direction. Length of these main entries is about 17,700 ft (4,210 m). Six longwall panels were mined on either side of the main entries from entry ends near a major fault (Joe's Valley

fault) that strikes in a north-south direction. These panels were roughly 780 ft (234 m) wide by 4,700 ft (1,140 m) long on the north side of the main entries and 810 ft (243 m) wide by 7,040 ft (2,112 m) long on the south side. Panels were parallel to the main entries.

FORMULATION OF THE PROBLEM

Finite element analysis is a mature subject and a popular method for solving boundary value problems in the mechanics of solids and other fields as well [e.g., Zienkiewicz, 1977; Bathe, 1982; Oden, 1972; Desai and Abel, 1972; Cook, 1974]. In stress analysis, equations of equilibrium, strain-displacement relationships, and stress-strain laws are requirements met under the constraints of tractions and displacements specified at the boundaries of a region of interest. The method is popular, especially in engineering, because of a relative ease of implementation compared with traditional finite difference methods. The method has important advantages in coping with non-linearity and complex geometry.

Finite element analysis of mining involves computation of stress, strain, and displacement fields induced by excavation. Rock response to an initial application of load is considered elastic. Indeed the elastic material model is perhaps the *de facto* standard model in solid mechanics. However, the range of a purely elastic response is limited by material strength. Beyond the elastic limit, flow and fracture occur, collectively, plastic deformation, i.e., "yielding". Although strictly speaking inelastic deformation is elastic-plastic deformation, "plastic" is used for brevity. Plastic deformation may be time-dependent and various combinations of elastic and plastic deformation are possible, e.g., elastic-viscoplastic deformation allows for time-dependent plasticity beyond the elastic limit.

Generally, excavation takes place in initially stressed ground, so changes in stress are computed. When stress changes are added to the initial stresses, post-excavation stresses are obtained. These stresses may then be used to determine a local factor of safety, the ratio of strength to stress in an element. A safety factor greater than 1.0 indicates a stress state in the range of a purely elastic response to load. A *computed* safety factor less than 1.0 indicates stress beyond the elastic limit, while a safety factor of 1.0 is at the elastic limit where further loading would cause yielding. Unloading from the elastic limit induces an elastic diminution of stress. Safety factors less than 1.0 are physically impossible because yielding prevents stress from exceeding the elastic limit. However, in a purely elastic analysis, computed safety factors may be less than 1.0.

Elastic analyses offer the important advantages of speed and simplicity. Although safety factor distributions based on elastic analysis may differ from elastic-plastic analyses, the differences are not considered important especially in consideration of questions that may arise about the plastic portion of an elastic-plastic material model. Generally, the effect of yielding is to “spread the load” by reducing peak stresses that would otherwise arise while increasing the region of elevated stress.

Mine Geology

A drill hole log of hole DH-7 was used to define the stratigraphic column at Crandall Canyon. This hole is centrally located in the area of interest. Figure 1 shows a color plot of the stratigraphic column used in subsequent analyses. The Hiawatha seam is the thin gray line at the 1,601 ft (480 m) depth. A thickness of 8 ft (3 m) is indicated. Roof and floor are sandstone.

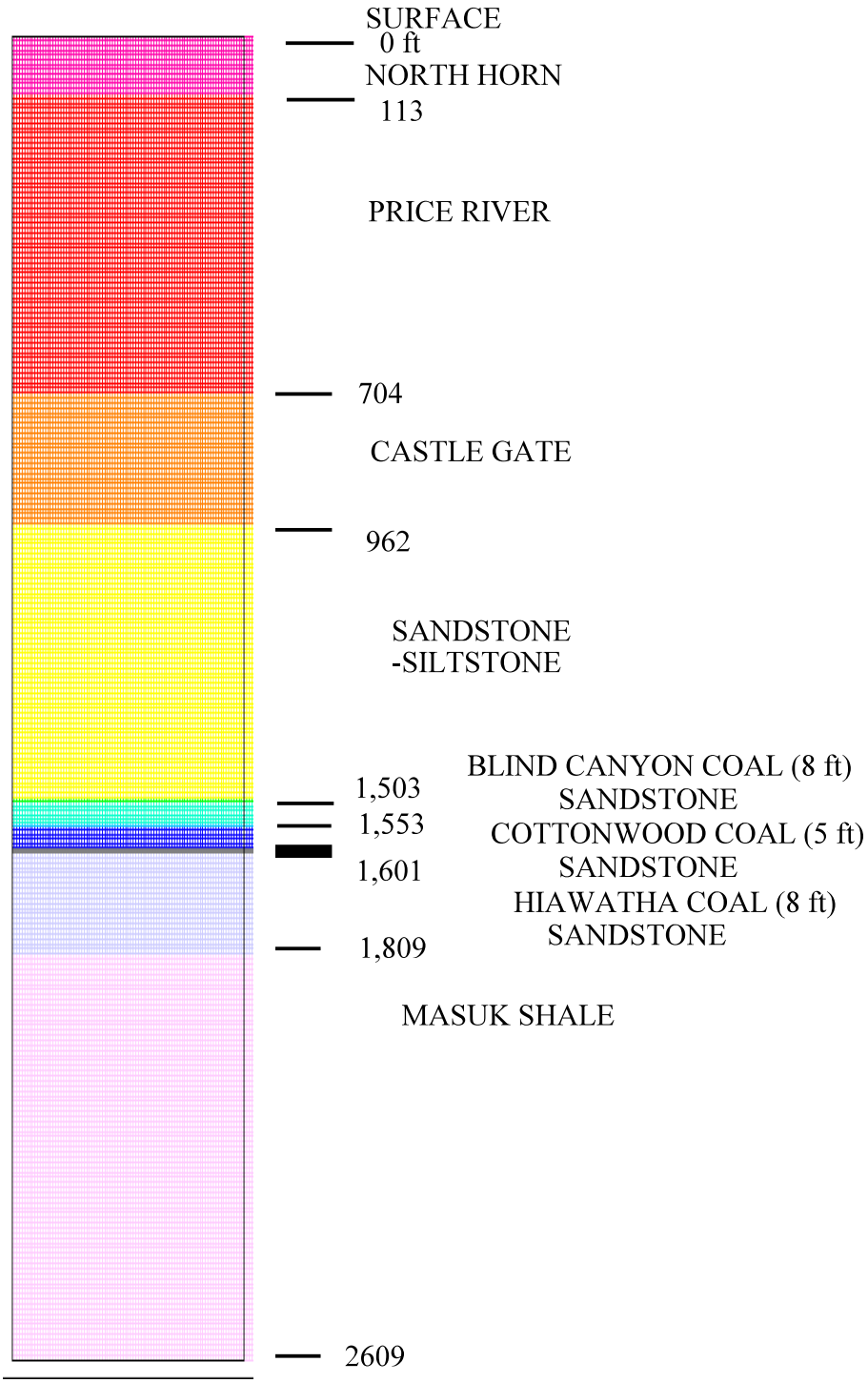

Figure 1. Stratigraphic column, formation names, depths in feet, seam names, and thicknesses (in parentheses in feet). There are 11 layers in the column.

Mine Geometry

The overall region used for analysis is shown in Figure 2 where the colors correspond to the same colors and rock types shown in the stratigraphic column (Figure 1). Details of the main entry geometry are shown in Figure 3. Elements in the mesh shown in Figures 2 and 3 are approximately 10 ft wide and 10 ft high (3.0x3.0 m), except at seam level where element height is 8 ft (2.4 m). Element size is a compromise between interest in detail at seam level and a larger view of panel and barrier pillar mining beyond the main entry development.

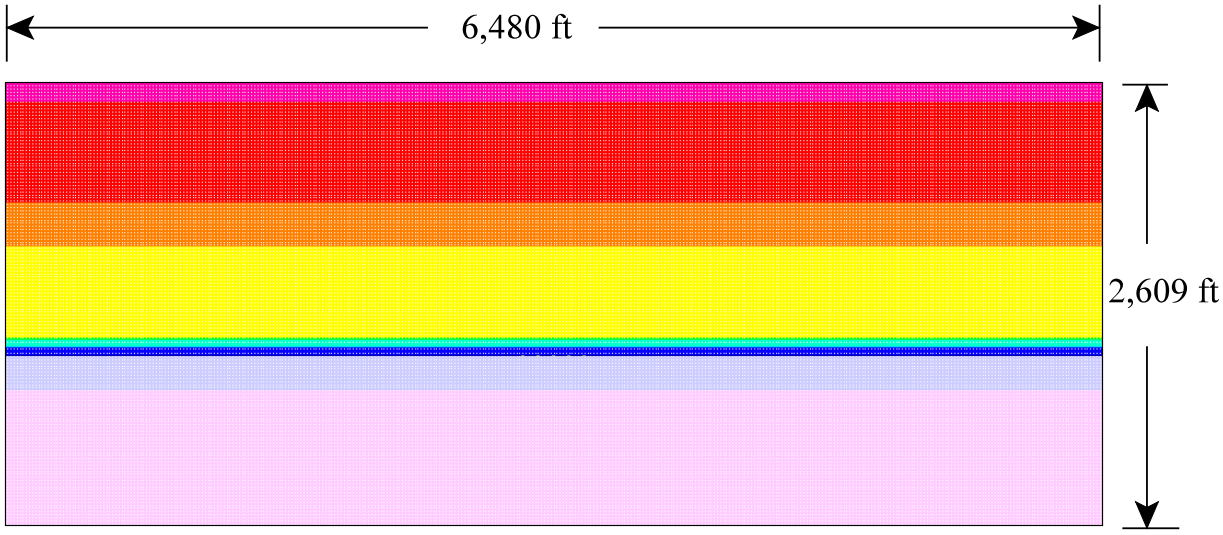

Figure 2. Overall finite element mesh geometry. There are 172,368 elements and 173,283 nodes in the mesh.

The mine geometry changes with development of the main entries and subsequent mining of longwall panels parallel to the mains and on both sides. Barrier pillars 450 ft (135 m) wide are left on both sides of the main entries as shown near seam level in Figure 4. Only 100 ft (30 m) of the future longwall panels are shown in Figure 4. Panels in the analyses are eventually mined 2,600 ft (780 m) on the north and south sides of the main entries. Panels, barrier pillars, main entries and entry pillars account for the 6,480 ft (1,944 m) wide mesh. Cross-cuts are not included in two-dimensional analyses.

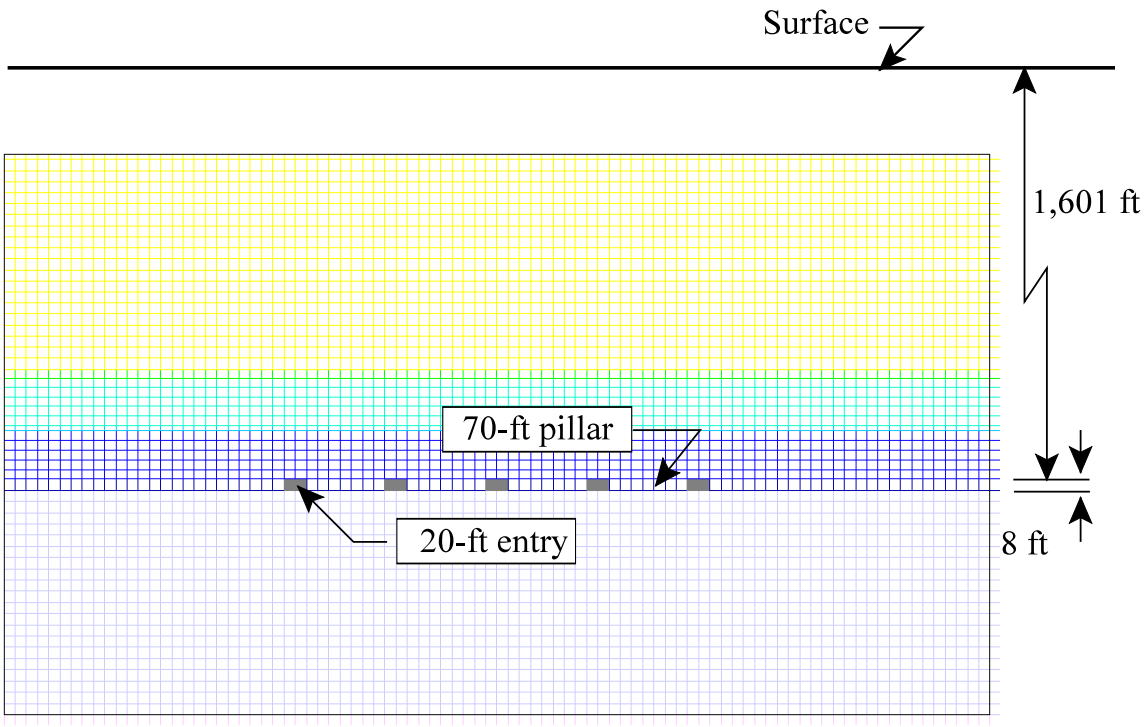

Figure 3. Geometry of the main entries. Coal seam elements are 10x8 ft (3.0x2.4 m).

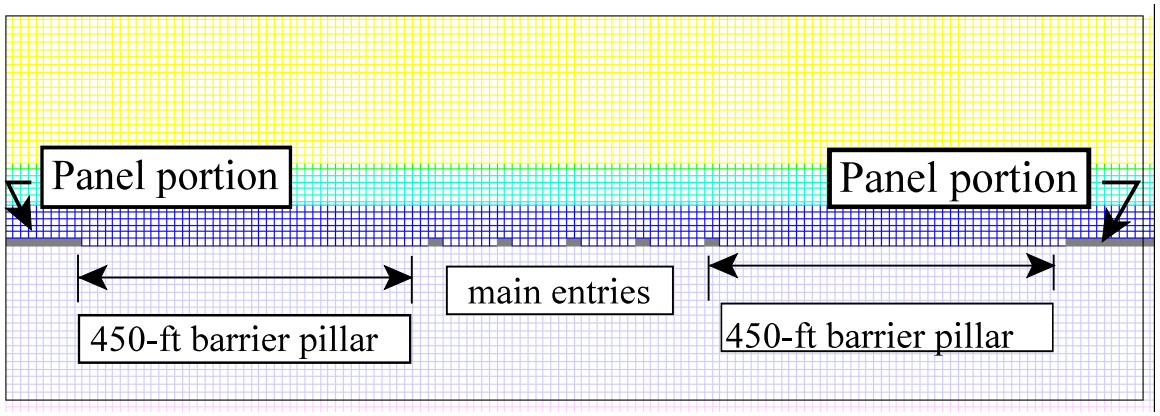

Figure 4. Expanded view at seam level showing main entries, adjacent barrier pillars, and 100 ft (30 m) of future longwall panel excavation.

Premining Stress

The premining stress field is associated with gravity loading only. This simple stress field assumes that the vertical stress before mining is the product of average specific weight of material times depth, or to a reasonable approximation, 1 psi per foot of depth (23 kPa/m of depth). Horizontal stresses are equal in all directions and are computed as one-fourth of the vertical premining stress. Thus, at the top of the Hiawatha seam, the vertical premining stress is 1,601 psi (11.04 MPa) and the horizontal stresses are 400 psi (2.76 MPa). Shear stresses relative to compass coordinates (x=east, y=north, z=up) are nil. Water and gas are considered absent, so these stresses are also the effective stresses before mining. When the depth of cover changes, the premining stresses also change in accordance with the assumed vertical stress gradient and ratio of horizontal to vertical premining stress.

Rock Properties

Rock properties of importance to the present study are the elastic moduli and strengths. The various strata in the geologic column are assumed to be homogeneous and isotropic, so only two independent elastic properties are required, and also only two independent strengths for each material. Young's modulus (E) and Poisson's ratio (ν) are the primary elastic properties and most easily measured. These properties are shown in Table 1 and were adapted from Jones (1994), Rao (1974), and from laboratory tests on core from holes near coal mines in the Book Cliffs field in central Utah. Unconfined compressive and tensile strengths, Co and To, respectively, are the basic strength properties and are also shown in Table 1. Other properties such as shear modulus and shear strength may be computed from the properties given in Table 1 on the basis of isotropy.

Table 1. Rock Properties.

Property / Material	E (10^6 psi)	ν	C_o (10^3 psi)	T_o (10^2 psi)
1. North Horn Formation	2.6	0.26	11.80	7.0
2. Price River Formation	3.2	0.26	9.98	3.8
3. Castle Gate Sandstone	3.0	0.22	9.59	4.3
4. Sand+Siltstone	3.1	0.24	13.50	11.9
5. Blind Canyon Coal	0.43	0.12	4.13	2.8
6. Roof/Floor Siltstone	2.8	0.23	12.18	12.9
7. Cottonwood Coal	0.43	0.12	4.13	2.8
8. Roof Sandstone	3.4	0.26	14.50	10.9
9. Hiawatha Coal	0.43	0.12	4.13	2.8
10. Floor Sandstone	3.4	0.26	11.72	11.7
11. Masuk Shale	2.2	0.35	10.30	0.60

Compressive strength of rock is generally dependent on confining pressure as shown in laboratory tests. The well-known Mohr-Coulomb strength criterion is one way of expressing confining pressure dependency. This criterion may be expressed in terms of the major and minor principal stress at failure in the form

$$(1/2)(\sigma_1 - \sigma_3) = (1/2)(\sigma_1 + \sigma_3)\sin(\phi) + (c)\cos(\phi) \qquad (1)$$

where $\sigma_1, \sigma_3, c, \text{and } \phi$ are the major principal stress, minor principal stress, cohesion and angle of internal friction, respectively, and compression is positive. The left side of (1) is the maximum shear stress, while the sum of the principal stresses on the right side is a mean normal stress in the plane of the major and minor principal stresses. Cohesion and angle of internal friction may be expressed in terms of the unconfined compressive and tensile strengths. Thus,

$$\sin(\phi) = \frac{C_o - T_o}{C_o + T_o}, \quad c = (\frac{1}{2})\sqrt{C_o T_o} \tag{2}$$

An alternative form of (1) that shows the direct dependency of compressive strength on confining pressure is

$$C_p = C_o + (\frac{C_o}{T_o})p \tag{3}$$

where C_p and p are compressive strength under confining pressure and confining pressure, respectively. Equation (3) has applicability to pillar strength because often a pillar is much wider than it is high and has a core confined by horizontal stress. The ratio of unconfined compressive strength to tensile strength in (3) is often 10 or greater and thus multiplies the confining pressure effect by an order of magnitude or more.

Often the increase of compressive strength with confining pressure is non-linear and moreover the intermediate principal stress may influence strength. A criterion that handles both possibilities is a non-linear form of the well-known Drucker-Prager criterion that may be expressed as

$$J_2^{N/2} = AI_1 + B \tag{4}$$

where compression is positive and $J_2, I_1, N, A, \text{and } B$ are second invariant of deviatoric stress, first invariant of stress, an exponent, and material properties, respectively. The variable $\sqrt{J_2}$ is a measure of shear stress intensity, while I_1 is a measure of the mean normal stress that includes the three principal stresses. The last two, A and B, may be expressed in terms of the unconfined compressive and tensile strengths, while the exponent (N) is decided upon by test data. A value

of 1 reduces (4) to the original Drucker-Prager criterion. A value of 2 allows for non-linearity and more realistic fits to test data. A value $N = 2$ is used in this study. The maximum value of $J_2^{1/2}$ for the given mean normal stress ($I_1 / 3$) can be extracted from (4). The ratio of this maximum value to the actual value is a factor of safety for the considered point. Thus, an element factor of safety $fs = J_2^{1/2}$ (strength) / $J_2^{1/2}$ (stress). This ratio has an analogy to the ratio of shear strength to shear stress. Uniaxial compression and tension are special cases included in this definition of element safety factor. Other definitions are certainly possible, but the one described here is embedded in UT2 and serves the important purpose of indicating the possibility of stress exceeding strength and thus the possibility of yielding.

Mining Sequence

The mining sequence involves several stages: (1) excavation of the main entries, (2) excavation of panels on either side of the main entries, (3) entry excavation in the north barrier pillar, (4) entry excavation in the south barrier pillar. Main entries are excavated in strata initially stressed under gravity loading alone. Stress changes induced by mining entries are added to the initial stresses to obtain the final stresses at the end of main entry excavation. These final stresses are the initial stresses for the next stage of excavation (panel mining) and so on.

Boundary Conditions

Displacements normal to the sides and bottom of the mesh shown in Figure 2 are not allowed, that is, they are fixed at zero. The top surface of the mesh is free to move as mining dictates. Initial conditions are boundary conditions in time. These are the stresses at the start of each excavation stage.

There is a possibility that computed seam closure, the relative displacement between roof and floor, may exceed mining height. This event is physically impossible and thus must be prohibited by appropriate boundary conditions. Because the bottom of the mesh is fixed in the vertical direction, floor heave is somewhat restricted relative to a mesh of greater vertical extent. Roof sag is not restricted, so specification of roof sag in an amount that prevents overlap of floor heave is a reasonable physical constraint to impose as an internal boundary condition. Where overlap of roof and floor does not occur, no constraint is necessary.

FINITE ELEMENT ANALYSIS

The main results of an analysis are stress, strain and displacements induced by mining. Visualization of information derived from these basic results assists in understanding strata mechanics associated with mining and in assessment of overall safety of a particular mining plan. Color contours of element safety factors are especially helpful. In two-dimensional analyses, variables such as widths of entries, pillars, panels and barriers may be changed at will as may other input data including stratigraphy and rock properties. The list of parameters is long; a design parameter study on the computer could be lengthy, indeed. However, in a case study, the input is fixed and thus computation time is greatly reduced. When the stratigraphic column extends to the surface, subsidence may be extracted from displacement output. If the actual subsidence profile is known, a match between finite element model output and mine measurements may be used to constrain the model in a reasonable manner.

Main Entry Mining

Figure 5 shows before and after views of main entry mining. The "before" view is just the mesh shown in Figure 3, but to the same scale as the "after" view that shows the distribution of the element safety factors according to the color scale in the figure. The three yellow bands are coal seams and show almost a uniform safety factor of 2.7 away from the main entries. Pillars between the entries and ribs of the outside entries show a slightly lower safety factor of 2.2. Roofs and floors show much higher safety factors (greater than 4.5) because of the greater strength of roof and floor strata. Pillar safety factors are with respect to compressive stress as inspection of the stress output file shows. A safety factor of 2 to 4 in compression is suggested in the literature [Obert and Duvall 1967], so the main entry system is considered safe.

Stress concentration in great detail is *not* obtained in this analysis stage because of the relatively coarse mesh that uses 10x8 ft (3.0x2.4m) coal seam elements about an entry 20 ft (6 m) wide by 8 ft (2.4 m) high. In fact, element stresses are average stresses over the area enclosed by an element. Stresses in a pillar rib element are average stresses over the 10 ft (3 m) distance into the rib and over the full mining height of 8 ft (2.4 m). A highly refined mesh would reveal details about an entry and perhaps compressive stress concentrations enough to cause yielding at entry ribs and tensile stress concentrations possibly high enough to cause roof and floor failure. Such effects would necessarily be localized within about a half-element thickness (5 ft, 1.5 m) because no failure in ribs, roof, and floor is indicated in elements adjacent to the main entries in Figure 5. Figure 6 shows the distribution of vertical and horizontal stress across the main entries and pillars. The U-shape pattern is typical of vertical stress after mining. The horizontal stress increases from zero at the ribs with distance into the rib rather rapidly because of element size.

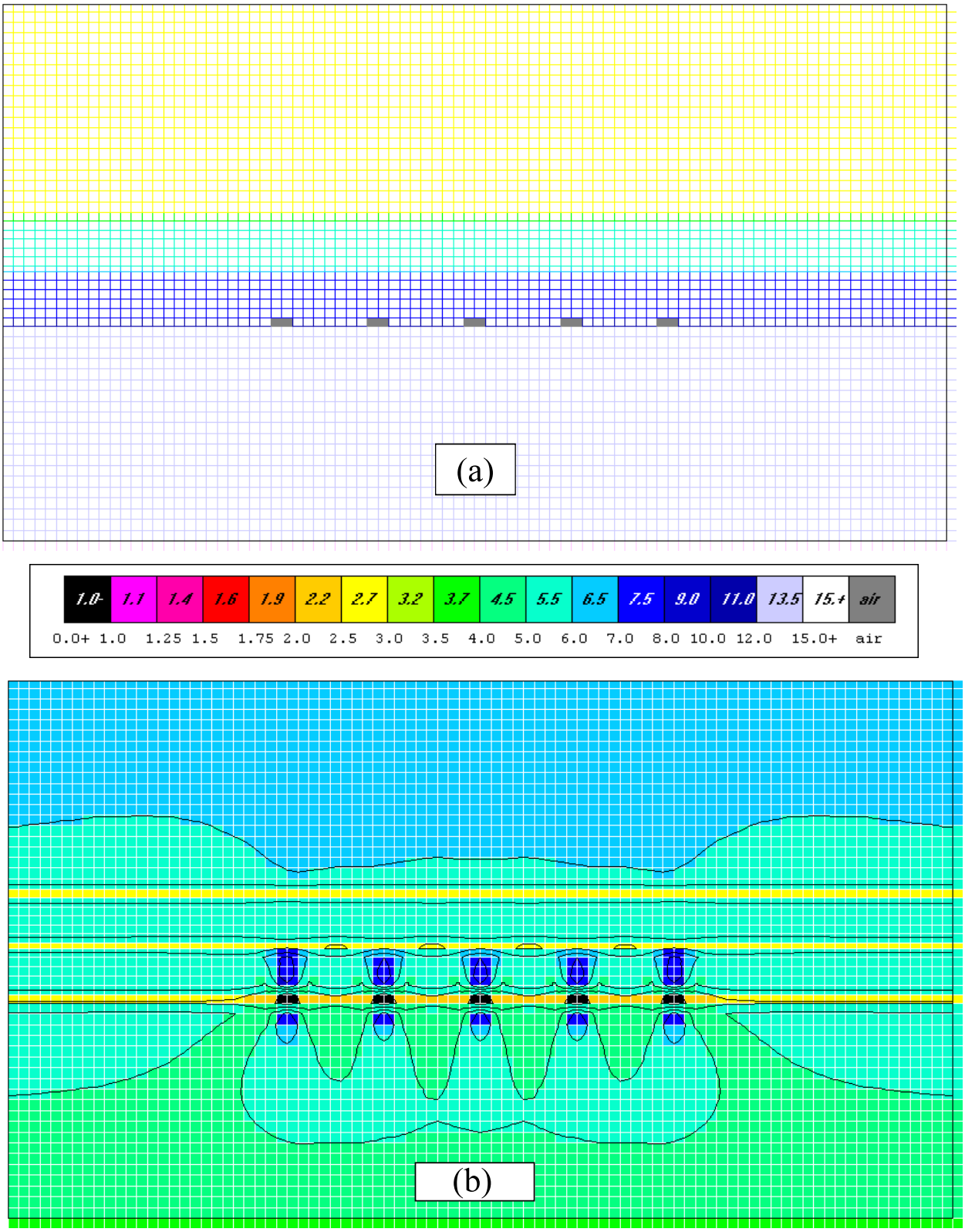

Figure 5. Element safety factor distribution. (a) before mining main entries, (b) after mining.

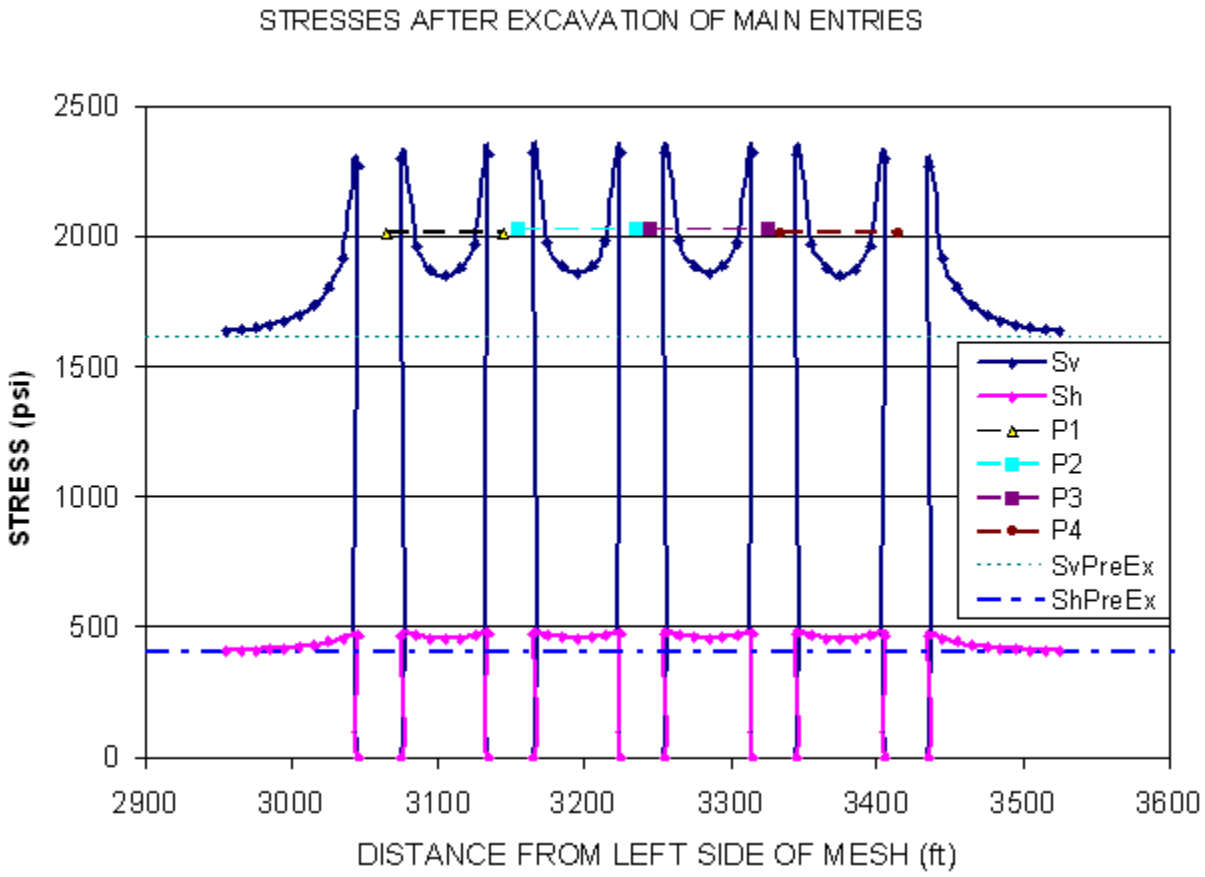

Figure 6. Stress distribution across the main entries and pillars after excavation. Sv=vertical stress, Sh=horizontal stress. Dashed lines are premining values.

The average vertical stress in each pillar in Figure 6 is shown by the horizontal lines labeled P1, P2, P3, and P4. These values are obtained from the finite element analysis and have an overall average of 2,021 psi (13.9 MPa). A tributary area or extraction ratio calculation gives a slightly higher average of 2,057 psi (14.2 MPa) because of the assumption of an infinitely long row of entries and pillars. The average vertical pillar stress is well below the unconfined compressive strength of coal. In fact, the ratio of strength to average vertical stress is a safety factor of sorts with a value of 2.0. Because the vertical stress varies across a pillar and horizontal stress increases confinement with distance into a pillar, the local element safety factor varies

through a pillar. This variation is shown in Figure 7 where data are from finite element results and the local factor of safety (*fs*) is based on the formulation used in UT2. Also shown in Figure 7 is a normalized vertical stress obtained by dividing the post-mining vertical stress (Sv) by the premining vertical stress (So), in essence, a stress concentration factor for vertical stress. The local safety factor is least at the pillar ribs where confinement is nil and vertical stress is high and greatest at the core of the pillar where confinement is high and vertical stress is less concentrated than at the rib. The close agreement between the tributary area calculation of vertical pillar stress after mining and the finite element results provides a check on the finite element analysis.

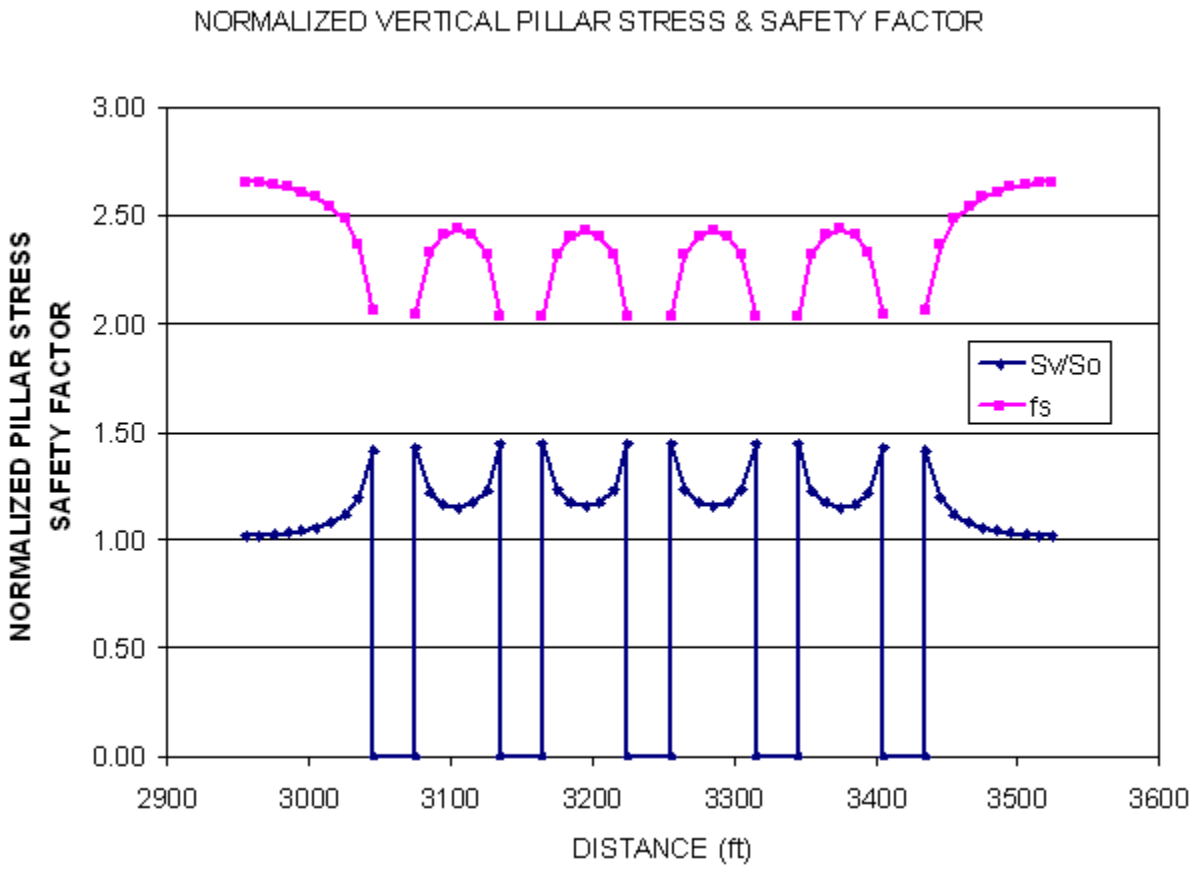

Figure 7. Pillar safety factor distribution from UT2 data and normalized vertical stress across the main entries and pillars.

Longwall Panel Mining

Six longwall panels were mined on the north and south sides of the main entries that were excavated in an east-west direction. For the most part, two panel entries were used for development. The chain pillars of the panel entries undoubtedly are lost as a panel is mined and are not considered in analysis of panel excavation effects on the main entries. Six panels approximately 780 ft to 810 ft (234 m to 243 m) wide were excavated on each side of the main entries. Barrier pillars approximately 450 ft (135 m) wide separate the nearest of these panels from the main entries. In the second stage of finite element analysis, panel mining extends 2,600 ft (780 m) on each side of the barrier pillars. The geometry of this stage of analysis is shown in Figures 2, 3, and 4.

Node Displacements and Subsidence. The first analysis of panel mining was only partially successful. While the solution process proceeded monotonically and convergence was excellent, roof and floor displacements over the central portions of the excavated panels indicated seam closure greater than seam thickness, a physical impossibility. A correction was applied in the second analysis that prevented excess seam closure. In this analysis, seam closure was set in a way that allowed maximum surface subsidence over the panel centers to approximate observed surface subsidence while preventing roof-floor overlap. Thus, seam level roof sag was restricted over the horizontal length of 1,300 ft (390 m) from panel centers (mesh sides). No restrictions on floor heave were imposed. Subsidence profiles across panels 13 through 17 on the south side of the main entries that were plotted for the years 1999 through 2002 indicated formation of a flat subsidence trough with about 5 ft (1.5 m) of surface subsidence.

Figure 8a shows displacements in the form of a deformed mesh after a second attempt at panel mining. The displacement scale is exaggerated relative to the distance scale in order to visualize the overall displacement pattern. Maximum displacement of 63 inches or about 5 ft (160 cm or about 1.5 m) occurs at the mesh sides, that is, over the centers of panel mining. Interestingly, 18 inches (46 cm) of subsidence occurs over the center of the main entries. Floor heave (upward displacement) is also maximum at the mesh sides but diminishes with distance to the main entries. At 130 ft (39 m) from the outside barrier pillar ribs, floor heave diminishes to zero. With further distance from the mesh sides towards the mesh center and center of the main entries, floor displacement is downwards indicating that the barrier pillars and entry pillars depress the floor under the weight transferred from panel mining. Figure 8b is a close up view of the deformed mesh about the main entries and only hints at entry roof sag and floor rise. The rough agreement between maximum subsidence obtained from finite element analysis and that observed in actual subsidence profiles, although indirectly imposed through seam closure, suggests the finite element model of panel mining is reasonable.

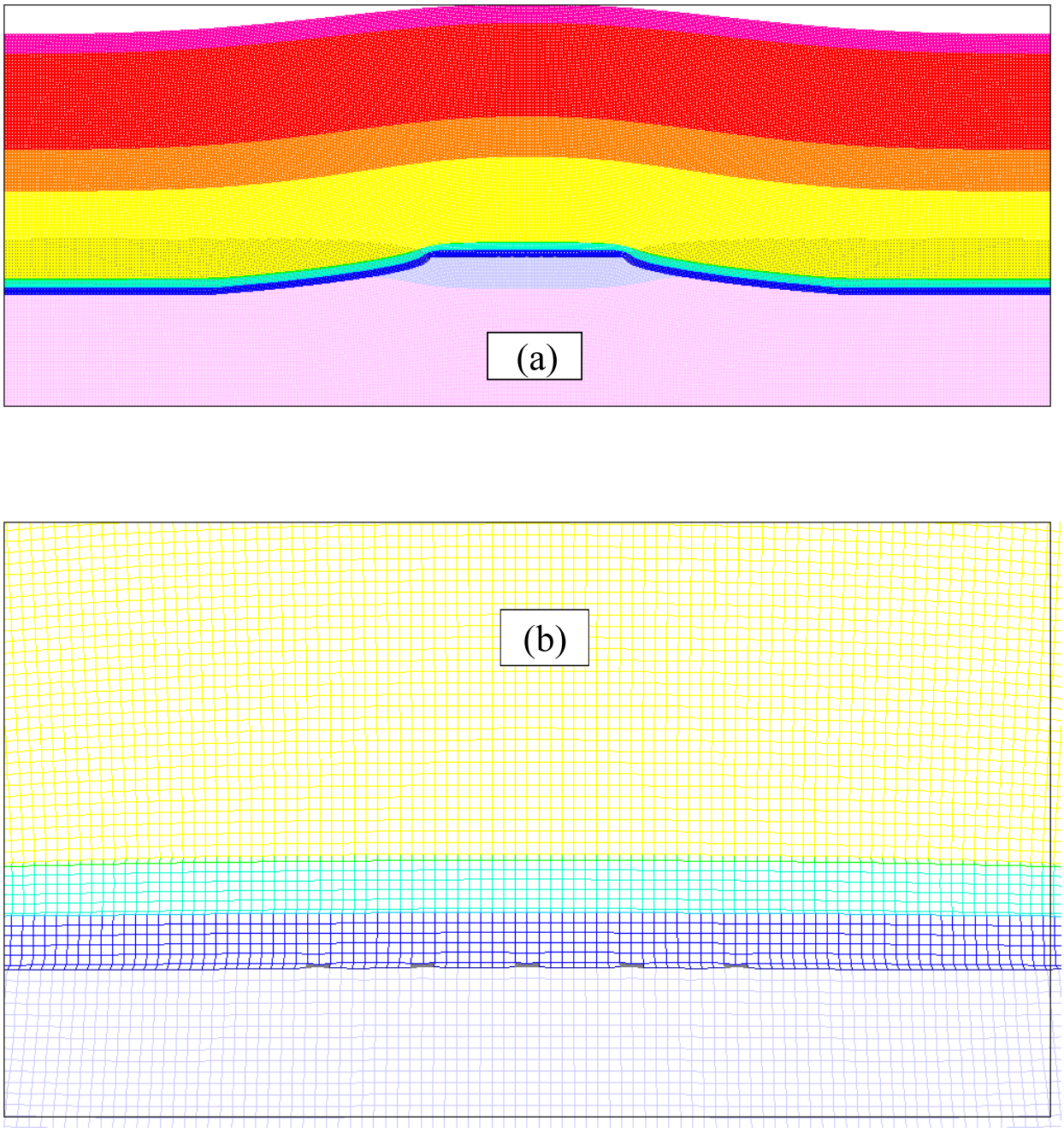

Figure 8. Displacements after panel and entry mining. (a) overall, (b) entries.

Element Safety Factor Distributions. Element safety factor distributions reveal at a glance areas that have reached the elastic limit and are therefore subject to yielding and areas well below the elastic limit and of much less concern. Safety and stability of an entry surrounded by an extensive zone of yielding would surely be threatened. A pillar with all elements stressed beyond the elastic limit would also be of great concern. Absence of extensive zones of yielding would be reassuring.

Figure 9 shows the overall distribution of element safety factors in two ways, one without contours that supplement the color coding and one with contours. The seemingly faded color is a result of the plot density that brings white element borders into close proximity and allows only a tiny area for coloring. The jumps in contours occur across strata interfaces where discontinuities in material properties occur. Disruption of contours occurs at seam level across portions of the seam that have been excavated (panels and entries). Symmetry of the contour pattern is apparent and as the pattern should be. The dark (black) regions of yielding are extensive. Near the surface above the main entries strata flexure leads to tensile failure. Much of the roof and floor yield is also tensile.

An expanded half-mesh view is shown in Figure 10 where the yield zones are more clearly seen. Strata flexure in tension and failure is indicated near seam level in the roof outside the barrier pillar rib. Floor failure below is also evident in Figure 10. Interestingly, yielding is small in the immediate sandstone floor, but is extensive in the Masuk shale below.

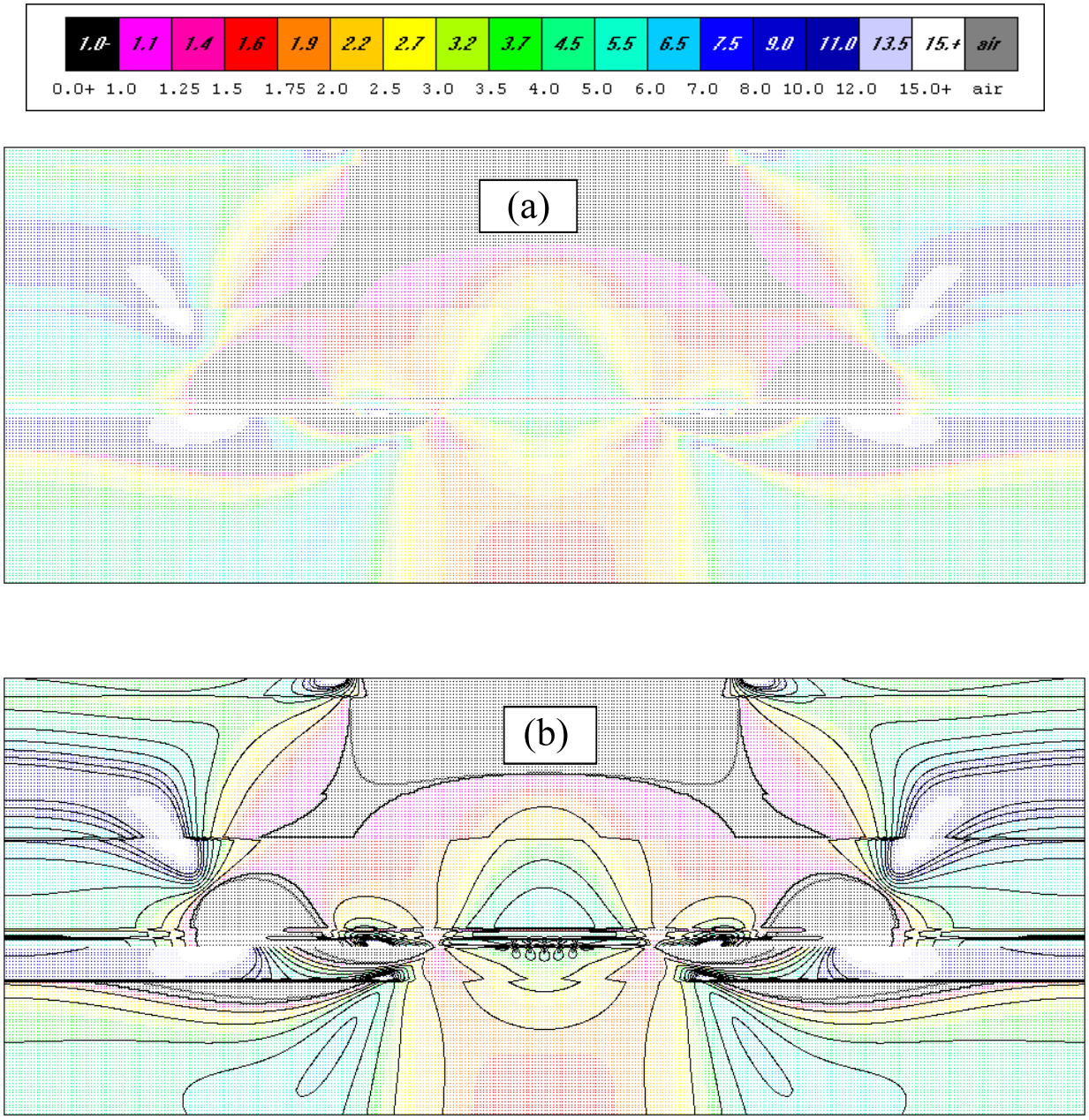

Figure 9. Whole mesh element safety factor distributions. (a) without line contours, (b) with.

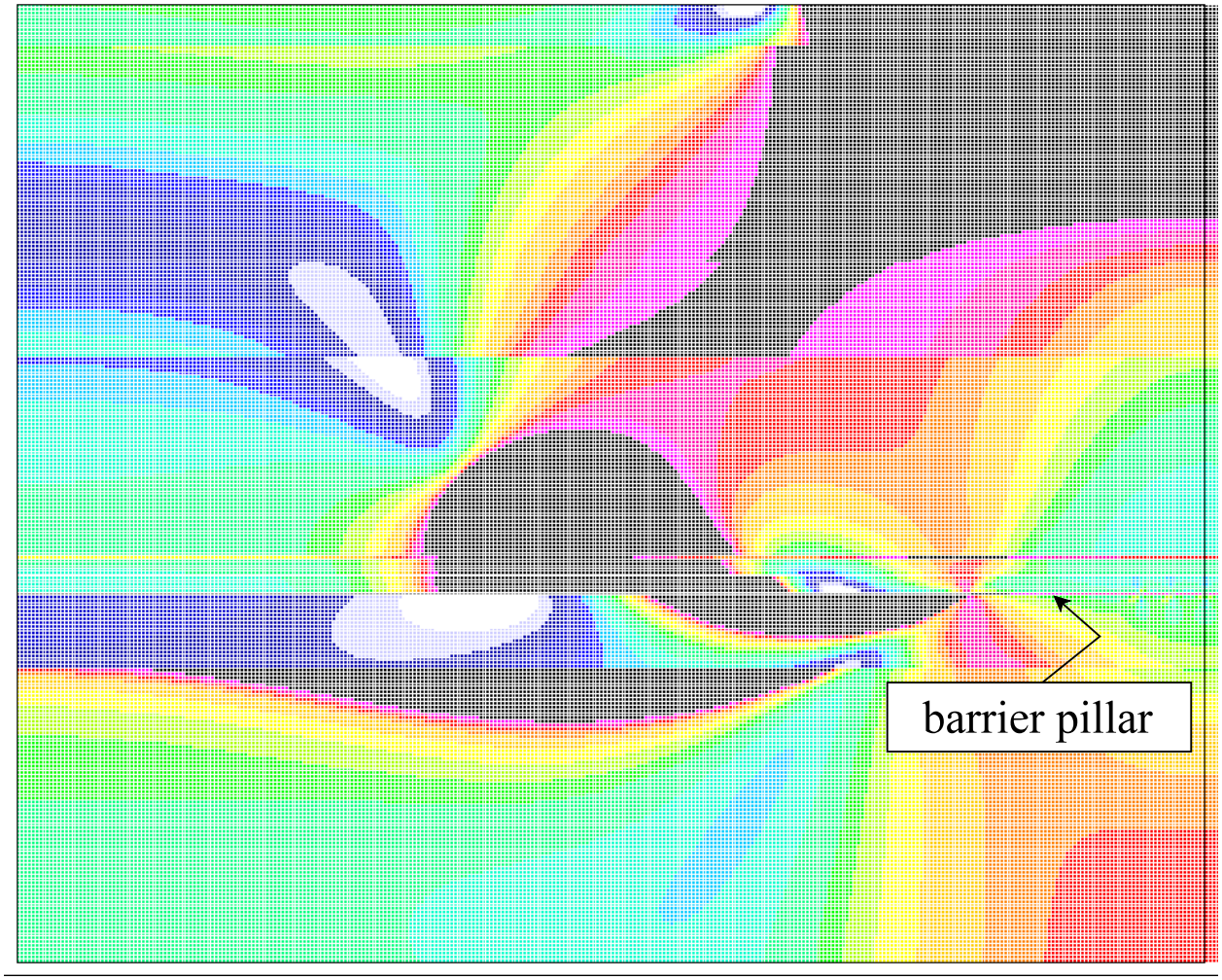

Figure 10. A half-mesh view of element safety factors showing dark (black) zones of yielding mainly in horizontal tension associated with strata flexure.

Yielding under high compressive stress penetrates the barrier pillar from the panel side a distance of 110 ft (33 m). Thus, about 25% of the barrier yields after panel excavation. This penetration is accompanied graphically by large horizontal excursions of the safety factor contour lines in Figure 11 which shows details of the element safety factor distribution in the vicinity of a barrier pillar. Half of the main entries are included in Figure 11. The remainder of the barrier pillar while not yielding is highly stressed with element safety factors no greater than 1.34. Yielding in the two overlying coal seams is evident in a region above the barrier pillar.

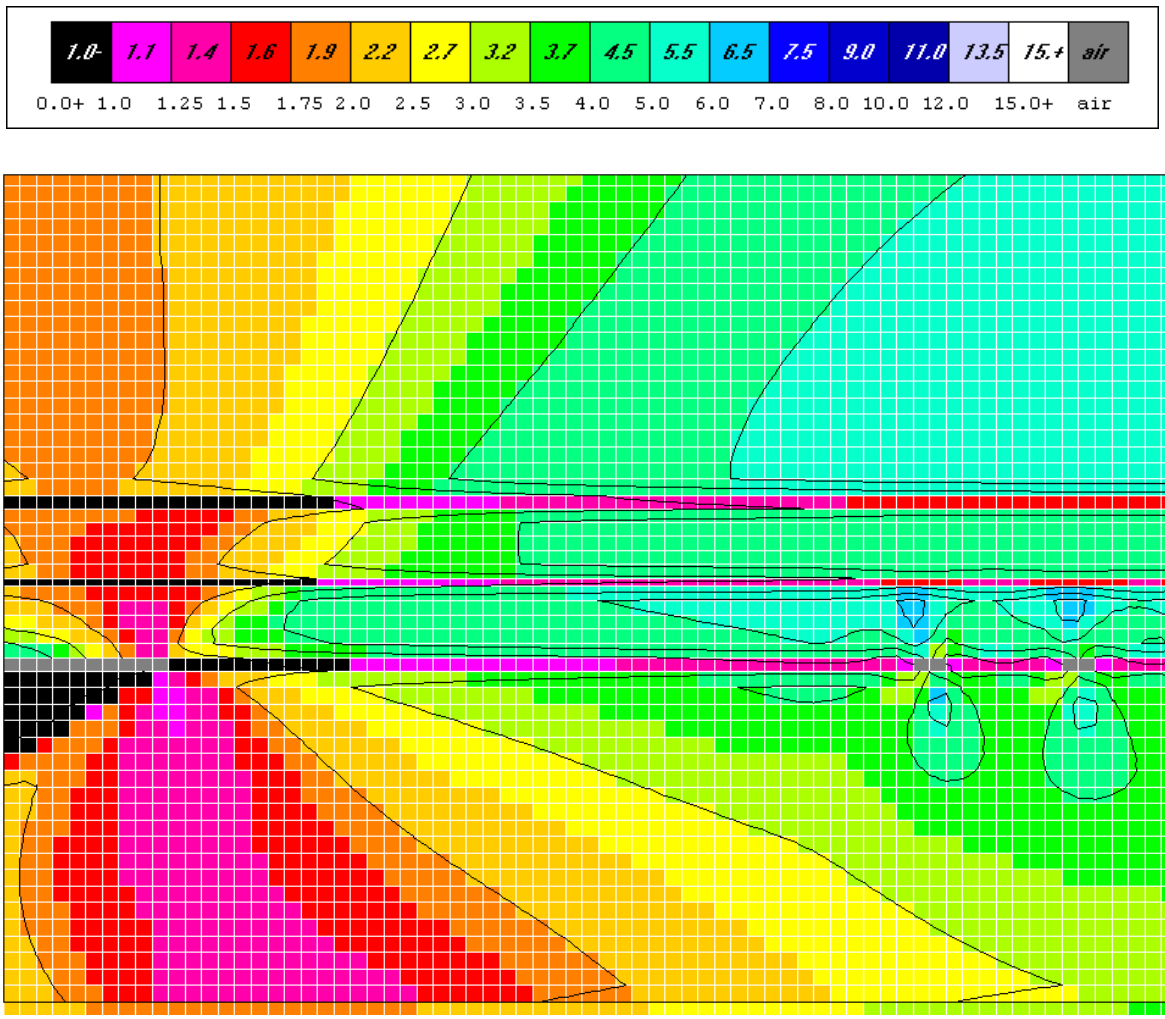

Figure 11. Element safety factors about a barrier pillar after panel mining.

Details of the element safety factor distribution about the main entries is shown in Figure 12. The pink and red zones indicate relatively low safety factors. The highest safety factor in the main entry pillars is 1.34, the same peak value in the barrier pillars on either side of the main entries. Thus, all pillar element safety factors are less than the minimum of 2 recommended by Obert and Duvall (1967). Roof and floor safety factors are in the 4 to 5 range. Although mesh refinement would lead to lower safety factors at the roof and floor of an entry, there appears to be no significant threat to roof and floor safety at this stage of mining.

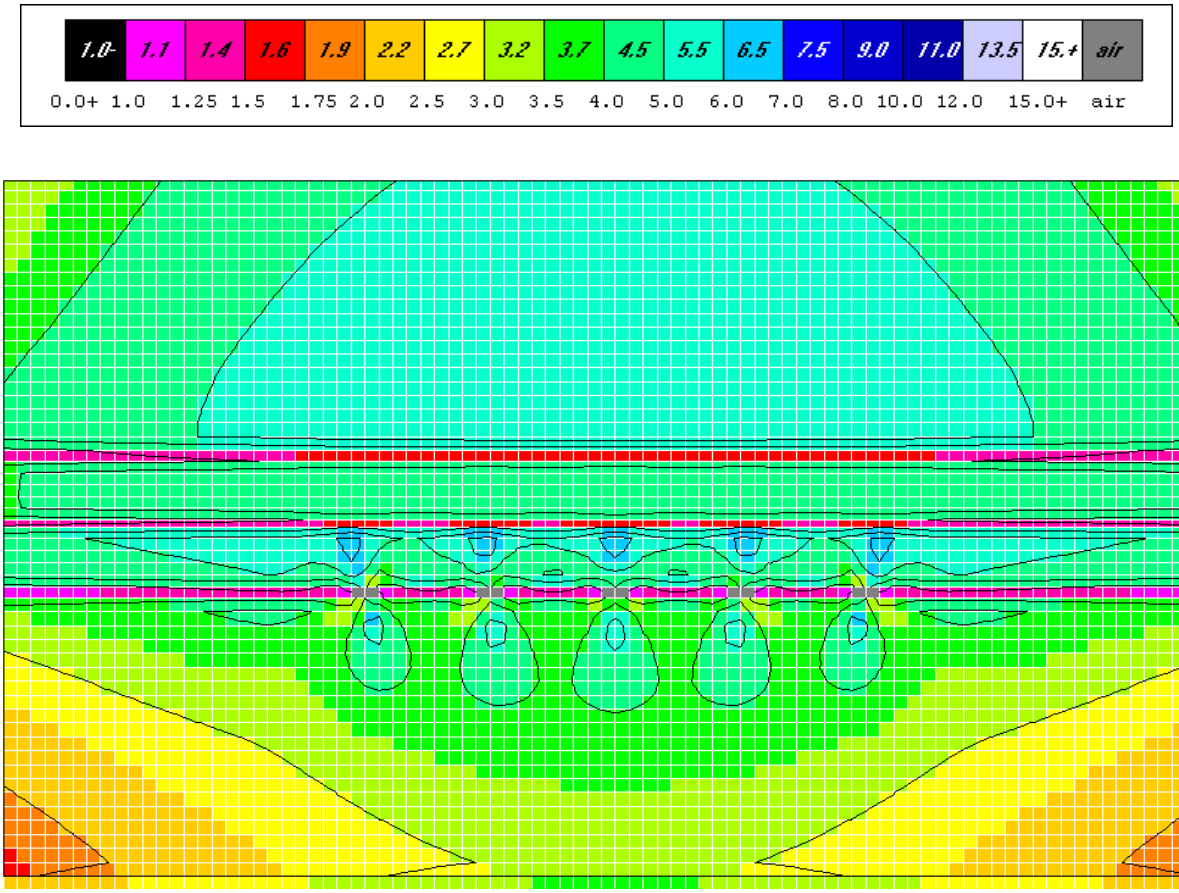

Figure 12. Distribution of element safety factors about the main entries after panel mining.

Barrier Pillar Entry Mining

Barrier pillar entry mining in the analysis consists of four entries 20 ft (6 m) wide separated by pillars 60 ft (18 m) wide. Two sets of such entries were mined, one on the north side and one on the south side of the original main entries. The north side barrier pillar entries were separated from the north side longwall panels by a pillar 140 ft (42 m) wide and from the main entries by a pillar 50 ft (15 m) wide. The south side barrier pillar entries were separated from the south side longwall panels by a 120 ft (36 m) wide pillar and from the original main entries by a 70 ft (21 m) pillar. These dimensions were estimated using the distance function in a drawing of the mine geometry. Without doubt, the as-mined dimensions differ from these

nominal dimensions. Provided such dimensional differences are small, finite element results should differ only slightly as well and not affect inferences from analysis results concerning overall safety of the mining plan.

North Barrier Pillar Mining. The third stage of analysis follows the first and second stages of main entry development and panel mining. This stage involves further entry and pillar development in the north barrier pillar. Mining geometry is illustrated in Figure 13 and shows four additional entries and associated pillars. Only 100 ft (30 m) of the 2,600 ft (780 m) of prior panel mining is shown in Figure 13. Mining height is 8 ft (2.4 m) as before.

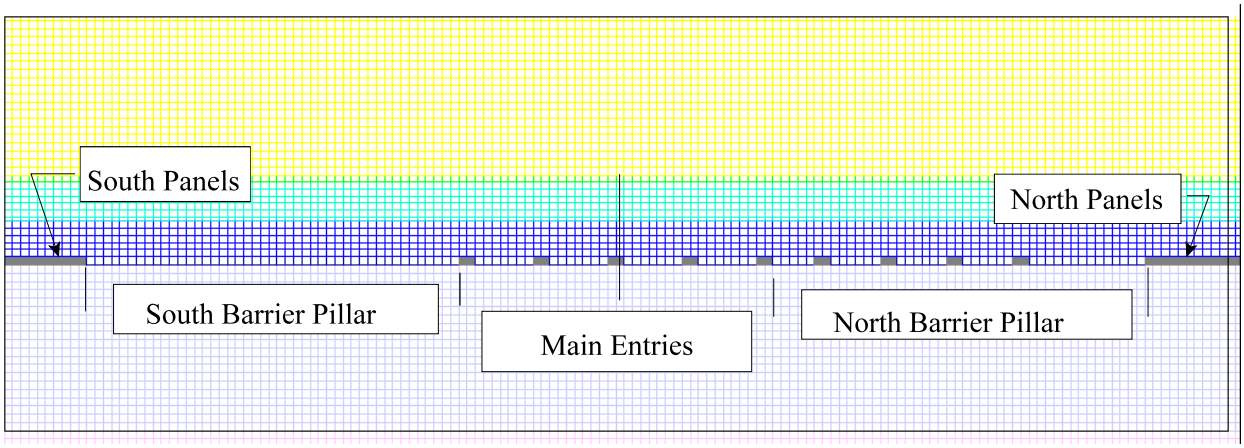

Figure 13. North barrier pillar entry geometry.

The distribution of element safety factors after entry development in the north barrier pillar is shown in Figure 14. Most elements in the north side barrier pillar are now at yield. Rib elements in pillars adjacent to the original main entries are also at yield. The outside entry of the original main entries shows ribs yielding in the pillar between it and the new north side barrier pillar entry. The south outside entry ribs shows yielding extending 10 ft (3 m) into the ribs. The highest safety factor in any pillar element in Figure 14 is 1.2.

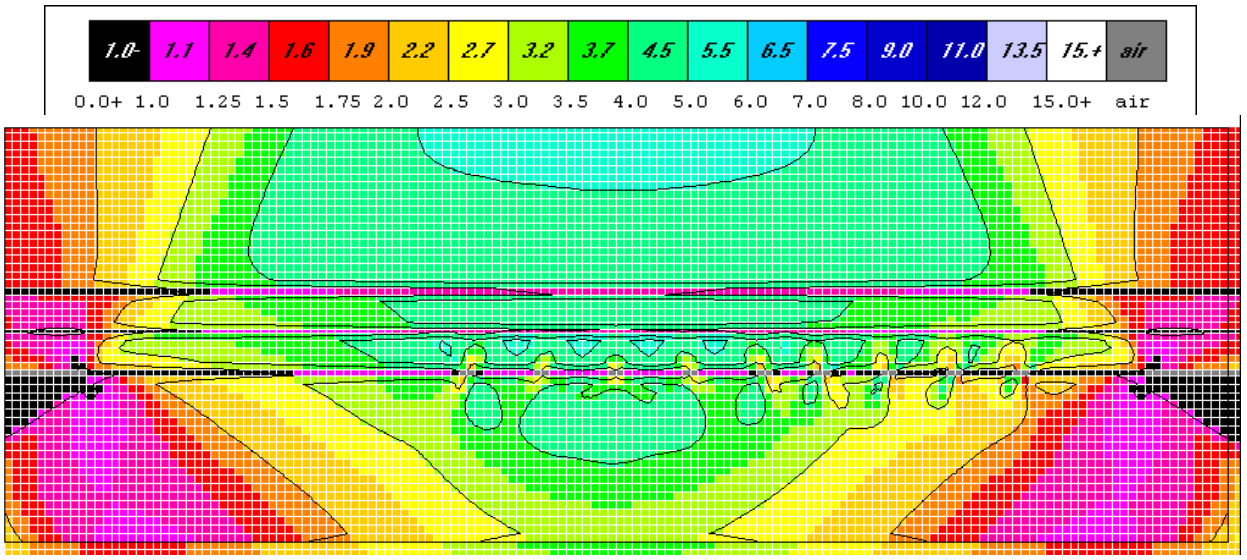

Figure 14. Element safety distribution after entry development in the north barrier pillar.

South Barrier Pillar Mining. The fourth and last stage of analysis is entry development in the south barrier pillar and follows entry development in the north barrier pillar. Mining geometry is illustrated in Figure 15 and shows four additional entries and associated pillars in the south barrier pillar. Only 100 ft (30 m) of prior panel mining is shown in Figure 15. Mining height is 8 ft (2.4 m). Entry and pillar widths in the south barrier pillar development are 20 ft (6 m) and 60 ft (18 m), respectively. Four additional entries are developed in the south barrier pillar.

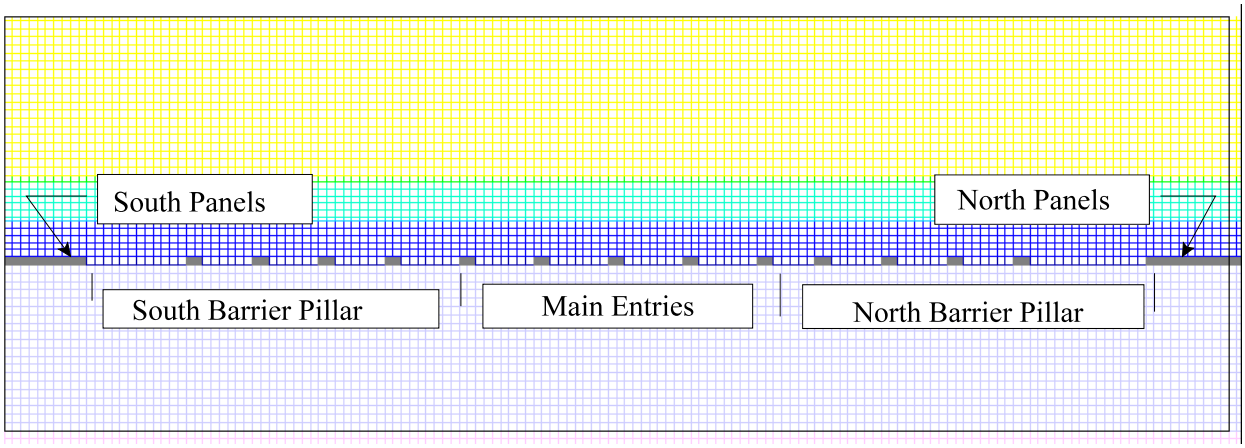

Figure 15. South barrier pillar mining geometry.

The distribution of element safety factors after entry development in the south barrier pillar is shown in Figure 16. Almost all elements in the south side barrier pillar are now at yield. Indeed all pillar elements across the mining horizon are close to yield. Peak vertical stress in the barrier pillars exceeds 38,400 psi (264.8 MPa), over 9 times the unconfined compressive strength of the coal. Horizontal stress exceeds 7,300 psi (50.3 MPa). Even so this high confining pressure is insufficient to prevent yielding. The lowest vertical pillar stress is about 6,000 psi (41.4 MPa), almost half again greater than the unconfined compressive strength of the coal; the lowest horizontal pillar stress is about 1,500 psi (10.3 MPa). Any release of horizontal confinement would likely result in rapid destruction of pillars. Additionally, entries nearest to the mined panels are showing reduced roof and floor safety factors. Yield zones extend to depth in the floor. Overlying coal seams are also yielding or are very close to yielding over portions of the barrier pillars, as seen in Figure 16.

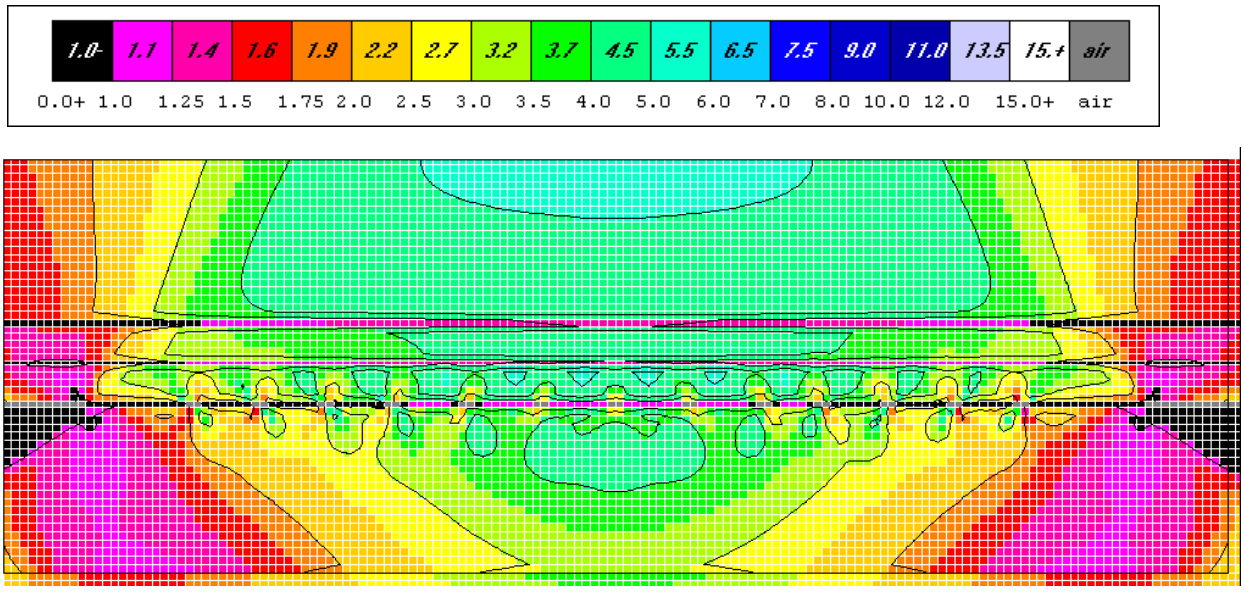

Figure 16. Element safety distribution after entry development in the south barrier pillar.

Figure 17 shows the distribution of element safety factors about the original main entries after entry mining in the north and south barrier pillars. Roof and floor element safety factors have decreased significantly from the original values obtained during development prior to longwall panel mining and range between 2 and 4, as seen in the color code. Roof and floor element safety factors about the new entries mined in the barrier pillars are lower, roughly in the range of 2 to 4 in Figure 17.

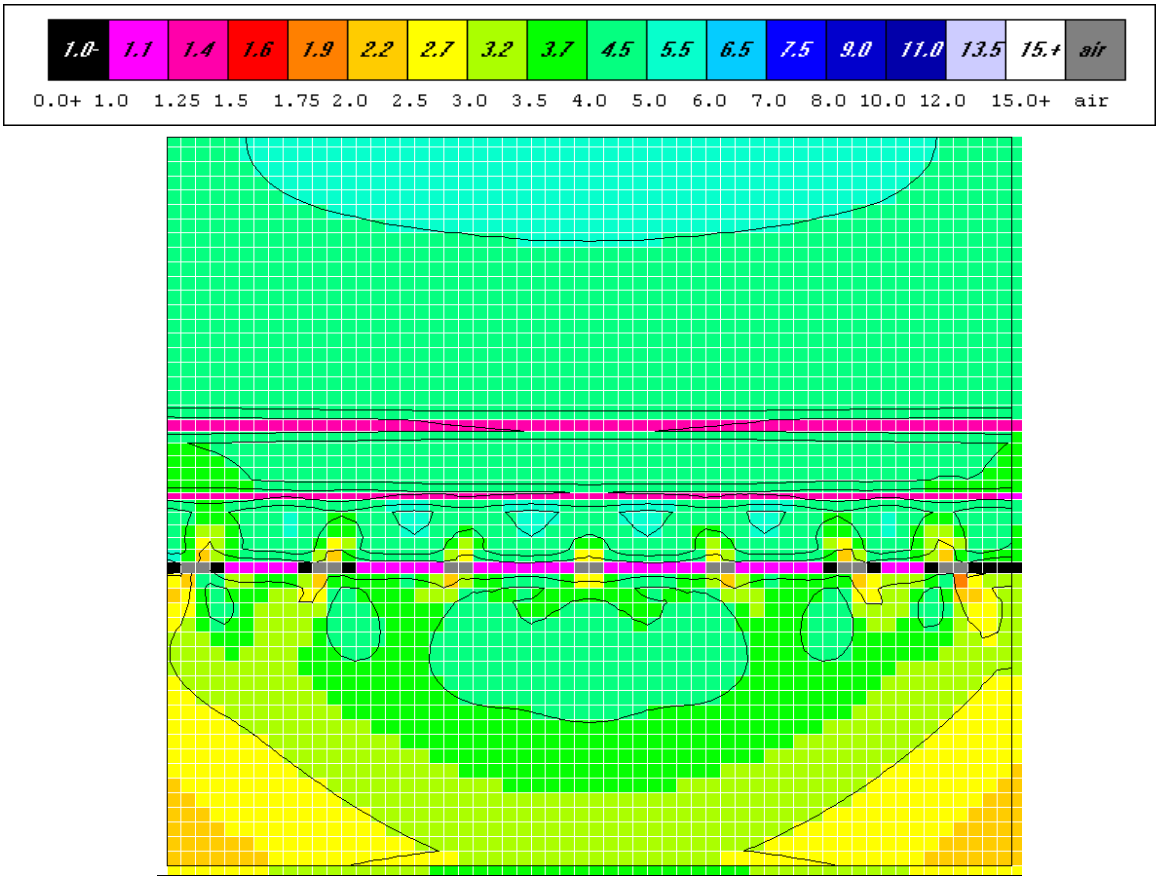

Figure 17. Distribution of element safety factors about the original main entries after development in the north and south barrier pillars.

The distribution of horizontal and vertical element stresses after main entry development, panel mining, and entry development in the north and south barrier pillars is shown in Figure 18 where gaps are entry elements. The very high vertical stresses on the ribs of the barrier pillars

adjacent to the panels mined north and south of the barrier pillars is striking. Although these extreme peaks in vertical stress diminish rapidly across the pillars, they remain well above the unconfined compressive strength of the coal, also shown in Figure 18. Recall the analysis is elastic. If yielding were allowed as in an elastic-plastic analysis, these peaks would diminish and the extent of yielding would likely spread across regions of the pillars that have not yielded according to the elastic results. Horizontal confinement in rib elements at the ribs of the barrier pillars, where the vertical stress is high, is because of averaging over the width of rib elements. The actual horizontal stress at the rib must be zero. The high analysis value is associated with mesh refinement and the use of a 10 ft (3 m) wide element. A lower horizontal stress would enhance the spread of pillar yielding. Again, purely elastic behavior leads to an underestimate of the extent of yielding that is indicated by elements with a safety factor less than one.

A tributary area calculation of the average pillar stress across the entire seam is also shown in Figure 18 as is the finite element analysis result. These two values agree within one percent and lend credence to the analysis. In essence, the calculation shows that the requirement for equilibrium of stress in the vertical direction is satisfied in the course of four stages of mining. Any analysis result, regardless of method, should meet this requirement.

Figure 19 shows the distribution of element safety factors at seam level. Safety factors less than one are a consequence of a purely elastic calculation. Safety factors less than one indicate a potential for shedding stress to adjacent elements.

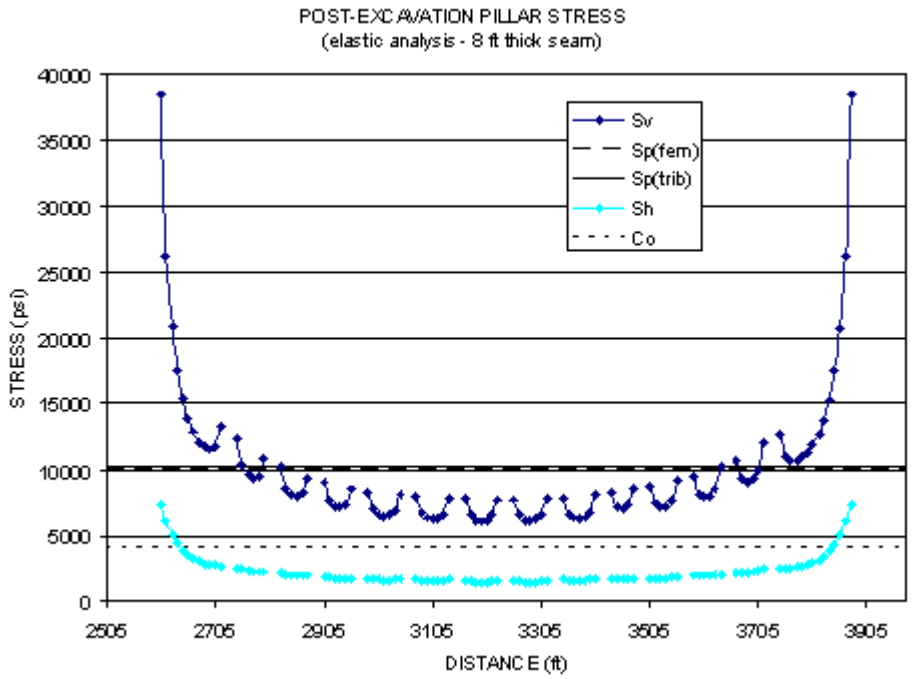

Figure 18. Post-excavation pillar stress distribution. Sv=premining vertical stress. Sp=average pillar stress, fem=finite element method, trib=tributary area, Co=unconfined compressive strength.

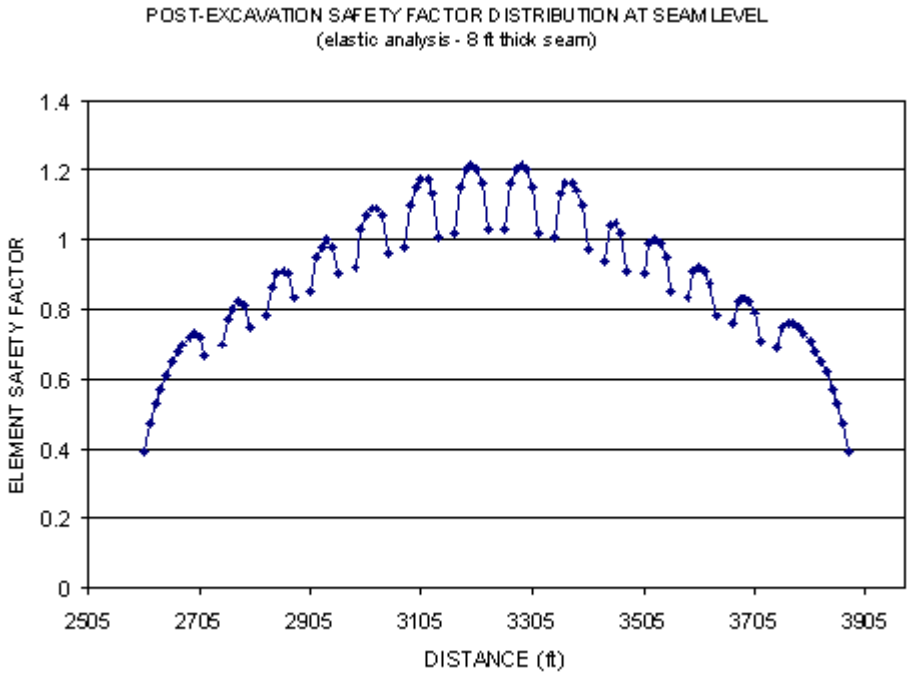

Figure 19. Post-excavation element safety factor distribution.

DISCUSSION

Several questions that often arise about finite element analysis involve input data, two-dimensional analysis, and interpretation of output results. A brief discussion of these questions may not alleviate concerns, but does allow for some explanation and expression of opinion.

The first issue here is the proverbial one about quality of input data and consequences for output results. In fact, this question is present in all engineering analysis and is not unique to the finite element method or other computer-based models for stress analysis or for the analysis of business plans and so forth. Generally, the problem of mine excavation using UT2 is a well-posed mathematical problem in solid mechanics, so small variations in input data lead to only small variations in output. However, if there are errors in input, then the output will also be erroneous. For this reason, checks on results are important when available. An extraction ratio calculation after main entry excavation indicates reliable output at this stage of analysis. Subsidence results in agreement with mine observations, although indirectly imposed, also indicate reliable output.

Another question is the use of two-dimensional analyses in a three-dimensional world of underground coal mining. Here the long drive of main entries, over three miles, and the extensive mining on both sides of the main entries suggests a tunnel-like geometry amenable to two-dimensional analysis in a vertical cross-section. Depth varies over the main entries because of topography and certainly influences analysis results because greater depth is associated with higher premining stress. Depths ranged to 2,000 ft (600 m) or more. A depth of 1,601 ft (480 m) used in the analyses here is therefore relatively shallow. For this reason, any adverse results

would be of even more concern at greater depth. Thus, an optimistic view is taken using a relatively shallow depth.

Another question concerns the role of cross-cuts that are not seen in a vertical section across the mains and through the pillars between entries. The effect is to produce an optimistic or lower stress in pillars because the additional load transferred to pillars from cross-cuts is not taken into account. An adjustment can be made to increase pillar load (Pariseau, 1981) but this was not done for the sake of analysis clarity. Cross-cuts also lead to greater roof spans at entry intersections with cross-cuts and thus more complex strata flexure in roof and floor, but again this complication was avoided with error on the side of optimism. A threat to roof or floor safety in two-dimensional analysis would indicate a greater threat in a three-dimensional analysis.

Mesh refinement is always a question of interest in any numerical analysis of stress. Large elements average out stress and may mask yielding that would be observed with smaller elements. Large is relative to excavation size. Tabular excavations are very wide compared to height and thus represent a challenge for numerical analysis. A compromise is always necessary between desire for detail and problem size and run time limitations. In any case, a coarse mesh results in optimistic output, lower element stresses and also lower displacements. For example, a roof element 10x10 ft (3.0x3.0 m) over a 20-ft (6 m) wide entry would certainly mask stress concentration in the roof compared with roof elements 1x1 ft (0.3x0.3 m). However, 100 more small elements per large element would be required. If this requirement were extended over the mesh used, more than 17 million elements would be needed, an impractical number for engineering applications.

A more subtle question that arises in “stress analysis” concerns material behavior. A closely related question concerns relationships between laboratory and mine scale rock properties. These questions are of much interest in rock mechanics research for which there is no general consensus and that are well-beyond the scope of this report. An elastic material model was used here as were laboratory rock properties. Strengths were used to compute the limit to a purely elastic response and element safety factors. Generally, rock masses contain discontinuities such as joints and cleats that are absent in laboratory-scale test specimens. Consequently, rock masses tend to be weaker and more compliant than laboratory test results would indicate. The result is an optimistic analysis of stress because the higher laboratory moduli and strengths used lead to smaller displacements and less yielding. If an adverse result is observed using rock properties from laboratory tests, results for the mine would likely be worse.

Inelastic behavior of rock under low confinement is likely to be “brittle” with inelasticity appearing in the form of cracking or “damage”. A falling compressive stress-strain curve is often observed in the laboratory in tests under displacement control past the peak of the curve. Without displacement control, fast, violent failure of the test specimen is likely. While a rising stress-strain curve beyond the elastic limit is strain-hardening, a falling curve indicates “strain-softening”. The first is intrinsically stable, while the latter is unstable. Introduction of strain-softening is likely to make a potentially adverse situation, say, with respect to pillar stress, a catastrophic case. Again, a purely elastic model is optimistic because of the avoidance of complex inelastic behavior that may lead to catastrophic failures.

A potentially important inelastic effect absent in elastic analyses is “caving”. Caving over longwall panels is considered to relieve load on shield supports at the face and on chain pillars in panel entries because the length of a cantilever roof beam immediately above the supports is shortened by tensile failure and thus reduces “weight” on the supports. Caving certainly occurs over longwall panels. How high into the remote roof caving propagates is an open question that is sometimes addressed by rules of thumb or experience in a particular mining district. Strata flexure still occurs above the caved zone and transfers load to pillars remaining. Thick, massive sandstones in roof and floor may transfer load over large spans and if failure ensues, large scale collapse is possible. However, reliable caving models, those that initiate and propagate caving from first principals, are not available, and thus, the question of caving effects is left open.

CONCLUSION

Finite element analysis of barrier pillar mining at Crandall Canyon indicates a decidedly unsafe, unstable situation in the making. This conclusion is based on a two-dimensional elastic analysis of a vertical section transverse to the main entries and parallel longwall panels outside of barrier pillars adjacent to the main entries. Elasticity is the de facto standard model for engineering design of bridges, skyscrapers, concrete dams and similar structures throughout the world. Approximations in the analyses here are generally on the optimistic side, so that an adverse situation evident in output data is likely to be worse. For example, complications such as damage in pillar ribs from locally high stress concentration is ignored. Another example is the neglect of load transfer to pillars from cross-cut excavation that would be in addition to load transfer associated with entry excavation. A relatively shallow depth of 1,601 ft (480 m) was

used; actual depth ranges to 2,000 ft (600 m). No pillar extraction was considered after entry development in the barrier pillars. Transfer of load to the remaining pillars during pillar mining in the barrier pillars would increase stress about the entries and remaining pillars as would consideration of greater depth. Both increase outby the considered analysis section.

Elastic behavior is optimistic because stress may exceed strength in a purely elastic analysis. Thus, if an unsafe condition is inferred from results of an elastic analysis, then caution is certainly indicated. In an elastic-plastic analysis, stresses above strength are relieved by fracture and flow of ground ("yielding"). Reduction of peak stress by yielding is likely to cause the zone of fracture and flow (yield zone) to spread to adjacent ground. Yielding by fracture is accompanied by a sudden loss of strength and is associated with fast failure. Glass breakage is an example of fast failure. Yielding by flow may also be accompanied by reduction in strength ("strain softening") which is also unstable and may to lead to fast failure.

However, yielding by flow may also be slow as loss of strength occurs in time. Unfortunately, time effects in strata mechanics are not well understood. Creep, that is, time-dependent flow, to failure may occur in a matter of minutes, hours, or years. Elasticity may also be delayed, that is, strain may not occur instantaneously with stress. In this regard, there are many mathematical models of time-dependent (rheological) material behavior available for analysis, but reliable calculations for engineering design are problematic. Successful forecasts of time to failure in rock mechanics are rare, if they exist at all. In any event, long-term strength is less than short term strength (determined by laboratory tests) used in elastic analysis here. Again, elastic analysis is optimistic because of the use of higher strength.

A multi-stage mining sequence was followed in the analysis here. Main entries were mined first. A tributary area check on pillar stress confirmed finite element results. Entry roofs, pillars, and floors were well within the elastic limit; no yielding was indicated.

Panel mining on both sides of the main entries was done next. During this stage, displacements were constrained in the finite element model to prevent physically impossible overlap of roof and floor strata at seam level during the panel mining stage. This constraint assisted in achieving reasonable agreement between measured subsidence and finite element results. Results indicated 25% of the barrier pillars yielded, while the remaining portions were near yield. Entry pillar safety factors decreased significantly to 1.3; roof and floor safety factors also decreased but remained in the elastic domain.

Entry mining in the north barrier pillar led to yielding of the remaining portion of this pillar and a significant penetration of yielding into the south barrier pillar. The highest safety factor in any pillar, including main entry pillars was 1.2; the lowest was 0.4. Subsequent entry development in the south barrier caused further yielding. The greatest vertical stress in a rib element was more than nine times the unconfined compressive strength of coal. Extensive zones of strata flexure and tensile yielding were observed in roof and floor. A tributary area calculation of average vertical stress at the conclusion of the last mining stage showed close agreement with finite element results.

The large excess of vertical rib stress over strength indicates a potential for rapid destruction of the rib with expulsion of the broken coal into the adjacent entry. The presence of

thick, strong sandstone in roof and floor strata would reinforce this expectation. The broken coal could fill the entry and perhaps restore some horizontal confinement. If a bulking porosity of 0.25 is assumed, then rib failure would extend 60 ft (18 m) into a rib. The extent of failure into a single rib would be less, if both entry ribs failed. Photographs show entries partially filled with broken coal under intact roof. If bottom coal were left, then floor heave could occur, and similarly, if top coal were left. Failure of either top or bottom coal is a release mechanism of horizontal confinement. Another expectation of large, horizontal motion of rib coal into entries would be evidence of shear slip at contacts between roof and floor sandstones, perhaps in the form of "fault" gouge, that is, finely pulverized coal.

In the opinion of the writer, were these finite element model results available in advance, mining in barrier pillars at Crandall Canyon would not be justified.

REFERENCES

Bathe, K.-L., (1982) *Finite Element Procedures in Engineering Analysis*. Englewood Cliffs, N. J., Prentice-Hall, pp 735.

Desai, C. S., and J. F. Abel (1972) *Introduction to the Finite Element Method for Engineering Analysis*. Van Nostrand Reinhold Co., N. Y., pp 477.

Cook, R. D. (1972) *Concepts and Applications of Finite Element Analysis*. John Wiley & Sons, Inc., N. Y., pp 402.

Jones, R. E. (1994) *Investigation of Sandstone Escarpment Stability in the Vicinity of Longwall Mining Operations*. M. S. Thesis, Department of Mining Engineering, University of Utah.

Obert, L. and W. I. Duvall (1967) *Rock Mechanics and the Design of Structures in Rock*. John Wiley & Sons, Inc., N. Y., pg 490.

Oden, J. T. (1972) *Finite Elements of Nonlinear Continua*. N.Y., McGraw-Hill, pp 432.

Pariseau, W. G. (1981) Inexpensive but Technically Sound Mine Pillar Design Analysis. *Intl. J. for Numerical and Analytical Methods in Geomechanics.* Vol. 5, No. 4, pg 429-447.

Pariseau, W. G. (2007) *Finite Element Analysis of Inter-Panel Barrier Pillar Width at the Aberdeen (Tower) Mine.* Department of Mining Engineering, University of Utah and Bureau of Land Management, Salt Lake City, Utah.

Rao, T. V. (1974) *Two Dimensional Stability Evaluation of a Single Entry Longwall Mining System.* M. S. Thesis, Department of Mining Engineering, University of Utah.

Zienkiewicz, O. C. (1977) *The Finite Element Method* (3rd ed). N. Y., McGraw-Hill, pp 787.

Appendix R - Description of BEM Numerical Models

AAI developed numerical models for Crandall Canyon Mine as early as 1995. Between 1995 and 2004, AAI performed several design/modeling projects using a program called EXPAREA. According to AAI:

> *"This program was developed at the University of Minnesota by Dr. S. Crouch and Dr. Starfield (Starfield and Crouch (1973), St. John (1978)). It was initially used for Project Salt Vault in the early days of the Nuclear Waste program. It uses the displacement discontinuity method. The development of the program and later variations such as MULSIM were further developed at the University of Minnesota under funding from the USBM [US Bureau of Mines]. AAI has used the program since 1979 for design of underground thin-seam mines, particularly for coal mines."*

However, in 2006, AAI elected to use another program, LaModel[5], to model ground behavior at the mine. According to NIOSH[26]:

> *"LAMODEL is software that uses boundary-elements for calculating the stresses and displacements in coal mines or other thin, tabular seams or veins. It can be used to investigate and optimize pillar sizes and layout in relation to pillar stress, multiseam stress, or bump potential (energy release). LAMODEL simulates the overburden as a stack of homogeneous isotropic layers with frictionless interfaces, and with each layer having the identical elastic modulus, Poisson's Ratio, and thickness. This "homogeneous stratification" formulation does not require specific material properties for each individual layer, and yet it still provides a realistic suppleness to the overburden that is not possible with the classic, homogeneous isotropic elastic overburden used in previous boundary element formulations such as MULSIM or BESOL. LAMODEL consists of three separate programs - LAMPRE, LAMODEL, and LAMPLT. You must install all three programs to use LAMODEL:*
>
> *LAMPRE is the pre-processor that facilitates creating the input file for LAMODEL. LAMPRE accepts all of the numerical parameters input for LAMODEL and allows graphical input of the material codes for the seam grids. Also, a "Material Wizard" helps generate reasonable coal properties and appropriate yield zones on coal pillars.*
>
> *LAMODEL calculates the stresses and displacements at the seam level from the user's input file. Model runs can take several minutes to several days depending on the computer speed and model complexity. The output from LAMODEL is stored for subsequent analysis by LAMPLT, the post-processing program.*
>
> *LAMPLT is the post-processor that allows the user to plot and analyze the output from LAMODEL."*

Appendix S - Back-Analysis of the Crandall Canyon Mine Using the LaModel Program

by
Keith A. Heasley, Ph.D., P.E.
West Virginia University

Back Analysis of the Crandall Canyon Mine Using the LaModel Program

By

Keith A. Heasley, Ph.D., P.E.
June 20, 2008

Executive Summary

On August 6th, 2007, the Crandall Canyon Mine in Utah collapsed entrapping six miners. It appeared that a large area of pillars in the Main West and South Barrier sections of the mine had bumped in a brief time period, filling the mine entries with coal from the failed pillars and entrapping the six miners working in the South Barrier section. Ten days later, during the heroic rescue effort, another bump occurred thereby killing three of the rescue workers, including one federal inspector, and injuring six other rescue workers. A few days after the August 16th incident, a panel of ground control experts determined that the Main West area was structurally un-stable and underground rescue attempts halted. Subsequently the mine was abandoned and sealed.

The objective of this investigation is to utilize the LaModel boundary-element program along with the best available information to back-analyze the August 6th, 2007 collapse at the Crandall Canyon Mine in order to better understand the geometric and geo-mechanical factors which contributed to that collapse. Ultimately, it is hoped that this back-analysis will help determine improvements in mine design that can be made in the future to eliminate similar type events.

In order to determine the optimum parameter values for matching the observed mine behavior, to assess the sensitivity of the model results to the input values, and to investigate various triggering mechanisms, an extensive parametric analysis was performed. This analysis examined: different overburden properties, gob properties, coal behavior and triggering mechanisms. In all, over 230 different models were run to perform the parameter optimization, sensitivity analysis and trigger investigation.

Based on this extensive back analysis of the Crandall Canyon Mine using the LaModel program and with the benefit of hindsight from the March bump and August collapse, a number of conclusions can be made concerning the mine design and August 6th collapse:

1) Overall, the Main West and adjacent North and South Barrier sections were primed for a massive pillar collapse because of the large area of equal size pillars and the near unity safety factors. This large area of undersized pillars was the fundamental cause of the collapse.
   a. The pillars and inter-panel barriers in this portion of the Crandall Canyon Mine essentially constitute a large area of similar size pillars, one of the essential ingredients for a massive pillar collapse.
   b. The high overburden (2200 ft) was causing considerable development stress on the pillars in this area, and bringing pillar development safety factors below 1.4.
   c. Considerable longwall abutment stress was overriding the barrier pillars between the active sections and the old longwall gobs.
2) The abutment stress from the active North Barrier retreat section was key to the March 10th bump occurrence and the modeling indicated that the North Barrier abutment stress contributed to the August 6th pillar collapse.
3) From the modeling, it is not clear exactly what triggered the August collapse. A number of factors or combination of factors could have been the final perturbation that initiated the collapse of the undersized pillars in the Main West area.
4) LaModel analysis demonstrated that the active pillar recovery mining in the South Barrier section could certainly have been the trigger that initiated the August collapse; however, the modeling by itself does not indicate if the active mining was the most likely trigger.

Table of Contents

Page

List of Figures

Page

1. Objective

The objective of this investigation is to utilize the LaModel boundary-element program along with the best available information to back-analyze the August 6th, 2007 collapse at the Crandall Canyon Mine in order to better understand the geometric and geo-mechanical factors which contributed to that collapse. A secondary objective of this work is to perform a parametric analysis of the pertinent input parameters to assess the sensitivity of the model results to the input values. Ultimately, it is hoped that this back-analysis will help determine improvements in mine design that can be made in the future to eliminate similar type events.

2. Background

2.1 The Crandall Canyon Mine

On August 6th, 2007, the Crandall Canyon Mine in Utah collapsed entrapping six miners. It appeared that a large area of pillars in the Main West and South Barrier sections of the mine had bumped in a brief time period, filling the mine entries with coal from the failed pillars and entrapping the six miners working in the South Barrier section. The seismic event associated with the initial accident registered 3.9 on the Richter scale. Ten days later during the heroic rescue effort, another bump occurred thereby killing three of the rescue workers, including one federal inspector, and injuring six other rescue workers. A few days after the August 16th incident, a panel of ground control experts determined that the Main West area was structurally unstable and posed a significant risk to anyone entering the area. At this point, underground rescue attempts halted and subsequently the mine was abandoned and sealed.

2.2 The LaModel Program

The LaModel program is used to model the stresses and displacements on thin tabular deposits such as coal seams. It use the displacement-discontinuity (DD) variation of the boundary-element method, and because of this formulation, it is able to analyze large areas of single or multiple-seam coal mines (Heasley, 1998). LaModel is unique among boundary element codes because the overburden material includes laminations which give the model a very realistic flexibility for stratified sedimentary geologies and multiple-seam mines. Using LaModel, the total vertical stresses and displacements in the coal seam are calculated, and also, the individual effects of multiple-seam stress interactions and topographic relief can be separated and analyzed individually.

Since LaModel's original introduction in 1996, it has continually been upgraded (based on user requests) and modernized as operating systems and programming languages have changed. The present program is written in Microsoft Visual C++ and runs in the windows operating system. It can be used to calculate convergence, vertical stress, overburden stress, element safety factors, pillar safety factors, intra-seam subsidence, etc. on single and multiple seams with complex geometries and variable topography. Presently, the program can analyze a 1000 x 1000 grid with 6 different material models and 26 different individual in-

seam materials. It uses a forms-based system for inputting model parameters and a graphical interface for creating the mine grid. Also, it includes a utility referred to as a "Wizard" for automatically calculating coal pillars with a Mark-Bienawski pillar strength and another utility to assist with the development of "standard" gob properties. Recently, the LaModel program was interfaced with AutoCAD to allow mine plans and overburden contours to be automatically imported into the corresponding seam and overburden grids. Also, the output from LaModel can be downloaded into AutoCAD and overlain on the mine map for enhanced analysis and graphical display.

2.2.1 Calibrating LaModel:

The accuracy of a LaModel analysis depends entirely on the accuracy of the input parameters. Therefore, the input parameters need to be calibrated with the best available information, either: measured, observed, or empirically or numerically derived. However, in calibrating the model, the user also needs to consider that the mathematics in LaModel are only a simplified approximation of the true mechanical response of the overburden and because of the mathematical simplifications built into the program, the input parameters may need to be appropriately adjusted to reconcile the program limitations.

In particular, after many years of experience with the program, it is clear that in many situations the overburden model in LaModel is not as flexible as the true overburden. The laminated overburden model in LaModel is inherently more flexible than a homogeneous elastic overburden as used in previous displacement-discontinuity codes and it is more flexible than a stratified elastic model without bedding plane slip as used in many finite-element programs. However, using reasonable values of input parameters, the LaModel program still does not produce the level of seam convergence and/or surface subsidence as measured in the field. It is believed that this displacement limitation in the model may be due to the lack of any consideration for vertical joint movement in the program. The laminated model makes a good attempt at simulating bedding plane slip in the overburden, but it does not consider any overburden movement due to vertical/sub-vertical joint slip, thereby limiting the amount of calculated displacements.

Knowing the inherent limitations of LaModel, the user can either calibrate for realistic stress output or for realistic displacement output. In general, it is not possible to accurately model both with the same set of material parameters. If the user calibrates the model to produce realistic stress values, then the input parameters are optimized to match as closely as possible the observed/measured stress levels from the field, and it is likely that the calculated displacement values will be low. On the other hand, if the user optimizes the input parameters to produce realistic displacement/subsidence values, then generally, the calculated stress values will be inaccurate. Historically, the vast majority of LaModel users have been interested in calculating realistic stresses and loads, and in this back-analysis of the pillar stability at the Crandall Canyon Mine realistic stress and load calculations are also the primary objective.

When actually building a model, the geometry of the mining in the seams and the topography are fairly well known and fairly accurately discretized into LaModel grids. The most critical input parameters with regard to accurately calculating stresses and loads, and, therefore, pillar stability and safety factors, are then:

- The Rock Mass Stiffness
- The Gob Stiffness
- The Coal Strength

These three parameters are always fundamentally important to accurate modeling with LaModel and particularly so in simulations analyzing abutment stress transfer (from gob areas) and pillar stability as in the Crandall Canyon Mine situation. During model calibration, it is critical to note that these parameters are strongly interrelated, and because of the model geo-mechanics, the parameters need to be calibrated in the order shown above. With this sequence of parameter calibration, the calibrated value of the subsequent parameters is determined by the chosen value of the previous parameters, and changing the value of any of the preceding parameters will require re-calibration of the subsequent parameters. The model calibration process as it relates to each of these parameters is discussed in more detail below.

2.2.1.1 Rock Mass Stiffness: The stiffness of the rock mass in LaModel is primarily determined by two parameters, the rock mass modulus and the rock mass lamination thickness. Increasing the modulus or increasing the lamination thickness of the rock mass will increase the stiffness of the overburden. With a stiffer overburden: 1) the extent of the abutment stresses will increase, 2) the convergence over the gob areas will decrease and 3) the multiple seam stress concentrations will be smoothed over a larger area. When calibrating for realistic stress output, the rock mass stiffness should be calibrated to produce a realistic extent of abutment zone at the edge of the critical gob areas. Since changes in either the modulus or lamination thickness cause a similar response in the model, it is most efficient to keep one parameter constant and only adjust the other. When calibrating the rock mass stiffness, it has been found to be most efficient to initially select a rock mass modulus and then solely adjust the lamination thickness for the model calibration.

In calibrating the lamination thickness for a model based on the extent of the abutment zone, it would be best to use specific field measurements of the abutment zone from the mine. However, often these field measurements are not available. In this case, visual observations of the extent of the abutment zone can often be used. Most operations personnel in a mine have a fairly good idea of how far the stress effects can be seen from an adjacent gob.

Without any field measurements or observations, general historical field measurements can be used. For instance, historical field measurements would indicate that, on average, the extent of the abutment zone (D) at depth (H) (with both terms expressed in units of ft) should be (Mark and Chase, 1997; Mark, 1992):

$$D = 9.3\sqrt{H} \qquad (2.1)$$

or that 90% of the abutment load should be within:

$$D = 5\sqrt{H} \qquad (2.2)$$

Once the extent of the abutment zone (D) at a given site is determined, an equation recently derived from the fundamental laminated overburden model can be used to determine

the lamination thickness (t) required to match that abutment extent based on the value of some of the other site parameters:

$$t = \frac{2E_s\sqrt{12(1-v^2)}}{E \times M} \times \left(\frac{D - d}{\ln(1 - L_g)} \right)^2 \qquad (2.3)$$

Where:

- E = The elastic modulus of the overburden
- v = The Poisson's Ratio of the overburden
- E_s = The elastic modulus of the seam
- M = The seam thickness
- d = The extent of the coal yielding at the edge of the gob
- L_g = The fraction of gob load within distance D

As mentioned previously, there is a practical trade-off between getting a realistic stress distribution and getting realistic convergence. Equation 2.3 provides an optimum lamination thickness to use for matching the desired abutment stress extent; it should not be used for determining the optimum lamination thickness for accurately calculating displacement and/or subsidence values. Furthermore, when using equation 2.3, the user is fairly accurately matching the "global" stress transfer in the field with the global stress transfer in the model. In many practical mining situations, the more "local" stress transfer between adjacent pillars or between adjacent multiple seams is probably determined by the local flexing of the thinner strata laminations in the immediate roof or interburden. To optimally match these more local effects or to compromise between matching global and local stress transfer, a thinner lamination thickness than determined by equation 2.3 may be appropriate.

2.2.1.2 Gob Stiffness: In a LaModel analysis with gob areas, an accurate input stiffness for the gob (in relation to the stiffness of the rock mass) is critical to accurately calculating pillar stresses and safety factors. The relative stiffness of the gob determines how much overburden weight is carried by the gob; and therefore, not transferred to the surrounding pillars as an abutment stress. This means that a stiffer gob carries more load and the surrounding pillars carry less, while a softer gob carries less load and the surrounding pillars carry more. In LaModel, three models are available to simulate gob behavior: 1) linear-elastic, 2) bilinear and 3) strain-hardening. The gob wizard available in LamPre is designed to assist the user in developing strain-hardening input parameters.

In the strain hardening model, the stiffness of the gob is primarily determined by adjusting the "Final Modulus" (Heasley, 1998; Pappas and Mark, 1993; Zipf, 1992). A higher final modulus gives a stiffer gob and a lower modulus value produces a softer gob material. Given that the behavior of the gob is so critical in determining the pillar stresses and safety factors, it is a sad fact that our knowledge of insitu gob properties and stresses is very poor.

For a calibrated LaModel analysis, it is imperative that the gob stiffness be calibrated with the best available information on the amount of abutment load (or gob load) experienced at that mine. Once again, it would be best to use specific field measurements of the abutment load or gob load from the mine in order to determine realistic gob stiffness. However, these

types of field measurements are quite rare (and sometimes of questionable accuracy). Also, visual observations are not very useful for estimating abutment loads or gob loads; and therefore, general empirical information is quite often the only available data.

In order to calibrate the gob stiffness for a practical situation, it is best to consider a number of general guiding factors. For a first approximation, a comparison of the present gob width and the critical gob width for the given depth can provide some insight. For a critical (or supercritical) panel width (where the maximum amount of subsidence has been achieved), it would be expected that the peak gob load in the middle of the panel would approach the insitu overburden load. As the depth increases from the critical situation and the gob width becomes more subcritical, a laminated overburden analysis with a linear gob material would suggest that the peak gob load would increase linearly with depth from the load level in the critical case (Chase et al., 2002; Heasley, 2000).

The critical depth (H_c) for a given gob width (P) and abutment angle (ß) can be calculated as:

$$H_c = \frac{P}{2 \times \tan(ß)} \tag{2.4}$$

Where:

P = Panel Width (ft)

β = Abutment Angle

and then the expected average gob stress ($s_{gob\text{-}lam\text{-}av}$) at the actual seam depth (H) can be calculated as:

$$s_{gob\text{-}lam-av} = \left(\frac{H}{H_c}\right)\left(\frac{H_c \times d}{2 \times 144}\right) = \left(\frac{H \times d}{288}\right) \tag{2.5}$$

Where:

H = Seam Depth (ft)

d = Overburden Density (lbs/cu ft)

Equation 2.5, which is based on a laminated overburden and a linear elastic gob, implies that the average gob stress for a subcritical panel is solely a function of the depth and equal to half of the insitu stress. (In reality, gob material is generally considered to be strain-hardening and therefore, equation 2.5 may underestimate the actual gob loading.)

Another factor to consider in estimating the gob stiffness and the abutment loading is the abutment angle concept utilized in ALPS and ARMPS. In both these programs, an average abutment angle of 21° was determined from a large empirical database and is used to calculate the abutment loading. Using the abutment angle concept and the geometry shown in Figure 2.1, the average gob stress ($s_{gob\text{-}sup\text{-}av}$) for a supercritical panel can be calculated as:

$$s_{gob\text{-}sup-av} = \left(\frac{H \times d}{144}\right)\left(\frac{P - (H \times \tan ß)}{P}\right) \tag{2.6}$$

Where:

H = Seam Depth (ft)

d = Overburden Density (lbs/cu ft)

P = Panel Width (ft)
β = Abutment Angle

Similarly, the average gob stress ($s_{gob\text{-}sub\text{-}av}$) for a subcritical panel can be calculated from the geometry in Figure 2.1 as:

$$s_{gob\text{-}sub\text{-}av} = \frac{P}{4}\left(\frac{1}{\tan ß}\right)\left(\frac{d}{144}\right) \qquad (2.7)$$

Equation 2.7, which is based on the abutment angle concept of gob loading, implies that the average gob stress for a subcritical panel (with an assumed abutment angle) is solely a function of the panel width.

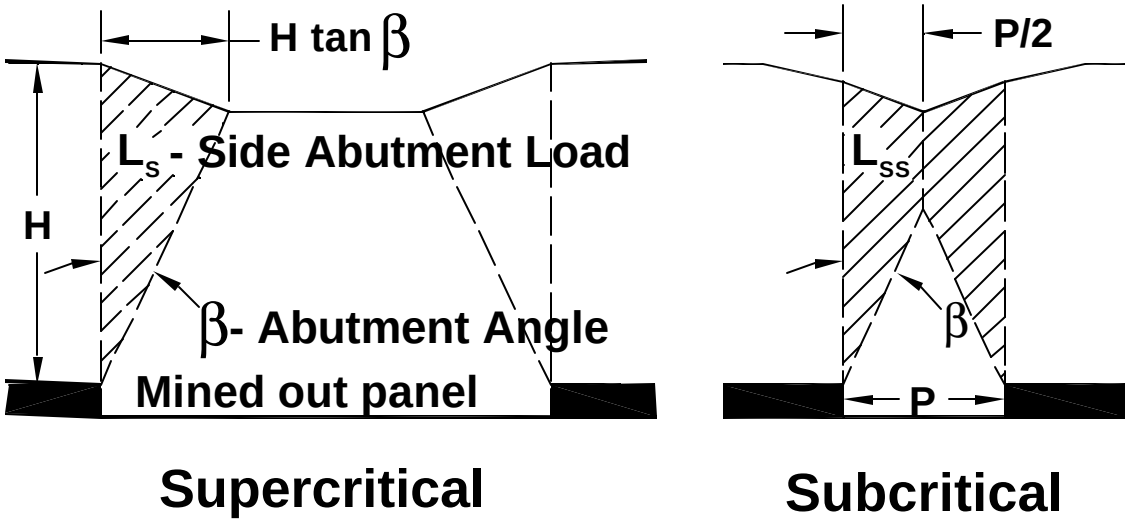

Figure 2.1 Conceptualization of the abutment angle.

Recent work has noted that the concept of a constant abutment angle as used in ALPS and ARMPS appears to breakdown under deeper cover (see Figure 2.2)(Chase et al., 2002; Heasley, 2000). In particular, for room-and-pillar retreat panels deeper than 1250 ft, it was found that a stability factor of 0.8 (for strong roof) could be successfully used in ARMPS, as opposed to a required stability factor of 1.5 for panels less than 650 ft deep. One of the more likely explanations for this reduction in allowable stability factor is that the actual pillar abutment loading may be less than predicted by using the constant abutment angle concept (Chase et al., 2002). Colwell found a similar situation with deep longwall panels in Australia where the measured abutment stresses were much less than predicted with a 21° abutment angle (Colwell et al., 1999).

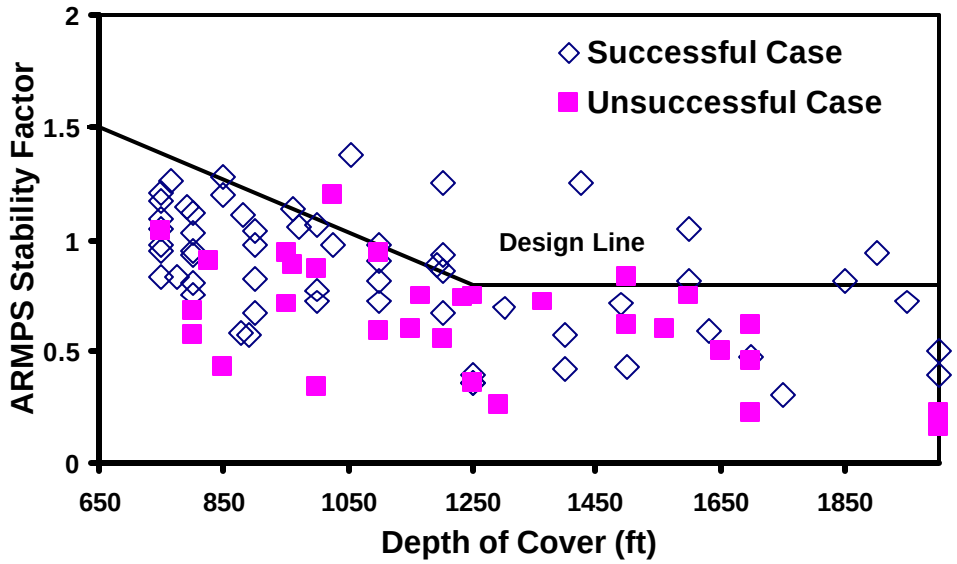

Figure 2.2 Suggested stability factors for the ARMPS deep-cover database.

The degree to which a constant abutment angle might overestimate the abutment loading can be investigated by comparing the recommended NIOSH stability factors for shallow and deep cover. Below 650 ft, a stability factor greater than 1.5 is recommended but, at depths greater than 1250 ft, 0.8 is acceptable. Since higher coal strengths have not been correlated with greater depth, it is most likely that the lower stability factor recommendation is due to an overestimate of applied stress or load. Based on the NIOSH recommendations, it appears that the abutment loading based on the constant abutment angle of 21° could be as much as 1.875 (1.5/0.8) times higher than actual loading experienced in the field. Implementing this adjustment produces the following equation for an adjusted average gob load for a subcritical panel based on the abutment angle concept (given without derivation):

$$s_{\text{gob-adj-av}} = \left[1 - \left(\frac{0.8}{1.5}\right) * \left(\frac{(4H * \tan ß) - P}{4H * \tan ß}\right)\right] * \left(\frac{H * d}{144}\right) \qquad (2.8)$$

Where:

H = Seam Depth (ft)
d = Overburden Density (lbs/cu ft)
P = Panel Width (ft)
β = Abutment Angle

The preceding discussion on gob stiffness and loading has produced several competing concepts/equations. Equation 2.5, which is based on a laminated overburden model and a linear elastic gob, implies that the average gob stress for a subcritical panel is solely a function of the depth. Equation 2.7, which is based on the abutment angle concept of gob loading, implies that the average gob stress for a subcritical panel is solely a function of the panel width. Equation 2.8 modifies the abutment angle concept in an attempt to produce more realistic results for panels deeper than 1250 ft.

It is not entirely clear which concept or equation provides the most realistic estimates of gob stress. From recent experience, Equation 2.7 appears to provide a lower bound for realistic gob stresses and Equation 2.8 appears to provide an upper bound. Equation 2.5 is between the bounds set by equations 2.7 & 2.8 and may provide a reasonable starting point for further calibration. Regardless of which equation is chosen as a starting point, it is clear that a realistic gob/abutment loading is critical to a realistic model result and that the gob stiffness should be carefully analyzed and calibrated in a realistic model.

If the user desires to calibrate the abutment and/or gob loading in the model based on a laminated approximation or a specific abutment angle, then either equation 2.5, 2.7 or 2.8, depending on the situation, could be used to determine the average gob loading. Each of these equations provides an estimate of average gob stress. After choosing among them, the user would need to run several models with various gob stiffnesses (in LaModel or LaM2D), measure the average gob loading in the model, and then choose the final gob modulus which best fits the estimated gob stress.

2.2.1.3 Coal Strength: Accurate insitu coal strength is another value which is very difficult to obtain and yet is critical to determining accurate pillar safety factors. It is difficult to get a representative laboratory test value for the coal strength and scaling the laboratory values to accurate insitu coal pillar values is not very straightforward or precise (Mark and Barton, 1997). For the default coal strength in LaModel, 900 psi (S_i) is used in conjunction with the Mark-Bieniawski pillar strength formula (Mark, 1999):

$$S_p = S_i\left[0.64 + 0.54\left(\frac{w}{h}\right) - 0.18\left(\frac{w^2}{lh}\right)\right] \qquad (2.9)$$

Where:

S_p = Pillar Strength (psi)
S_i = Insitu Coal Strength (psi)
w = Pillar Width
l = Pillar Length
h = Pillar Height

This formula also implies a stress gradient from the pillar rib that can be calculated as:

$$s_p(x) = S_i\left(0.64 + 2.16\left(\frac{x}{h}\right)\right) \qquad (2.10)$$

Where:

$s_p(x)$ = Peak Coal Stress (psi)
x = Distance into Pillar
S_i = Insitu Coal Strength (psi)
h = Pillar Height

The best technique to determine appropriate coal strength for LaModel is to back analyze a previous mining situation (similar to the situation in question) where the coal was close to,

or past, failure. Back-analysis is an iterative process in which coal strength is increased or decreased to determine a value that provides model results consistent with the actual observed failure. This back analysis should, of course, use the previously determined optimum values of the lamination thickness and gob stiffness. If there are no situations available where the coal was close to failure, then the back-analysis can at least determine a minimum insitu coal strength with some thought of how much stronger the coal may be, or the default average of 900 psi can be used.

The 900 psi insitu coal strength that is the default in LaModel comes from the databases used to create the ALPS and ARMPS program and is supported by considerable empirical data. It is the author's opinion that insitu coal strengths calculated from laboratory tests are not more valid than the default 900 psi, due to the inaccuracies inherent to the testing and scaling process for coal strength. If the LaModel user chooses to deviate very much from the default 900 psi, they should have a very strong justification, preferably a suitable back analysis as described above.

2.2.1.4 Post-Failure Coal Behavior: The present understanding of the post failure behavior of coal pillars is very limited, and most of this understanding comes from the analysis of coal specimens tested in the laboratory, not pillars in the field (Barron, 1992; Das, 1986). It is generally understood that a slender coal specimen tested past its ultimate strength will initially reach maximum peak strength at the point of "failure" and then, with further strain, the specimen will "soften" (carry increasingly less load as it continues to be deformed) until the broken coal reaches a final "residual" strength. In general, as the specimen width-to-height ratio increases or the confining pressure on the specimen increases, the peak strength will increase, the residual strength will increase, and the softening modulus will flatten. At a particular width-to-height ratio (Das found this to be approximately 8:1) or confining stress, the specimen will no longer soften after elastic failure, but will become essentially "elastic-plastic". At higher width-to-height ratios or confining pressure, the coal specimens actually become "strain-hardening", where they carry increasing load with increasing deformation after elastic failure. There is also some information that indicates that coal in the field may actually become pseudo-ductile at very high confining stresses (Barron, 1992; Heasley and Barron, 1988).

When the post-failure behavior of coal pillars needs to be accurately simulated (as is the case with this back-analysis of Crandall Canyon Mine), "residual strength" and "residual strain" must be determined accurately. These parameters essentially define the pillar post-failure behavior. Some insights to residual strength and residual strain have been provided by laboratory tests where the peak and residual strength are seen to increase with increased confining pressure (or distance into the pillar) while the softening modulus decreases with increased confinement. These trends are also seen/assumed to be valid in the field.

Some pioneering work in trying to accurately quantify the strain softening behavior of coal pillars for boundary-element modeling was done by Karabin and Evanto (1999). In this work, they developed an equation from field measurements which estimated an ultimate residual stress level (s_r):

$$s_r(x) = (0.2254 \times \ln(x)) s_p(x) \qquad (2.11)$$

Where:

$\sigma_r(x)$ = Residual Stress (psi)
$\sigma_p(x)$ = Peak Stress (psi)
x = Distance into Pillar

and the strain level (ε_r) for the final residual stress:

$$\varepsilon_r(x) = 4 \times \varepsilon_p(x) \qquad (2.12)$$

Where:
$\varepsilon_r(x)$ = Residual Strain (psi)
$\varepsilon_p(x)$ = Peak Strain (psi)
x = Distance into Pillar

These post-failure stress-strain relationships are consistent with trends in the load/deflection response of coal samples as described above; however, Karabin and Evanto certainly note that these properties are only "first approximations" and must be verified for accuracy. For use in LaModel or any boundary element model, these are some of the only post-failure coal properties calculations available. Certainly, this is an area for additional research. (It should be noted in equation 2.11 that the value, "0.2254" essentially determines the global magnitude of the residual stress in this strain-softening coal model and that the value of "4" in equation 2.12 essentially determines the global magnitude of the residual strain value in this strain-softening model. For LaModel calibration purposes, these single values can be adjusted in order to vary the residual strength or strain of the coal model.)

2.2.2 LaModel and Bumps:

The term "bump" is used in this report to describe the sudden violent failure of a coal pillar or rib which ejects coal into the adjacent openings. At the present time, the exact mechanics of coal bumps are not completely understood. However, a lot of research has been done to understand the bump phenomenon, and a lot of progress has been made. Bumps are known to be associated with deep cover, competent strata and retreat mining which concentrates overburden stress. Also, it is known that bump behavior can be triggered in laboratory specimens by using a "soft" loading system or by suddenly releasing confining stresses. The past bump research has produced many significant improvements in minimizing or eliminating coal bumps (in some situations) through better mine designs and cut sequencing. However, in general, it is still not possible to precisely predict whether a particular pillar or mine plan will bump, nor is it generally possible to predict the exact timing of a bump event. Bump prediction can be readily compared to earthquake prediction. The general area and nature of certain earthquakes (bumps) are well understood, but predicting the exact timing, location and magnitude of the next earthquake (bump) is still beyond the present scientific capability.

In LaModel, a bump is simply simulated as a pillar (or coal) failure. LaModel does not calculate any of the details of the coal or overburden failure mechanics; the program does not consider whether a bump occurs from simply overloading the coal or whether there is some external loading mechanism or sudden loss of confinement. However, coal that bumps has to be at, or very near, its ultimate failure strength at the time of the bump; therefore, it is reasonable to associate the point of coal failure in LaModel simulations with potential coal

bumps. Since LaModel does not have any dynamic capabilities, it cannot distinguish between a gentle controlled pillar failure and a violent pillar bump. However, that distinction can generally be determined from the geology and/or history of the mine. In some mines, the pillars fail gently while in other mines, with "bump-prone" conditions, pillar failure is likely to occur as a bump. Therefore, in a bump-prone mine or in bump-prone conditions, it can be assumed that any pillar failure could be a potential bump.

2.2.3 LaModel and Massive Pillar Collapses:

The term massive pillar collapse (also called "cascading pillar failures", "domino-type failures" or "pillar runs") refers to the situation in a room-and-pillar mine where a large area of undersized pillars dynamically fails. In a massive pillar collapse, it is generally assumed that one pillar fails (for some reason), it sheds its load to the adjacent pillars, causing them to fail, and so forth (Mark et al,, 1997). This phenomenon has occurred a dozen or so times in the U.S, and has been fairly well documented and analyzed (Mark et al., 1997; Zipf, 1996). The basic condition for a massive pillar collapse is a large area of pillars loaded almost to failure. Generally, the roof and floor must be fairly competent or they would yield and relieve the pressure on the pillars. Also, the pillars have to be strain-softening in order for them to shed load and propagate the collapse. (On initial inspection, the Crandall Canyon Mine failure certainly appears to be consistent with a massive pillar collapse; however, the depth of the mine workings, the size of the collapse area and the bump-type failure set this failure outside of the previous database of massive pillar collapses.)

In LaModel, a massive pillar collapse is simulated when a "small" change in the mining condition results in a "large" number of pillars failing over a "large" area. The small change in mining condition can be any one (or combination) of a number of items: an additional cut or two, the pulling of another pillar, a small drop in coal strength (e.g. deterioration over time), the sudden movement on a fault or joint, etc. Of course, in LaModel, as in reality, to accurately simulate the massive pillar collapse, a large area of pillars must be close to failure and they must be strain-softening.

2.2.4 LaModel and Time and Homogeneity:

A complete discussion of LaModel calibration must also address time and homogeneity. In a LaModel analysis, the solutions are static. The model converges on a static solution of stresses and displacements based on the given geometry and material properties. In reality, we know that geologic materials change over time without necessarily any outside stress or displacement influence. Coal pillars can slough, weaken and fail, roof rock can crack, soften and fall, and floors can heave, etc. In fact, the geo-mechanical environment in a mine is very dynamic. Not only is the geometry constantly changing due to the active mining, but the pillars, roof and floor are continuously adjusting to the stresses through time. Generally, the geo-mechanical adjustment to new stresses initially occurs quickly and then slows exponentially as time advances.

In a LaModel analysis, geologic materials are assumed to be perfectly homogeneous. The material behavior is identical at different locations in the model and the stresses and displacements are continuous and smooth from one location to another and from one step to the next. In reality, we know that geologic material is not homogeneous. The rock and coal have bedding planes, joints and other discontinuities, and the intrinsic material properties can change dramatically (10-20% or more) in very short distances. Similarly, failure in a mine is

not typically continuous and smooth. The roof and floor can appear essentially stable and then suddenly fail, pillars can suddenly slough or fail and certainly large cave/gob areas are known to advance in a stepwise fashion.

Since LaModel does not inherently account for the effects of time or inhomogeneity, the user needs to consider these factors in the analysis and interpretation of any results. For instance, in a given cut sequence, LaModel may indicate that a certain pillar has just barely failed. In reality, considering time, it may take a little while for the pillar to ultimately fail, or considering homogeneity, the pillar may be a little weaker or stronger than modeled and may fail a little sooner or later in the cut sequence. The static and homogenous nature of LaModel actually resists sudden changes in stability. The classic example is the analysis of a large area of equal size (strain-softening) pillars. A LaModel analysis may show that all of these "equal" pillars have exactly the same stability factor that is a bit greater than one; and therefore, the area is stable. In reality, the pillars have some statistical distribution of strength, and the stability factor of each individual pillar is slightly different. So, even if the average stability factor of the section is greater than one, once the weakest pillar fails and sheds it load, this can overload the adjacent pillars and the whole section can collapse.

To account for the assumptions regarding time and homogeneity inherent in LaModel, users must use some intuition to properly assess the realistic stability of the modeled mine plan. For example, the user needs to consider how the result might change if the material weakens over time, or if there is some variation in material properties. In an analysis of a massive pillar collapse with LaModel, small changes in material properties and/or geometry can cause large changes in pillar stability. Time dependent behavior or a local inhomogeneity in the material properties can have a large effect on the real stability of the situation and greatly affect the correspondence between the model and reality. Therefore, it is very difficult to "exactly" model unstable mining situations with LaModel; however, the general instability can easily be modeled.

2.2.5 Pillar Safety Factors in LaModel:

Recently, the capability of calculating safety factors was added to the LaModel program (Hardy and Heasley, 1996). For the strain-softening and elastic-plastic material models, the safety factor is calculated as the ratio between the peak strain defined for that particular element and the applied strain:

$$SF = \frac{e_p}{e_a} \tag{2.13}$$

Where:

SF = Safety Factor
e_p = Peak Strain
e_a = Applied strain

For the linear elastic model, which has no pre-defined peak stress or strain, the strain safety factor is set to a default value of 10 (in order to adjust the scaling).

Conventionally, safety factors are calculated on a stress basis, rather than a strain basis. However, stress based calculations can be problematic when determining safety factors in the post-failure range in LaModel as inappropriate values result for the elastic-plastic and strain-softening material models. The strain-based safety factor calculation detailed above yields values equivalent to the stress-based calculation in the pre-failure range but also gives

appropriate values in the post-failure range for all the materials. Safety factors below 1.0 indicate that an element has failed. Values lower than 1.0 provide a measure of the amount of strain that has occurred beyond failure. For instance, an element which has compressed to twice the peak strain will generate a safety factor of 0.5. Therefore, the strain-based safety factor as shown in Equation 2.13 above is used throughout LaModel.

In LaModel, the safety factor is initially calculated for each individual element and this value can be displayed in the output. However, most users desire to know the safety factor for the entire pillar. In order to provide a pillar safety factor, safety factors from each individual element comprising a pillar are averaged. This algorithm is easy to implement, but does not necessarily give a pillar safety factor which equates to the safety factor that would be determined from a traditional analysis of the full stress-strain curve for the pillar. The safety factor calculation is accurate for the stress-strain curve of the individual elements, but when the element safety factors are averaged over the pillar, the average does not give a traditional safety factor result.

With strain-softening elements, the peak stress and peak strain are determined from the insitu coal strength, the coal modulus, and the distance of the element into the pillar (see equation 2.10). For the weaker elements at the edge of the pillar, the peak stress is reached at much lower levels of strain than the elements in the confined core of the pillar. After the edge elements reach peak stress, they soften as pillar strain continues and the interior elements move towards failure. At the point of peak pillar strength (the "traditional" point of failure and a unity safety factor) only a few elements in the core of the pillar are still in the elastic range and have safety factors greater than one. Thus, the overall safety factor for the pillar calculated from an average of the elements will be much lower than one. The exact magnitude of this reduced safety factor is determined by: the size and shape of the pillar, the amount of strain-softening in the elements, and the flexibility of the rock mass. Since the pillar elements do not reach peak stress at the same time, the ultimate strength of the pillar is not the sum of the ultimate strengths of the elements. In particular, the pillar peak stress is affected by the degree of strain softening input to the elements. (For a pillar made of elastic-perfectly plastic materials as generated by the LaModel coal wizard, the peak strength of the pillar will be the weighted sum of the peak strength of the elements.)

For an individual pillar, a comparison between the pillar stress-strain curve and the averaged pillar safety factor calculated in LaModel can be observed by plotting these values on the same graph (see Figure 2.3). The exact values for these plots are determined by calculating the stress value and safety factor for each pillar element at various strain values. Next, at each strain level, the stress values and safety factors are weighted by the number of each type of element in the pillar and then finally, the total weighted stress and safety factor values are averaged by the total number of elements in the pillar. The plot in Figure 2.3 show the values for a 60 X 70 foot pillar as used in the North Barrier Section of the Crandall Canyon Mine. With the amount of strain-softening in the elements of this pillar and the dimensions of the pillar, the peak stress in the pillar corresponds to a safety factor of 0.55, quite a bit below 1.0. (In the following analysis of the Crandall Canyon Mine, the pillar safety factors where adjusted so that the point of peak stress corresponded to a pillar safety factor of 1.0. As an example, for this pillar, the pillar safety factor calculated by LaModel would be divided by 0.55 to get the adjusted safety factor.)

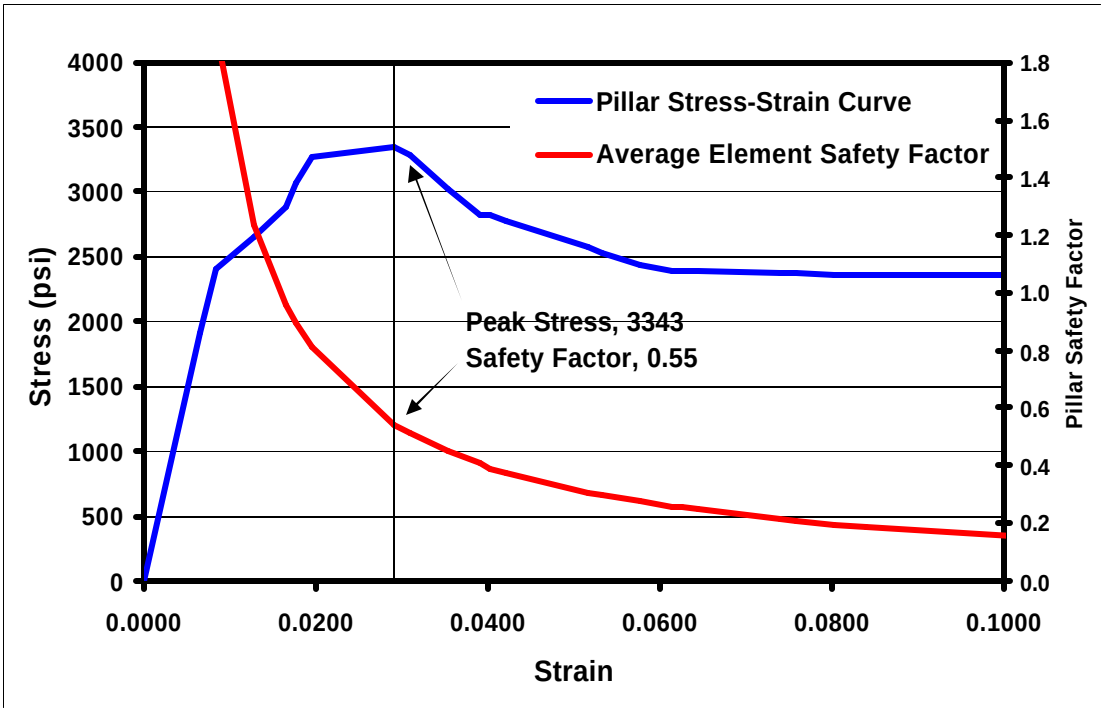

Figure 2.3. Stress-strain and safety factor curves for the North Barrier 60 X 70 ft pillar.

3. The LaModel Analysis

3.1 Approach

The major effort in this back-analysis was directed toward calibrating the critical rock mass, gob and coal properties to provide the best LaModel simulation of what we know happened at Crandall Canyon Mine. Initially, the mine and overburden geometries of the Main West area of the mine were developed into LaModel mine and overburden grids. Then, the rock mass stiffness was calibrated against the expected abutment load distribution (i.e., extent) consistent with empirical averages and local experience. Next, the gob behavior was calibrated to provide reasonable abutment and gob loading magnitudes. For the coal properties, the peak strength was primarily determined from back analyzing a March 10th bump in the Main West North Barrier section, and the strain-softening behavior was optimized from the back-analysis of the August 6, 2007, event. Throughout the back-analysis, a wide range of reasonable input parameter values were investigated to optimize the agreement between the model and the observed reality. Also, a number of different events that could have triggered the August 6th collapse were investigated with the basic model.

3.2 Basic Calibration Points

Knowledge of the actual mining conditions and the scenarios in which they occurred served as the basis for calibrating the LaModel model to the reality of the mining situation at Crandall Canyon Mine. A number of particular locations, situations and conditions were used as distinct calibration points.

3.2.1 Main West:

During the initial mining of the Main West section, the pillars were assumed to be stable, although some difficulties were encountered in this area and the safety factor under the deepest cover was probably not very high (see Figure 3.1). When longwall Panel 12 to the north and Panel 13 to the South were being mined, the abutment stress effects were seen in the outside entries of Main West and additional support was installed. When the Main West section was eventually sealed, some of the intersections had fallen and the pillars were in poor shape.

3.2.2 North Barrier:

When the North Barrier Section was initially developed, the section was fairly stable. Under the lower cover at the western end of the section, the pillar retreat was fairly successful. As the retreat line moved under the deeper cover to the east, pillar line stresses increased and became untenable in the 137-138 crosscut area where a couple of pillar rows were then skipped. After mining a couple of pillars between crosscuts 134 and 135, a bump (pillar failure) occurred that effected: the two rows of pillars inby, a number of pillar ribs and the barriers along the bleeder entry, and one to two rows of pillars outby crosscut 134 (see Figure 3.2). At this point, the section was abandoned and sealed shortly after that.

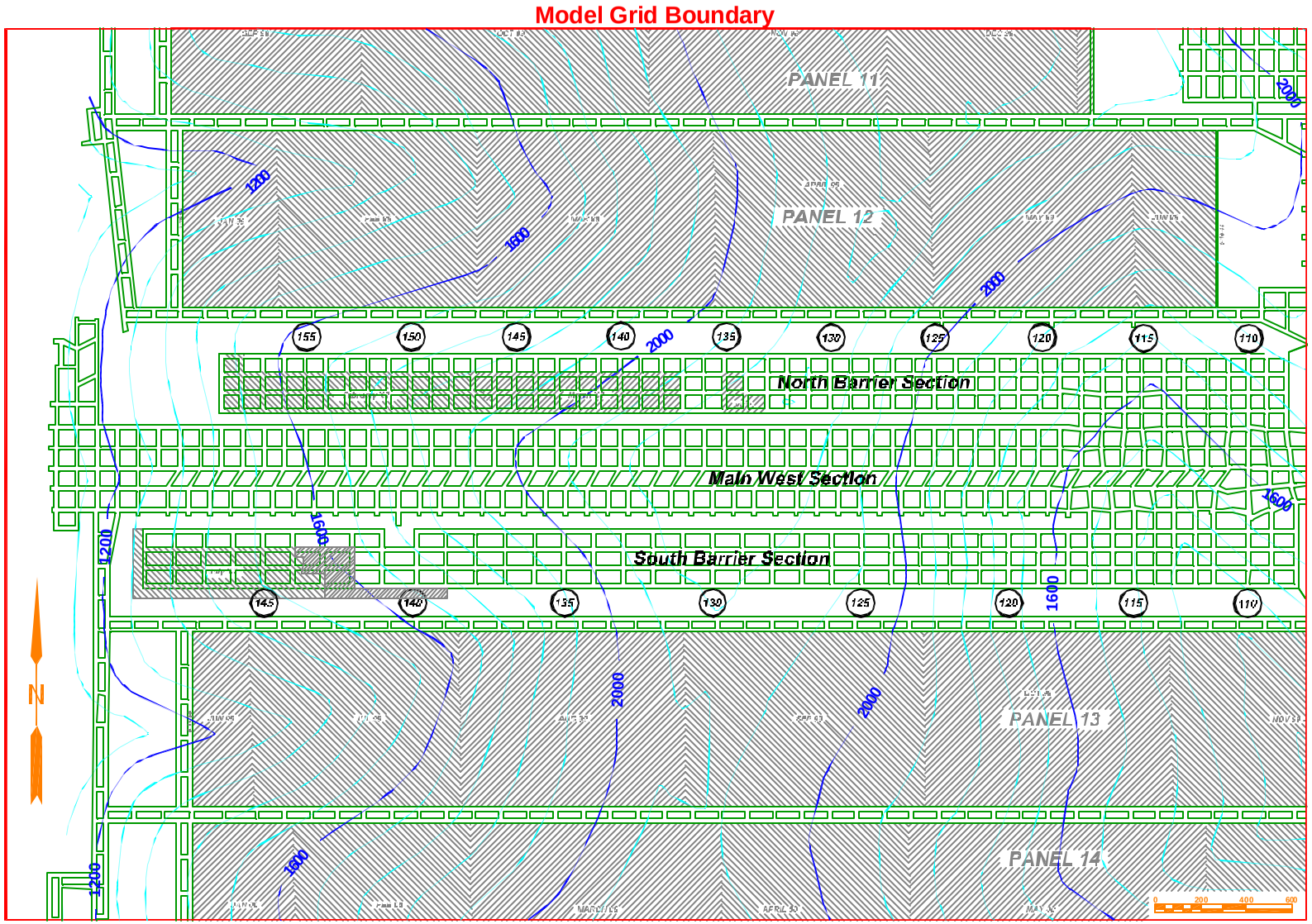

Figure 3.1 Map of the Main West area.

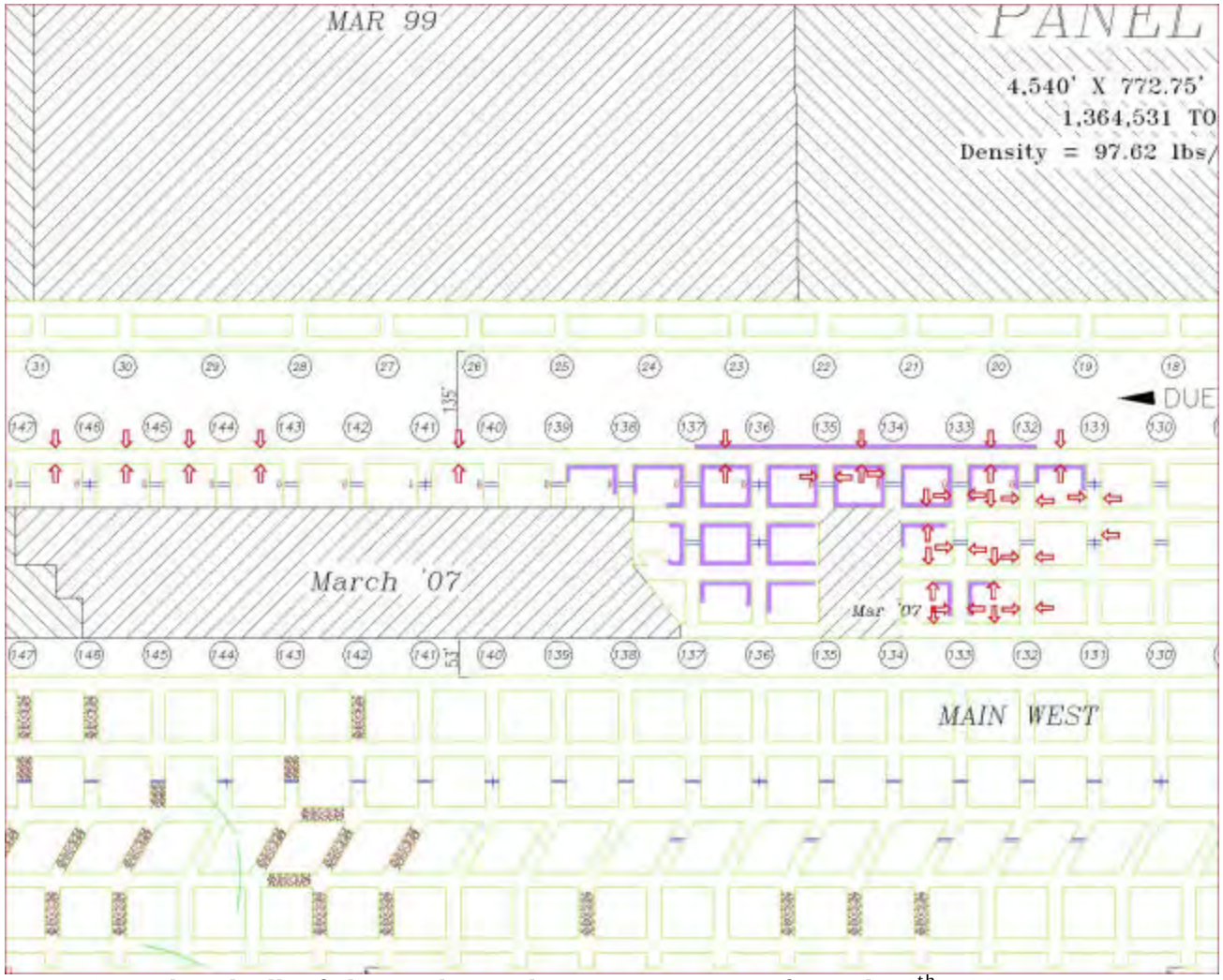

Figure 3.2 Rib and pillar failure in the North Barrier section as of March 16th, 2007.

3.2.3 South Barrier:

When the South Barrier section was developed, the section was fairly stable. Also, as the section retreated to crosscut 142, the conditions were mostly manageable. There were some signs of high stress and some bumping noted in the section before the August 6th, 2007 collapse.

3.2.4 Results of The August 6th Collapse:

Immediately after the August 6th, 2007, collapse, it appeared that the pillars in the South Barrier Section inby crosscut 120 had bumped and filled the entries with coal. Stress effects from the collapse were visibly evident in the pillar ribs as far outby as crosscut 116 in the South Barrier and Main West Sections. On the inby end of the South Barrier, video from the drillholes revealed that there was still several feet of open entry at the intersections of cross cuts 137-138 and entry #2, but that the entries and crosscuts were bumped full of coal. Further inby the South Barrier section in the bleeder area at crosscut 142, the entry was half filled with bumped coal, and at the end of the bleeder at crosscut 147, the entry was wide open. Observations made during the rescue operation indicated that the remaining south barrier had certainly bumped on the north rib and subsequent analysis indicates that it may have completely failed under the deepest cover.

A Richter 3.9 seismic event was associated with the collapse. Subsequent analysis of the initial part of this event locates it over the barrier pillar between the Main West and South Barrier sections at about crosscut 143. After the collapse, seismic activity was located along a North-South line through the whole Main West area around crosscut 120 and around crosscuts 141 to 146.

3.3 The LaModel Grid

The LaModel simulation of the Main West area encompassed the entire Main West, North Barrier and South Barrier Sections so that all of the areas of interest could be included within one grid. Thus, the west and east boundaries of the model were set as shown in Figure 3.1. The north and south boundaries were established to include the full abutment loading from both the northern and southern longwall mining districts for at least a couple of panels. So, anticipating a symmetric boundary condition, model boundaries were set in the middle of the longwall panels, 1-1/2 panels from the north and south barriers (see Figure 3.1).

For determining an optimum element size, a number of factors were considered. First, the desired model area shown in Figure 3.1 is approximately 6000 X 4000 ft. Presently, LaModel is limited to a maximum grid size of 1000 X 1000 elements; therefore, the required element size must be greater than 6 ft. Second, the pillar sizes were examined. The pillars are 80 X 92 ft on centers in the North Barrier section, 90 X 92 ft on centers in the Main West section, and 80 X 130 ft on centers in the South Barrier section. Also, in this deep cover, high stress situation, it was desired to have a pillar yield zone that would extend completely through the 120 ft wide barriers to the north and south of the room-and-pillar sections. So, considering all of these factors, a 10 ft wide element was chosen. This width fits most of the pillar dimensions fairly well and can easily span the 6000 ft grid width. Also, with a 10 ft wide element, the 120 ft wide barrier will only require 12 yield zone elements to reach to the middle of the pillar (two element codes are required to define each yield zone in models developed for this report).

Five and 6 ft wide elements were also considered. However, in the case of the 5 ft element, a 5000 ft wide grid would not span the desired model area, it does not fit the pillar dimensions any better than the 10 ft element, and it would take 24 yield elements to represent the larger barrier pillars. In the case of the 6 ft element, a 6000 ft grid just barely spans the desired model area, it does not fit the pillar dimensions any better than the 10 ft element, and it would take 20 yield elements to cover the larger barrier pillars.

In the final grid, 10 ft elements were used and overall dimensions were set at 570 elements in the east-west direction and 390 elements in the north-south direction with a grid boundary as shown in Figure 3.1. The actual mine grid was automatically generated from the AutoCAD mine map of the Main West area with some manual editing to enforce 2 element entry widths and rectangular pillars.

For inputting the overburden information to the model, an overburden grid was developed that was 1500 ft wider on all 4 sides than the model grid and used 100 ft wide elements on an 87 X 69 element grid. This overburden grid was then automatically generated from the AutoCAD topographic lines as shown in Figure 3.1. The result of the overburden grid generation process is the calculated overburden stress on the coal seam as shown in Figure 3.3. In the plotted overburden stress, it can be seen how the laminated model softens the effects of the ridges and valleys in the topography. Also, a couple other points should be noted in this plot. First, the north-south trending ridge centered over crosscuts 130 in both the North and South Barrier sections dominates the overburden stress. From the center part of this ridge, the overburden stresses drop quickly to both the east and west, or both the inby and outby ends of the North Barrier, Main West and South Barrier Sections. Also, the slightly higher overburden stress above longwall Panel 12 should be noted. This higher stress is probably carried to some extent by the abutment onto the North Barrier section.

3.4 Calibrating the Critical Parameters

3.4.1 Determining the Rock Mass Lamination Thickness:

Equation 2.3 was used to determine an appropriate lamination thickness to give a realistic extent of the abutment zone in this model. In this equation, the rock mass was assumed to have an elastic modulus of 3,000,000 psi and a Poisson's ratio of 0.25. The coal seam was assumed to have an elastic modulus of 300,000 psi and to average 8 ft thick. A "high average" overburden depth of 2000 ft was used resulting in a full abutment extent (Equation 2.1) of 416 ft and 90% of the abutment load (Equation 2.2) within 224 ft. Using a yield zone depth of 40 ft (consistent with the extent of yielding actually observed in the model), the required lamination thickness was calculated as 533 ft. As part of the parametric analysis discussed later, lamination thicknesses of 300, 500 and 600 ft were investigated. Ultimately, the 500 ft value appeared to match the observed conditions best and was subsequently used in the optimum model.

For Crandall Canyon Mine, Equations 2.1 and 2.3 appear to be fairly appropriate. The mine noted the effects of increasing stresses in the Main West section when the adjacent longwalls were retreating and these longwalls are some 430 ft away. Also, the Wasatch Plateau area and the Crandall Canyon Mine are known for stiff massive sandstones in the overburden which would help bridge and transfer the abutment stresses for considerable distances and, therefore, help justify thicker model lamination.

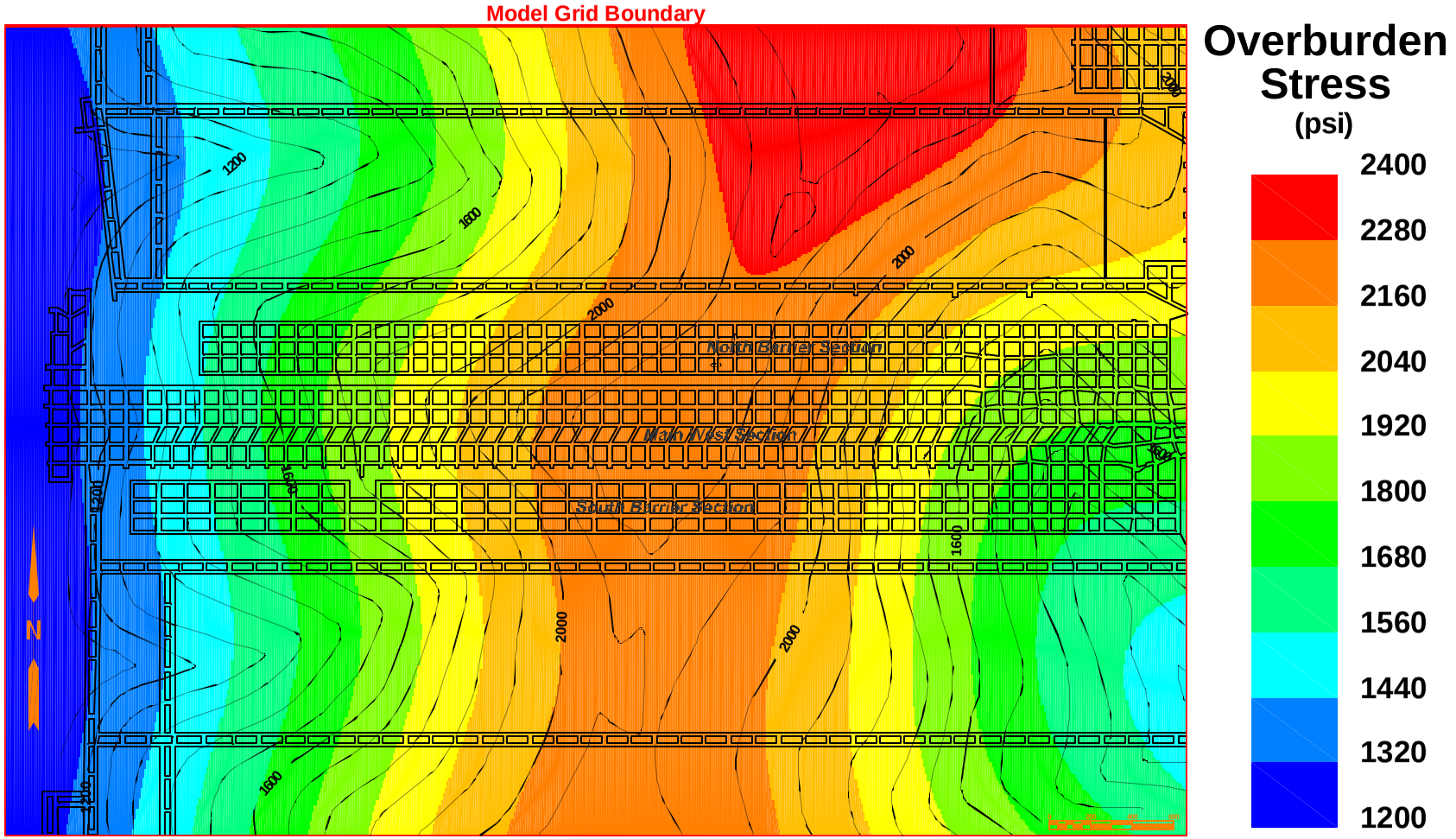

Figure 3.3. Overburden stress as calculated by LaModel.

3.4.2 Determining the Gob Stiffness:

A number of factors were examined to optimize gob loading and gob stiffness in the model. First, Equation 2.4 was used with an 800 ft wide panel at 2000 ft of cover and an abutment angle of 21º to calculate a critical seam depth of 1042 ft. Then, using Equation 2.5, the laminated overburden model would suggest that an average gob loading of 1125 psi would be appropriate. Next, the gob loading as used in ALPS and ARMPS was calculated using Equation 2.7 with an abutment angle of 21º and an overburden density of 162 lbs/cu ft. This results in an average gob stress of 586 psi and a corresponding abutment load of 1659 psi. However, with the 2000+ feet of overburden the "correction" factor of 1.875 was applied to the abutment load resulting in a suggested average gob loading (Equation 2.8) of 1362 psi.

From these various calculations of gob loading, the average gob stress value of 586 psi, (73% abutment load) as determined by the abutment angle concept, is considered a very lower bound. The average gob loading of 1362 psi, (38% abutment load) as determined by adjusting the abutment loading by the 1.875 "deep-cover" factor, is considered an upper bound. The actual gob loading is probably somewhere in between, but choosing the exact value is very difficult. In this mining situation at the very deepest part of the ARMPS deep-cover database, the tendency might be to start on the high end of gob loading range, something in the 1000-1300 psi range, but with the stiff competent overburden at the mine, the gob loading would tend to be less.

To investigate the appropriate final gob modulus to use in the model, a simple grid was built of the Crandall Canyon Mine without any barrier mining in the Main West area. The depth was set at 2000 ft and then various combinations of lamination thickness and final gob modulus were input and the resultant average gob stress adjacent to the Main West area was determined. The results of this parametric analysis are shown in Table 1 and Figure 3.4. In these results, it is easy to see that, for a given lamination thickness, increasing the final gob modulus increases the average stress on the gob. Also, it is clear that for a given final gob modulus, increasing the lamination thickness reduces the average stress on the gob.

In the parametric analysis discussed later, average gob stresses of 800 – 1400 psi were evaluated. Ultimately, gob stress around 900 psi (60% abutment loading) was determined to be best for matching the observed results. With the 500 ft lamination thickness this gob stress translates to a final gob modulus of 250,000 psi (see Table 1 and Figure 3.4).

Table 3.1 Average Gob Stress as a function of lamination thickness and final gob modulus.

Final Modulus (psi)	Average Gob Stress (psi)		
	Lamination Thickness		
	300 ft	500 ft	600 ft
100,000	680	435	365
200,000	1066	763	662
300,000	1305	1012	903
400,000	1467	1198	1094
500,000	1581	1340	1242
600,000	1668	1449	1359
700,000	1735	1538	1455

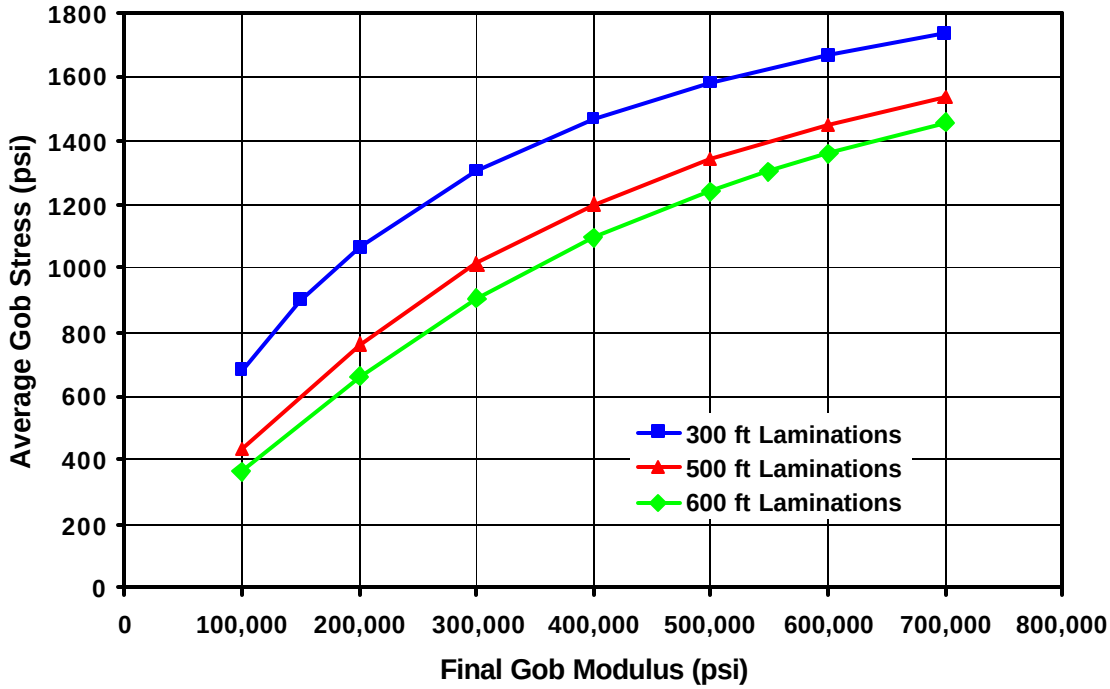

Figure 3.4 Average gob stress as a function of lamination thickness and final gob modulus.

3.4.3 Determining the Coal Strength:

In determining appropriate coal strength, a couple of simple analyses provided significant insight. The pillars in the Main West Section were certainly stable when they were mined, and the overburden stress plot (Figure 3.3) shows some 2200 psi of insitu stress. With 90 X 92 ft centers and 20 ft wide openings, the extraction ratio would be 39.1% and the assumed tributary area stress on these pillars would be 3614 psi. Using the Mark-Bieniawski pillar

strength formula, this implies that the insitu coal strength must be at least 943 psi. Similarly, evaluating the 80 X 92 ft pillars in the North Barrier section and the 80 X 130 ft pillars in the South Barrier section (with 18 ft wide entries), implies a minimum coal strength of 965 psi and 813 psi, respectively. This analysis assumes tributary area loading, but with the narrow panels and competent overburden, this may not be the case causing the true pillar loading to be somewhat less. From underground observations, these pillars did not appear to be too close to failure on development; and therefore, the insitu coal strength could be higher than the calculated minimum. However, considering that the Main West was showing considerable weakness when it was eventually sealed, the safety factors on development were certainly not excessive.

Another simple analysis which can provide some insight is to compare the pillar design in the North Barrier section to the design in the South Barrier section. Based on the above analysis, and comparing the 965 psi minimum strength in the North Barrier to the 813 psi minimum strength in the South Barrier implies that the larger pillars in the South Barrier section provide a 16% stronger design than the pillars in the North Barrier section.

3.4.3.1 Back Analysis of North Barrier Bump: Ultimately, the best information for computing the insitu coal strength at Crandall Canyon Mine is the pillar bump that occurred on March 10th, 2007, in the North Barrier Section (see Figure 3.2). A back-analysis of this event can provide reasonably reliable insitu coal strength to use in the further analysis of the subsequent collapse. To develop a back-analysis of the North Barrier Section bump, a six step LaModel run was developed to represent the cut sequence leading up to the bump. This model starts when the pillar retreat line is at crosscut 141, and retreats the pillar line one crosscut per step until the point when the bump occurred (i.e., after the pillars were pulled at crosscut 134 (see Figure 3.5)). For this back-analysis, Figure 3.2 was used as the primary calibration objective. This figure indicates that 2 rows of pillars inby crosscut 135 failed and bumped and that 1 to 2 rows of pillars outby crosscut 134 failed and bumped, also, the failures appear to be more prevalent towards the north. To calibrate the model, the coal strength was adjusted until the calculated conditions matched the observed conditions as closely as possible. Figure 3.5 shows the results of this calibration process. (Note: the safety factors in Figure 3.5 were adjusted so that the peak pillar strength in the North Barrier pillars corresponds to a safety factor of 1.0. This same adjustment was made to all pillar safety factors plots in this report.)

In the back-analysis of the North Barrier bump shown in Figure 3.5, the lamination thickness was set at 500 ft, the final modulus of the gob was set at 300,000 psi, and the coal strength was calibrated to an input value of 1325 psi (in the strain softening equations of 2.11 and 2.12). For the strain softening coal behavior, the residual stress was calculated using equation 2.11 with a factor of 0.188 (essentially a 30% reduction from the peak stress), and the residual strain was calculated with equation 2.12 using a peak stress multiplication factor of 2. The resultant pillar strength correlates to a Mark-Bieniawski pillar strength with an insitu coal strength of 927 psi.

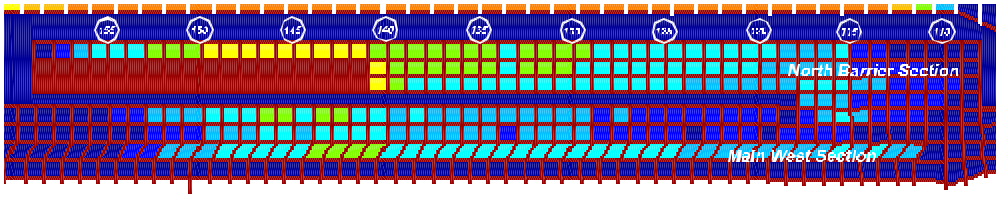

A. Retreat Line at XC 141

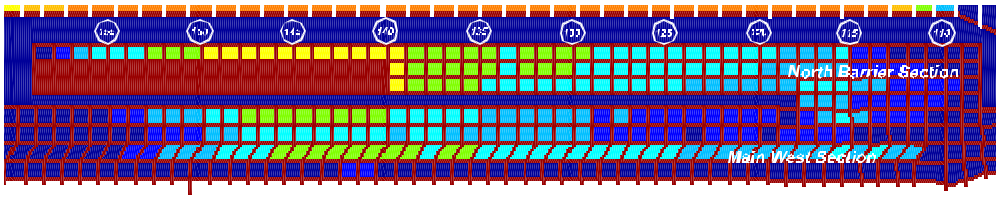

B. Retreat Line at XC 140

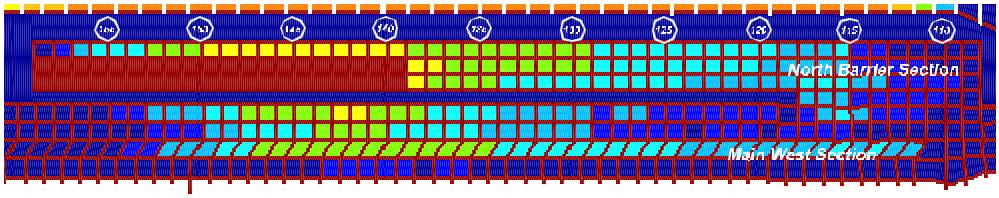

C. Retreat Line at XC 139

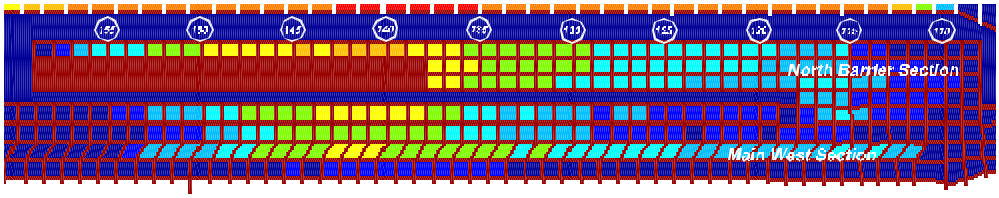

D. Retreat Line at XC 138

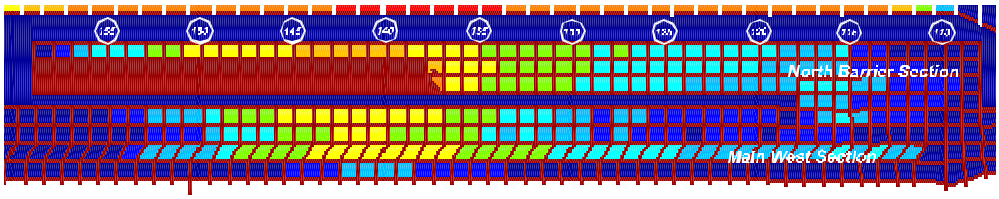

E. Retreat Line at XC 138.5

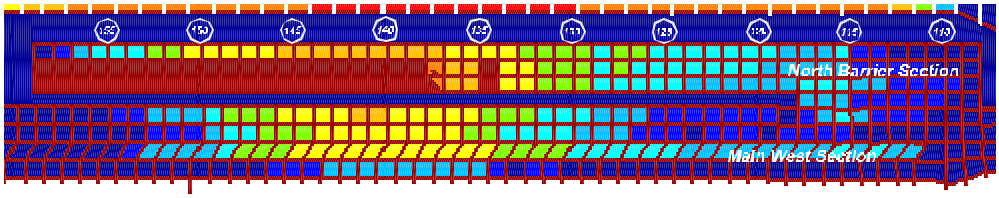

F. Retreat Line at XC 134

Figure 3.5 Analysis of North Barrier bump.

The model results illustrated in Figure 3.5 agree reasonably well with the observed behavior. When the retreat line is at crosscut 141 (see Figure 3.5A), the model shows that two pillars on the retreat line have safety factors slightly less than one. This is a pretty typical response of a room-and-pillar retreat section. These pillars on the retreat line (although the model shows failure) may not fail in the short amount of time that they are under this stress condition, and often can be safely extracted. (However, if the section is allowed to sit idle for a length of time, these pillars may indeed fail.) As the North Barrier Section continues to retreat under deeper cover (the deepest cover is essentially crosscuts 131-132, see Figure 3.1), safety factors on the retreat line decrease. When the retreat line is at crosscut 138 (see Figure 3.5D & E), the model now shows that two full rows of pillars on the retreat line have safety factors less than one. It was at this point that deteriorating ground conditions prompted mine personnel to stop recovering pillars, move the section a couple rows outby, and continue retreating. The mine then extracted two pillars between crosscut 134 and 135 and the bump occurred. In the calibrated model, the extraction of the two pillars between crosscut 134 and 135 caused 4 pillars to fail outby, 2 pillars to fail to the north and the 4 pillars inby to fail more, or soften considerably. These calibrated pillar conditions appear to match the observed conditions in Figure 3.2 fairly well. Also, this response in the model, where a small mining step causes a large amount of failure, is certainly indicative of a dynamic event, such as the bump in this case.

It should also be noted in Figure 3.5, that as the North Barrier Section is retreated, considerable failure also occurs in the Main West Section. This response was seen in all of the calibrated models indicating that if the coal strength is adjusted to fail at the pillar geometry of the bump, then pillars in the Main West will also fail. This reaction seems entirely reasonable considering that: 1) the pillars in the Main West are only about 2% stronger than the pillars in the North Barrier Section, 2) the overburden stress is a little greater over the Main West than either the North or South Barrier sections, and 3) the abutment loading from the North Barrier gob can easily transfer over the intervening 50 ft wide barrier just as it transfers further inby in the North Barrier section. It is not believed that this amount of failure in the Main West section actually occurred at this time. Some adjustments to the model to correct this apparent inconsistency in the sequence of observed failure are discussed later in section 3.5.1.

In performing this back-analysis of the North Barrier Section with various sets of parameter properties (see the parametric analysis section), a couple of important points become evident. First, once the coal strength is reduced in the calibration process to a development safety factor under the deepest cover of 1.4 or less, retreating the pillar line into the high stress, deep cover area will cause significant pillar failure at the retreat line (at some point) due to the combination of the high development stress from the deep cover and the abutment stress from the retreat line. The exact location of the significant pillar failure will move further west under the shallower cover if the coal is weaker or the failure point will move further east under the deeper cover if the coal is stronger. Second, it is apparent from the occurrence of the bump, and the model definitely indicates, that moving the face two rows of pillars outby the old retreat line was not sufficient to isolate it from the previous retreat line abutment stresses in the given conditions.

3.5 Analyzing the August 6th Collapse

Once the optimum lamination thickness and gob modulus were developed (within the given resolution) and the coal strength was calibrated from the North Barrier bump, the parameters were set to use LaModel to back-analyze the August 6th, 2007, collapse at the Crandall Canyon Mine. For this collapse analysis, a six step model was developed:

1. Development of the Main West Section
2. Development of the North Barrier Section
3. Final retreat of the North Barrier Section
4. Development of the South Barrier Section
5. Final retreat of the South Barrier Section
6. Final retreat of the South Barrier Section, with bump triggers.

When performing this back-analysis, a number of critical calibration conditions needed to be met. For step 1, the Main West Section should be stable on development. Similarly, for step 2, the North Barrier Section should be stable on development. For step 3, the pillar failure in the North Barrier Section should be consistent with Figure 3.2. For step 4, the South Barrier Section should be stable on development. Finally, for Step 6, after the bump event, pillar failure should cover the middle portion of the South barrier Section and extend outby to crosscut 122 to 124. Also, pillar failure (and pillar bumps) should extend into the face area at least to crosscut 138 with some moderate pillar bumping at crosscut 142 (as indicated by the drillholes).

3.5.1 Primary Results:

The primary results of the initial back-analysis model for the Crandall Canyon Mine are shown in Figures 3.6-3.8. Figure 3.6 show the average pillar and individual element safety factors for step 3 which is the March 2007 bump geometry. Figure 3.6a is identical to Figure 3.5f and pillar failure in this plot was discussed above. Figure 3.6b shows the individual element safety factors calculated in the model for the bump geometry (step 3). By examining the element safety factors, it can be seen that the 50 ft wide barrier between the Main West and the North Barrier sections is indicating substantial failure between crosscut 137 and crosscut 144. Figure 3.6 also clearly shows the effect of the depth of cover on the pillar safety factors which increase rapidly as the cover drops below 2000 ft west of crosscut 145 and east of crosscut 125. Similarly, under the deepest cover between crosscuts 129 and 134, many pillars have not yet failed but they have very low safety factors and are close to failure. Finally, this figure indicates that the abutment stress from the active retreat gob is one of the primary factors driving the bump and the pillar failure; and therefore, the pillar failure radiates out from the active gob area. In addition, the deep cover stress is seen as a significant factor in propagating the pillar failure to the east.

Figure 3.7 shows the average pillar and individual element safety factors calculated by the model after the South Barrier section was developed and retreated to its final configuration. Several important observations can be made from this figure. First, on development and partial retreat, the pillars in the central portion of the South Barrier section (crosscuts 120–138) are shown to be fairly stable with the lowest safety factors.

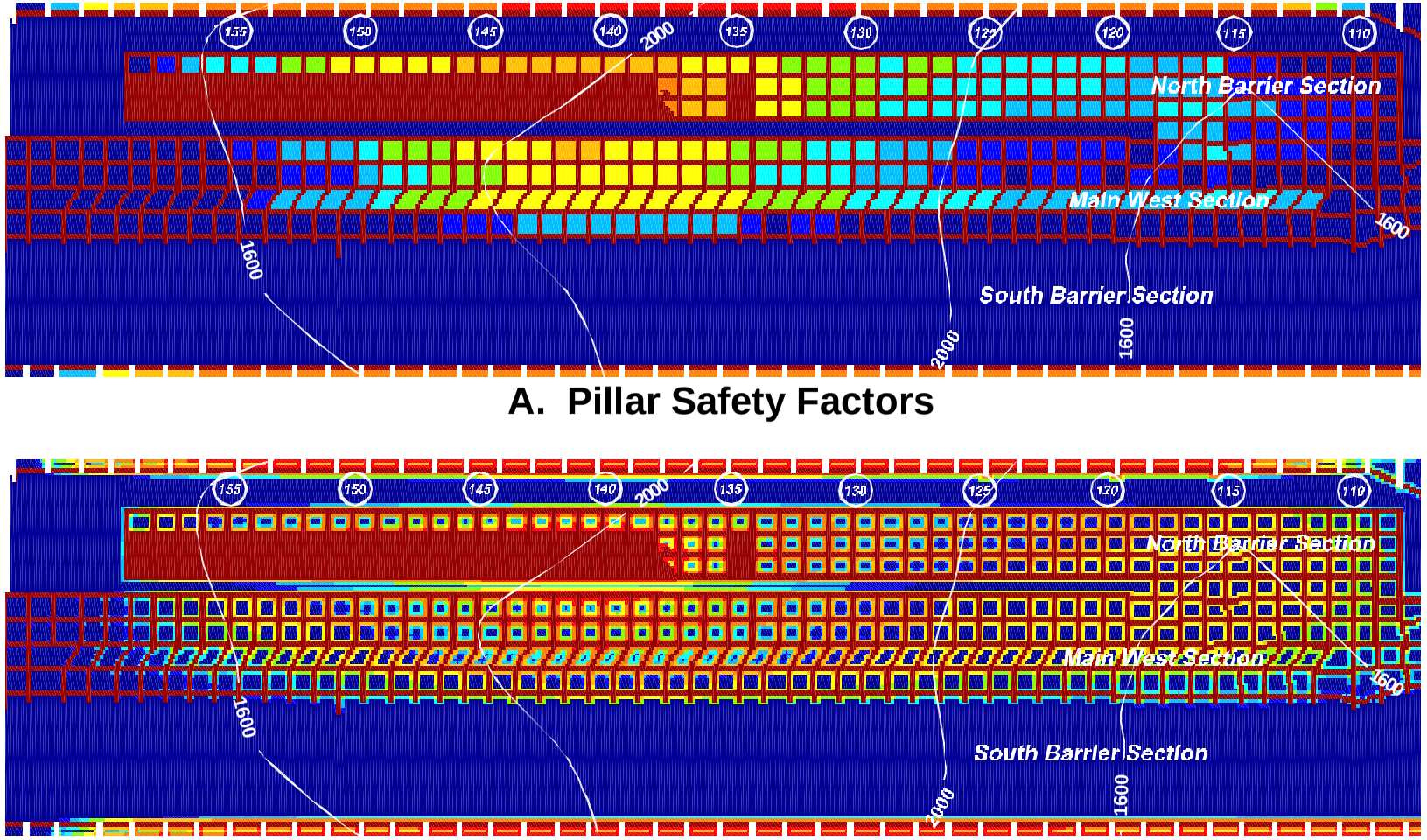

Figure 3.6 Plot of pillar and element safety factors for step 3.

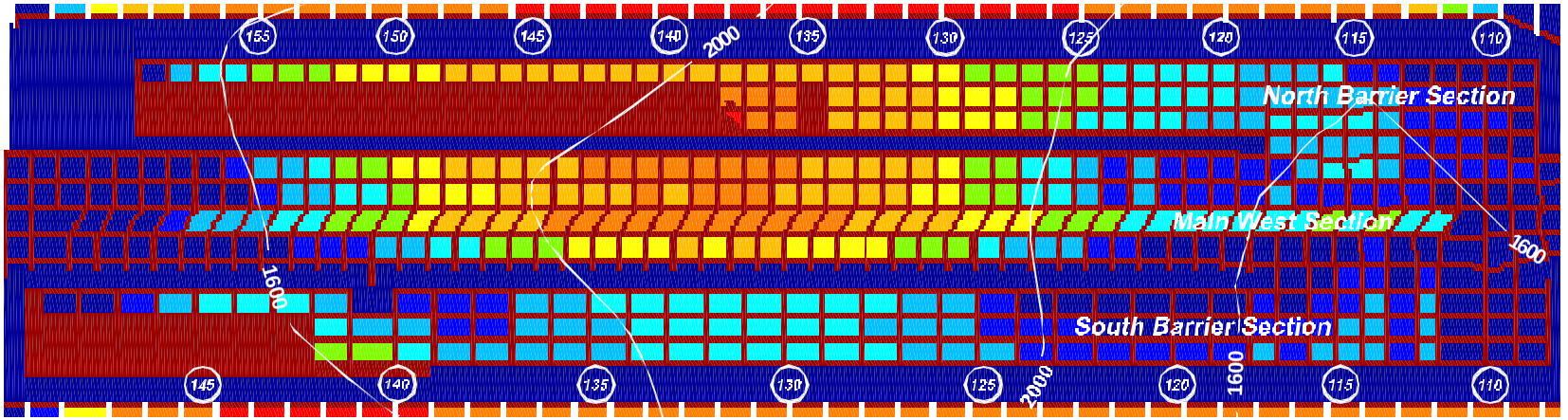

A. Pillar Safety Factors

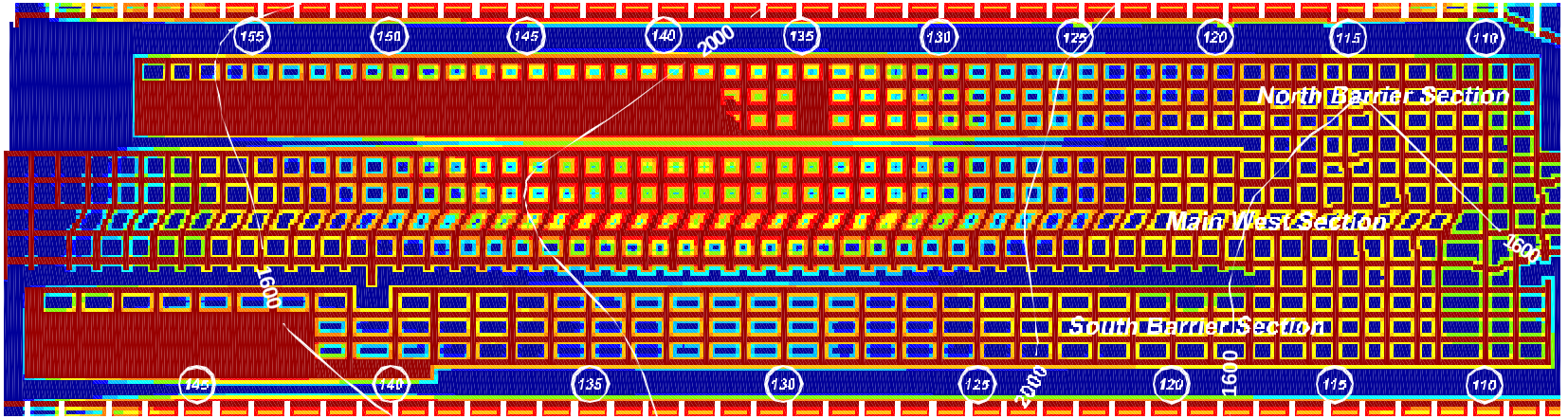

B. Element Safety Factors

Figure 3.7 Plot of pillar and element safety factors for step 5.

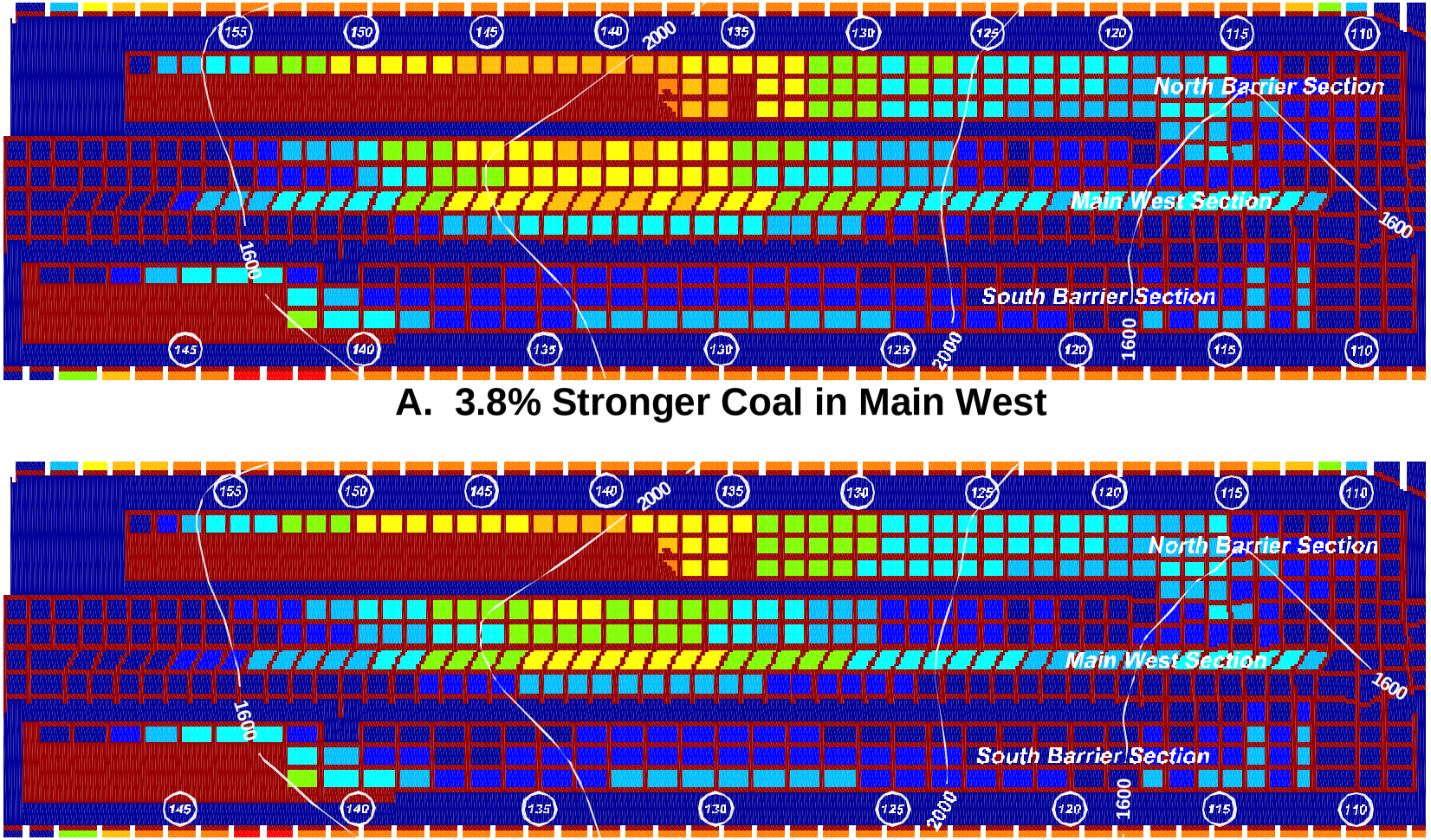

Figure 3.8 Plot of pillar safety factors with coal strength adjusted in Main West.

around 1.2-1.4. As previously noted, these pillars are about 16% stronger than the pillars in the Main West or North Barrier sections, and this stability is undoubtedly a result of this higher strength. Next, it can be seen by examining the pillar safety factors from crosscut 139-145 in the South Barrier section that the stresses from the active retreat line/working section are fairly isolated from the potentially unstable pillars under the deeper cover to the east. The retreat line is under relatively shallow cover and there are five rows of fairly stable pillars (safety factors up to 1.8) between the active mining and the 2000 ft cover line.

Finally, it can be seen by comparing Figure 3.7 with the previous Figure 3.6 that the small increase in stress from the development of the South Barrier section has caused considerable additional pillar failure in the Main West and North Barrier sections. Fourteen additional pillars have failed in the North Barrier section and 46 additional pillars have failed in the Main West section. There is no evidence to support whether this degree of failure actually did or did not occur. It does not seem reasonable that a failure of this magnitude could have gone unnoticed during development of the South Barrier section. However, the failure may have been very gradual. More likely, the difference in Main West pillar failure between Figure 3.6 and 3.7 was part of the collapse on August 6th. Regardless, this model response certainly indicates how sensitive the Main West and North Barrier geometries are to any slight change in loading condition.

To maintain general stability in the Main West through the final retreat position of the South Barrier does not take much of a change in the model. A 50 psi (3.8%) increase in coal strength in just the Main West reduces the number of failed pillars in the Main West from 76 to 33 (see Figure 3.8a), and a 75 psi (5.7%) increase in coal strength reduces the pillar failure in the Main West to 12 pillars (see Figure 3.8b). However, either of these increases in coal strength in the Main West adversely affects the degree of fit to the March 2007 bump, but not too much (see Figure 3.8). The only strong justification for increasing the strength of the coal in the Main West in the model above the calibrated strength is to postpone the pillar failure until the August collapse. There is not much physical evidence that the Main West coal is any different than the coal in the North and South Barrier sections. On one hand, the coal in the Main West might be expected to be weaker than in the surrounding sections because it had been standing for 10+ years. However, there are a variety of possible explanations for pillars in this area not to exhibit lower strength. For example, the floor may have yielded enough over time to allow some overburden stress to bridge the section and functionally reduce the pillar load or roof falls and/or gobbed crosscuts may functionally provide additional confinement to the pillars. Any number of small changes in the loading condition of the Main West section could account for the pillars not failing at exactly the point indicated by the model. This is one point where the back-analysis model does not easily/smoothly match the perceived reality of the Crandall Canyon Mine; however, certainly a 4-6% increase in the stability of the Main West pillars (for any number of possible reasons) would be easily conceivable considering the natural variability of the geologic and mining systems.

3.5.2 Triggering the Collapse of the South Barrier Section:

It can be seen in Figure 3.7a, that when the pillars in the Main West do start to fail, there is reluctance for the failure to propagate south past the barrier pillar and into the South Barrier Section. However, we know that this failure did occur on August 6th. To investigate what possible conditions may have triggered the collapse, or what conditions or parameter

changes are necessary to replicate the observed South Barrier failure in the model, a number of different trigger scenarios were investigated.

A classic boundary-element technique used to check the stability of a potentially unstable mining plan is to simulate the extraction of a few pillars in the model (i.e., cause a small stress increase) and observe the magnitude of the resultant changes. In the optimized Crandall Canyon Mine model, four pillars (with a safety factor around 1) were removed between crosscut 128 and 132 on the south side of the Main West. The results of this perturbation are shown in Figure 3.9; it can be observed that the removal of the pillars has indeed caused 25 pillars to fail in the South Barrier section between crosscuts 125 and 134. Comparing this figure with Figure 3.7, it can also be observed that additional pillars in the Main West have failed between crosscut 124 and 129, and that the stability of the barrier between the sections has greatly decreased. The final pillar failure results shown in the South Barrier section of Figure 3.9 are not quite as extensive as observed in the field, but it does demonstrate that a relatively small change in the model conditions can cause the pillar failure to continue into the South Barrier section.

3.5.2.1 Reduced Coal Strength: The next triggering technique was to reduce the coal strength in the Main West by 50 psi or 3.8%. The results of this investigation are shown in Figure 3.10. Figure 3.10a shows that the small strength reduction has caused 37 pillars to fail in the South Barrier section between crosscuts 124 and 137, also many more pillars have failed in the Main West section. Figure 3.10b includes the removal of four pillars in the Main West and shows that the failure in the South Barrier section has encompassed the face area (crosscuts 137 to 139) and several pillars in the bleeder area (crosscuts 141 to 143). If Figures 3.8a and 3.10a are compared, it can be seen that a 7.7% reduction in the coal strength of the Main West pillars will cause 37 pillars to fail in the South Barrier section and 94 additional pillars to fail in the Main West. This large number of pillar failures in the model due to a relatively small decrease in coal strength effectively simulates the observed August 6th collapse. Seeing these model results, it certainly seems reasonable and plausible that the strength of the Main West pillars may have degraded from the effects of time and the northern abutment stresses, and a massive pillar collapse initiated which swept through the Main West pillars and down through the South Barrier section.

3.5.2.2 Joint Slip: The seismic event that accompanied the August 6th collapse was analyzed by personnel at the University of Utah Seismological Stations. The seismic signal was consistent with a collapse event but there was a small component of shear. Thus, it seems plausible that movement along one of the pervasive vertical joint surfaces known to exist on the mine property may have initiated the collapse (or certainly have contributed to the collapse). In order to simulate this possibility, a simple joint model was added to a special version of LaModel as part of this investigation. This joint model simulates a frictionless vertical plane in the LaModel grid, such that the plane does not allow any transfer of shearing or bending stresses across the joint. Basically, the plane is inserted between two rows or columns of the LaModel grid, and the program calculates the modified seam stresses and displacements that result from the addition of the joint.

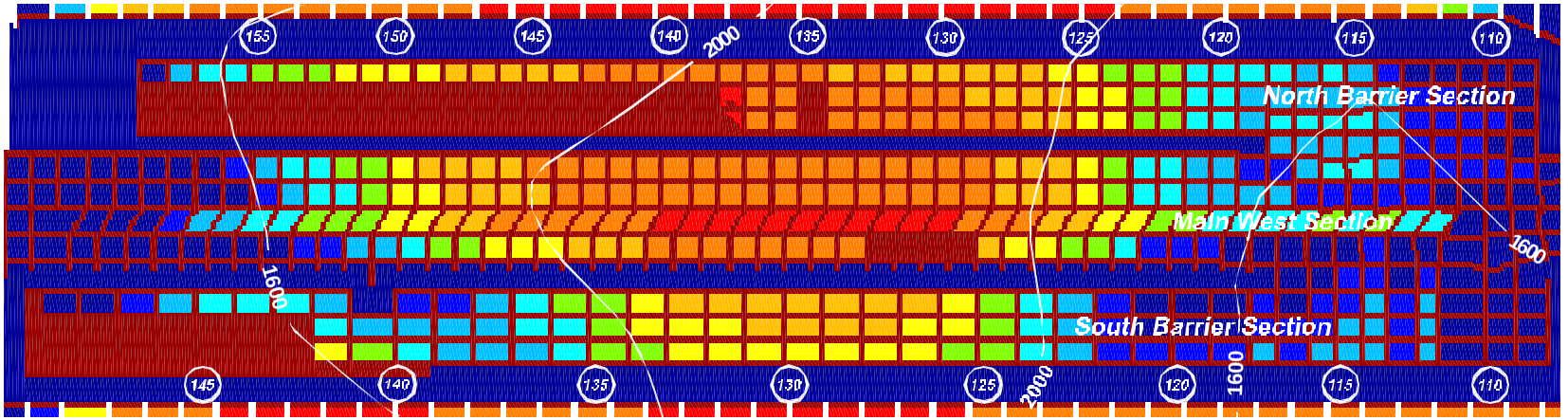

A. Pillar Safety Factors

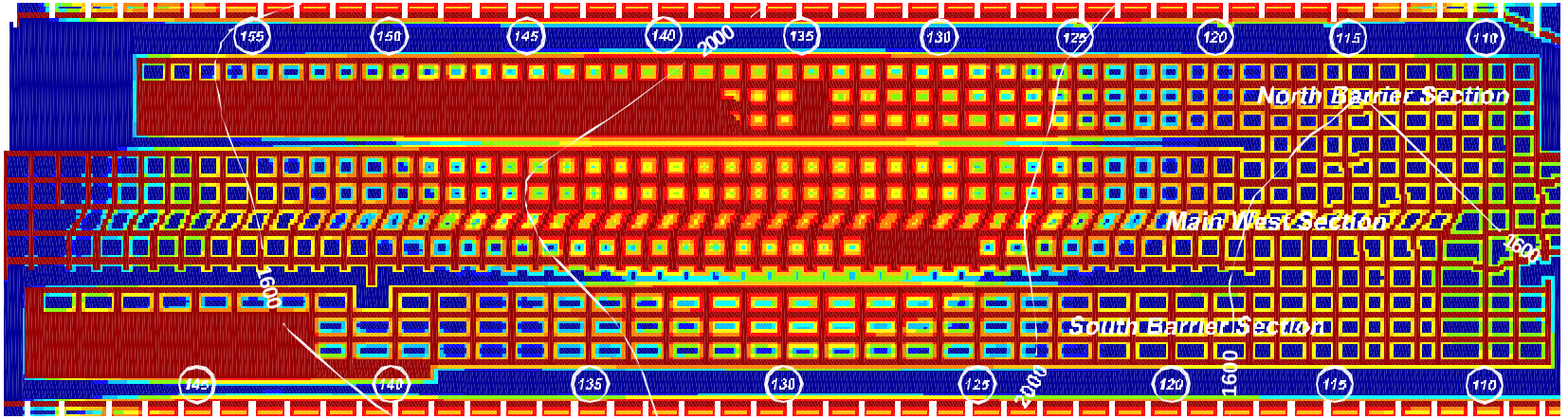

B. Element Safety Factors

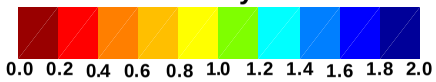

Figure 3.9 Plot of pillar and element safety factors for step 6 with 4 pillars removed.

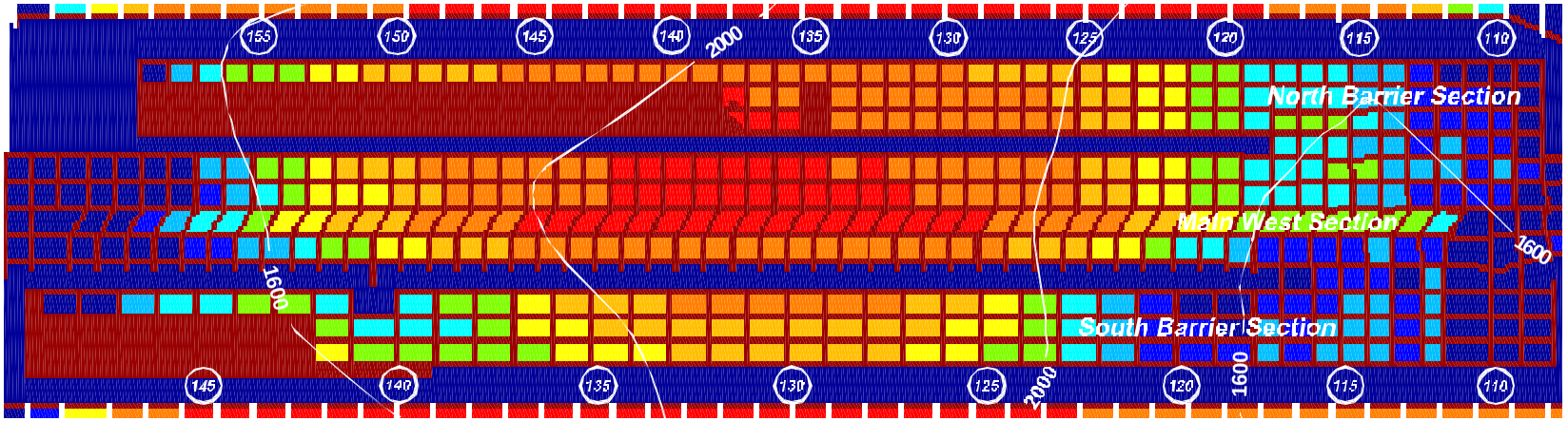

A. Step 5 - South Barrier Retreated

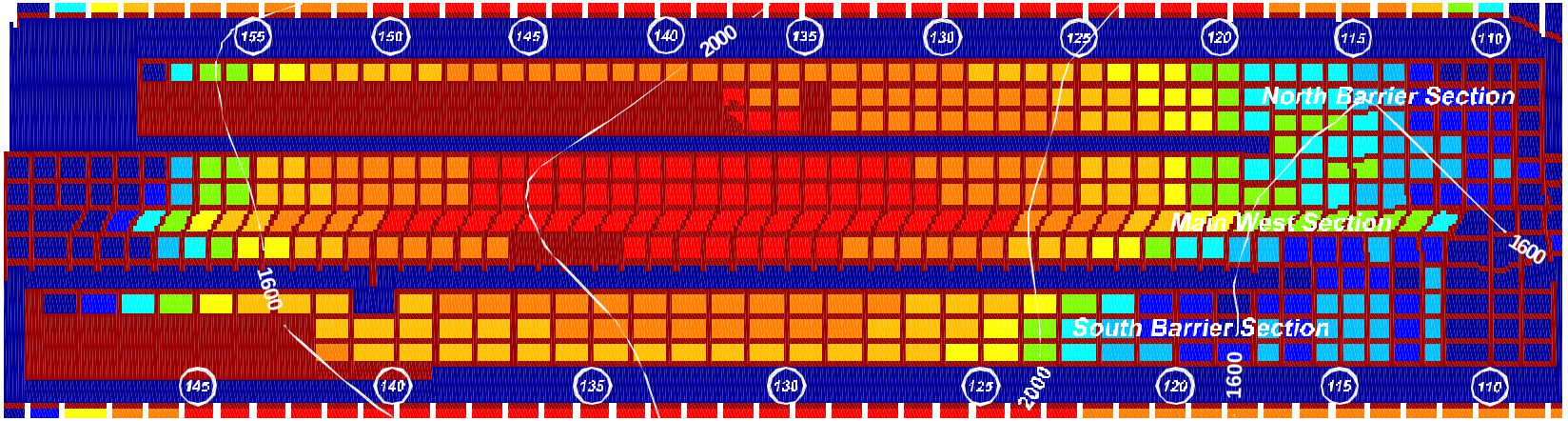

B. Step 6 - 4 Pillars Removed in Main West

Figure 3.10 Plot of pillar safety factors for weakened coal in the Main West.

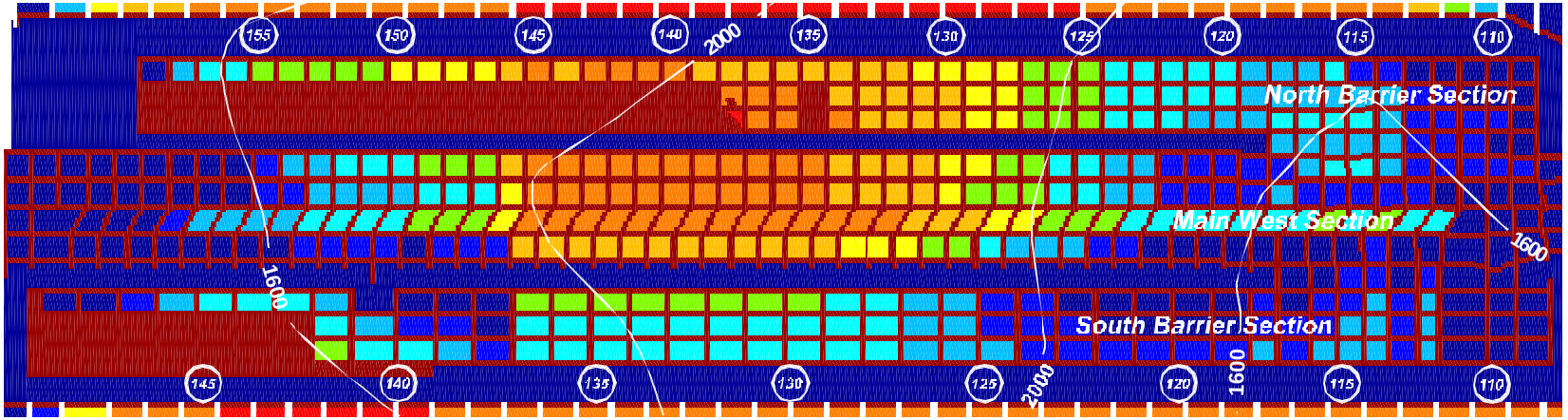

A. Step 5 - South Barrier Retreated with a Fault

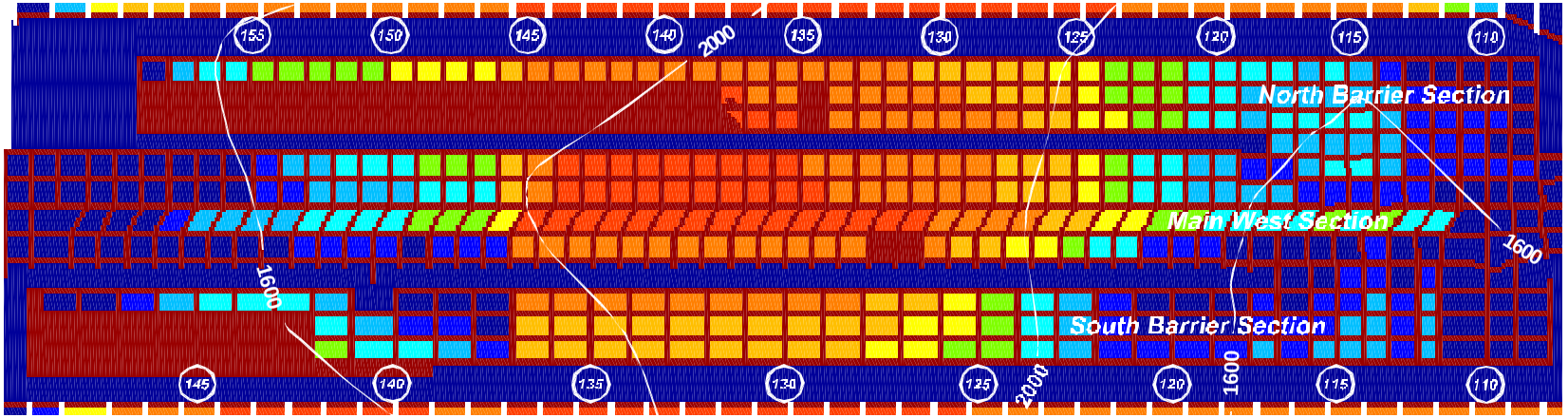

B. Step 6 - 2 Pillars Removed in Main West with a Fault

Figure 3.11 Plot of pillar safety factors for the model with a joint at crosscut 137.

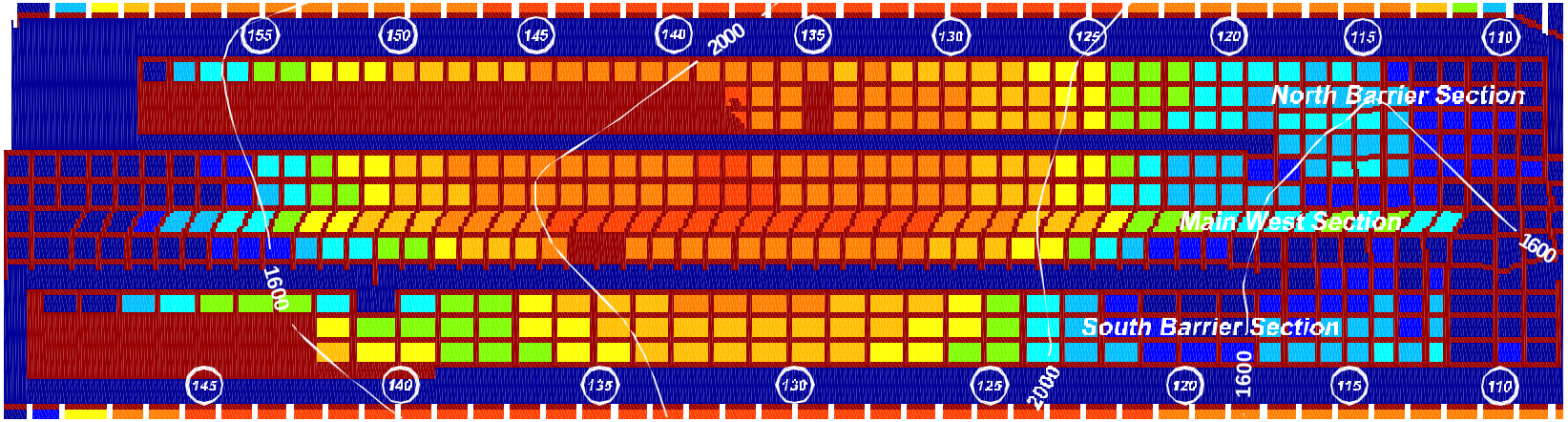

A. Step 6 - 2 Pillars Removed in Main West

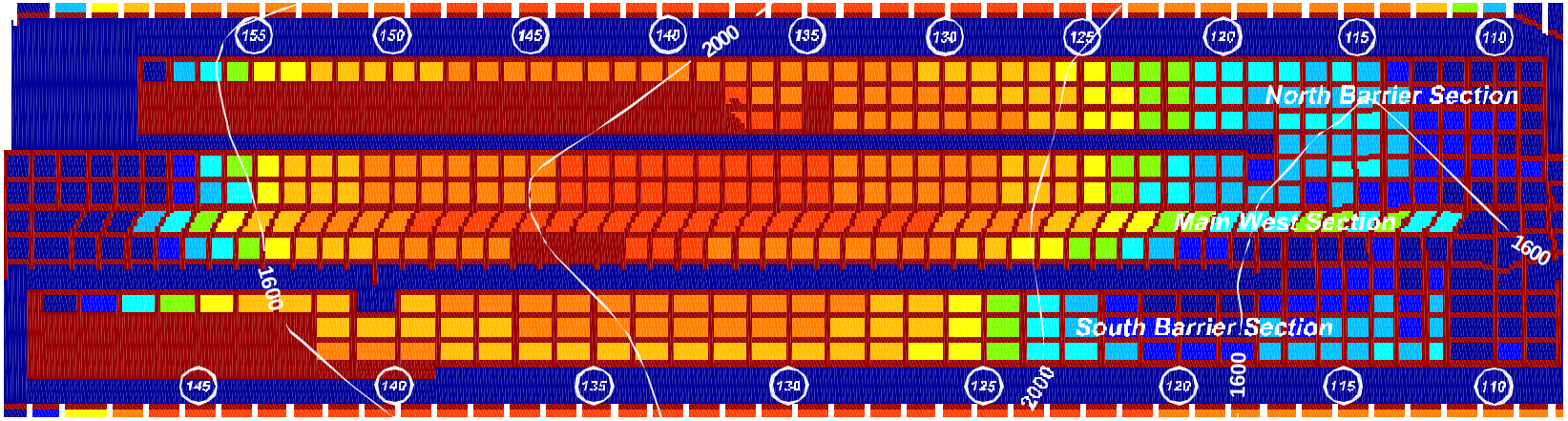

B. Step 7 - 4 Pillars Removed in Main West

Figure 3.12 Plot of pillar safety factors for softer gob in the southern panels.

For the analysis of a possible fault trigger, the joint was placed at crosscut 137 of the South Barrier section and oriented in a north-south direction between the columns of the LaModel grid. The results of this joint analysis are shown in Figure 3.11. Figure 3.11a indicates that the addition of the joint by itself does not cause any failure in the South Barrier section, but the joint with a couple pillars removed in the Main West causes 35 pillars to fail in the South Barrier section. This analysis indicates that a sudden change in stresses due to slip along a joint in the roof certainly could have been a factor in triggering the collapse seen on August 6th.

3.5.2.3 Softer Southern Gob: Given that pillars in the South Barrier section are 16% stronger than the pillars in the North Barrier section and 14% stronger than the pillars in the Main West section, and that overburden loading in the south appears a little less than in the Main West, one would anticipate that pillars in the Main West would have failed before the South Barrier pillars, as seen in the previous models. This actually may have occurred and gone unnoticed, but it is also possible that failure in both areas occurred simultaneously. To account for this simultaneous failure, it seems reasonable to hypothesize that the abutment loading from the southern longwall panels may have been higher than the abutment loading from the northern longwall panels. In the north, longwall panel 12 (see Figure 3.1) was the last longwall in the northern district, whereas longwall panel 13 to the south of the South Barrier section was the first longwall panel in the southern district. This configuration may have resulted in a higher abutment load from the southern longwalls, or the southern geology may have been a little stiffer or more massive causing additional abutment load.

To simulate additional abutment load from the southern longwall, the gob modulus in the south was reduced from 300,000 psi to 250,000 psi. Nominally, this reduces the average gob loading from 1013 psi to 888 psi, and increases the abutment load from 1187 psi to 1312 psi (10.5%). The results of this loading condition are shown in Figure 3.12 where it can be clearly seen that the increased southern abutment loading certainly increases the amount of failure in the Southern Barrier section. By comparing Figure 3.12b with 3.8a, it can be seen that the softer southern gob has caused an additional 23 pillars to fail and caused the failure to encompass the face area in the South Barrier section. Also, the softer southern gob has made the South Barrier section more likely to fail as a "natural" extension of failure in the Main West (see Figure 3.12a)

3.6 Parametric Analysis

In order to assess the sensitivity of the model results to the input values and to determine the optimum parameter values for matching the observed mine behavior, an extensive parametric analysis was performed. This analysis examined: 3 different lamination thicknesses (300 ft, 500ft and 600 ft); final gob moduli ranging from 100,000 psi to 700,000 psi; strain-softening coal strengths ranging from 1150 psi to 1450 psi (corresponding to a Mark-Bieniawski insitu coal strengths of 835 psi to 1115 psi); post-failure residual coal strength reductions of 20%, 30% and 40%, and several different mechanisms for triggering the collapse. In all, over 230 models were evaluated.

In a back-analysis, such as this investigation of the Crandall Canyon Mine collapse, there are an infinite number of parameter combinations that might be analyzed. The resolution of each optimized parameter (and therefore the accuracy of the back-analysis) can always be

further improved. Obviously, there is a practical time constraint and also, it is only reasonable to refine the parameters to within the overall accuracy of the general input values. In this case, with a geo-mechanical model, an accuracy of 10-20% seems more than sufficient. In this back-analysis, the smallest resolution of the critical parameters was:

- Lamination Thickness 100 ft
- Final Gob Modulus 50,000 psi
- Coal Strength 25 psi
- Residual Strength Reduction 10%

To investigate the optimum lamination thickness, 300 ft, 500 ft and 600 ft thicknesses were examined (with a fixed rock mass modulus of 3,000,000 psi). The 300 ft lamination thickness has an abutment extent of around 180 ft and, in general, it showed a relatively local influence of the abutment stresses from the gob areas. The longwall abutment stresses did not appropriately influence the North and South Barrier sections and the North Barrier section gob did not project sufficient abutment stress into the bump area. On the other hand, the 600 ft lamination thickness had an effective (90% of abutment load) abutment extent of around 235 ft; however, this thickness had a tendency to over-extend the abutment zones and cause the coal failures to travel further than observed. Of the three lamination thicknesses investigated, the 500 ft thickness appeared to be most realistic. If the lamination thickness were to be further refined, the next selection would be in the 300 to 500 ft range.

A fairly wide range of final gob moduli and the resultant abutment loads were investigated. When the abutment loads reached 65-75% of the overburden load, it was found that the North and South Barrier sections were beginning to fail on development. Also, this high abutment loading produced stresses in the barrier sections that were very biased towards the gob, much more than was actually experienced. On the other end of the spectrum, when the abutment loading was reduced to 30-40% of the overburden load, the low abutment stress ceased to be much of a factor in the modeled failure. At this point, the pillar failures were primarily driven by just the tributary overburden load. In this scenario, very low coal strengths were required to recreate a wide spread failure in the model. However these low strength pillars were close to failure on development and this behavior was not observed. The abutment loading was ultimately found to be most realistic in the 55-65% range (highest in the south) resulting in a final gob modulus between 200,000 and 300,000 psi (with the 500 ft lamination thickness).

The coal strengths in the model were readily calibrated using the North Barrier bump geometry once a lamination thickness and abutment loading was determined. The calibrated coal strength essentially correlated with the modeled abutment loading. Increasing the abutment load required a corresponding increase in coal strength to calibrate the model. Conversely, decreasing the abutment load required a decrease in the coal strength for a realistic calibration. The final optimized strain-softening coal strength was in the 1300-1400 psi range corresponding to Mark-Bieniawski formula insitu coal strengths of 910-980 psi.

The final critical parameter that was investigated in the parametric analysis was the post failure coal behavior. In this investigation, coal strength reductions of 20%, 30% and 40% after pillar failure were examined. Essentially, the magnitude of strength reduction determines the tendency for the pillar failures to propagate (or run) and generate a massive pillar collapse. With the 20% reduction, it was difficult for the model to produce the pillar

run that was observed. The pillars failed, but did not run across large areas of the sections. On the other hand, with the 40% reduction in coal strength, the pillar failures ran too far, out to around crosscut 115. Of the post-failure coal strength reductions examined, the 30% level produced the best results. If this value were to be further refined, it would be increased in order to get the pillar failures to spread further outby crosscut 124 in the South Barrier section as was observed.

The magnitude of the post failure reduction in coal strength in this model necessary to simulate the observed pillar behavior is somewhat surprising. The classic laboratory tests by Das (1986) would indicate that a 60 ft wide pillar in an 8 ft seam (w/h=7.5) would be close to elastic, perfectly-plastic behavior and would not have much strain-softening behavior. Obviously, there was a massive pillar collapse; and therefore, the pillars had to exhibit significant strain-softening behavior. It is not clear whether this magnitude of strain-softening behavior is: typical for a pillar with a width-to-height of 7.5, a behavior unique to the seam at this mine, an effect of the bump-type pillar failure, a manifestation of the veracity/dynamics of the pillar collapse or has some other explanation.

3.7 Final Back Analysis Model

In the initial model analyzed in section 3.5 above, all of the coal and gob at different locations have identical properties. However, it was shown that this assumption causes the pillars in the Main West section to fail too soon and the pillars in the South Barrier to be difficult to fail. It was also shown that a small (<8%) change in the coal strength or loading condition in the Main West pillars would make their behavior correlate well with observed conditions and that a small change (10.5%) in the southern abutment loading brings the South Barrier pillars' behavior closer to observations. So, by combining all of these adjustments into one model, a final back-analysis model of the Crandall Canyon Mine can be developed that:

- Accurately simulates the March 10th, 2007 bump,
- Accurately simulates the South Barrier section development, and
- Accurately simulates the final August 6th collapse.

In this model, the lamination thickness was set at 500 ft, the final modulus of the north gob was set at 250,000 psi, and the final modulus of the southern gob was set at 200,000 psi. The coal strength in the North and South Barrier sections was set at 1300 psi and coal strength in the Main West was set at 1400 psi. For the strain softening coal behavior, the residual stress was set with a 30% reduction from the peak stress.

The results from this final back analysis model are shown in Figure 3.13 and 3.14. In Figure 3.13a, the March 2007 bump is simulated with fairly good correlation to the observed results in Figure 3.2. In this final model, only one pillar has failed in the Main West at the time of the bump. Figure 3.13b shows the development and retreat of the South Barrier section. In this final model, the pillars in the South Barrier section have fairly good stability, although some 42 pillars have failed in the Main West. Then, in Figure 3.14 after perturbing the model by removing 6 pillars, the August 6th collapse is simulated. The removal of the six trigger pillars has caused 106 additional pillars to fail in the Main West and 59 pillars to fail in the South Barrier section. The failure runs from crosscut 123 in the South Barrier section

in to crosscut 146 in the bleeder area. This final model does a fairly good job of simulating most of the critical observation of the geo-mechanical behavior at the Crandall Canyon Mine.

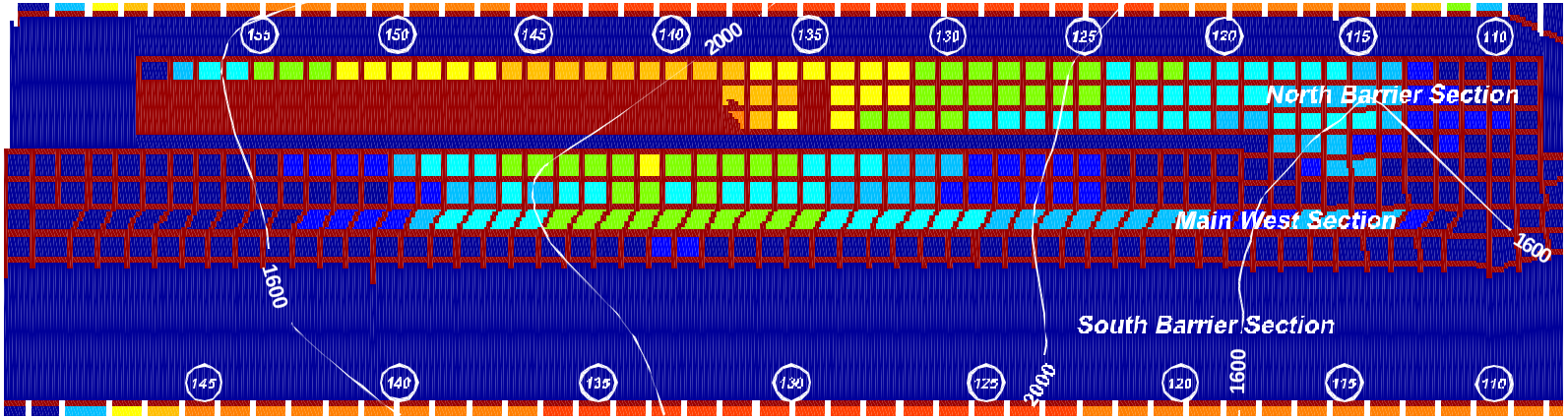

A. Step 3 - North Barrier Bump

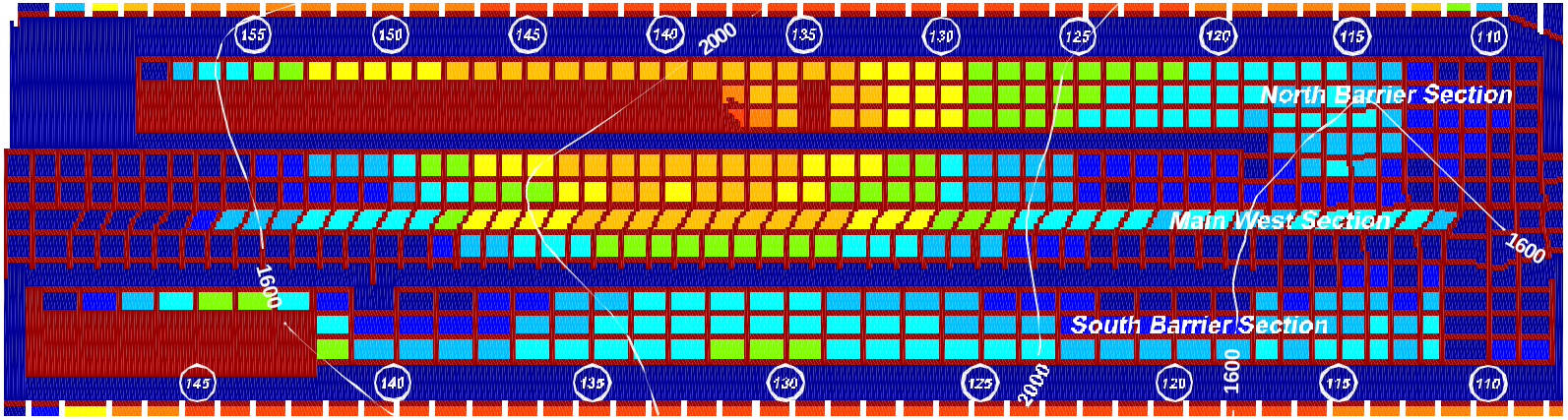

B. Step 5 - South Barrier Retreated

Figure 3.13 Final model of Crandall Canyon Mine – steps 3 & 5.

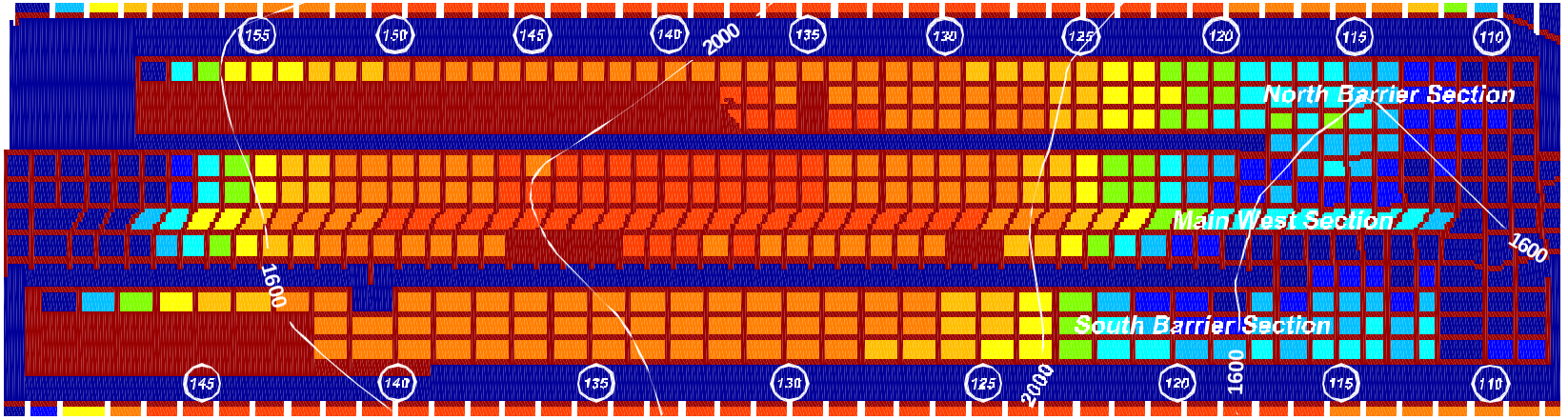

A. Step 9 - Pillar Safety Factors

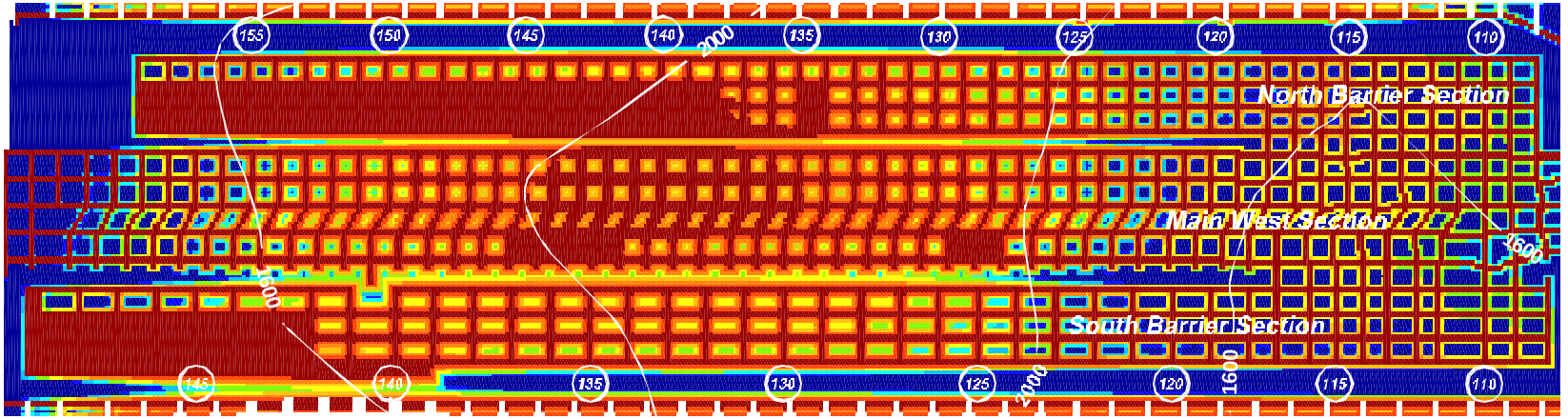

B. Step 9 - Element Safety Factors

Figure 3.14 Final model of Crandall Canyon Mine - step 9.

4. Summary

In this back analysis of the Crandall Canyon Mine, a six step base model of the mining in the Main West area was initially developed. The mine grid for the model was sized to cover the entire area of interest with a 10 ft element size that sufficiently fit the pillar sizes and entry widths. An appropriate overburden grid was also developed. This base model included a step for each of the critical stages in the mining of this area: development of the Main West Section, development of the North Barrier Section, final retreat of the North Barrier Section, development of the South Barrier Section, and final retreat of the South Barrier Section.

Next, calibrated values for the critical input parameters: rock mass stiffness, gob stiffness and coal strength, were developed. The rock mass stiffness was calibrated against the expected abutment load distribution (i.e., extent) consistent with empirical averages and local experience. The gob behavior was calibrated to provide reasonable abutment and gob loading magnitudes. The peak strength of the coal was primarily determined from back analyzing the March 10th bump in the Main West North Barrier section, and the strain-softening behavior was optimized from back-analysis of the August 6th, 2007, event. Throughout this calibration process, a number of particular locations, situations, and conditions were used as distinct calibration points.

As part of calibrating the critical input parameters, a wide range of reasonable sets of input parameter values were investigated (a parametric study) to optimize agreement between the model and the observed reality, and to assess the sensitivity of the model results to changes in the critical input parameters. Also, a number of different events that could have triggered the August 6th collapse were investigated with the basic model. In total, over 230 different sets of input parameters were evaluated, and from this extensive analysis a broad understanding of the factors that affected ground conditions at Crandall Canyon Mine was developed. Also, a pretty clear picture of the range of reasonable input values for the critical parameters was developed: lamination thickness, 300-600 ft; gob load, 25-60% of insitu load; coal strength, 1250-1450 psi - 20-40% strain softening.

In all of these models (with different sets of lamination thicknesses and gob loadings), once the coal strength was calibrated to the North Barrier bump, LaModel naturally showed that the pillars in the Main West were also close to failure. Once the South Barrier was subsequently developed, the model showed that it was very likely for the entire Main West and South Barrier sections to collapse upon the South Barrier development, or just a small perturbation was needed to initiate the collapse. Different sets of lamination thickness and coal strength primarily just determined the exact timing and extent of the collapse. With the initial base model where all of the coal and gob in different areas are maintained at the same strength, the critical input parameters which best matched the known collapse conditions at the Crandall Canyon Mine were: a lamination thickness = 500 ft, a gob load = 40% of insitu load, and a coal strength = 1325 psi with 30% strain softening (see Figures 3.5-3.12).

In the initial optimized base model were all of the coal and gob have identical properties, it was noted that the pillars in the Main West section seemed to fail a little too soon (or too easy) while the pillars in the South Barrier seemed to resist failure. Relaxing the condition that all of the coal and gob have the same properties, a final model was developed that fits the known conditions a bit better than the optimized base model (See Figures 3.13 and 3.14). In this final model, the Main West coal strength was raised to 1400 psi while the rest of the coal strength was lowered slightly to 1300 psi, Also, the south gob load was decreased to

36% of insitu load. With these two changes, the final model accurately simulates the March 10th, 2007 bump and minimizes the pillar failure in the Main West at that time. Also, the final model now more accurately simulates the final August 6th collapse with the simultaneous failure of 106 pillars in the Main West and 59 pillars in the South Barrier section. The collapse runs from crosscut 123 in the South Barrier section completely through the active section to crosscut 146 in the South Barrier bleeder area (see Figure 3.14).

5. Conclusions

Based on the extensive back analysis of the Crandall Canyon Mine using the LaModel program describe above, and with the benefit of hindsight from the March bump and August collapse, a number of conclusions can be made concerning the mine design and the August 6th collapse.

1) Overall, the Main West and adjacent North and South Barrier sections were primed for a massive pillar collapse because of the large area of equal size pillars with near unity safety factors. This large area of undersized pillars was the fundamental cause of the collapse.

    a. The pillars and inter-panel barriers in this portion of the Crandall Canyon Mine essentially constitute a large area of similar size pillars. The pillars in the North Barrier and Main West section are essentially the same size and strength. Also, the inter-panel barrier pillars between the Main West section and the North and South Barrier sections have a comparable strength (+15%) to the pillars in the sections. The pillars in the South Barrier section are stronger than the pillars in the North Barrier and Main West sections, but only by about 16%. Therefore, the South Barrier section pillars might also be included as part of the large area of equal size pillars. This large area of similar size pillars is one of the essential ingredients for a massive pillar collapse (Mark et al., 1997; Zipf and Mark, 1996).

    b. The high overburden (2200 ft) was causing considerable development stress on the pillars in this area and bringing pillar development safety factors below 1.4.

    c. Considerable longwall abutment stress was overriding the barrier pillars between the active sections and the old longwall gobs. In the north, the abutment stress from Panel 12 was overriding the North Barrier section and in the south the abutment stress from Panel 13 was overriding the South Barrier Section.

2) The abutment stress from the active North Barrier retreat section was key to the March 10th bump occurrence and the modeling indicated that the North Barrier abutment stress contributed to the August 6th pillar collapse.

3) From the modeling, it was not clear exactly what triggered the August collapse. A number of factors or combination of factors could have been the perturbation that initiated the collapse. Likely candidates include: the active retreat mining in the South

Barrier section, random pillar failure, a joint slip in the overburden, a gradual weakening of the coal over time, a change in the abutment loading, etc. The boundary element modeling identified a number of possible triggers, but by itself could not distinguish the most likely trigger.

4) LaModel analysis demonstrated that the active pillar recovery mining in the South Barrier section could certainly have been the trigger that initiated the August collapse; however, the modeling by itself does not indicate if the active mining was the most likely trigger. Certainly removing more coal in the South Barrier section contributed to the ultimate collapse by applying additional load to the outby area that was primed to collapse. In fact, if the active mining was not the specific trigger on August 6th, then it is fairly certain that as the South Barrier section had retreated further under the deeper cover, it would have eventually triggered the collapse of the undersized pillars in the Main West area.

References

Barron, K., 1992, "A Revised Model for Coal Pillars," Proceedings of the Workshop on Coal Pillar Mechanics and Design, BuMines IC 9315, p. 144-157.

Chase, F., C. Mark and K. Heasley, 2002, "Deep Cover Pillar Extraction in the U.S. Coalfields," Proceedings of the 21st International Conference on Ground Control in Mining, Morgantown, WV, Aug. 6-8, p. 68-80.

Das, M. N., 1986, "Influence of Width/Height ratio on Postfailure Behavior of Coal," International Jounral of Mining and Geological Engineering, vol. 4, p. 79-87.

Hardy, R. and K. A. Heasley, 2006, "Enhancements to the LaModel Stress Analysis Program", Society of Mining Engineers Annual Meeting, St. Louis, Missouri, March 26-29, Pre-print 06-067, 7 pp.

Heasley, K. A, 2000, "The Forgotten Denominator, Pillar Loading", Proceedings of the 4th North American Rock Mechanics Symposium, Seattle, WA, July 31-Aug. 3, p. 457-464.

Heasley, K. A., 1998, "Numerical Modeling of Coal Mines with a Laminated Displacement-Discontinuity Code", Ph.D. Dissertation, Colorado School of Mines, May, 187 pp.

Heasley, K. A. and K. Barron, 1988, "A Case Study of gate Pillar Response to Longwall Mining in Bump-Prone Strata," Proceedings of the 3rd Annual Longwall USA Exhibition and Conference, Chicago, MacLean-Hunter, p. 92-105

Karabin, G. and M. Evanto, 1999, "Experience with the Boundary-Element Method of Numerical Modeling to Resolve Complex Ground Control Problems," Proceedings of the Second International Workshop on Coal Pillar Mechanics and Design, NIOSH IC 9448, p. 89-113.

Mark, C., 1999, "Empirical Methods for Coal Pillar Design," Proceedings of the Second International Workshop on Coal Pillar Mechanics and Design, NIOSH IC 9448, p. 145-154.

Mark, C. and F. E. Chase, 1997, "Analysis of Retreat Mining Pillar Stability (ARMPS)," Proceedings of New Technology for Ground Control in Retreat Mining, NIOSH IC 9446, p. 17-34.

Mark, C. and T. M. Barton, 1997, "Pillar Design and Coal Strength," Proceedings of New Technology for Ground Control in Retreat Mining, NIOSH IC 9446, p. 49-59.

Mark, C., F.E. Chase and R. K. Zipf, 1997, "Preventing Massive Pillar Collapses in Coal Mines," Proceedings of New Technology for Ground Control in Retreat Mining, NIOSH IC 9446, p. 35-48.

Mark, C., 1992, "Analysis of Longwall Pillar Stability (ALPS); an update," Proceedings of the Workshop on Coal Pillar Mechanics and Design, BuMines IC 9315, p. 238-249.

Mark, C., 1990, "Pillar Design Methods for Longwall Mining, BuMines IC 9247.

Pappas, D. M. and C. Mark, 1993, "Behavior of Simulated Longwall Gob Material," BuMines RI 9458.

Zipf, R. K. and C. Mark, 1996, "Design Methods to Control Violent Pillar Failures in Room-and-Pillar Mines," Proceedings of the 15th International Conference on Ground Control in Mining, Golden, CO, Colorado School of Mines, p. 225-264.

Zipf, R. K., 1992, "MULSIM/NL Theoretical and Programmer's Manual," BuMines IC 9321.

Appendix T - Abutment Load Transfer

The magnitude of abutment load transferred to mine workings adjacent to a gob area depends on the mechanical characteristics of the gob, the mechanical characteristics of the strata, and the extraction geometry (e.g. width, height, and overburden depth). Unfortunately, the mechanics of caving strata is not well established in the mining literature. Predictions of abutment loads and load distribution often rely on empirical relationships derived from field data or rules of thumb based on experience or theory. For example, one rule of thumb suggests that abutment loads would be anticipated at distance up to about one panel width away regardless of depth. Another relates the distance to overburden depth:

$$W_s = 9.3\sqrt{h}$$

where W_s = width of the side abutment (or influenced zone), feet
h = overburden depth, feet

Experience has shown that these approaches provide useful insight. However, predictions of magnitude and distribution become much more reliable when they are based on mine-specific measurements and observations.

Between June 1995 and January 1996, Neil & Associates (NAA) conducted field studies in the 6th Right yield-abutment gateroad system at Crandall Canyon Mine. This study provided data on ground behavior including information relative to abutment stress transfer. Measurements indicated that stress changes due to abutment loading could be detected at a distance of more than 280 feet ahead of the advancing longwall face. Similarly, changes were measured adjacent to the extracted panel (side abutment loads) more than 170 feet away. These measurements were made at a location beneath 1,100 feet of overburden.

Appendix U - Coal Properties Input

Agapito Associates Inc. (AAI) assigned calculated coal properties using a "method of slices" approach to approximate the load bearing capacity of pillars in LaModel. The method assumes that the strength of a pillar element is a function of its distance from the nearest rib. AAI modeled the Crandall Canyon Mine workings using 5-foot elements. As illustrated in Table 15, eight sets of peak and residual strength values were calculated to correspond to depths up to 37.5 feet from a pillar rib. These parameters were determined using the following relationships:

$$\sigma_v = S_i[0.71 + 1.74(\frac{x}{h})] \qquad \text{(Equation 1)}$$

where σ_v = Confined coal strength
S_i = In situ coal unconfined strength
x = Distance from the nearest rib
h = Pillar height

$$\varepsilon_v = \sigma_v / E \qquad \text{(Equation 2)}$$

where ε_v = Peak strain
σ_v = Confined coal strength
E = Coal elastic modulus

$$\sigma_r = 0.2254 \times \ln(x) \times \sigma_v \qquad \text{(Equation 3)}$$

where σ_r = Residual stress
x = Distance from the nearest rib, and
σ_v = Confined coal strength

$$\varepsilon_r = 4 \times \varepsilon_v \qquad \text{(Equation 4)}$$

where ε_r = Residual strain
ε_v = Peak strain.

Table 15 - LaModel Confined Coal Strength

Confined Coal Distance into Rib (ft)	Confined Strength (psi)	Peak Strain	Residual Strength (psi)	Residual Strain
2.5	2,059	0.004	425	0.017
7.5	3,845	0.008	1,746	0.032
12.5	5,631	0.012	3,206	0.047
17.5	7,417	0.016	4,785	0.062
22.5	9,203	0.019	6,459	0.077
27.5	10,989	0.023	8,209	0.092
32.5	12,775	0.027	10,025	0.107
37.5	14,562	0.031	11,896	0.122

These relationships are very similar to those that Karabin and Evanto[14] proposed to be used as a first approximation of stress and strain values for a strain softening coal model. AAI used a constant of 0.71 in the confined coal strength formula whereas Karabin and Evanto used 0.78. Also, Karabin and Evanto used two points to define the post-peak slope of the stress-strain curve whereas AAI used only one. As illustrated in Figure 114, the slope of the post-peak curve that

AAI used departs somewhat from that proposed by Karabin and Evanto. However, this approach is reasonable given the assumptions inherent in using strain softening properties. Karabin and Evanto acknowledged that information was lacking at the time that they wrote their paper:

> *"The strain-softening approach has been identified as a reasonable method of describing coal seam behavior. While that concept has been widely discussed, little specific information is available concerning the actual construction of a strain-softening model."*

Unfortunately, little research has been done to improve our understanding of strain-softening behavior in coal since this was written.

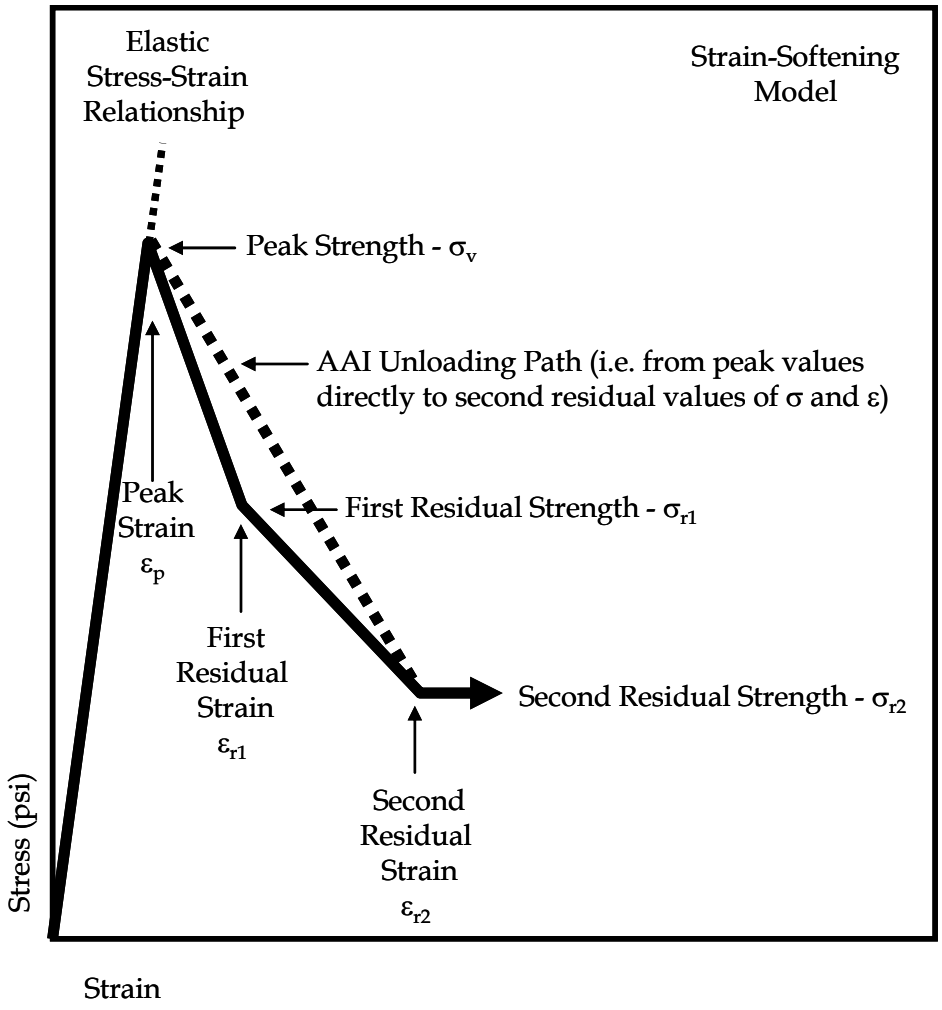

Figure 114 - General Strain-Softening Element Characteristics

Traditionally, strain softening properties have been deployed in a displacement-discontinuity pillar model as a series of concentric rings with the weakest material on the perimeter and progressively stronger materials approaching the center (see Figure 115)[14]. In reality, pillar corners experience less confinement and, therefore, have lower peak strengths. However, this simplification (i.e., not considering corner effects) has proven to be generally acceptable. At least one BEM program, BESOL, assigned yielding properties in this manner when the user elected to use the program's "automatic yield allocation" feature.

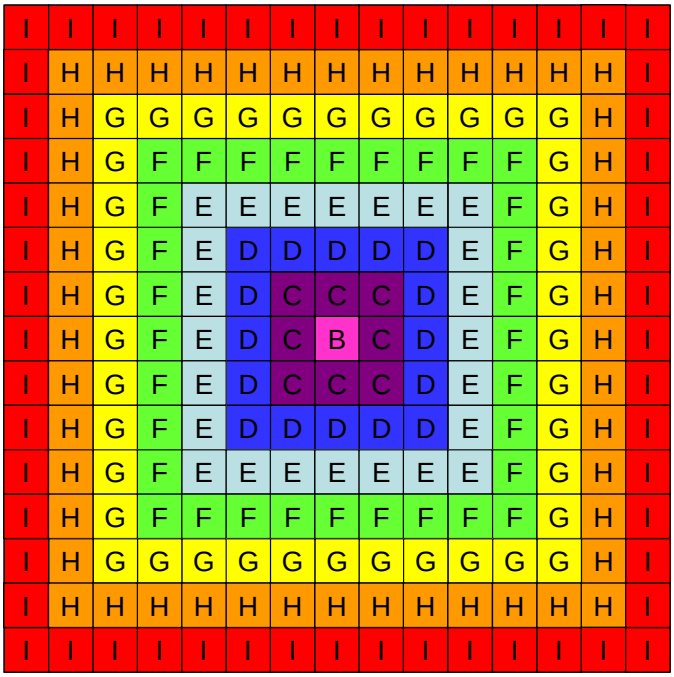

Figure 115 - Traditional Strain-Softening Element Distribution

The LaModel preprocessor, LamPre, has an automatic yield property allocation feature. However, the "apply yield zone" utility in LaModel distributes properties in the manner illustrated in Figure 116. This distribution provides a separate element designation (i.e., letter code) for corners so that modeled pillar strengths can be more consistent with empirically derived pillar strength formulas and the assumed stress gradient.

LaModel provides up to 26 different material property inputs. These properties can be deployed manually in any manner deemed appropriate by the user. However, LamPre's automatic yielding property allocation utility limits the depth of yielding to 4 elements. Although the utility utilizes nine material properties, the depth of the yield zone is still limited to four elements deep. One of the nine codes represents linear elastic behavior, four represent yielding ribs, and four are slightly lower strength yielding elements used to more accurately represent reduced corner confinement.

Models constructed by AAI utilized eight strain-softening material properties (as shown in Table 1 of AAI's July 2006 report). These properties are consistent with equations 2 through 5 using in situ coal strength (S_i) of 1640 psi and element depths (from the ribline) from 2.5 to 37.5 feet. However, the properties actually were deployed in AAI's models as illustrated in Figure 116. One result of this element configuration is to limit the maximum depth of pillar yielding to 20 feet when 5-foot elements are used. Another is to substantially increase the modeled pillar strength beyond the value that traditional pillar strength formulae (such as those used to determine Equation 2) would predict.

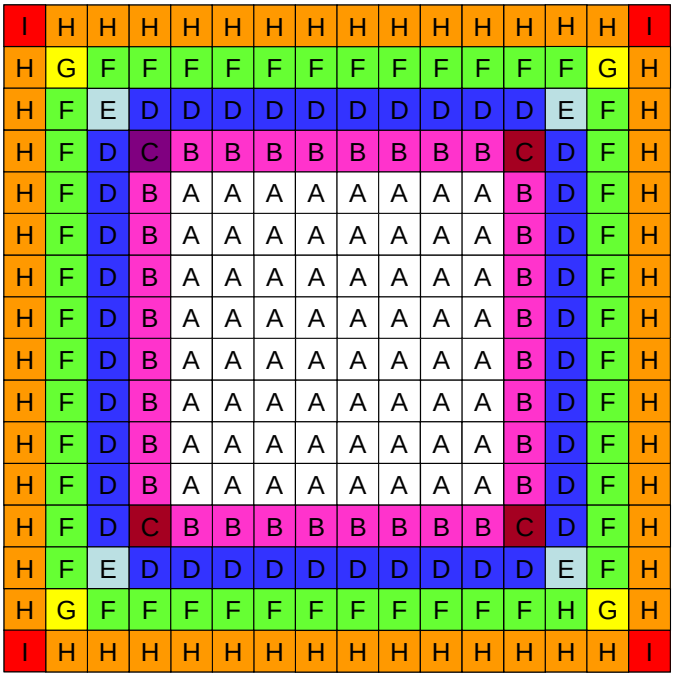

Figure 116 - Strain-Softening Element Distribution to Account for Corner Effects (as Deployed by AAI)

If eight elements (“B” through “I”) are assigned yielding (e.g., strain-softening properties), as distributed and shown in Figure 115, any pillar 16 elements wide or less would be comprised of “yieldable” elements. If 5-foot wide elements are employed, pillars up to 80 feet would be capable of yielding and transferring load to adjacent pillars once the peak strengths of the elements within the pillar were exceeded. In contrast, the same properties distributed as shown in Figure 116 will provide full yielding only for pillars up to 8 elements wide, which is 40 feet in width (8 elements x 5 feet/element). The group of elements labeled “A” in Figure 116 corresponds to linear elastic elements that have no peak strength and cannot transfer load to adjacent structures. In effect, any pillar over 40 feet in width will be represented in the model with a linearly elastic core that will not fail.

Appendix V - Rock Mass Properties

AAI indicated in a written response to the investigation team that the rock mass modulus was modified from $1x10^6$ psi used in their calibrated EXPAREA model to $2x10^6$ psi to account for the reduced stiffness introduced by the laminated rock mass used in LaModel. However, the engineer who conducted the work subsequently indicated that he had used the default elastic modulus in LamPre (i.e. $3x10^6$ psi) and evaluated the response of their model to lamination thicknesses of 25 and 50 feet. He noted no difference between the two thickness values and opted to use 25 feet thereafter.

In his dissertation, Heasley[5] provides equations that represent the relationship between convergence in the laminated overburden used in LaModel and homogeneous elastic rock masses used in other boundary element models. First, he notes that the seam convergence across a two-dimensional slot for the laminated model (s_l) as a function of the distance from the panel centerline (x) can be determined as:

$$s_l(x) = \frac{\sqrt{12(1-\nu^{2)}}}{t}\frac{q}{E}(L^2 - x^2) \qquad \text{Equation 1}$$

where: s = seam convergence,
x = distance from the panel centerline,
υ = rock mass Poisson's ratio,
t = layer or lamination thickness,
q = overburden stress,
E = rock mass elastic modulus, and
L = half width of longwall panel.

A comparable equation for convergence in a homogeneous, isotropic, elastic overburden (s_h) is provided by Jaeger and Cook[27]:

$$s_h(x) = 4(1-\nu^2)\frac{q}{E}\sqrt{(L^2 - x^2)} \qquad \text{Equation 2}$$

Heasley equates these relationships and solves for the lamination thickness (t) corresponding to the convergence at the center of the panel (x=0):

$$s_l(0) = \frac{\sqrt{12(1-\nu^{2)}}}{t}\frac{q}{E}L^2 = 4(1-\nu^2)\frac{q}{E}L = s_h(0) \qquad \text{Equation 3}$$

Assuming that the elastic modulus in both cases is constant, the result is:

$$t = \sqrt{\frac{3}{4}}\frac{L}{\sqrt{1-\nu^2}} \qquad \text{Equation 4}$$

However, in the present case, AAI increased the modulus threefold. To account for dissimilar moduli, equations 1 and 2 can be solved in a similar manner to yield the following relationship:

$$t = \sqrt{\frac{3}{4}}\frac{E_{HOMOGENEOUS}}{E_{LAMINATED}}\frac{L}{\sqrt{1-\nu^2}} \qquad \text{Equation 5}$$

Equation 5 indicates that the required thickness is reduced by a factor of three as a result of increasing the rock mass modulus for the laminated model. However, if we assume a panel half-width of 117 meters (385 feet or half the width of an average 770-foot wide longwall panel), the estimated lamination thickness is 35 meters (115 feet) which is more than four times greater than the 25-foot thickness that AAI used. The effect of thin laminations is that stress will be concentrated more at the edges of openings rather than be distributed farther away.

Appendix W - MSHA Main West 2006 ARMPS

As part of a plan review involving the AAI August 2006 analysis for pillar recovery in the Main West North and South Barriers inby crosscut 107, MSHA District 9 conducted an independent ARMPS study. Based on the 9 Left – 1st North pillar recovery panel, MSHA established that a minimum ARMPS PStF should be 0.42. To assess the North Barrier section pillar recovery, a model was constructed where the sealed portion of the Main West entries and the North Barrier section entries were combined to form the 9-entry geometry shown in Figure 117. The projected South Barrier section pillar recovery was also studied. In a manner similar to the North Barrier section, the South Barrier section pillar recovery was modeled as the 9-entry geometry shown in Figure 118 where Main West and South Barrier section pillars are combined.

In the North Barrier section analysis, the pillar extraction row included all nine entries as if pillar recovery included extracting pillars from Main West and the barrier separating Main West and the North Barrier section. In the South Barrier section analysis, the pillar extraction row also included all nine entries with the barrier separating Main West and the South Barrier section modeled as an extracted section pillar. This layout generates low pillar stability values in order to model a worse case scenario, considering that only two pillars per row were to be recovered in the North and South Barrier sections, and not eight pillars per row as modeled by MSHA. The MSHA Main West 2006 analysis did not address barrier pillar stability factors.

At 2,000 feet of overburden, the MSHA Main West 2006 ARMPS pillar stability values are under the 0.42 MSHA derived minimum criteria for the pillar stability values. The MSHA analysis led to further discussion between Owens and GRI concerning the AAI study. After discussing MSHA's concerns with GRI, Owens agreed with AAI's analysis.

At the time of the MSHA 2006 study, 80 x 92-foot center pillars were proposed for the South Barrier section. MSHA District 9 did not run ARMPS studies for the as-mined South Barrier section pillar design having 80 x 130-foot center pillars and a 40-foot barrier slab cut.

Example of MSHA North Barrier ARMPS Model

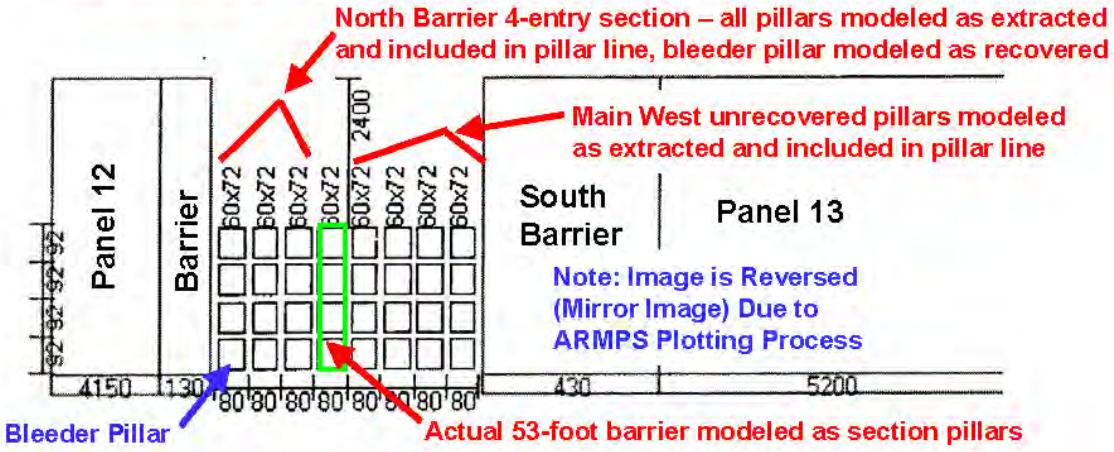


```
[DEVELOPMENT GEOMETRY PARAMETERS]
Entry Height.....8 (ft)
Depth of Cover.....2000 (ft)
Crosscut Angle.....90 (deg)
Entry Width.....20 (ft)
Number of Entries.....9
Crosscut Spacing.....92 (ft)
Center to Center Distance #1.....80 (ft)
Center to Center Distance #2.....80 (ft)
Center to Center Distance #3.....80 (ft)
Center to Center Distance #4.....80 (ft)
Center to Center Distance #5.....80 (ft)
Center to Center Distance #6.....80 (ft)
Center to Center Distance #7.....80 (ft)
Center to Center Distance #8.....80 (ft)

[DEFAULT PARAMETERS]
In Situ Coal Strength.....900 (psi)
Unit Weight of Overburden.....162 (pcf)
Breadth of AMZ.....223 (ft)
AMZ set automatically

[RETREAT MINING PARAMETERS]
Loading Condition.....TWO SIDES + ACTIVE GOB
Extend of Active Gob.....2400 (ft)
Abutment Angle of Active Gob.....21 (deg)
Extend of First Gob.....4150 (ft)
Abutment Angle of 1st Gob.....21 (deg)
Barrier Pillar Width of 1st Gob.....130 (ft)
Depth of Slab Cut in Barrier Pillar of 1st Gob....0 (ft)
Extend of Second Gob.....5200 (ft)
Abutment Angle of 2nd Gob.....21 (deg)
Barrier Pillar Width of 2nd Gob.....430 (ft)
Depth of Slab Cut in Barrier Pillar of 2nd Gob....0 (ft)

[ARMPS STABILITY FACTORS]

DEVELOPMENT.....0.84
ACTIVE GOB.....0.54
ONE SIDE + ACTIVE GOB.....0.34
TWO SIDES + ACTIVE GOB.....0.34
```

ARMPS PStF noted to be under 0.42 MSHA derived threshold

Figure 117 - North Barrier MSHA 2006 ARMPS Model

Example of MSHA South Barrier ARMPS Model

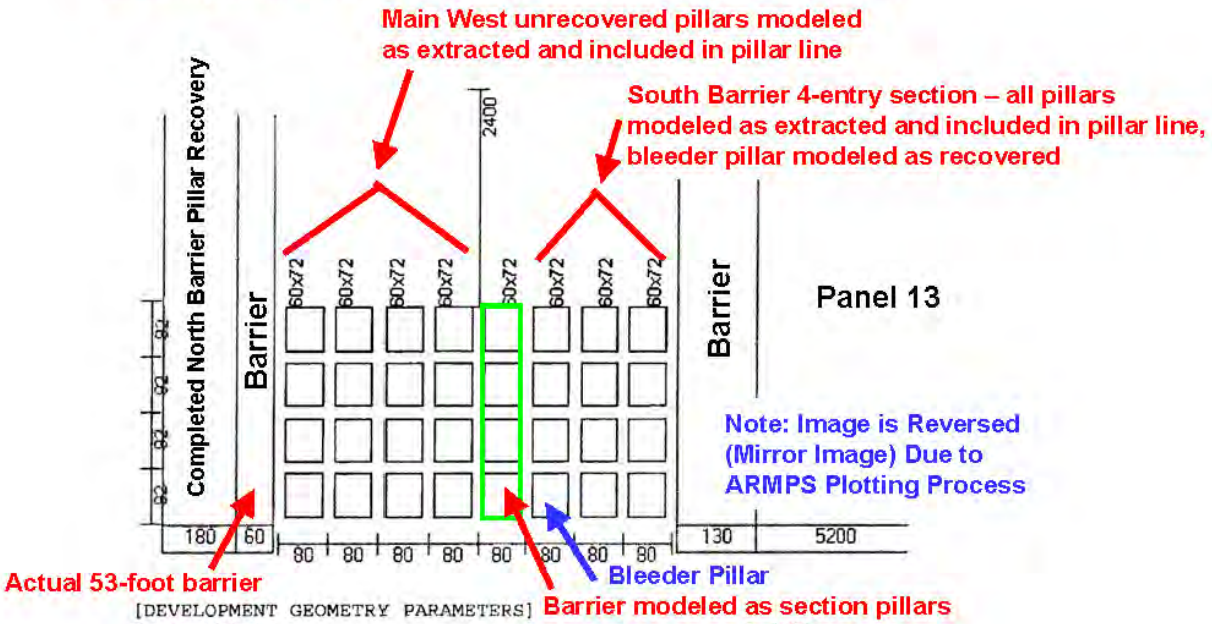


```
[DEVELOPMENT GEOMETRY PARAMETERS]
Entry Height.....8 (ft)
Depth of Cover.....2000 (ft)
Crosscut Angle.....90 (deg)
Entry Width.....20 (ft)
Number of Entries.....9
Crosscut Spacing.....92 (ft)
Center to Center Distance #1.....80 (ft)
Center to Center Distance #2.....80 (ft)
Center to Center Distance #3.....80 (ft)
Center to Center Distance #4.....80 (ft)
Center to Center Distance #5.....80 (ft)
Center to Center Distance #6.....80 (ft)
Center to Center Distance #7.....80 (ft)
Center to Center Distance #8.....80 (ft)

[DEFAULT PARAMETERS]
In Situ Coal Strength.....900 (psi)
Unit Weight of Overburden.....162 (pcf)
Breadth of AMZ.....223 (ft)
AMZ set automatically

[RETREAT MINING PARAMETERS]
Loading Condition.....TWO SIDES + ACTIVE GOB
Extend of Active Gob.....2400 (ft)
Abutment Angle of Active Gob.....21 (deg)
Extend of First Gob.....180 (ft)
Abutment Angle of 1st Gob.....21 (deg)
Barrier Pillar Width of 1st Gob.....60 (ft)
Depth of Slab Cut in Barrier Pillar of 1st Gob....0 (ft)
Extend of Second Gob.....5200 (ft)
Abutment Angle of 2nd Gob.....21 (deg)
Barrier Pillar Width of 2nd Gob.....130 (ft)
Depth of Slab Cut in Barrier Pillar of 2nd Gob....0 (ft)

[ARMPS STABILITY FACTORS]

DEVELOPMENT.....0.84
ACTIVE GOB.....0.54
ONE SIDE + ACTIVE GOB.....0.38
TWO SIDES + ACTIVE GOB.....0.27
```

ARMPS PStF noted to be under 0.42 MSHA derived threshold

Figure 118 - South Barrier MSHA 2006 ARMPS Model

Appendix X - Mine Ventilation Plan

The mine ventilation plan in effect at the time of the accident was submitted January 5, 2006, and approved on July 27, 2006. The plan superseded all previously approved ventilation plans with exception of amendments for pillar recovery in South Mains, sealing of 1st South Mains and South Mains, and the ventilation map accepted on July 6, 2007. At the time of the accident, pillar recovery in South Mains had been completed. The approved plan to seal 1st South Mains and South Mains had not been implemented.

The plans to develop and recover pillars in the Main West barrier pillars consisted of five separate plan amendments. Separate plans were submitted for the development and recovery of each barrier and a site specific plan for the drilling of drainage boreholes into an adjacent sealed area. An amendment to permanently seal the North Barrier section was also submitted. A description of each amendment follows.

The amendment to the ventilation plan for the development of the North Barrier section dated November 10, 2006, was received by MSHA on November 15, 2006, and was approved on November 21, 2006. The plan states that a separate roof control plan amendment would be submitted. Four entries were projected into the North Barrier. Entries were numbered from left to right with Nos. 1 and 2 entries projected to be intake air courses, No. 3 entry was projected as the isolated section belt, and No. 4 entry was projected as the return air course. The intake air split ventilated the Main West seals prior to ventilating the working section. The seals were to be examined in accordance with 30 CFR 75.360(b)(5).

The ventilation plan amendment to recover pillars in the North Barrier section was dated and received by MSHA on February 3, 2007, and was approved February 9, 2007. The plan required a measurement point location (MPL) to be established at the deepest point of penetration or at the edge of accumulated (roofed) water. The mine map provided after the accident indicated that mining was stopped short of the location shown on the approved plan. Pillar recovery was initiated approximately 92 feet inby crosscut 158. Measurements indicating the quantity, quality, and direction of air at the MPL were not recorded in the weekly examination record book as required by 30 CFR 75.364.

A ventilation plan amendment to drill boreholes between the North Barrier section and the sealed portion of Main West dated February 8, 2007, was approved February 14, 2007. The stated intent of the boreholes was to drain any water that may accumulate in the North Barrier section into the sealed portion of Main West.

The ventilation plan amendment to seal the North Barrier section dated March 14, 2007, was received by MSHA on March 15, 2007, and provisionally approved on March 16, 2007. The plan specifies that cementitious foam alternative seals would be installed in the four entries of the North Barrier section between crosscuts 118 and 119. The stoppings in crosscut 118 were removed to establish ventilation across the seal line.

The ventilation plan amendment to develop entries in the Main West South Barrier was received by MSHA on March 22, 2007, and approved on March 23, 2007. Four entries were projected into the Main West South Barrier. The No. 1 entry was projected to be an intake air course, Nos. 2 and 3 entries were projected as the section belt and common entries, and No. 4 entry was projected as the return air course.

The ventilation plan amendment to recover pillars in the South Barrier section dated May 16, 2007, was received by MSHA on May 21, 2007, and approved on June 1, 2007. The plan allowed pillar recovery between the Nos. 1 and 3 entries, and slabbing of the barrier south of the No. 1 entry (except between crosscuts 139 and 142). The ventilation plan depicted pillar recovery between the No. 1 and No. 2 entries and slabbing of the barrier to the south between crosscuts 139 to 142. However, the approved roof control plan was revised to afford additional protection to the bleeder system by not permitting any pillar recovery between crosscuts 139 and 142, including slab cuts from the barrier (refer to *South Barrier Section - Pillar Recovery Plan*).

The plan amendment approved June 1, 2007, shows an MPL location at the inby end of the bleeder entry as well as an alternate MPL location if water was allowed to accumulate. A copy of this amendment is included at the end of this appendix. The alternate location was to be at "the edge of accumulated (roofed) water." The plan also states that "Entries will be maintained to keep the entries free of standing water in excessive depths which would prevent safe travel." Mining was conducted approximately 40 feet inby crosscut 149.

Mining conducted inby the last crosscut did not provide for an MPL to be established at the deepest point of penetration as required in the approved plan. The bleeder entry did not extend to the deepest point of penetration. Measurements indicating the quantity, quality and direction of the MPL were not recorded in the weekly examination record book as required by 30 CFR 75.364.

A revised ventilation map dated June 2007 was received by MSHA on July 2, 2007. Mining development was shown to crosscut 141 of the South Barrier section. The map depicted the section as being ventilated with 51,546 cubic feet per minute (cfm) of intake air at crosscut 121. The section regulator between crosscuts 107 to 108 is shown with an air quantity of 60,687 cfm. The return air includes 11,980 cfm of belt air being dumped through a regulator adjacent to the number 6 belt drive. The intake and return quantities on the map are also recorded in the weekly examination book for the week ending June 23, 2007 under the location *"Main West #139-#39."*

UNDERGROUND MINE FILE
DATE FWD. 6-5-07
INITIALS Am

Surname	Date
	5-29-07
	5-29-07
	5/30/07
	5-29-07
	5/31

Coal Mine Safety and Health
District 9

JUN 01 2007

Gary Peacock
General Manager
Genwal Resources, Inc.
P.O. Box 1077
Price, UT 84501

RE: Crandall Canyon Mine
ID No. 42-01715
Ventilation Plan Amendment

Dear Mr. Peacock:

The enclosed plan amendment, dated May 16, 2007, consisting of a cover letter and Plate Nos. 5 and 6, addressing retreat mining in the Main-West South-Barrier Panel, is approved in accordance with 30 CFR §75.370(a)(1). This amendment will be incorporated into the Ventilation Plan approved on July 27, 2006.

This approval supersedes the following:

1. The Ventilation Plan amendment approved on February 9, 2007, addressing pillar extraction in the North Barrier of main west.

2. The Ventilation Plan amendment approved on February 14, 2007, addressing drilling boreholes between the north block of Main West and the sealed portion of Main West.

This approval is site specific and will terminate upon completion of the project.

A copy of this approval shall be made available to the miners and reviewed with all miners affected by this plan.

Sincerely,

/s/ Allyn C. Davis

Allyn C. Davis
District Manager

Enclosure

cc: Tom Hurst

APPROVED
JUN - 1 2007
CMSH

bcc: EC Plan File (Original Surname w/Original Plan)
McAlester Dust (Copy of Surname w/Copy of Plan)
Price #2 FO (Copy of Surname w/Copy of Plan)
Price #2 UMF (Copy of Surname w/Copy of Plan)
(Copy of Surname w/Copy of Plan)
VG - Plan File (Copy of Surname w/Copy of Plan)
VG - Chron V* (Copy of Surname)
D-9 Chron * (Copy of Surname)
Lan/coal/vent/jf/4201715/8660-B4-A14

Crandall Canyon Mine
a subsidiary

Hwy31 MP 33, Huntington, UT 84528
PO Box 1077, Price, UT 84501
Phone: (435) 888-4000
Fax: (435) 888-4002

UtahAmerican Energy, Inc.

8660 B4-A 14

May 16, 2007

Mr. Allyn C. Davis
District Manager
Coal Mine Safety and Health
P.O. Box 25367
Denver, Colorado 80225

Re: Crandall Canyon Mine ID# 42-01715 Ventilation Plan for Pillaring Main West South Barrier

Dear Mr. Davis:

Please find attached for your review and approval, a ventilation plan for mining the South Barrier of Main West at our Crandall Canyon Mine. The plan consists of one page of text and 2 Plates.

Please contact me with any questions at 435.888.4023.

Sincerely,

Tom Hurst

Tom Hurst
Mining Engineer
435.888.4023

Crandall Canyon Mine
MSHA ID Number 42-01715
Main West South Barrier Pillar Ventilation

The mine is currently developing entries in the south barrier block of the Main West Area. This plan is for the ventilation for the pillar recovery of the developed area of the south barrier block.

The bleeder system proposes is a wrap around bleeder type. The bleeder measurement point location (MPL) will be located at the deepest point of penetration or the edge of accumulated (roofed) water. The pillar recovery proposed by this plan will be done in accordance with the approved Roof Control Plan. Examinations of the bleeder will be conducted in accordance with 30 CFR Part 75.364. The MPL proposed for the #4 entry of the Main West south barrier would be moved outby if water accumulations were to occur. In conjunction with the retreating MPL, the stopping immediately inby the newly established MPL will be removed to insure sufficient airflow in the bleeders. Plate 5, Pillar Ventilation, shows the ventilation after pillaring has began. Plate 6, Continuing Pillar Ventilation, shows the ventilation with water accumulations sufficient to require an alternate MPL because of roofed water inby the pillar line.

The elevations in this area of the mine are down dip to the beginning of the pillar line. This proposal is to conduct weekly examinations in accordance with 30 CFR Part 75.364 at the toe of any accumulated water (roofed) on the return side of the bleeders. It is not anticipated that accumulations of water will be a significant problem in this area. The alternate MPL is proposed in the event water accumulates, preventing travel inby in the bleeder entry.

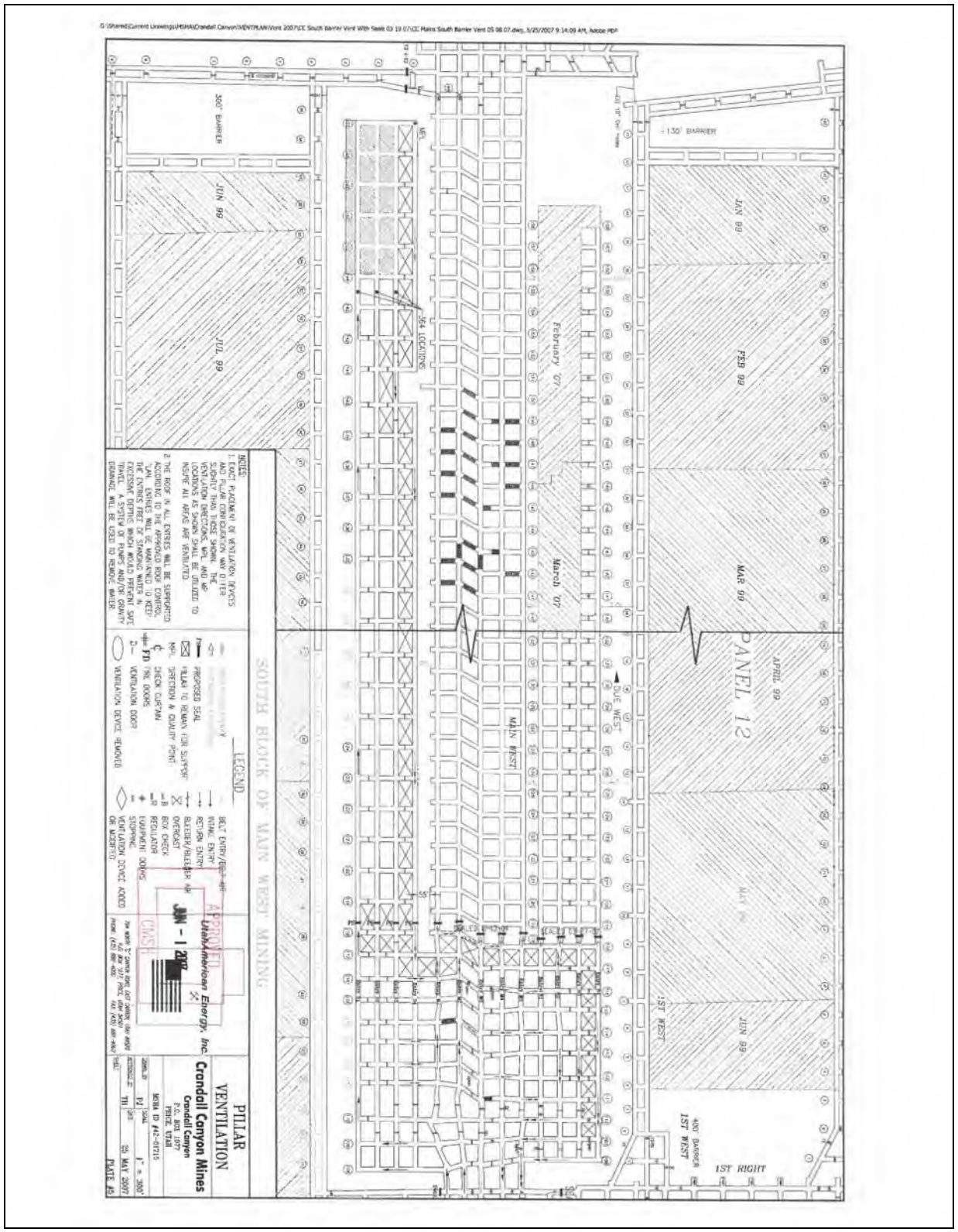
PILLAR VENTILATION
Crandall Canyon Mines
Crandall Canyon
P.O. BOX 1077
HUNTINGTON, UTAH
MSHA ID #42-01715
SCALE: 1" = 300'
DATE: 25 MAY 2007
PLATE #5
SOUTH BLOCK OF MAIN WEST MINING
PANEL 12
PROPOSED SEAL
PILLAR TO REMAIN FOR SUPPORT
INSPECTION & QUALITY POINT
CHECK CURTAIN
TRAL DOORS
VENTILATION DOOR
VENTILATION DEVICE REMOVED
BELT ENTRY/EGRESS AIR
INTAKE ENTRY
RETURN ENTRY
BULKHEAD/BLEEDER
OVERCAST
BOX CHECK
REGULATOR
EQUIPMENT DOORS
STOPPING
VENTILATION DEVICE ADDED OR MODIFIED
APPROVED
UtahAmerican Energy, Inc.
JUN - 1 2007
CMSHA
300' BARRIER
+130' BARRIER
400' BARRIER
264 LOCATIONS
DUE WEST
MAIN WEST
1ST WEST
1ST RIGHT
JAN 99
FEB 99
MAR 99
APRIL 99
MAY 99
JUN 99
JUL 99
February '07
March '07

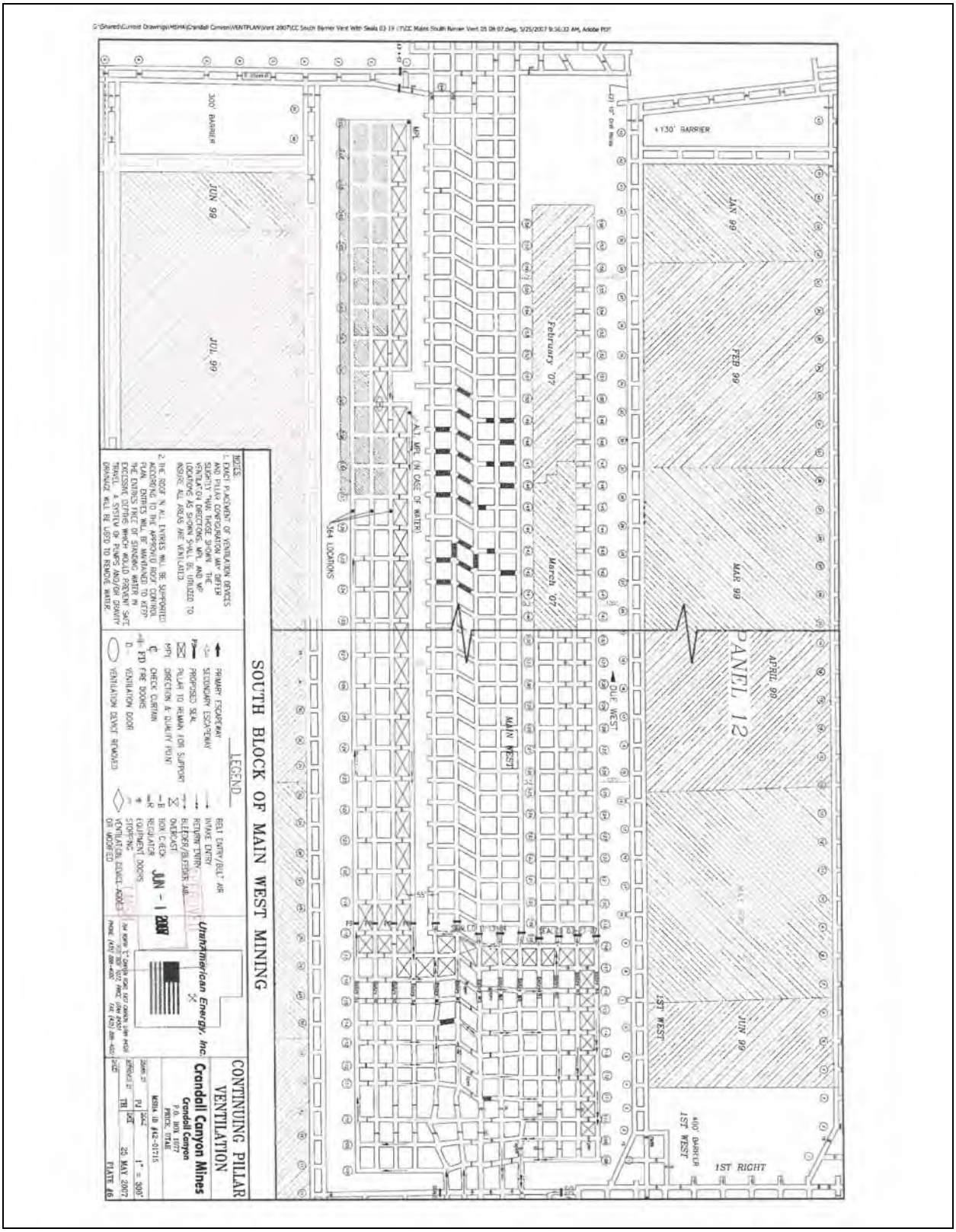
SOUTH BLOCK OF MAIN WEST MINING
CONTINUING PILLAR VENTILATION
Crandall Canyon Mines
Crandall Canyon
PANEL 12
MAIN WEST
1ST WEST
1ST RIGHT
JAN 99
FEB 99
MAR 99
APRIL 99
JUN 99
JUL 99
February '07
March '07
300' BARRIER
130' BARRIER
400' BARRIER
364 LOCATIONS
ALL MPL ON CASE OF WATER
MPL
GULF WEST
LEGEND
NOTES:
PRIMARY ESCAPEWAY
SECONDARY ESCAPEWAY
PROPOSED SEAL
PILLAR TO REMAIN FOR SUPPORT
DIRECTION & QUANTITY FROM
CHECK CURTAIN
FIRE DOORS
VENTILATION DOOR
VENTILATION DEVICE REMOVED
BELT ENTRY/BELT AIR
INTAKE ENTRY
RETURN ENTRY
BLEEDER/BLEEDER AIR
OVERCAST
BOX CHECK
REGULATOR
EQUIPMENT DOORS
STOPPING
VENTILATION DEVICE ADDED OR MODIFIED
Utah American Energy, Inc.
JUN - 1 2007
DIV. OF OIL, GAS & MINING
MSHA ID #42-01715
PANEL 12
SCALE
1" = 300'
DATE
25 MAY 2007
PLATE #6

Appendix Y - Glossary of Mining Terms as used in this Report

Abutment - In coal mining, (1) the weight of the rocks above a narrow roadway is transferred to the solid coal along the sides, which act as abutments of the arch of strata spanning the roadway; and (2) the weight of the rocks over a longwall face is transferred to the front abutment, that is, the solid coal ahead of the face and the back abutment, that is, the settled packs behind the face.

Act - The Federal Mine Safety and Health Act of 1977.

Active workings - Any place in a coal mine where miners are normally required to work or travel.

Advance - Mining in the same direction, or order of sequence; first mining as distinguished from retreat.

Agent – Any person charged with responsibility for the operation of all or a part of a coal or other mine or the supervision of the miners in a coal or other mine.

Air split - The division of a current of air into two or more parts.

Air course - An entry or a set of entries separated from other entries by stoppings, overcasts, other ventilation control devices, or by solid blocks of coal or rock so that any mixing of air currents between each is limited to leakage. Also known as an airway.

AMS Operator - The person(s) designated by the mine operator, who is located on the surface of the mine and monitors the malfunction, alert, and alarm signals of the AMS and notifies appropriate personnel of these signals.

Angle of dip - The angle at which strata or mineral deposits are inclined to the horizontal plane.

Angle of draw - In coal mine subsidence, this angle is assumed to bisect the angle between the vertical and the angle of repose of the material and is 20° for flat seams. For dipping seams, the angle of break increases, being 35.8° from the vertical for a 40° dip. The main break occurs over the seam at an angle from the vertical equal to half the dip.

Angle of repose - The maximum angle from horizontal at which a given material will rest on a given surface without sliding or rolling.

Arching - Fracture processes around a mine opening, leading to stabilization by an arching effect.

Atmospheric Monitoring System (AMS) - A network consisting of hardware and software meeting the requirements of 30 CFR 75.351 and 75.1103–2 and capable of: measuring atmospheric parameters; transmitting the measurements to a designated surface location; providing alert and alarm signals; processing and cataloging atmospheric data; and, providing reports. Frequently used for early-warning fire detection and to monitor the operational status of mining equipment.

Azimuth - A surveying term that references the angle measured clockwise from any meridian (the established line of reference). The bearing is used to designate direction. The bearing of a line is the acute horizontal angle between the meridian and the line.

Back-Analysis - A process in which known failures or successes are evaluated to determine the relationship of engineering parameters to outcomes.

Barricading - Enclosing part of a mine to prevent inflow of noxious gasses from a mine fire or an explosion. If men are unable to escape, they retreat as far as possible, select some working place with plenty of space, short-circuit the air from this place, build a barricade, and remain behind it until rescued.

Barrier - Barrier pillars are solid blocks of coal left between two mines or sections of a mine to prevent accidents due to inrushes of water, gas, or from explosions or a mine fire; also used for a pillar left to protect active workings from a squeeze.

Beam - A bar or straight girder used to support a span of roof between two support props or walls.

Beam building - The creation of a strong, inflexible beam by bolting or otherwise fastening together several weaker layers. In coal mining this is the intended basis for roof bolting.

Bearing plate - A plate used to distribute a given load; in roof bolting, the plate used between the bolt head and the roof.

Bed - A stratum of coal or other sedimentary deposit.

Belt air course - The entry in which a belt is located and any adjacent entry(ies) not separated from the belt entry by permanent ventilation controls, including any entries in series with the belt entry, terminating at a return regulator, a section loading point, or the surface.

Belt conveyor - A looped belt on which coal or other materials can be carried and which is generally constructed of flame-resistant material or of reinforced rubber or rubber-like substance.

Bit - The hardened and strengthened device at the end of a drill rod that transmits the energy of breakage to the rock. The size of the bit determines the size of the hole. A bit may be either detachable from or integral with its supporting drill rod.

Bituminous coal – A middle rank coal (between sub-bituminous and anthracite) formed by additional pressure and heat on lignite. Usually has a high Btu value and may be referred to as "soft coal."

Bleeder entries - Special entries developed and maintained as part of the bleeder system and designed to continuously move air from pillared areas into a return air course or to the surface of the mine.

Bleeder system - a ventilation network used to ventilate pillared areas in underground coal mines and designed to continuously dilute and move air-methane mixtures and other gases,

dusts, and fumes from the worked-out area away from active workings and into a return air course or to the surface of the mine.

Borehole - Any deep or long drill-hole, usually associated with a diamond drill.

Bottom - Floor or underlying surface of an underground excavation.

Boss - Any member of the managerial ranks who is directly in charge of miners (e.g., "shift-boss," "face-boss," "fire-boss," etc.).

Brattice or brattice cloth - Fire-resistant fabric or plastic partition used in a mine passage to confine the air and force it into the working place; also termed "curtain," "rag," "line brattice," "line canvas," or "line curtain."

Bounce - A heavy sudden often noisy blow or thump; sudden spalling off of the sides of ribs and pillars due to the excessive pressure; any dull, hollow, or thumping sound produced by movement or fracturing of strata as a result of mining operations; also known as a bump.

Bump – see definition for "Bounce."

Bump Prone Ground[28] – Strong, stiff roof and floor strata not prone to failing or heaving when subjected to high stress (e.g., deep overburden); also can refer to locations where bumps or bursts have historically occurred.

Burst - An explosive breaking of coal or rock in a mine due to pressure; the sudden and violent failure of overstressed rock resulting in the instantaneous release of large amounts of accumulated energy where coal or rock is suddenly expelled from failed pillars. In coal mines they may or may not be accompanied by a copious discharge of methane, carbon dioxide, or coal dust; also called outburst; bounce; bump; rock burst.

Can – A brand name type of floor-to-roof support constructed of prefabricated steel sheet metal cylinders filled with light-weight concrete.

Cap - A miner's safety helmet.

Certified - Describes a person who has passed an examination to do a required job.

Cleat - The vertical cleavage of coal seams. The main set of joints along which coal breaks when mined.

Coal - A solid, brittle, more or less distinctly stratified combustible carbonaceous rock, formed by partial to complete decomposition of vegetation; varies in color from dark brown to black; not fusible without decomposition and very insoluble.

Coal reserves - Measured tonnages of coal that have been calculated to occur in a coal seam within a particular property.

Coda Magnitude – The coda magnitude (M_C) is based on the length of the seismic signal and calibrated to provide similar results with the local magnitude (M_L) or Richter scale for naturally occurring earthquakes.

Competent rock - Rock which, because of its physical and geological characteristics, is capable of sustaining openings without any structural support except pillars and walls left during mining (stalls, light props, and roof bolts are not considered structural support).

Contact - The place or surface where two different kinds of rocks meet. Applies to sedimentary rocks, as the contact between a limestone and a sandstone, for example, and to metamorphic rocks; and it is especially applicable between igneous intrusions and their walls.

Continuous mining machine - A machine that removes coal from the face and loads that coal into cars without the use of cutting machines, drills, or explosives.

Contour - An imaginary line that connects all points on a surface having the same elevation.

Convergence – Reduction of entry height; closure between the mine floor and the mine roof.

Core sample – A cylinder sample generally 1-5" in diameter drilled out of an area to determine the geologic and chemical analysis of the overburden and coal.

Cover - The overburden of any deposit.

Crib - A roof support of prop timbers or ties, laid in alternate cross-layers, log-cabin style.

Cribbing - The construction of cribs or timbers laid at right angles to each other, sometimes filled with earth, as a roof support or as a support for machinery.

Crosscut - A passageway driven between parallel entries or air courses for ventilation purposes.

Curtain – see definition for “Brattice.”

Cycle mining - A system of mining in more than one working place at a time, that is, a continuous mining machine takes a lift from the face and moves to another face while permanent roof support is established in the previous working face.

Depth - The word alone generally denotes vertical depth below the surface. In the case of boreholes it may mean the distance reached from the beginning of the hole, the borehole depth, or the inclined depth.

Detectors - Specialized chemical or electronic instruments used to detect mine gases.

Development mining - Work undertaken to open up coal reserves prior to pillar recovery.

Dilute - To lower the concentration of a mixture; in this case the concentration of any hazardous gas in mine air by addition of fresh intake air.

Dip - The inclination of a geologic structure (bed, vein, fault, etc.) from the horizontal; dip is always measured downwards at right angles to the strike.

Double Difference Method – A technique to improve the precision of the location of seismic events by determining the relative location between multiple events. When combined with a known location, it can improve the accuracy of the locations.

Drainage - The process of removing surplus ground or surface water either by artificial means or by gravity flow.

Drift - A horizontal passage underground. A drift follows the vein, as distinguished from a crosscut that intersects it, or a level or gallery, which may do either.

Drift mine – An underground coal mine in which the entry or access is above water level and generally on the slope of a hill, driven horizontally into a coal seam.

Dump - To unload; specifically, a load of coal or waste; the mechanism for unloading, e.g. a car dump (sometimes called tipple); or, the pile created by such unloading, e.g. a waste dump (also called heap, pile, tip, spoil pike, etc.).

Entry - An underground horizontal or near-horizontal passage used for haulage, ventilation, or as a mainway; a coal heading; a working place where the coal is extracted from the seam in the initial mining; same as "gate" and "roadway," both British terms.

Extraction - The process of mining and removal of cal or ore from a mine.

Face – The exposed area of a coal bed from which coal is being extracted.

Face cleat - The principal cleavage plane or joint at right angles to the stratification of the coal seam.

Fall - A mass of roof rock or coal which has fallen in any part of a mine.

Fan signal - Automation device designed to give alarm if the main fan slows down or stops.

Fault - A slip-surface between two portions of the earth's surface that have moved relative to each other. A fault is a failure surface and is evidence of severe earth stresses.

Fault zone - A fault, instead of being a single clean fracture, may be a zone hundreds or thousands of feet wide. The fault zone consists of numerous interlacing small faults or a confused zone of gouge, breccia, or mylonite.

Feeder - A machine that feeds coal onto a conveyor belt evenly.

Floor - That part of any underground working upon which a person walks or upon which haulage equipment travels; simply the bottom or underlying surface of an underground excavation.

Formation – Any assemblage of rocks which have some character in common, whether of origin, age, or composition. Often, the word is loosely used to indicate anything that has been formed or brought into its present shape.

Fracture - A general term to include any kind of discontinuity in a body of rock if produced by mechanical failure, whether by shear stress or tensile stress. Fractures include faults, shears, joints, and planes of fracture cleavage.

Fresh Air Base – Mine rescue teams establish a fresh air base (FAB) under controlled ventilation at the entrance to unexplored areas. The FAB includes a hardwired communications system running to the surface command center. The FAB serves as a safe retreat and as a communication hub between the exploring teams and the command center.

Gob - The term applied to that part of the mine from which the coal pillars have been recovered and the rock that falls into the void; also called goaf. Also, refers to loose waste in a mine.

Grading - Digging up the bottom to give more headroom in roadways.

Ground control - Measures taken to prevent roof falls or coal bursts.

Ground pressure - The pressure to which a rock formation is subjected by the weight of the superimposed rock and rock material or by diastrophic forces created by movements in the rocks forming the earth's crust. Such pressures may be great enough to cause rocks having a low compressional strength to deform and be squeezed into and close a borehole or other underground opening not adequately strengthened by an artificial support, such as casing or timber.

Haulage - The horizontal transport of ore, coal, supplies, and waste.

Haulageway - Any underground entry or passageway that is designed for transport of mined material, personnel, or equipment, usually by the installation of track or belt conveyor.

Heaving - Applied to the rising of the bottom after removal of the coal.

Horizon - In geology, any given definite position or interval in the stratigraphic column or the scheme of stratigraphic classification; generally used in a relative sense.

Hydraulic - Of or pertaining to fluids in motion. Hydraulic cement has a composition which permits it to set quickly under water. Hydraulic jacks lift through the force transmitted to the movable part of the jack by a liquid. Hydraulic control refers to the mechanical control of various parts of machines, such as coal cutters, loaders, etc., through the operation or action of hydraulic cylinders.

Immediate roof - The roof strata immediately above the coalbed, requiring support during the excavation of coal.

Inby – Into the mine; in the direction of the working face.

In situ - In the natural or original position. Applied to a rock, soil, or fossil when occurring in the situation in which it was originally formed or deposited.

Intake air - Air that has not yet ventilated the last working place on any split of any working section, or any worked-out area, whether pillared or nonpillared.

Isopach - A line, on a map, drawn through points of equal thickness of a designated unit.

Jackpot - A cap-shaped unit designed for pre-stressing prop-type supports developed by New Concept Mining.

Joint - A divisional plane or surface that divides a rock and along which there has been no visible movement parallel to the plane or surface.

Lamp - The electric cap lamp worn for visibility.

Layout - The design or pattern of the main roadways and workings. The proper layout of mine workings is the responsibility of the manager aided by the planning department.

Lift - The amount of coal obtained from a continuous mining machine in one mining cycle.

Line Curtain - Fire-resistant fabric or plastic partition used in a mine passage to confine the air and force it into the working place; also termed “line brattice” or “line canvas.”

Lithology - The character of a rock described in terms of its structure, color, mineral composition, grain size, and arrangement of its component parts; all those visible features that in the aggregate impart individuality of the rock. Lithology is the basis of correlation in coal mines and commonly is reliable over a distance of a few miles.

Loading point – The point where coal or ore is loaded onto conveyors.

Local Magnitude – The local magnitude (M_L) or Richter scale is a logarithmic scale originally devised by Charles Richter to quantify the intensity of California earthquakes and has been adopted for use around the world.

Longwall mining – One of three major underground coal mining methods currently in use. Employs a steal plow, or rotation drum, which is pulled mechanically back and forth across a face of coal that is usually several hundred feet long. The loosened coal falls onto a conveyor for removal from the mine.

Loose coal - Coal fragments larger in size than coal dust.

Main entry - A main haulage road. Where the coal has cleats, main entries are driven at right angles to the face cleats.

Main fan - A mechanical ventilator installed at the surface; operates by either exhausting or blowing to induce airflow through the mine.

Man trip - A carrier of mine personnel, by rail or rubber tire, to and from the work area.

Methane – A potentially explosive gas formed naturally from the decay of vegetative matter, similar to that which formed coal. Methane, which is the principal component of natural gas, is frequently encountered in underground coal mining operations and is kept within safe limits through the use of extensive mine ventilation systems.

Methane monitor - An electronic instrument often mounted on a piece of mining equipment that detects and measures the methane content of mine air.

Miner – Any individual working in a coal or other mine.

Mobile bridge continuous haulage system - A system of movable conveyors that carry coal from a continuous mining machine to the section belt allowing the machine to advance over short distances without interrupting the mining and loading operation.

Mobile Command Center Vehicle – Class A motor home equipped with communication equipment, conference facility, and office equipment maintained by MSHA's Mine Emergency Operations unit.

MSHA - Mine Safety and Health Administration; the federal agency which regulates coal mine safety and health.

Operator - Any owner, lessee, or other person who operates, controls, or supervises a coal or other mine or any independent contractor performing services or construction at such mine.

Outburst Accident - coal or rock outburst that cause withdrawal of miners or which disrupts regular mining activity for more than one hour (even if no miners are injured).

Outby - Nearer to or toward the mine entrance, and hence farther from the working face; the opposite of inby.

Overburden – Layers of soil and rock covering a coal seam; also referred to as "depth of cover."

Overcast - Enclosed airway which permits one air current to pass over another without interruption.

Pager Phone – A telephone system approved for use in coal mines and capable of broadcasting voice messages over a loud speaker.

Panel - A coal mining block that generally comprises one operating unit.

Parting - (1) A small joint in coal or rock; (2) a layer of rock in a coal seam; (3) a side track or turnout in a haulage road.

Percentage extraction - The proportion of a coal seam which is removed from the mine. The remainder may represent coal in pillars or coal which is too thin or inferior to mine or lost in mining. Shallow coal mines working under townships, reservoirs, etc., may extract 50%, or less, of the entire seam, the remainder being left as pillars to protect the surface. Under favorable conditions, longwall mining may extract from 80 to 95% of the entire seam. With pillar methods of working, the extraction ranges from 50 to 90% depending on local conditions.

Permissible - That which is allowable or permitted. It is most widely applied to mine equipment and explosives of all kinds which are similar in all respects to samples that have passed certain tests of the MSHA and can be used with safety in accordance with specified conditions where hazards from explosive gas or coal dust exist.

Permit – As it pertains to mining, a document issued by a regulatory agency that gives approval for mining operations to take place.

Pillar - An area of coal left to support the overlying strata in a mine; sometimes left permanently to support surface structures.

Pillared area - Describes that part of a mine from which the pillars have been removed; also known as robbed out area.

Pillar line - The line that roughly follows the rear edges of coal pillars that are being recovered during retreat mining; the line along which the roof of a coal mine is expected to break.

Pillar recovery - Any reduction in pillar size during retreat mining. Refers to the systematic removal of the coal pillars between rooms or chambers to regulate the subsidence of the roof; also termed “pillar robbing,” “bridging back” the pillar, “drawing” the pillar, or “pulling” the pillar.

Portal - The surface entrance to a mine.

Post - The vertical member of a timber set.

Prop - Coal mining term for any single post used as roof support. Props may be timber or steel; if steel--screwed, yieldable, or hydraulic.

Qualified Person - (1) An individual deemed qualified by MSHA and designated by the operator to make tests and examinations required by this 30 CFR part 75; and (2) An individual deemed, in accordance with minimum requirements established by MSHA, qualified by training, education, and experience, to perform electrical work, to maintain electrical equipment, and to conduct examinations and tests of all electrical equipment.

Rag – see definition for “Brattice.”

Recovery - The proportion or percentage of coal or ore mined from the original seam or deposit.

Regulator - Device (wall, door) used to control the volume of air in an air split.

Reserve – That portion of the identified coal resource that can be economically mined at the time of determination. The reserve is derived by applying a recovery factor to that component of the identified coal resource designated as the reserve base.

Resin bolting - A method of permanent roof support in which steel rods are grouted with resin.

Resources – Concentrations of coal in such forms that economic extraction is currently or may become feasible. Coal resources broken down by identified and undiscovered resources.

Identified coal resources are classified as demonstrated and inferred. Demonstrated resources are further broken down as measured and indicated. Undiscovered resources are broken down as hypothetical and speculative.

Retreat mining - A system of robbing pillars in which the robbing line, or line through the faces of the pillars being extracted, retreats from the boundary toward the shaft or mine mouth.

Return air - Air that has ventilated (or mixed with air that has ventilated) the last working place on any split of any working section, or any worked-out area, whether pillared or nonpillared.

Rib - The side of a pillar or the wall of an entry; the solid coal on the side of any underground passage.

Rider - A thin seam of coal overlying a thicker one.

Rob - To extract pillars of coal previously left for support.

Rock Dust - Pulverized limestone, dolomite, gypsum, anhydrite, shale, adobe, or other inert material, preferably light colored. Rock dust is applied to underground areas of coal mines to increase the incombustible content of mine dust so that it will not propagate an explosion.

RocProp - A type of hydraulically wedged standing roof support, registered trademark of Mine Support Products.

Roof - The stratum of rock or other material above a coal seam; the overhead surface of a coal working place; same as “back” or “top.”

Roof bolt - A long steel bolt driven into the roof of underground excavations to support the roof, preventing and limiting the extent of roof falls. The unit consists of the bolt (up to 4 feet long), steel plate, expansion shell, and pal nut. The use of roof bolts eliminates the need for timbering by fastening together, or “laminating,” several weaker layers of roof strata to build a “beam.”

Roof Coal – A layer of coal immediately above the mine opening as a result of leaving the upper horizon of the coalbed unmined, usually to protect weak shale in the immediate roof from weathering; also known as “head coal” or “top coal.”

Roof fall - A coal mine cave-in, especially in active areas such as entries.

Roof jack - A screw- or pump-type hydraulic extension post made of steel and used as temporary roof support.

Roof sag - The sinking, bending, or curving of the roof, especially in the middle, from weight or pressure.

Roof stress - Unbalanced internal forces in the roof or sides, created when coal is extracted.

Roof support – Posts, jacks, roof bolts and beams used to support the rock overlying a coal seam in an underground mine. A good roof support plan is part of mine safety and coal extraction.

Room and pillar mining – A method of underground mining in which approximately half of the coal is left in place to support the roof of the active mining area. Large "pillars" are left while "rooms" of coal are extracted.

Safety factor - The ratio of the ultimate breaking strength of the material to the force exerted against it.

Sandstone - A sedimentary rock consisting of quartz sand united by some cementing material, such as iron oxide or calcium carbonate.

Scaling - Removal of loose rock from the roof or walls. This work is dangerous and a long bar (called a scaling bar) is often used.

Scoop - A rubber tired-, battery- or diesel-powered piece of equipment designed for cleaning roadways and hauling supplies.

Seam - A stratum or bed of coal.

Section - A portion of the working area of a mine.

Self-contained breathing apparatus - A self-contained supply of oxygen used during rescue work from coal mine fires and explosions.

Self-contained self-rescuer (SCSR) – A type of closed-circuit, self-contained breathing apparatus approved by MSHA and NIOSH under 42 CFR part 84 for escape only from underground mines. The device is capable of sustaining life in atmospheres containing deficient oxygen.

Self-rescuer – A small filtering device carried by a coal miner underground, either on his belt or in his pocket, to provide him with immediate protection against carbon monoxide and smoke in case of a mine fire or explosion. It is a small canister with a mouthpiece directly attached to it. The wearer breathes through the mouth, the nose being closed by a clip. The canister contains a layer of fused calcium chloride that absorbs water vapor from the mine air. The device is used for escape purposes only and does not sustain life in atmospheres containing deficient oxygen. Filter self-rescuers approved by MSHA and NIOSH under 42 CFR part 84 provide at least one hour of protection against carbon monoxide.

Shaft - A primary vertical or non-vertical opening through mine strata used for ventilation or drainage and/or for hoisting of personnel or materials; connects the surface with underground workings.

Shale - A rock formed by consolidation of clay, mud, or silt, having a laminated structure and composed of minerals essentially unaltered since deposition.

Shift - The number of hours or the part of any day worked.

Shuttle car – A self-discharging vehicle, generally with rubber tires, used for receiving coal from the loading or mining machine and transferring it to an underground loading point, mine railway, or belt conveyor system.

Slabbing – A method of mining pillars in which successive lifts are cut from one side of the pillar.

Sloughing - The slow crumbling and falling away of material from roof, rib, and face.

Spad – A spad is a flat spike hammered into the mine ceiling from which is threaded a plumbline to serve as an underground survey station. A sight spad, is a station that allows a mine foreman to visually align entries or breaks from the main spad.

Span - The horizontal distance between the side supports or solid abutments.

Split - Any division or branch of the ventilating current or the workings ventilated by one branch. Also, to divide a pillar by driving one or more roads through it.

Squeeze - The settling, without breaking, of the roof and the gradual upheaval of the floor of a mine due to the weight of the overlying strata.

Step-Up Foreman – A crewmember who acts in a supervisory role during a foreman's absence.

Strike - The direction of the line of intersection of a bed or vein with the horizontal plane. The strike of a bed is the direction of a straight line that connects two points of equal elevation on the bed.

Stump - Any small pillar.

Stopping – A permanent wall built across unused crosscuts or entries to separate air courses and prevent the air from short circuiting.

Subsidence – The gradual sinking, or sometimes abrupt collapse, of the rock and soil layers into an underground mine.

Sump - A place in a mine that is used as a collecting point for drainage water.

Support - The all-important function of keeping the mine workings open. As a verb, it refers to this function; as a noun it refers to all the equipment and materials--timber, roof bolts, concrete, steel, etc.--that are used to carry out this function.

Tailgate - A subsidiary gate road to a conveyor face as opposed to a main gate. The tailgate commonly acts as the return airway and supplies road to the face.

Tailpiece - Also known as foot section pulley. The pulley or roller in the tail or foot section of a belt conveyor around which the belt runs.

Timber - A collective term for underground wooden supports.

Time of Useful Consciousness – Also known as "**Effective Performance Time.**" These interchangeable terms describe the period of time between the interruption of the oxygen supply or exposure to an oxygen-poor environment and the time when a person is unable to perform duties effectively, such as putting on oxygen equipment or taking corrective action.

Ton – A short or net ton is equal to 2,000 pounds.

Top - A mine roof; same as “back.”

Tractor - A piece of self-propelled equipment that pulls trailers, skids, or personnel carriers. Also used for supplies.

Tram - Used in connection with moving self-propelled mining equipment (i.e., to tram or move a machine).

Transfer point - Location in the materials handling system, either haulage or hoisting, where bulk material is transferred between conveyances.

Underground mine – Also known as a "deep" mine. Usually located several hundred feet below the earth's surface, an underground mine's coal is removed mechanically and transferred by shuttle car or conveyor to the surface.

Velocity - Rate of airflow in lineal feet per minute.

Ventilation - The provision of a directed flow of fresh and return air along all underground roadways, traveling roads, workings, and service parts.

Violation - The breaking of any state or federal mining law.

Water Gauge (standard U-tube) - Instrument that measures differential pressures in inches of water.

Wedge - A piece of wood tapering to a thin edge and used for tightening in conventional timbering.

Weight - Fracturing and lowering of the roof strata at the face as a result of mining operations, as in “taking weight.”

Worked out area - An area where mining has been completed, whether pillared or nonpillared, excluding developing entries, return air courses, and intake air courses.

Working - When a coal seam is being squeezed by pressure from roof and floor, it emits creaking noises and is said to be “working.” This often serves as a warning to the miners that additional support is needed.

Working face - Any place in a coal mine in which work of extracting coal from its natural deposit in the earth is performed during the mining cycle.

Working place - The area of a coal mine inby the last open crosscut.

Workings - The entire system of openings in a mine for the purpose of exploitation.

Working section - All areas of the coal mine from the loading point of the section to and including the working faces.

Appendix Z - References

[1] USBM dictionary 1996.

[2] Pechmann, J.C., Arabasz, W.J., Pankow, K.L., and Burlacu, R.L., 2008, Seismological report on the August 6, 2007 Crandall Canyon Mine Collapse in Utah, submitted to *Seismological Research Letters*.

[3] Ford, S.R., Dreger, D.S., and Walter, W.R., 2008, Source characterization of the August 6, 2007 Crandall Canyon Mine seismic event in central Utah, submitted to *Seismological Research Letters*.

[4] Pariseau, W.G., 1978, Interpretation of Rock Mechanics Data (Vol. II), (A Guide to Using UTAH2), USBM OFR 47-80, June 1978, 41pp.

[5] Heasley, K.A., 1998, Numerical Modeling of Coal Mines with a Laminated Displacement-Discontinuity Code, Ph.D. Thesis, Colorado School of Mines

[6] Mark, C., ARMPS v.5.1.18 Help file, Stability Factors.

[7] Chase, F.E., Mark, C., and Heasley, K.A., 2002, Deep Cover Pillar Extraction in the U.S. Coalfields, Proceedings of the 21st International Conference on Ground Control in Mining, Morgantown, WV, West Virginia University.

[8] Koehler, J.R., and Tadolini, S.C., 1995, Practical Design Methods for Barrier Pillars, USBM Information Circular 9427, 19 pp.

[9] Goodrich, R.R., Agapito, J.F.T., Pollastro, C., LaFrentz, L., and Fleck, K., 1999, Long load transfer distances at the Deer Creek Mine, Rock Mechanics for Industry, 37th U.S. Rock Mechanics Symposium, Vail, CO, June 6-9, 1999, p. 517-523.

[10] Abel Jr., J.F., 1988, Soft Rock Pillars, International Journal of Mining and Geological Engineering, Vo. 6, pp. 215-248.

[11] Barrientos, G., and Parker, J., 1974, Use of the Pressure Arch in Mine Design at White Pine, Trans. SME of AIME, Vol. 255, pp. 75-82.

[12] Gilbride, L.J., and Hardy, M.P., 2004, Interpanel Barriers for Deep Western U.S. Longwall Mining, Proceedings of the 23rd International Conference on Ground Control in Mining, August 2004, 7 pp.

[13] Karabin, G.J., and Evanto, M.A., 1999, Experience with the Boundary-Element Method of Numerical Modeling to Resolve Complex Ground Control Problems, Proceedings of the Second International Workshop on Coal Pillar Mechanics and Design, NIOSH IC 9448, pp. 89-113.

[14] Karabin, G.J. and Evanto, M.A., 1994 Experience with the Boundary Element Method of Numerical Modeling as a Tool to Resolve Complex Ground Control Problems, Proceedings of the 13th International Conference on Ground Control in Mining, Morgantown, WV, pp. 201-213.

[15] Chase, F. and C. Mark, 1997, Analysis of Retreat Mining Pillar Stability (ARMPS), Proceedings: New Technology for Ground Control in Retreat Mining, eds. C. Mark and R. Tuchman, NIOSH IC 9446, March 1997, p. 17-34.

[16] Miller, T.M., and Mazur, P.O. (Fermilab), 1983, Oxygen Deficiency Hazards Associated with Liquefied Gas Systems Development of a Program of Controls, FERMILAB-TM-1163, Jan 1983, 30pp.

[17] http://www.cdc.gov/niosh/mining/statistics/disall.htm

[18] Lexan (LEXAN) is a registered trademark for General Electric's (now SABIC Innovative Plastics) brand of highly durable polycarbonate resin thermoplastic intended to replace glass where the need for strength justifies its higher cost.

[19] Chase, F.E., R.K. Zipf, and C. Mark (1994) "The Massive Collapse of Coal Pillars- Case Histories in the U.S.," Proceedings of the 13th International Conference on Ground Control in Mining. West Virginia University, Morgantown, WV, pp. 69-80.

[20] Maleki, H. (1995) "An Analysis of Violent Failure in U.S. Coal Mines – Case Studies," Proceedings: Mechanics and Mitigation of Violent Failure in Coal and Hard-Rock Mines, Bureau of Mines, SP 01-95, pp. 5-25.

[21] NSA Engineering, Inc., 2000, "Final Report – Review of Current Yielding Gate Road Design Approaches and Applications in U.S. Longwall Operations," January 7, 2000, 77 pp. (included as Appendix 11 in UNSW/SCT Collaborative ACARP Project C9018, "Systems approach to pillar design: Module 1 – Pillar design procedures," January 2005).

[22] Peng, S.S., 1992, Surface Subsidence Engineering, Society for Mining, Metallurgy, and Exploration, Inc., Littleton, CO, 161 pp.

[23] Agioutantis, Z., and Karmis, M., 2003, Surface Deformation Prediction System (SDPS), Virginia Polytechnic Institute and State University, Blacksburg, VA, p. 42.

[24] Arabasz W.J., 2007, Presentation to Utah Mining Commission, November 2007

[25] Waldhauser, F., and Ellsworth, W.L., 2000, A double difference earthquake location algorithm: Method and application to the northern Hayward fault, *Bulletin of the Seismological Society of America* 90, 1353-1368.

[26] http://www.cdc.gov/niosh/mining/products/product54.htm

[27] Jaeger, J.C., and Cook, N.G.W., 1979, Fundamental of Rock Mechanics, London: Chapman and Hall.

[28] Iannacchione, A.T., and Zelanko, J.C., 1995, Occurrence and Remediation of Coal Mine Bumps: A Historical Review, Proceedings: Mechanics and Mitigation of Violent Failure in Coal and Hard-Rock Mines, USBM, May 1995.